http://researchcommons.waikato.ac.nz/

Research Commons at the University of Waikato

Copyright Statement:

The digital copy of this thesis is protected by the Copyright Act 1994 (New Zealand).

The thesis may be consulted by you, provided you comply with the provisions of the Act and the following conditions of use:

- Any use you make of these documents or images must be for research or private study purposes only, and you may not make them available to any other person.
- Authors control the copyright of their thesis. You will recognise the author's right to be identified as the author of the thesis, and due acknowledgement will be made to the author where appropriate.
- You will obtain the author's permission before publishing any material from the thesis.

Reservoir Life Expectancy in Relation to Climate and Land-Use Changes: Case Study of the Mangla Reservoir in Pakistan

A thesis submitted in fulfilment

of the requirements for the degree of

Doctor of Philosophy

in

Water Resources Engineering

at

The University of Waikato

by

Saleem Sarwar

THE UNIVERSITY OF WAIKATO

Te Whare Wānanga o Waikato

2013

Abstract

The dams and reservoirs are one of the largest sources to store surface water. The escalating water crisis in the new millennium has made it very important to preserve available water and in turn to preserve the storage capacity of dams and reservoirs. Dams and reservoirs lose their capacity due to sedimentation. Climate change and land-use changes have the potential to generate more sediment load hence accelerating this depleting process. An example is the Mangla Dam in Pakistan - the second largest dam in the country. Agriculture in the Punjab province, with almost 65% of the country's population, is dependent on this dam. Due to sedimentation, the Mangla Reservoir has already lost 20% of its original storage capacity and an accelerated capacity loss is expected due to climate and land-use changes in the future.

The main aim of this research is to develop an integrated framework, which incorporates hydrological and sediment models with climate and land-use components to assess the impacts on the Mangla Reservoir sedimentation and reservoir life. Economic analysis is incorporated to identify adaptation options in relation to climate change and land-use planning and management for sustainable development in the area. The research aims to provide a practical methodology relying on limited available data. The hydrologic model was calibrated for various reaches in the reservoir catchment for flows and sediment discharge. There is a close agreement between observed and simulated flow and sediment, and the overall trend of the observed flow hydrograph and sediment discharge is simulated well by the model. The assessment of climate change impacts on reservoir life requires a transient climate change scenario, since the reservoir is subject to continuing climate dynamics, and changes in any future time will have

compound effects on reservoir life. In addition to mean climate factors, climate change will have a more profound impact on climate variability, which will likely lead to a more intensified and frequent extreme rainfall events than is currently experienced. Rainfall is the main driving factor of river sediment load, especially extreme rainfall events, which can cause exceptionally high sediment load compared to normal rainfall events. Therefore impacts of climate change was investigated by transient climate change scenarios from 1980 to 2098 constructed through bias correction of General Circulation Models (GCM) daily simulation outputs for the observed weather stations in the catchment. Land-use change scenarios were generated for two broad conditions based on socio-economic data and physical factors influencing the land-use: (i) pro-agriculture scenario and (ii) pro-industrialization scenario.

The impact of climate and land-use changes on the reservoir life was then investigated by using various combinations of climate change scenarios and land-use change scenarios. The results show that both climate and land-use changes can have significant impacts on the Mangla basin sediment transported by the river to the dam reservoir; climate change has a large impact on the annual sediment load, monthly variation in the sediment load, and in turn the reservoir life. The superimposed effects of land-use on climate change can exacerbate or reduce such impacts. Land-use change has the potential to effectively reduce climate change impacts. Therefore various land-use management measures were further evaluated based on economic analysis as adaptation options to mitigate the climate change impacts.

Acknowledgments

First of all the author would like to express his deep sense of profound gratitude to Allah who endowed him with the capabilities to complete this research study. A research of this size involves the invaluable contributions of many different people so it would not be possible without the support of many people. Your kindness, generosity and support made this three year study an enjoyable, learning and team building experience.

I am deeply indebted to my wonderful supervisors, Dr Wei Ye, Prof Janet F. Bornman, Associate. Professor Brendan Hicks and Dr Yinpeng Li at the Science & Engineering Faculty, University of Waikato, for their highly professional advice, dynamic supervision, excellent guidance and consistent technical and moral support during the development of this study. I am extremely thankful to Dr Wei Ye and Prof Janet F. Bornman whose swift response on comments and guidance made completion of this study possible in time. Special acknowledgment to Dr Chonghua Yin for helping me with the climate change scenarios. I would like to express my sincere thanks to CLIMsystems for granting me a partial grant for this study and providing SimCLIM software for the climate change analysis. All the data I used for this study were collected with the help of colleagues and friends. My thanks to EngrShafiq, Executive engineer at WAPDA for helping me to gather large sets of hydrological and climate data.

I would like to express my heartiest gratitude to the whole IGCC staff: Prof Neil Ericksen, Dr Peter Kouwenhoven, Dr Peter Urich, Prof Richard Warrick, Dr Lisa Storey, Matthew Dooley, Marian Holdaway and students (Chonghua, Meng and Electra) for their support and help. In addition, many thanks to my Hamilton friends Iqbal, Sohail, Salman, Noor, Khalid, Irfan and many others for their love

and moral support in Hamilton, New Zealand. Thanks are also due to all my friends in Pakistan.

Finally I express my gratitude to my beloved parents, brothers (Mushtaq, Sajjad and Salman), sisters, my wife and Muaz for their continuous moral and financial support, prayers and love throughout my career. I love you all.

This PhD thesis is dedicated to my father, Ch Muhammad Sarwar and mother,

Parveen Kausar

TABLE OF CONTENTS

List of Figures

List of Tables

CHAPTER ONE
INTRODUCTION

1.1 Background and problem

Fresh water is one of the most valuable assets for any human civilization. The dependency of a country's overall economy on this resource is due to inevitable demand for water from all sectors of human activities. Dams and reservoirs have served mankind as storage of fresh water for thousands of years. To date, there are over 50000 large dams (structure height higher than 15 m) throughout the world that are used for hydropower, irrigation and drinking purposes (Berga, 2008; Caston et al., 2009). Reservoirs are even more important for communities living in arid and semi-arid regions, because of scarcity of water resources. Pakistan is one of the world's most arid countries with an average annual rainfall of less than 240 mm. The agricultural sector is regarded as the backbone of Pakistan's economy. It contributes 25% of the GDP and employs more than 50% of the labour force. Because of the low annual rainfall, Pakistan's agrarian economy relies on two major reservoirs, the Tarbela Dam on the Indus River and the Mangla Dam on the Jhelum River for irrigation (Archer and Fowler, 2008). Out of its total geographical area of nearly 80 million hectares, the cultivated area is around 22 million hectares. The majority of this area, i.e., 19 million hectares, is covered by irrigation (Agricultural Statistics of Pakistan, 2005 – 2006). Irrigated land supplies more than 90% of agricultural production and most of the food for the country. The agricultural sector is the major user of water and its consumption will continue to dominate water demand.

However, dams have been designed traditionally as non-renewable resources. Their productive lives are gradually reduced because rivers refill reservoirs with

transport sediments that choke off reservoir storage capacity (Morris and Fan, 1998). The global average annual storage loss of reservoirs is about 1% but varies dramatically between 0.1% to 2.3% among river basins due to different land-use and land cover as well as other geological conditions (Chaudhry and Akhtar, 2009). For example, the Welbedacht Dam on the Caledon River in South Africa the main water source for Bloemfontein has lost 86% of its original storage capacity since completion in 1973, with a third lost within the first three years (Adams et al., 2001). In Pakistan, the Tarbela Reservoir has lost 30% of gross capacity in the period 1974 - 2006, with an average annual storage loss close to 1% or a total storage loss of 0.132 Billion Cubic Meters (BCM) (Haq I and Abbas, 2006). In terms of its initial construction cost of US $2.63 billion, an estimated US $789 million have been lost due to storage loss only. Other additional losses include reduction of irrigation water and power supplies (Dams, 2000). A more rapid rate of sedimentation is forecasted, with the reservoir largely filling up by 2030 (TAMS Consultants Inc., 1997). A similar situation is occurring for other large reservoirs in Pakistan. The Mangla Reservoir has lost 20% storage since it started in 1967, and Chasma has lost almost 43% storage capacity in 23 years (Planning Commision of Pakistan, 2005).

With the last century being particularly concerned with the development of reservoir storage, more emphasis is now required to conserve storage. It is important to convert today's inventory of non-sustainable reservoirs into sustainable assets for future generations (White, 2005). The Indus River and its tributaries naturally carry a high sediment load. Improper management systems and lack of appropriate soil conservation measures have generated additional sedimentation in the reservoirs along the river system. For the rest of this century

and beyond, climate change and associated enhanced climate variability will also play important roles in Pakistan water resource planning in relation to reservoir management. This will likely be a consequence of the strong impact expected from climate change (Huntington, 2006; Change et al., 2007), changes in precipitation patterns affecting water availability and runoff directly, and in turn the river sediment, as well as changes in temperature, radiation and humidity, which affect have evapotranspiration. As has been observed, floods caused by extreme rainfall usually give rise to more soil erosion than normal river flow. Global warming will enhance both the global and possibly regional hydrological cycles, making flooding more frequent in many areas. However, the amount of increase for any given climate change scenario is uncertain (Frederick and Major, 1997). It is therefore important for Pakistan, from a socio-economic perspective, to estimate the potential effects of climate change on the timing and magnitude of stream discharge.

Consequently, a systematic assessment of soil erosion/sedimentation with high spatial and temporal resolutions is required for Pakistan in order to support strategic decision making on water resource related to dam development projects and reservoir management practice. Although empirical relationships have been used in the past, which simply simulated rainfall-runoff relationships adopted from other similar agro-climatic zones, great uncertainty remains by using this method because it does not properly reflect the complex interactions that take place in the Pakistan river basins. Thus, a comprehensive understanding of hydrological processes in the Pakistan river basins is a pre-requisite for successful water management and climate change impact adaptation planning.

1.2 Objectives of the study

This research aims to investigate reservoir life under future change scenarios of climate and land use. Accordingly, the main objective of the thesis is to develop a systematic framework for analysing the impacts of climate change and land use changes on reservoir life, assessing the vulnerability in the future and identifying potential adaptation options.

The key research questions are:

What is the current status of sediment deposition in the reservoir?

- How will this evolve under future climate and land-use change scenarios?
- What are the vulnerabilities that lead to reservoir sedimentation?
- What adaptation options are feasible to reduce the vulnerabilities?
- Which adaptation options would be optimal to enhance reservoir life or reduce sedimentation processes?

The tasks

- Simulation of the dynamic hydrological processes and deposition of sediment at the reservoir catchment by selection of an appropriate hydrologic model.
- Development of transient projection of the climate and land use change scenarios for this century.

- Assessment of the potential risk of the reservoir (storage capacity) under future climate and land use changes by addressing hydrological/sedimentation processes and corresponding economic consequences.

1.3 Research design and methodology

The study is based on the following conditions, which underline the logical formulation of the framework:

a) The basin is used as the basic planning, data aggregation and computational unit. This provides the advantage of having a complete hydrologic cycle for an integrated river basin management methodology in which the river basin is taken as one control unit.

b) Transient climate change data are obtained from bias correction of the daily outputs from GCM models for the observed meteorological stations in the basin. The bias correction procedure is used to eliminate systematic errors in GCM simulations.

c) Land use changes are projected on the basis of current and predicted socio-economic activities in the basin. Future changes are built on a simple spatial model driven by the changes of key factors.

d) Explicit uncertainty analysis: The future of reservoir life is highly uncertain, and thus the uncertainty associated with the conclusions and outcomes of the assessment must be clearly defined. The assessment has used a set of scenarios to explore possible future trends based on different types of plausible hypotheses. The inherent uncertainties in

climate change and land use projections are dealt with using a range of change possibilities.

e) Hydrological processes in the basin are processed using the Soil and Water Assessment Tool (SWAT) (Jayakrishnan et al., 2005), which is a computationally efficient model and the simulation results can be output on daily, monthly or annual steps.

f) The climate and land-use change components are integrated into SWAT to develop an integrated framework for the prediction of changes in flow and sedimentation in the future.

The framework incorporates the integration of several modules. The details of each module are described as follows and illustrated in Figure 1.1.

1.4 Modules and models

The proposed conceptual framework consists of a series of direct/indirect interactive components. However, according to their respective functions inside the framework, they can be grouped into three large interrelated functional modules:

a) Hydro/Sediment Routing-Climatic module (HSRC)

b) Socio-Economic/Land-use analysis module (SELU)

c) Adaptation Options Analysis Module (AOAM)

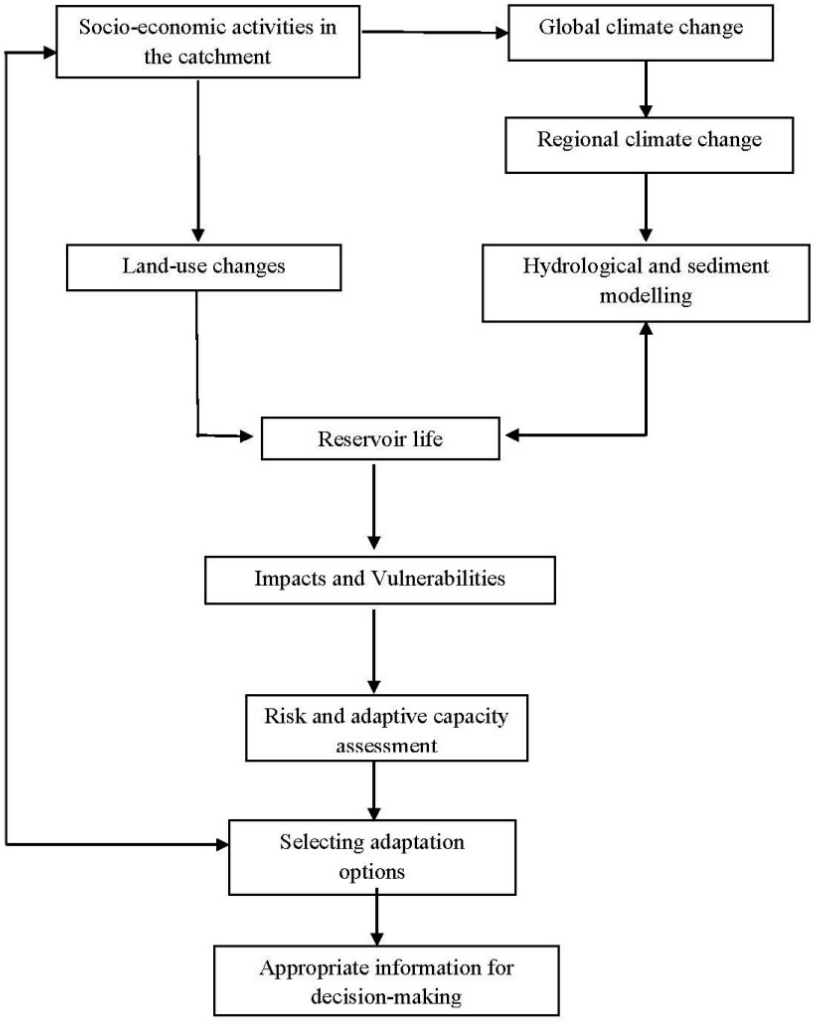

Figure. 1.1: Integrated framework of reservoir life

1.4.1 Hydro/sediment routing-climatic module (HSRC)

This module includes a hydrologic and climatic component to simulate the hydrologic and flow routing processes for predicting the potential changes in the sediment load of the reservoir. It provided a set of plausible and standard hydrologic scenarios for the study to simulate reservoir sedimentation under future climate change scenarios in addition to the baseline condition. The module involves the following procedures:

a) Construction of the baseline climate scenario. The identification, selection, and application of a baseline are the crucial steps in the climate change impact analytical process. Detailed current climate data on a daily time scale were acquired from the Meteorological Department of Pakistan and Water and Power Development Authority Pakistan (WAPDA).

b) Future climate change scenarios were developed from General Circulation Models (GCMs). At present, GCMs are widely recognized as the most appropriate tools for providing the transient global climate simulations and exploring future climate change scenarios. GCMs are physically based on the principle of fluid mechanics and describe global climate variables using 3-dimensional grids. Although GCMs are generally sufficient to reproduce the large scale climate features, their resolution is not fine enough for accurate local climate simulations. Downscaling techniques are normally used for regional scale simulation based on GCM results. The two categories of downscaling are dynamic and statistical downscaling, which are used to nest regional climate models into the GCM. However, the downscaling data were not available for the case study area. Instead, a transient climate change scenario was constructed through bias correction of simulated climate data (rainfall and temperature) obtained from different GCMs.

c) The hydrologic processes in SWAT are based on a distributed hydrology modelling (Jayakrishnan et al., 2005) for providing the spatial information of water distribution in a basin. The climate change impact on river sediment production was analyzed using different sensitivities and future

scenario data to drive the SWAT model for simulating the spatial-temporal component of the sediment in the basin, and ultimately at the outlet/reservoir.

d) The outputs of this module, including the simulations from baseline and future climate scenarios, feed to other modules as a set of common hydrologic inputs, while sensitivity parameters were used to obtain and explore how reservoir sediment may respond to climate change and to identify which hydrological processes are more vulnerable than others.

1.4.2 Socio-economic/land-use analysis module (SELU)

The land-use change module was used to identify current land use types and to group them based on their hydrological characteristics. This module is also used to produce scenarios for current and future land use changes in the basin. The purpose of this module is to analyse the potential socio-economic consequences of climate change impacts on the reservoir. It is known that socio-economic factors in addition the driving forces for land use changes (Taylor et al., 2009). This module includes the following steps:

a) Construction of a baseline socio-economic scenario based on historical statistics and global land cover data was done by downscaling national future socio-economic development scenarios to the regional/basin scales.

b) The basin/regional socio-economic scenarios were then developed in combination with the adaptation options from the module (AOAM). The national scale socio-economic development scenario data were

downscaled to the basin/regional scale through a regionalization method by extrapolation.

c) By adding basin/regional specific factors to the socio-economic scenario, alternative “scenarios” of the future were developed at appropriate time periods (between 20 and 50 years into the future). In detail, this study uses multiple scenarios to characterize four alternative futures for the priority basin. This approach can account for a wide variety of possible futures (Figure 1.2):

- S 1 is a reference scenario, which does not consider climate change.
- S 2 is a reference scenario that considers climate change, but not adaptation.
- S 3 is a projection in which development will proceed, taking climate change into account through adaptation policies that may attempt to preserve current economic activities and socio-economic conditions (adaptation 1).
- Scenario 4 is very similar to the S2, but only adaptation policies are significantly different with the emphasis, e.g., on how to optimize the structure of different water use sectors, and then to predict the reservoir life under local future climate and socio-economic scenarios (adaptation 2) (Figure 1.3).

The outputs are a set of socio-economic and land-use change scenarios. It should be pointed out that this module is closely linked to the HSRC module and AOAM module. The socio-economic scenarios vary dramatically with various adaptation options.

The next task in the study was to make projections about how socio-economic conditions will change in the future under a selected scenario. These changes are used to combine with the baseline to depict the possible future changes or prospects. The latter are then fed into the land use changes to predict reservoir sedimentation in the basin.

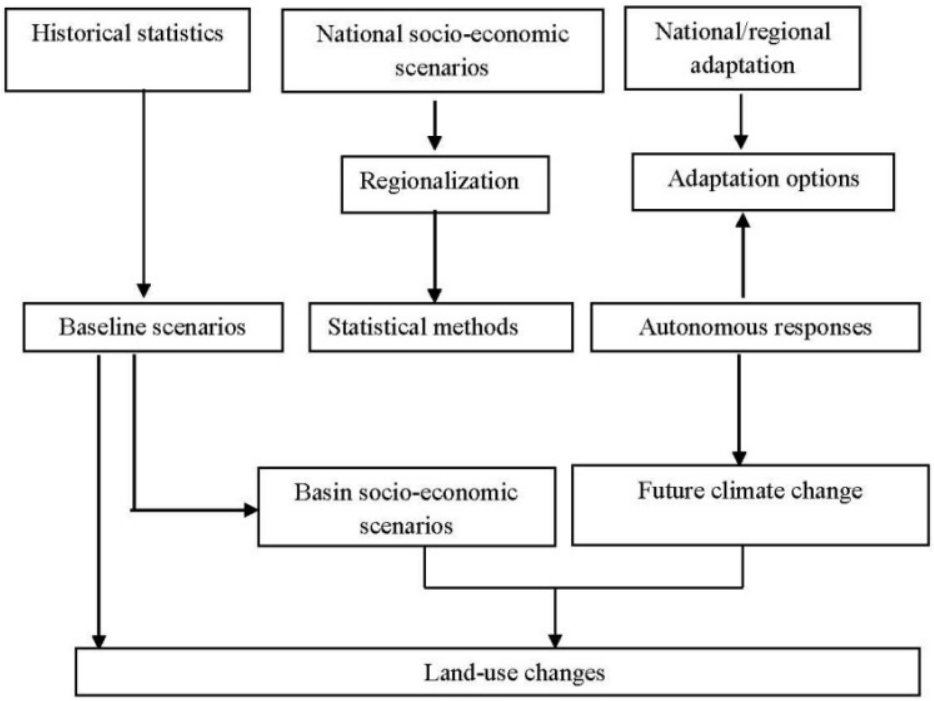

Figure 1.2: Scheme of procedures for assessing the impacts of land-use changes in a river basin

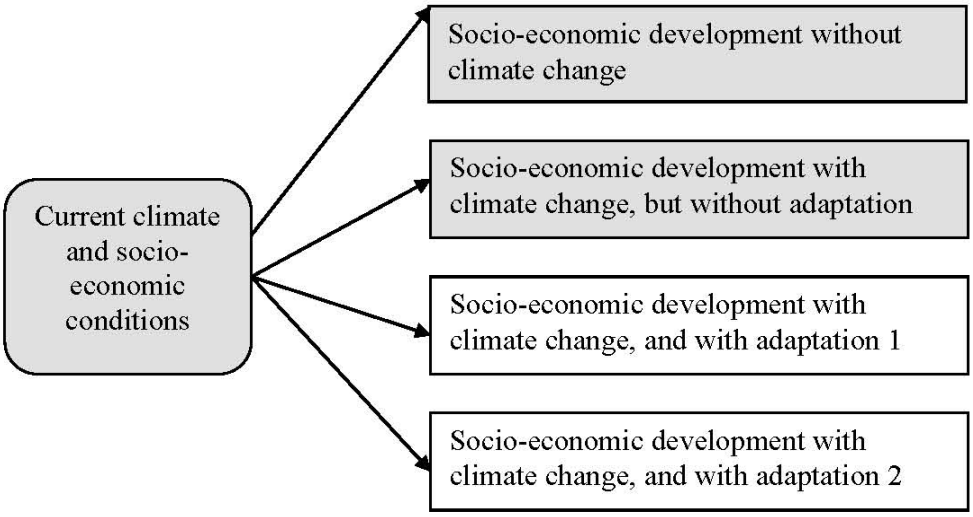

Figure 1.3: Schematic view of the multiple scenarios approach (Malone and Rovere, 2004)

1.4.3 Adaptation options analysis module (AOAM)

The adaptation assessment module, based on a unified risk management framework, was used to integrate the information from the above modules. Firstly, the vulnerability of the reservoir sedimentation brought about by climate change and land use was assessed. Secondly, a series of potential adaptation options to reduce the vulnerability of sedimentation in the reservoir was identified. The purpose of this module was to assess the current and future vulnerability of reservoir life, and identify potential consequences of adaptation options for the catchment as a whole.

The method involves the following steps:

a) Assessing current climate related reservoir sedimentation vulnerability and potential future risks according to the baseline climate and socio-economic scenarios, respectively.

b) Determining the impact of reservoir vulnerability on the economic growth of the area.

c) Scoping and identifying adaptation options for enhancing reservoir life based on the above analysis. Identifying priorities from the array of possible adaptation options.

d) Assessing those feasible adaptation options under future climate and constructed socio-economic scenarios.

The end product, namely the final result of the whole modeling framework, is envisaged as a multi-indicator system characterizing the reservoir life together with a set of most desirable adaptation options (Figure 1.4).

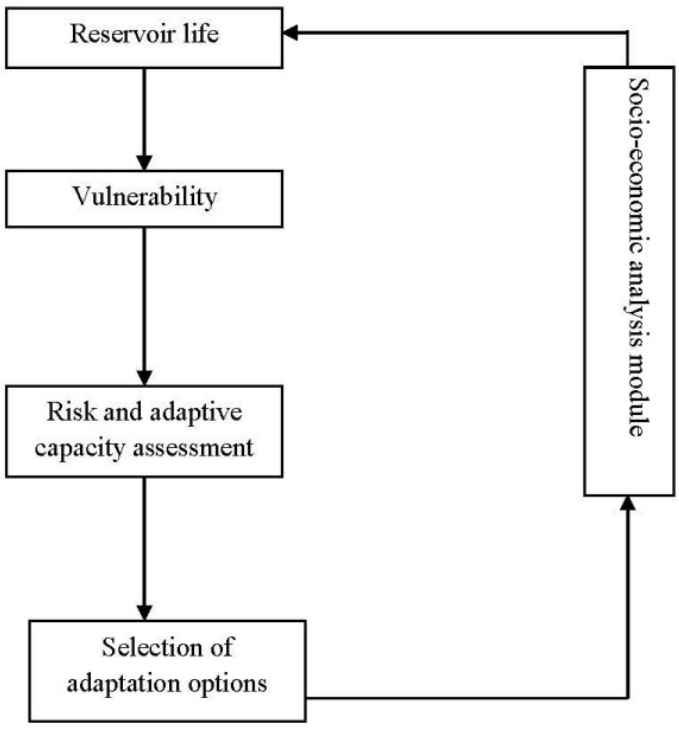

Figure 1.4: Schematic view of the adaptation option analysis

1.5 Conceptual framework

The conceptual framework (Figure 1.1) for this study was designed following the guiding principles given above. The framework integrates some merits of other popular integrated assessment modelling (Alcamo et al., 2003), and has a clear flow associated with the consequences of each stage.

Firstly, the framework starts with how future socio-economic and climate change have an impact on reservoir sedimentation. Secondly, the vulnerability is identified and the impacts on reservoir life deduced. Thirdly, a feasibility analysis is done for the adaptation options. An integrated assessment of these options is carried out within the framework in terms of their interactions with other components. For example, over a course of time, they may affect the socio-economic and land use activities in the basin, which in turn would have an impact on the reservoir life. Finally, a set of most desirable adaptation options are identified for the catchment under climate change. Within the framework, almost all of the components are related to the decision-making process either directly or indirectly. The entire process is integrated via a typical compartment modelling approach (McKinney and Lockwood, 1999). With this approach, there is a loose connection between the socio-economic and hydrological components, and only output data are usually transferred between the components through the predefined interface. That is, output of one component becomes input for the next and can be an iterative process.

1.6 Dissertation structure

Chapter 1 introduces the reservoir sedimentation or dam silting at a global level as well as in the context of Pakistan. Keeping in mind reservoir management issues

under future climate and land-use changes, research questions and objectives are outlined in this chapter. Furthermore a brief overview of the methodology (integrated framework for the reservoir life) is described. Chapter 2 outlines the lessons learned from review of the literature relating to (i) issues in reservoir sedimentation worldwide and in Pakistan; (ii) The impact of climate and land use changes on the reservoir sedimentation; (iii) Existing models for hydrological and sedimentation studies and application of the SWAT model; and (iv) Impact of reservoir life or reduction of flows on agriculture yield and economy. Chapter 3 describes the study area and its features. Chapters 4 to 6 describe the methodology adopted for hydrological modelling, climate change scenario development and land use change scenarios, respectively. Chapter 7 describes the integrated results derived from the methodologies in Chapters 4, 5 and 6 and economic analysis based on future climate change with adaptation options. Chapter 8 sets out the conclusions from the study and suggestions for the way forward to improve reservoir life.

CHAPTER TWO
LITERATURE REVIEW

This chapter provides an overview of the case study area, and reviews past research on reservoir sedimentation. It presents the research advances in reservoir sedimentation as well as climate, land use and integrated water resources management. The impact of reductions in reservoir life and/or river flows on agricultural yield and regional economy are also addressed. Key messages and knowledge gaps are identified.

2.1 Introduction

Freshwater is about 2.5% of the total 1,386 BCM (billion cubic metre) of water on Earth. Only one-third of this amount is available for human use (Postel et al., 1996). The consumption of freshwater for human use has increased almost three times during the last 50 years. The total water withdrawn increased from 1382 km^3/year in 1950 to 3973 km^3/year in 2000 and global projections forecast that water consumption will further increase to 5235 km^3/year by 2025 (Clarke and King, 2004). More than half of the available freshwater supplies (surface and subsurface) have already been used for human activities. Due to increasing demands from agricultural, industrial and residential uses, this proportion is still increasing (Postel et al., 1996; Vörösmarty et al., 2000). Figure 2.1 shows the world national availability of freshwater through average river flows and groundwater recharge in 2000. It is estimated that 5 out of 8 people will be living in conditions of water stress (per capita water availability less than 1,700 m^3/year) or scarcity (per capita water availability less than 1000 m^3/year) by 2025 (Falkenmark et al., 1989; Arnell, 1999). By 2050, some 40% of the world's

population will probably experience water shortages (Gadgil, 1998; Kuylenstierna et al., 1998; Hamdy et al., 2003).

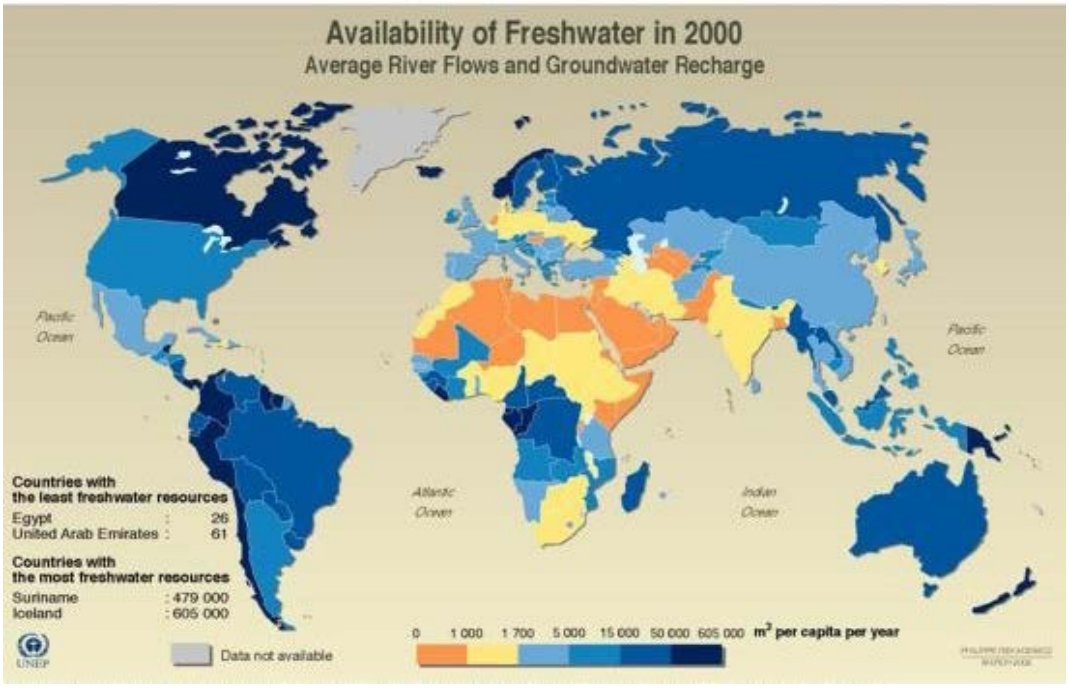

Figure 2.1: World national availability of fresh water in 2000 (Rosen, 2000)

The surface water plays an important role in the water supply for human activities. The increase in human population has had serious impacts on river and deltaic systems through enhanced fertilizer usage, damming, deforestation, and many other land-use changes in the last 50 years (Meybeck and Vorosmarty, 2005; Syvitski et al., 2005). Due to the uneven distribution of rainfall, both spatially and temporally, there is a shortage of potable and agricultural water in many countries (Vörösmarty et al., 2000). For example, although 30% of the world's renewable water resources are concentrated in Asia (Shiklomanov and Rodda, 2003), countries like China still have water shortages in certain regions. Consequently, some of China's major river systems (e.g., Huanghe and Changjiag Rivers) have

been dramatically altered by human activities in an attempt to remedy these water limitations.

Dams and reservoirs are the prominent source for storing surface water. They are critical components of a nation's water control infrastructure. Dams and their associated reservoirs represent a key component of water resource development in many areas of the world and have been constructed on many rivers, in order to provide water storage for irrigation, flood control and power generation.

2.2 Overview of surface water issues in Pakistan

Pakistan, lying in the South Asian region, has diverse landscapes and varied terrain as it's elevation changes from just above sea level from the Indian Ocean to the world's second highest mountain – K2 (PEPA, 2005). Despite being mostly arid, four distinct seasons occur in Pakistan. The country's high population growth rate is placing a severe strain on its natural resource. According to projections from the Pakistan Environmental Protection Act (PEPA, 2005), the country's population will reach 173 million by 2020 and 221 million by 2025. The available water per capita would be less than 1,000 m^3/year (water scarcity threshold) from 2010 onwards (PEPA, 2005).

The Indus River and its tributaries provide the main source of surface water for Pakistan. It includes on the eastern side, the Jhelum, Chenab, Ravi, Beas and Sutlej Rivers and on the western side, the Kabul River along with its main tributaries, i.e., Swat, Panjkora and Kunhar rivers. The total catchment area of the Indus River System (IRS) is 970,500 km^2, of which about 56%, i.e., 530,000 km^2, lies in Pakistan. Figure 2.2 illustrates the average water availability in Pakistan. Dependency on a single river system, i.e., IRS, means that Pakistan is vulnerable

due to the lack of a multiplicity of river basins and diversity of water resources that occur in many other countries (World Bank, 2005). The Indus River catchment receives about 193 BCM fresh water from combined sources of glacier melt, snow melt and rainfall. With regard to the irrigation system of the IRS, there is a significant amount of water losses in rivers, canal and seepage with only 144 BCM water available at farm level.

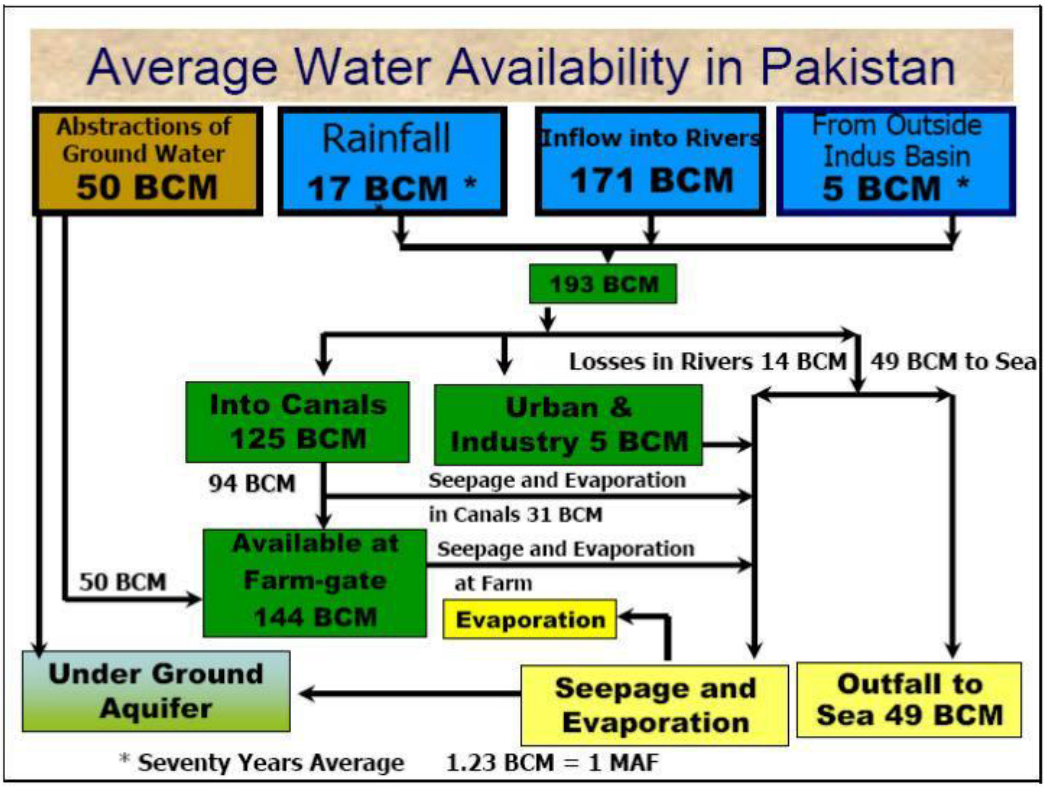

Figure 2.2: Average water availability in Pakistan (GCISC, 2005)

Pakistan has an agro-based economy with 70% of the people involved in agriculture. The Mangla and Tarbela dams, the two largest reservoirs in Pakistan, are multipurpose. These dams revolutionized the country's agriculture by increasing the irrigation command area and cultivatable land in Pakistan. These

two large dams increase total cultivatable area by 20% and provide almost one third of the country's electricity supply (Archer et al., 2010).

2.3 Reservoirs and sedimentation

There are more than 45,000 dams in the world. Most of them were constructed in the 20th Century (Dams, 2000). About 20% sediment generated in world river systems is retained in the reservoir of dams (Syvitski et al., 1998), and globally the total loss in reservoir storage is almost 1% annually due to sedimentation (Mahmood, 1987). The rate of sediment varies dramatically as the differences of river basin and impoundment characteristics control the rate and pattern of the sedimentation deposition in the reservoir (Small et al., 2003). The rates of storage loss in the Asian nations are generally higher than the world average of 1%. China and India are losing 2.3 and 0.5% respectively of storage capacity annually because of the low forest cover (China 16.5% and India 23%) and high erosion. However, the annual loss rates in Japan and Southeast Asia are only 0.15 and 0.3% respectively due to the high forest cover and relatively low sediment yield (Liu et al., 2001). Reservoir sedimentation can considerably reduce water availability (De Araújo et al., 2006). It also causes reservoir morphology to change towards a more open geometry, enhancing evaporation losses.

Globally, each reservoir is usually provided with certain rules following operational curves to suit the intended uses by taking into consideration the structural stability restriction of the reservoir. These operational rules have significant influence on reservoir sedimentation. These basic rules, however, are not adhered to in most countries. Even in the United States, the basic operational rules for reservoirs have been neglected for almost half a century but have been

considered seriously now as a measure to mitigate reservoir sedimentation after emerging of intense sedimentation problems in reservoirs and rivers (Yang, 2006).

2.3.1 Sedimentation and land-use changes

Erosion is a consequence of complex interactions among climate (precipitation, temperature, wind speed and direction), geology (volcanic and tectonic activities), soils, topography (slope, catchment orientation, drainage basin area), and land-use/cover (White, 2005). Although there is a significant relationship between land-use and in stream water quality (Tong and Chen, 2002), the relative impacts of different types of land-use on the amount of surface water are yet to be ascertained and quantified.

The rate of sediment generated production, storage and transport characterizes the river setting over space and time. In recent times, the change in river setting is mainly controlled by climate change and human induced land-use changes. The response of the Holocene and/or contemporary fluvial dynamics to land-use change has been documented in various studies (Piegay et al., 2004; Hudson and Kesel, 2006). The relative importance of climate and land cover may vary, i.e., changes in land-use increase the sensitivity of river basins to climate disturbance (Macklin and Lewin, 2003). Furthermore, during the Holocene period, human technological and economic power has been progressively replacing climate as key factors in controlling sediment dynamics (Meybeck and Vorosmarty, 2005). However, the extent to which climatic events and/or human actions have had an impact on sediment fluxes in the landscape often remains unclear.

The impact of climate and land-use changes on the sediment transported from rivers to the oceans is largely dominated by forest conversion to cropland and is

further exacerbated by climate events (Yang et al., 2003; Ito, 2007). On the other hand, several researchers have questioned the impact of deforestation on large scale flooding, suggesting that these effects have been overestimated (Kiersch and Tognetti, 2002; Bruijnzeel, 2004) and that major sources of sediments may be from other human activities such as road construction, poorly constructed and maintained terraces, runoff from cultivated land such as coffee plantations or bank erosion (Sidle et al., 2006).

The onsite impacts of land-use changes such as conversion and breakdown of native vegetation, biodiversity loss and changes, soil degradation and change in water regimes have been well documented (Gardner and Gerrard, 2003; Sidle et al., 2006). Examples include clearance of indigenous forest to pastureland in the late 19th and 20th century which changed the sediment dynamics of the Waipaoa River, New Zealand (Gomez et al., 2007).

The offsite impacts, such as downstream land flooding, pollution, siltation and sedimentation of reservoirs are also caused by runoff and soil erosion. They can result in increased sediment discharge and elevated nutrient loads leading to a reduction in water quality and water availability to downstream users (Bruijnzeel, 2004). The erosion of soil resulting from land degradation, climate and land-use changes is a concern to upland farmers as well as to downstream users.

2.3.2 Sedimentation and climate change

Climate change is projected to accelerate, with associated changes in climate variability, which means very likely more frequent extreme events such as droughts and floods (Solomon et al., 2007). IPCC has provided assessments of scientific, technical and socio-economic information relevant for understanding

climate change and the human dimensions of mitigation and adaptation. For example, the Fourth Assessment Report (AR4) provides an overview of four narrative scenarios, A1, A2, B1, and B2 and creates six plausible global greenhouse gas emissions scenarios: A1F, A1B, A1T, A2, B1 and B2 (IPCC, 2007a). Each scenario corresponds to different environmental, social, economic and technological development roads that result in different levels of greenhouse gas (GHG) emissions. Future scenarios provide analysis of socio-economic development and describe the possible future state of the world (Christensen et al., 2007). For different scenarios from the Special Report on Emissions Scenarios (SRES), the IPCC Data Distribution Centre (IPCC DCC, http:// www.ipcc-data.org/) provides accessible climate model data.

The global average surface temperature by the 2020s is likely to increase around 1°C relative to the pre-industrial period (IPCC, 2007 b). By the end of the 21st century, the most likely increases are 3°C to 4°C for the high greenhouse house gas (GHG) emission scenarios and around 2°C for the low emission scenario (Meehl et al., 2007). The increased global temperature will alter global and regional hydrological cycles with further impacts on water resources.

The transition of land surface from a natural landscape to other land-use types dominated by human activities has influenced the rate of sediment carried by rivers and has set the background for changes that might occur during the 21st Century, including feedback effects between the changes in climate and land-use (Goudie, 2006; Walling, 2006). A number of studies have been carried out to estimate the potential effects of future climate change on soil erosion at the scale of small catchment (Boardman and Favis-Mortlock, 1993; Favis-Mortlock and

Boardman, 1995; Pruski and Nearing, 2002). It is important to determine the climate change impact on sediment transport in rivers because of its effect on the global geochemical cycles (Martin and Meybeck, 1979). Also the forecasting of sediment flux from drainage basins is necessary for the evaluation of proactive land-use policies and adaptation options for minimizing the climate change impact on river sediment discharge at local and regional scales (Ashmore and Church, 2001). As catchment characteristics also influence the sediment yield, it is not easy to differentiate the sediment caused by climate change. Thus there are uncertainties in the projection of climate change impact on suspended sediment (Walling and Fang, 2003), and most importantly in the rate of bed load deposited. Consequently, projections of fluvial sediment discharge due to climate change are not well documented compared to water discharge. Results obtained from numerical simulation models are used to look into the impact of different types of environmental change on fluvial sediment transport (Coulthard and Macklin, 2001; Syvitski et al., 2005). Many researchers have forecasted the flow and sediment for river basins under different climate change scenarios, such as the mean annual flow of suspended sediment for the Waipaoa River in New Zealand (Gomez et al., 2009). According to their findings, the impact of climate change may decrease the mean annual flow of the Waipaoa River at Matawhere up to 13% by 2030 and the mean annual flow could be 18 % less by 2080. The change in mean annual suspended sediment in 2030 may be difficult to predict, since there is large variation in the suspended sediment load.

Given the potential significant impact consequence from climate change, the special consideration of adaptation opportunities has been highlighted in climate change and water security studies (IPCC, 2007a). There is growing awareness of

the importance of water resources management and there has been increasing attention directed at sustainable management of water resources at regional (e.g., European Union, 2000) and global scales (ICWE, 1992; FAO., 2000; United Nations, 2006; World Water Council, 2006). Correspondingly, integrated water resources management has gradually become an active research field (Jønch-Clausen, 2004; Savenije and Van der Zaag, 2008).

Both adaptation and mitigation measures are essential to alleviate expected impacts of climate change on humans and their environment, and sustainable development can improve adaptive capacity and increase resilience (Klein et al., 2007). Although there is growing awareness of the need to integrate adaptation with sustainable development, to date there appears to be a lack of experience to achieve this objective (IPCC, 2007a), because of the paucity of models and tools that can be used to support the assessment of potential adaptation/mitigation measures and their associated cost benefits.

2.3.3 Pakistan and sedimentation problems

Pakistan is an agricultural country and its economy is based mainly on an irrigated agriculture (World Bank, 2005). Most parts of the country lie in semi-arid regions so that agriculture mainly relies on water supply from reservoirs. The reservoir sedimentation has caused much damage to the country's economy. The cost to replace lost reservoir storage is reported to be over US$13 billion, excluding other environmental and social costs incurred from additional dam development (Palmieri et al., 2003). Due to the increases in population and the per capita water demand, preserving existing reservoir water storage has become a high priority for Pakistan. Otherwise many of the country's dams will cease to be operational in

the near future, putting more economic and environmental burdens of construction of new dams on future generations.

The country's two largest reservoirs, Tarbela and Mangla, have gross capacities of 14.3 BCM and 7.2 BCM, respectively (Altaf-ur-Rehman, 2004). When designed, they were intended to maximize water use for irrigation with power generation being a secondary purpose. These reservoirs are handicapped by their inbuilt sediment and trapping capabilities, and have gradually been degraded. The useful lifetime of the Tarbela Reservoir on the Indus River is threatened by a sediment delta that is approaching the dam's intake tunnels that lead to a hydroelectric power station and are used for irrigation releases (Tate and Farquharson, 2000).

2.4 Assessment methodologies and model development

In the past decades, scientists have made significant advances in modelling water resources. Since the IPCC Third Assessment Report (TAR), over one hundred studies of the climate change effect on river flows have been published in scientific journals, and many more as internal reports. However, studies still tend to be heavily focused on Europe, North America, and Australia (IPCC, 2007a). Most of the modelling approaches have been focused on the interaction between atmospheric and hydrological processes (Rode et al., 2002; Horak and Owsinski, 2004), or on the impact of climate change on the hydrological regime (Shiklomanov and Rodda, 2003). For example, in the Colorado River Basin (USA), there have been six major studies on how changes in temperature and precipitation might affect annual runoff in the Colorado River (Christensen et al., 2004).

These studies have made significant advancements in the assessment of climate change impacts on hydrology and water resources. In particular, they provide a series of methodologies, including classical top down (Wood et al., 1997), multi-model ensembles (Christensen et al., 2007) as well as various downscaling approaches (Wood et al., 2004). However, climate change information and its impact on regional hydrology and water resource are still limited in developing countries.

Climate change will potentially have substantial impacts on reservoir life. To evaluate the impacts, it is necessary to consider the land-use changes that are likely to be altered and future climate patterns and extreme rainfall events. Some of the integrated models can be used for this, such as Hydro Trend (Syvitski et al., 1998), which simulates daily discharge hydraulics at the river mouth, including sediment load properties; and HIDROSED (Mamede et al., 2007), for analysis of the sedimentation and resulting water availability reduction in reservoirs.

2.5 Selection of the hydrologic model

In order to select the most suitable model for eventual integration for this research, a range of available hydrological models are explored and assessed. The selection needs not only to consider the research objective that determines the complexity and structure of the model, but also the data requirements because model development can be hindered by the data availability for model calibration and validation. For this research the selection criteria for a hydrological model should include the area of catchment hydrology, the spatial effects of land-use change on runoff generation, and water quality of sediment.

The term ‘model’ has been defined in numerous ways which has led to some confusion regarding its meaning in different contexts (Konikow and Bredehoeft, 1992). Generally, models are not exact representations of the physical system or processes but are instead conceptual representations and estimations using some mathematical equations. For the purposes of this research, a simplified version of hydrological (surface and ground water) systems and sediment transport dynamics is used, and reasonable alternative scenarios are predicted, tested and compared. The application and effectiveness of a model depends on how closely the mathematical equations reflect the physical systems being modelled. It is crucial to have a thorough comprehension of the physical system and the hypothesis implanted in the derivation of the mathematical equations in order to assess the effectiveness of the model (Kumar, 2000).

Numerous catchment scale models are available today, and most of these have capability to simulate hydrologic processes with or without nonpoint-source pollution, and a few also include economic components (Singh and Frevert, 2002). Many of these models are continuous simulation models as they are used to analyse long-term hydrological changes. These can be used for management practices especially for agricultural purposes (Borah and Bera, 2004). A brief description of these models is listed in Table 2.1.

Keeping in mind the above selection criteria, the Soil and Water Assessment Tool (SWAT) was selected for part of the integrated system to achieve the research objectives. SWAT is a physically-based model (spatially represents the catchment area) It requires information about weather, soil properties, topography, vegetation and land management practices.

2.5.1 Assessment of the performance of SWAT for hydrological studies

Several hydrological components in the SWAT model, such as surface runoff, evapotranspiration (ET), recharge, and stream flow have been developed and validated at small scales within the Erosion Productivity Impact Calculator (EPIC), Groundwater Loading Effects of Agricultural Management Systems (GLEAMS) and Simulation of Water Resources in Rural Basins (SWRRB) components. Surface flow and sub-surface flow in SWAT are interlinked and based on a linked surface and sub-surface flow model developed by Arnold et al. (1996). Current SWAT reach and reservoir routings are based on the ROTO approach which is developed to estimate flow and sediment yields in large basins using sub-area inputs from SWRRB. The SWAT model has been used for several studies (Srinivasan and Arnold, 1994; Arnold et al., 1998; Arnold and Allen, 1999; Arnold et al., 2001; Chu and Shirmohammadi, 2004) for simulation of flow and sediment for river basins for assessing different climate and land-use changes.

The SWAT model has also been used for simulating stream flows for two small catchments in South Western Canada (Etienne et al., 2008). The study shows that the model satisfactorily calibrated the mean annual flows but under estimated the dry season flows and over-estimated the wet season flows.

Application of the RUSLE equation within a tropical watershed requires complex input data that are not too complex or unattainable within a developing country, it is compatible with a Geographic Information System GIS, and it is easy to implement and understand from a functional perspective. Wischmeier and Smith, (1978). used in conjunction with a raster-based GIS, the RUSLE model can predict erosion potential on a cell by cell basis. This has distinct advantages when

attempting to identify the spatial patterns of soil loss present within a catchment. The GIS can then be used to isolate and query these locations to yield vital information about the role of individual variables in contributing to the observed erosion potential value.

Table 2.1: Overview of hydrological models

Model	Author	Model Type	capabilities
AGNP	(Young et al., 1987)	Continuous simulation model	To evaluate management decisions impacting water, sediment and chemical loadings within a water basin system
AnnAGNPS	(Bingner and Theurer, 2001)	Continuous simulation models	Enhanced features from AGNP for more comprehensive evaluation of the catchment
ANSWERS-Continuous	(Beasley et al., 1980)	Continuous simulation models	Simulate runoff, erosion, transport of dissolved nutrients and sediment
CASC2D	(Downer et al., 2002)	2 D model	Simulate rainfall run off from any temporally spatially varied rainfall event
DWSM	(Borah et al., 2002)	Distributed	Simulation of surface and subsurface storm water runoff
HSPF	(Bicknell et al., 1996)	Continuous simulation model	Nonpoint source run off simulation
KINEROS	(Woolhiser et al., 1990)	Continuous simulation model	Hydrological and nonpoint source pollution model
MIKE SHE	(Refsgaard and Storm, 1995)	Distributed model	Catchment scale hydrological and nonpoint source pollution model
PRMS Storm Mode	(Leavesley and Survey, 1983)	Continuous simulation model	Rainfall runoff simulation model
SWAT	(Arnold et al., 1998)	Semi distributed model	Predicting and assessing the impact of management of water and sediment.

The above studies indicate that SWAT can perform very well for hydrological and sedimentation studies for large as well as small catchments and the following conclusions have been drawn for the SWAT model, which also form the rationale for its use for this research:

- Efficient performance for hydrological and sedimentation studies for large catchment.
- Good simulation of flows monthly, seasonally and annually with satisfactory simulation on a daily basis.
- Satisfactory performance in catchments with snow melting process.
- Coupling possible with climate and land-use models to forecast future stream flows and sedimentation in catchments.
- Appropriate for use as a decision support model as it has the capability of modelling changes in land-use, management practices and climate change.

2.5.2 Description of the SWAT model

The SWAT Model computes runoff and discharge at each Hydrological Response Unit (HRU) and then aggregates to sub-catchment by an area-weighted average. HRU represents the spatial heterogeneity in terms of land cover, soil type and slope in a sub-catchment. Water balance is the basis of all simulations. The water balance of a catchment can be grouped into the land phase and the routing phase. The routing of water in HRU calculated is shown in Figure 2.3. The water balance in each HRU is described by four storage volumes: snow, soil profile, shallow

aquifer and deep aquifer (Jha et al., 2004). The runoff, sediment and nutrient are processed in each HRU and routed through streams, lakes and reservoirs.

The water balance in the land phase includes canopy water balance (representing rainfall interception) and soil water balance. The canopy water balance determines the amount of rainfall evaporated from the canopy. The soil water balance partitions the incoming rainfall into soil water content, surface runoff, actual evapotranspiration, plant uptake, infiltration and percolation, and return flow. In the end, flow is routed at HRU level for computation of the total runoff of the basin.

Once the water balance of the land phase is calculated, the flow is routed through the stream network. As the water flows in the reach or main channel, water loss occurs as a result of evaporation and transfer through the river bed. The water in the reach is also removed by municipalities, industry and irrigation demands. The wetlands, reservoirs and lakes also influence water routing.

Sediment yield in SWAT is estimated with the modified soil loss equation (MUSLE) (Williams and Berndt, 1972). Once sediment is calculated, it is routed in two phase deposition and degradation. These two processes operate simultaneously. The sediment deposited in the river or flood plain from sub-basin is computed using Stoke's Law (Chow et al., 1988). In the second phase, degradation (Bagnold's stream power equation) of the channel takes place simultaneously with deposition of the sedimentation. The hydrological and sediment component of the SWAT model is discussed with further details in the next section. Full details of the model can be found from Arnold et al. (1998) and Neitsch and Arnold (2005).

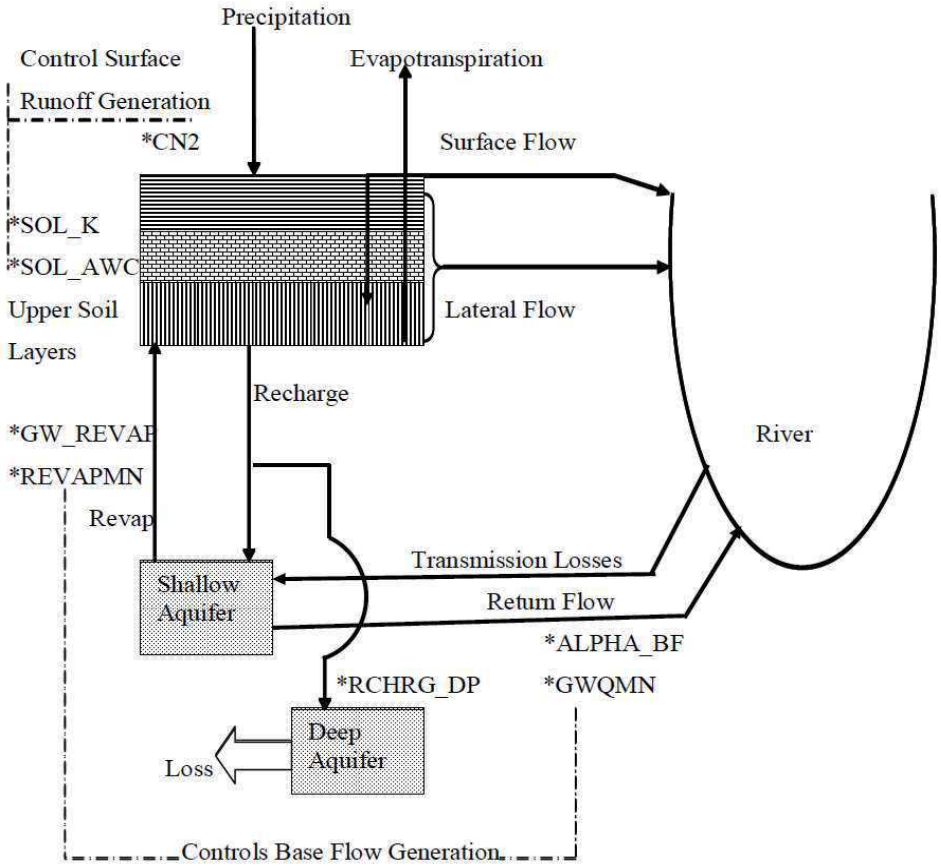

Figure 2.3: SWAT land phase process and control parameters (Mekonnen 2008). CN2: SCS Curve Number; SOL_K: soil hydraulic conductivity; SOL_AWC: soil available water capacity; GW_REVAP: Groundwater "revap" coefficient; REVAPMN: threshold depth of water in shallow aquifer baseflow; RCHRG_DP: deep aquifer percolation coefficient; ALPHA_BF: Baseflow alpha

2.5.3 Hydrological component of SWAT

The simulation of flow can be described in two hydrological components: the land phase and the routing phase. The land phase of the hydrologic component controls the water movement in the land and determines the water, sediment, nutrient and pesticide amount that is loaded into the main stream. Canopy storage, infiltration, redistribution, evapotranspiration, lateral sub-surface flow, surface runoff, ponds and tributary channel return flow are simulated in this hydrological component. The second component is the routing phase in which the water is routed in the

channel network of the basin, carrying the sediment, nutrients and pesticides to the outlet. In the land phase, equation 2.1 describes the hydrological cycle in the land phase.

$$SWt = SWo + \sum (R_{day} - Q_{surf} - E_a - W_{seep} - Q_{gw}) P_{USLE} LS_{USLE} CFRG \quad (2.1)$$

where SW_t is the final soil water content (mm), SW_0 is the initial soil water content (mm), t is the time step (day), R_{day} is the daily precipitation (mm). Q_{surf} is the surface runoff (mm), E_a is the evapotranspiration (mm), W_{seep} is the seepage from the soil bottom layer (mm) and Q_{gw} is the groundwater flow (mm).

With regard to the sediment component, the SWAT computes erosion caused by runoff and rainfall with the Modified Universal Soil Loss Equation (MUSLE) (Williams et al., 1996). (Equation 2.2)

$$sed = 11.8(Q_{surf} q_{peak} area_{hru})^{0.56} K_{USLE} C_{USLE} P_{USLE} LS_{USLE} CFRG \quad (2.2)$$

where *sed* is the sediment yield (tons/day), Q_{surf} is the surface runoff (mm/ha), q_{peak} is the peak runoff rate (m^3/s), $area_{hru}$ is the area of hydrological response unit (ha), K_{USLE} is the soil erodibility factor, C_{USLE} is the management cover, P_{USLE} is the support practice factor, LS_{USLE} is the topographic factor and *CFRG* is the coarse fragment factor. The detailed description of all these parameters can be found in the SWAT manual and also from Arnold et al. (1998) and Neitsch and Arnold (2005).

2.5.4 Simulation capabilities

SWAT is a physically based model that can be used to simulate flow and sediment for large basins. It can predict nonpoint source pollution. Furthermore, it can be

used for impact studies such as climate and land-use changes, and water quality loading. The model can be used in planning and decision making. It also simulates the major hydrologic components and their interactions simply and yet as realistically as possible (SWAT, 2009).

2.5.5 SWAT sensitivity, calibration and validation

The main objective of any hydrological model is to predict the hydrological cycle. It is very important to know the uncertainties in the model results prior to making any meaningful judgment (Himesh et al., 2000). The uncertainty in the model result depends upon the quality and nature of the model. The model can be optimized by reducing the model uncertainty through sensitivity analysis of the parameters. Finally, model performance should be checked using appropriate statistical and graphical tests.

2.5.6 Sensitivity analysis

The sensitivity of the model can be described as the rate of change in model output results with rate of change of model input data. It can provide good understanding for the behaviour of the modelling system, such as parameters and applicability of the model, thus increasing the confidence level in the prediction of the results of the model.

The SWAT model has the capability to make parameter selection for sensitivity analysis. It performs auto-sensitivity analysis using the principles of the Monte Carlo technique with a stratified sampling. The sensitivity analysis in the SWAT model can be performed by selecting up to 27 input parameters and 280 runs.

2.5.7 Calibration and validation

Calibration is setting or correcting the output value by changing values of input parameters in an attempt to match these with field conditions or observations within some acceptable criteria. The model calibration requires that field conditions at the study area be properly characterized otherwise it may result in a model calibrated to a set of unrepresentative conditions of the study area. Three calibration approaches are widely used by the scientific community. These include: 1) manual calibration, 2) automatic calibration and 3) a combination of the two. The most widely used approach is manual calibration. In manual calibration the modeller alters the model input parameters manually by comparing the simulated values with observed values until the two values come within a reasonable range. This process is time consuming and its success depends on the modeller expert judgment and his knowledge about the study area (Eckhardt and Arnold, 2001). Auto calibration is usually preferred as it is less time consuming and can use an extensive set of input parameters possibilities. Auto calibration uses a predefined algorithm to obtain optimum input parameters.

The SWAT model has two built-in calibration tools: the manual calibration helper and auto calibration. It has more than 30 input parameters that can be altered during the calibration period. For auto calibration the SWAT model uses Shuffled Complex Evolution Method algorithms to attain best-fit parameters (Green and Van Griensven, 2008).

2.6 Economics of reservoir sedimentation

Engineering literature emphasizes that even when a dam is structurally sustainable, the reservoir could become unsustainable due to sedimentation

accumulation. Although the importance of the effect of the silt and sedimentation on the reservoir due to land degradation in the upper catchment are widely known, there is limited quantitative economic analysis on such effects.

The consequences of soil erosion and reservoir sedimentation have onside as well as offside effects. The onside effects can be experienced by upstream land that reduces enriched nutrient contents and organic matter resulting in the decline of agricultural productivity (Pimentel et al., 1995). The offside effects means a reduction in reservoir capacity, enhancing flood risks, occurrence of muddy floods, and a shortened reservoir life (Verstraeten and Poesen, 1999). Particularly in most semi-arid and arid regions, soil erosion is one of the major threats to the conservation of soil and water resources. The potential risk of soil erosion in these regions is due to higher climatic instability to which the extreme intensive rainfall events, the poor vegetation cover and the existence of highly vulnerable soils on steep slopes all contribute (Raclot and Albergel, 2006; Al Ali et al., 2008). Fonseca et al. (1998) found high nutrient levels in the sediments of the two reservoirs compared to original soil nutrients in a Portuguese study. Similar results were also reported by Haregeweyn et al. (2008) who investigated 13 reservoirs in the semi-arid northern Ethiopian highlands. The enrichment in nutrients is caused by disintegration of finer soil particles from parent material and transport of these finer particles in the reservoir via runoff. The loss of nutrients from the soil may cause a significant threat to crop yield, as soil fertility is often already low (Haregeweyn et al., 2008). Furthermore, the nutrient rich sediments in reservoirs can cause aquatic life and water quality problems, particularly in drinking water reservoirs (Lahlou, 1996; Fonseca et al., 1998). Flushing the reservoir sedimentation through dredging and use of these high

nutrient sediments as fertilizer could be an option, depending on the economic viability (Fonseca et al., 1998; Haregeweyn et al., 2008) but only if concentrations of pesticides and herbicides are within acceptable ranges.

The downstream reservoir sedimentation effects have some severe implications such as sediment deposition that can compromise the safety of the impoundment structure, from spillway overtopping or cracking under increased pressure from the weight of the sediment (O'Reilly and Silberblatt, 2009). Furthermore, sediment deposition can also accelerate eutrophication of reservoirs through loss of water storage capacity and limiting flow, which subsequently limits dissolved oxygen content of the water column. Where reservoirs are used for irrigation storage for the surrounding agricultural landscape, runoff from these farms may have high nutrient content. The combination of these factors leads to eutrophic reservoir conditions of increased plant and algal growth in reservoirs (O'Reilly and Silberblatt, 2009).

The environmental impacts of the reservoirs are well documented. For example, Morris and Fan (1998) noted that the presence of a migration barrier to anadromous fish often prevents access to upstream spawning habitat. Downstream river morphology is caused by sediment transport in the upstream of the river (Morris and Fan, 1998). Deltas are formed in the river due to sedimentation resulting in bed armouring. This tends to erode river bed and banks that can accelerate bed armouring which may have ecological habitats (Owens et al., 2005). Channel siltation can also reduce the groundwater table in river bank areas and in coastal areas which may lead to saltwater intrusion, making these aquifers useless (Morris and Fan, 1998). Organic materials are integrated with sediment in

the reservoirs that are food sources of downstream ecosystems (Gasith and Resh, 1999).

Furthermore, reduced capacity of a reservoir due to sediment transport has direct impacts on the regional economy by reducing water for downstream land irrigation.

2.7 Summary

The key messages that can be drawn from the literature review are:

- The Pakistan economy is mainly based upon agriculture, with most of the regions lying in semi-arid areas relying heavily on rainfall and stored water in reservoirs. Tarbela and Mangla Dams, the two largest reservoirs, are losing their capacity very rapidly due to sedimentation.
- Climate change variability will likely accelerate in the future along with land-use changes, especially deforestation and more agricultural activities, further reducing the storage capacity of the dams.
- There have been major advances in the assessment of climate change impacts on hydrology and water resources. However, the integrated framework for evaluating the combined effect of climate change and land-use changes is still limited.
- Reservoir sedimentation has onside as well as offside effects resulting in upstream land degradation, flood risks, and changes in morphology of the river and the ecology. Furthermore, it has direct impacts on the

economy of the country, resulting in less agricultural yield and loss of hydropower capacity of the dams.

2.7.1 Key knowledge gaps identified from the literature review

These relate primarily to conditions in Pakistan.

- Observations and research related to climate change and sedimentation are patchy.
- An integrated management framework for surface water and sedimentation is lacking.

2.7.2 Contribution to the knowledge base

This research aims to make an original contribution to the knowledge base of climate change impacts on reservoir life as follows:

- The modelling work is an integration of a land-use, climate, and hydrological component with reservoir sedimentation. There are many existing models such as MIKE 11, MIKE SHE, and SWAT that integrate land-use components with hydrological ones. However, the changes in land-use components are not in a time series, nor are they policy oriented.
- The integrated model is developed for the Mangla basin, Pakistan, which is the first of its kind to be applied to a Pakistan catchment.
- The integrated work is applicable to both a larger and smaller catchment.

- Integrated Frame work that links climate and land-use part with hydrological part for the assessment of reservoir sediment for base line and future period.

- Land-use scenario algorithm was developed based upon socio economic and physical factors that is quite interesting, similarly use of transient time series for future scenarios was very new idea as most of the studies were using time slice data instead of transient time series data.

- The economic analysis carried out for this study to present the reservoir sedimentation in monetary terms was first of its kind of work in that region.
- The proposed integrated model can be used for policymakers and planners.

CHAPTER THREE
CHARACTERISTICS OF THE STUDY AREA AND DATA PREPARATION FOR THE MODEL DEVELOPMENT

3.1 Introduction

Pakistan is located in the Northwest of the South Asian subcontinent, lying between 24° to 37° north latitude and 61° to 75° east longitude. It borders with Iran in the west, Afghanistan in the northwest, China in the northeast, and India in the east. On the south side lies the Arabian Sea (Figure 3.1). The total land area is estimated at 804,000 km^2.

The Mangla basin is located on the northeast side of Pakistan. The Mangla Dam is the second largest in Pakistan and the 12th largest in the world. The main purpose of the dam is to store water for irrigation, although it produces more than 1,000 Mega Watts (MW) of electricity. The water stored in the dam is supplied to rice and wheat growing areas (Butt et al., 2010). Jhelum River is the main distributary feeding the Mangla Reservoir. The Jhelum River originates from the north-western side of PirPanjal and receives water from various tributaries of the southern slopes of the Great Himalaya. In addition to the rainfall, these tributaries are also partly fed by permanent snow and glacier melt. The Jhelum River valley starts narrowing down below Baramola. At Chakothi, the river enters the Pakistan Kashmir part and flows in a narrow gorge taking a turn in a general north-west direction. Along its way to the dam site the river is joined by a large number of streams and nullas. On its steep gorge course, the river takes a very sharp bend at Domel to flow southward along with its tributaries, namely, Neelam (Kishanganga) and Kunhar rivers. Two very important tributaries, Kanshi and Poonch, feed into the Jhelum River before it drains into the Mangla Reservoir (Figure 3.2).

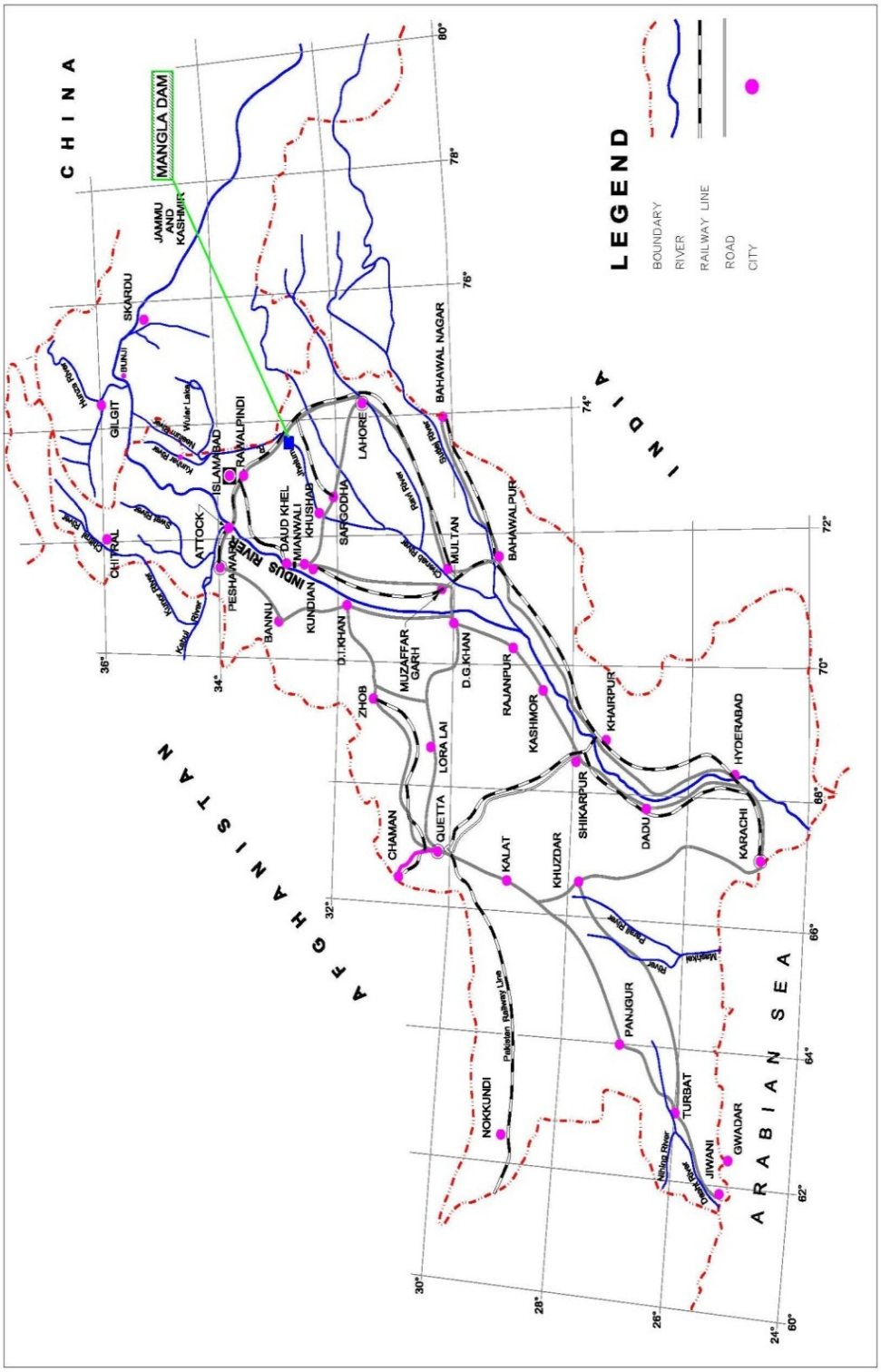

Figure 3.1: Map of Pakistan

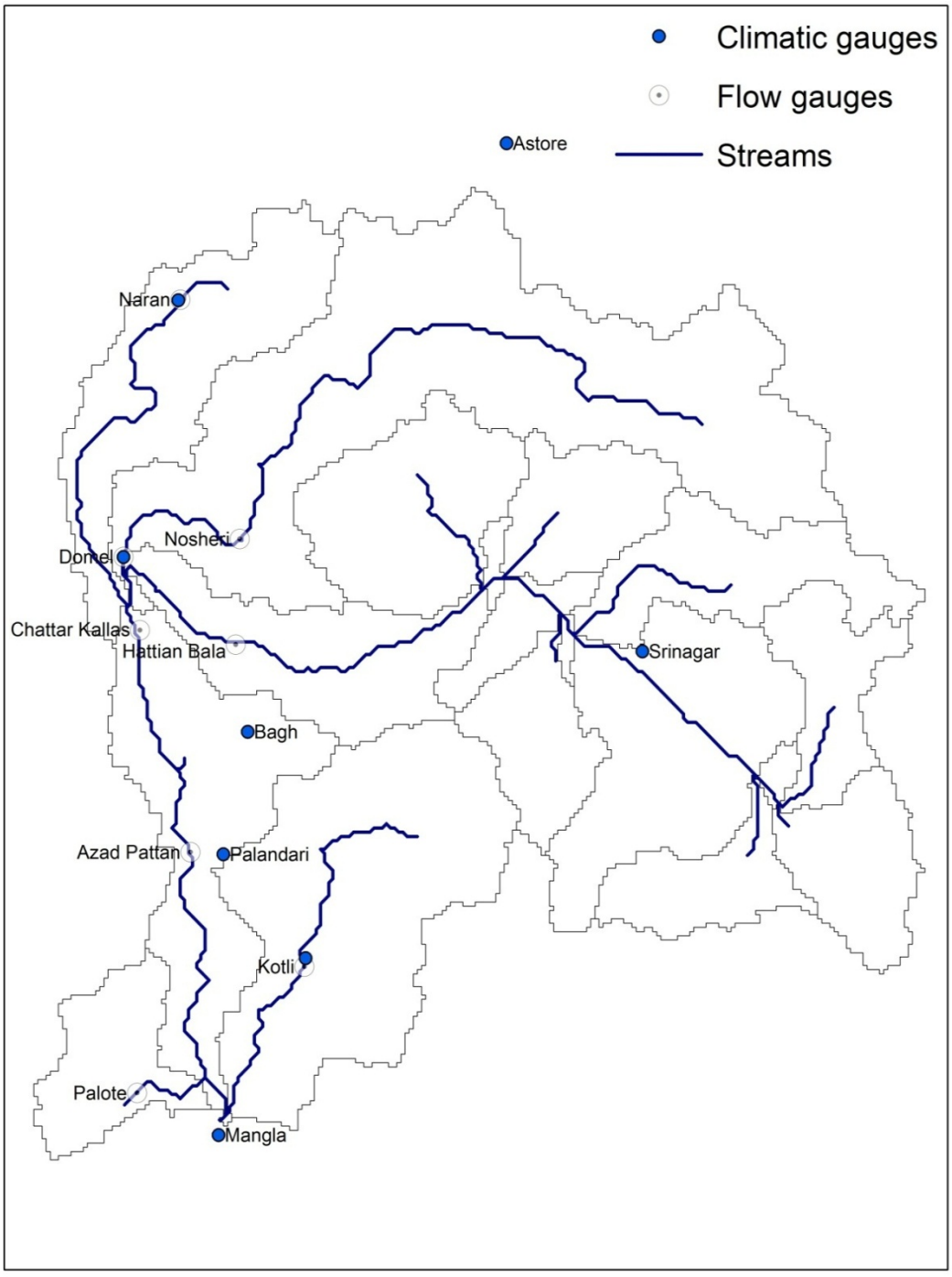

Figure 3.2: Location of the Mangla basin and climatic and hydrological observation stations

3.2 Climate

Besides latitude, the climate of the study area is directly related to its altitude. The altitude varies from north to south and so does the climate. The temperature changes from subtropical in the south with an elevation below 1,070 m to the temperate north with an elevation up to 3,650 m, and becomes very cold further north at elevations above 4,265 m. The average annual rainfall varies from around 945 mm in the south at Mangla to 1,415 mm in the north. The seasonal rainfall pattern is generally monsoonal. The autumn and winter rains are important, since their effectiveness is much greater under the prevailing low temperatures in these seasons. On the other hand, the spring and summer rains are received under high temperature and in torrential form. Summers are hot to very hot (30^{o}C at Mangla) in lower altitudinal zones, but are pleasant and colder at higher altitude.

To study the response of the climatological factors on the Mangla basin, analyses for rainfall and temperature were carried out for Astore, Bagh, Domel, Naran, Palandari, Kotli and Mangla climate stations in the Pakistan part of the basin using the period from 1990–2009. The location of the gauging stations is shown in Figure 3.2. Two different agencies collect the climate data in the upper Indus basin, i.e., the Pakistan Meteorological Department (PMD) and Surface Water Hydrology Project (SWHP) of Water and Power Development Authority (WAPDA). The main activity of SWHP stations is discharge measurements but at some of their gauging stations, SWHP also observes selected climate variables particularly rainfall. An inventory of the climate stations around the basin is given in Table 3.1. No data are available from Indian Kashmir, except for some monthly data for Srinagr from 1960–1990 (Archer and Fowler, 2008). The rainfall and

temperature data of the Srinagar gauging station was collected from the Indian Meteorological Department (IMD). Evaporation, relative humidity and wind speed parameters were analysed using the data from the Domel gauging station from 1970 –2009.

Table 3.1: Inventory of climate stations in and around the basin

Location	Latitude (°)	Longitude (°)	Elevation (MASL)	Operating Agency
Astore	35.20	74.50	5128	PMD
Bagh	33.97	73.76	1067	SWHP
Palandari	33.72	73.69	1402	SWHP
Domel/Muzaffarabad	34.37	73.47	686	SWHP/PMD
Naran	34.91	73.65	2363	SWHP
Kotli	33.49	73.89	610	SWHP
Mangla	33.12	73.64	282	SWHP
Srinagar	33.10	74.82	1584	IMD

3.2.1 Rainfall

There is a large spatial rainfall variation in the Mangla basin from an annual average of 944 mm in the sub-humid south to 1,453 mm at Kotli in the humid north and up to 2,024 mm at Muzaffarbad, but declining to 683 mm further north at Srinagr. The monthly variation in the rainfall over the period from 1990 to 2003 is between 70% and 130% (Figures 3.3 and 3.4). The northern and eastern part of the basin receives most of the rainfall in spring. About 50% of the annual rainfall for Srinagar and Naran stations occurs between January to April, with a further 14 and 29% from monsoon months. There is no gauging station in the upper part of

the basin, but the Astore station that lies in the Karakoram basin (neighbouring basin) supports the seasonal distribution for the high mountain areas of the Himalaya.

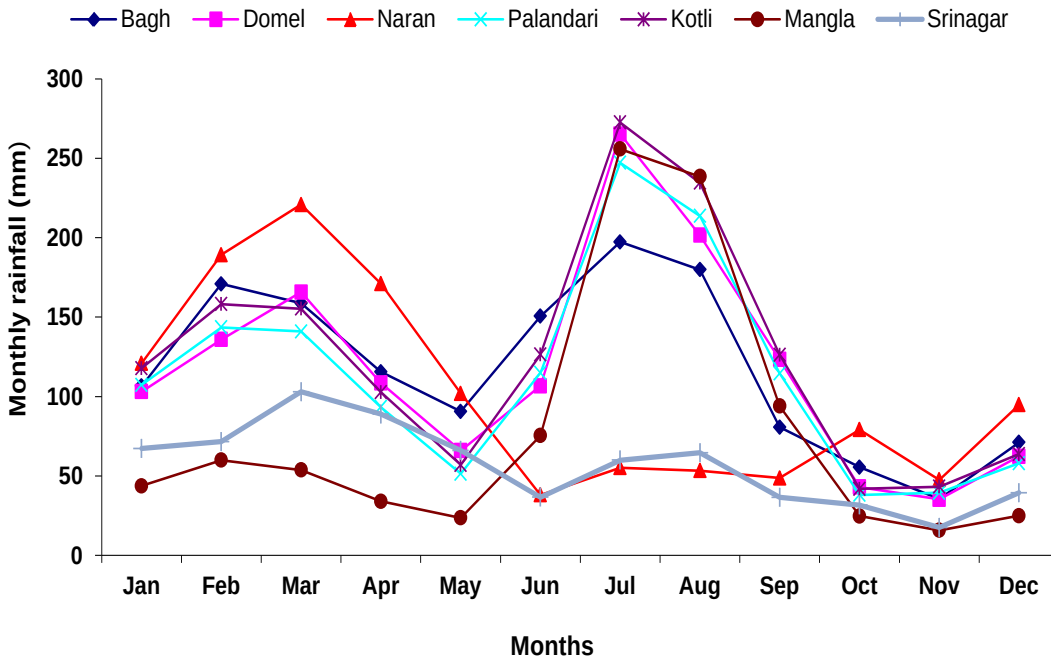

Figure 3.3: Monthly rainfall distribution in the Mangla basin

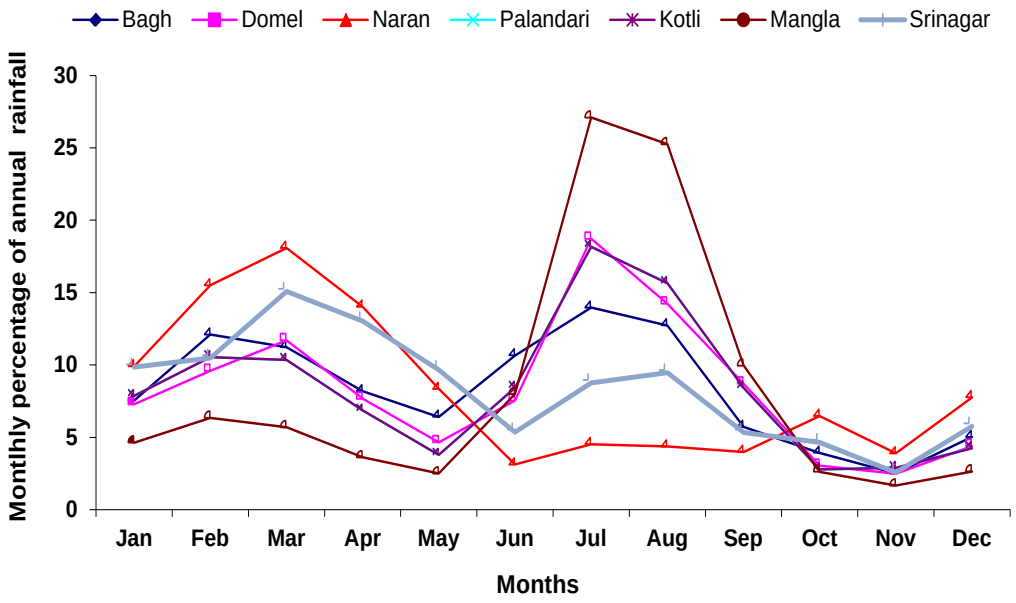

Figure 3.4: Mean monthly percentage of annual rainfall

3.2.2 Air temperature

The temperature in the basin varies greatly. In the northern part of the basin, temperatures frequently drop below 0°C in December to March. The southern part of the basin is relatively warmer and can be up to 40°C in June. Figures 3.5 and 3.6 show the average monthly maximum and minimum temperature for stations in the Mangla basin between 1990–2009.

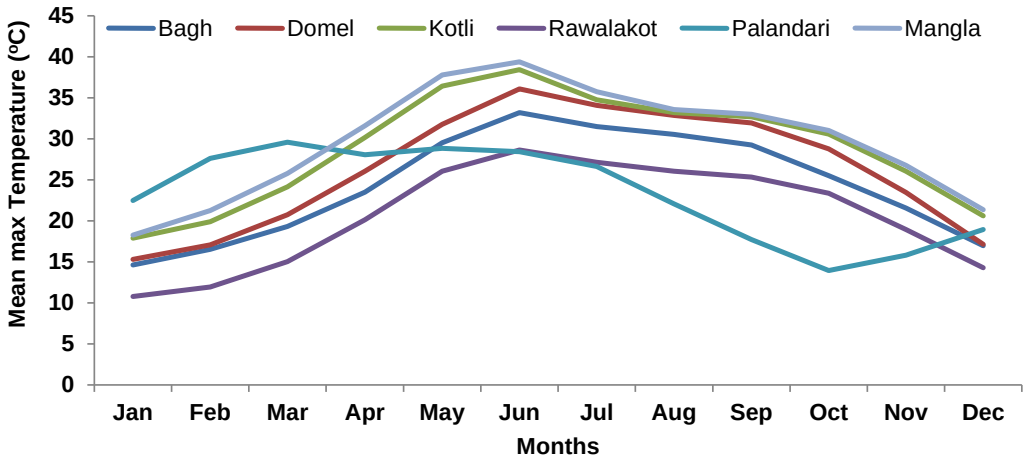

Figure 3.5: Average monthly maximum temperature

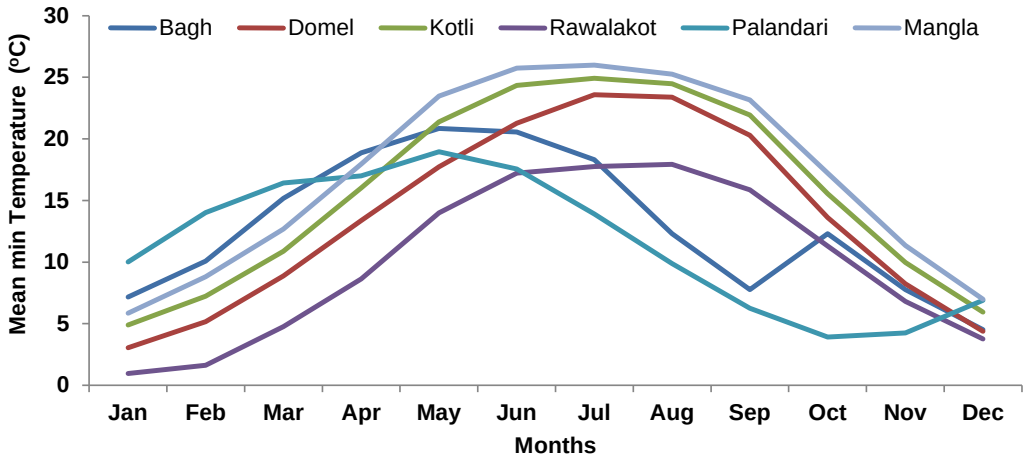

Figure 3.6: Average monthly minimum temperature

3.2.3 Evaporation, wind speed and relative humidity of the Mangla basin

As most of the basin area lies in the temperate zone, temperatures are mild, and evaporation remains moderate throughout the year. Evaporation, wind speed and relative humidity data are only available at the Domel station in the upper Jhelum basin. The temporal distribution of the average monthly evaporation is shown in Figure 3.7. June has the highest evaporation of 226 mm and December the lowest with 34 mm.

Annual evaporation over the Domel station is shown in Figure 3.8. The highest observed evaporation is 2515 mm in 1968 and the lowest, 725 mm in 2007.

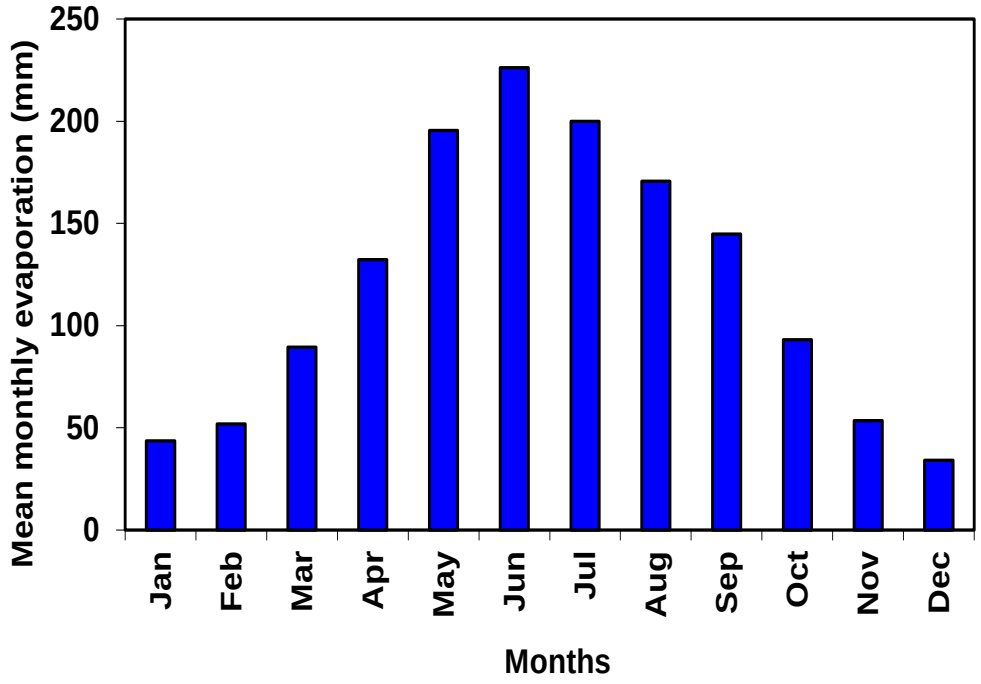

Figure 3.7: Average monthly evaporation at Domel

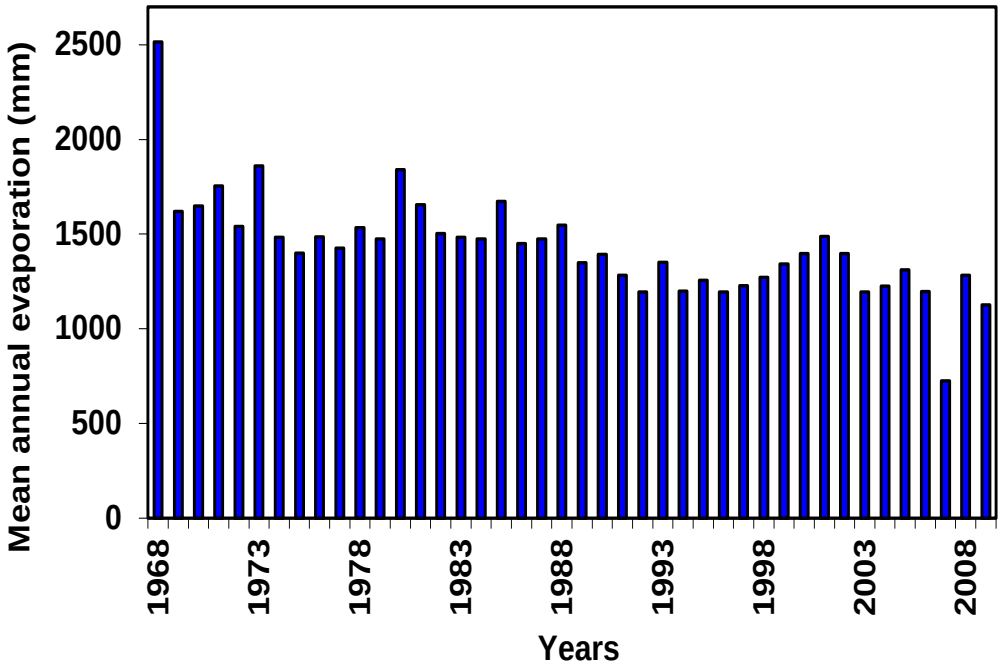

Figure 3.8: Mean annual evaporation at Domel

Average monthly wind speed distribution over the Domel is presented in Figure 3.9. Results show that March is the windiest month and August to December are calmer months. Figure 3.10 gives the annual average wind speeds for the last 40 years from 1968 to 2009, showing that the wind speed varies dramatically from year to year. In general, the average annual wind speed has decreased over time for the Domel area.

At the Domel (Muzzafarabad) climatological station relative humidity data were collected from SWHP for the period 1968 to 2009. Relative humidity is recorded at 08:00 and 17:00 daily. The mean relative humidity on a daily basis is calculated by taking the mean of both values. The relative humidity reached a maximum in August with a value of 77% and a minimum in June with a value of 56% (Figure 3.11).

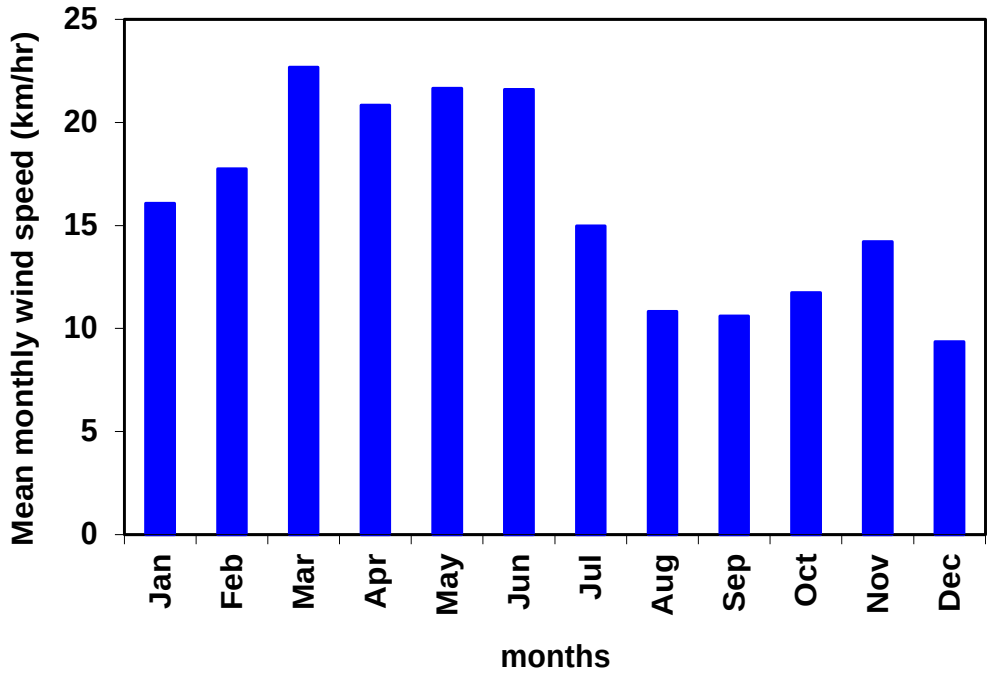

Figure 3.9: Mean monthly wind speed at Domel

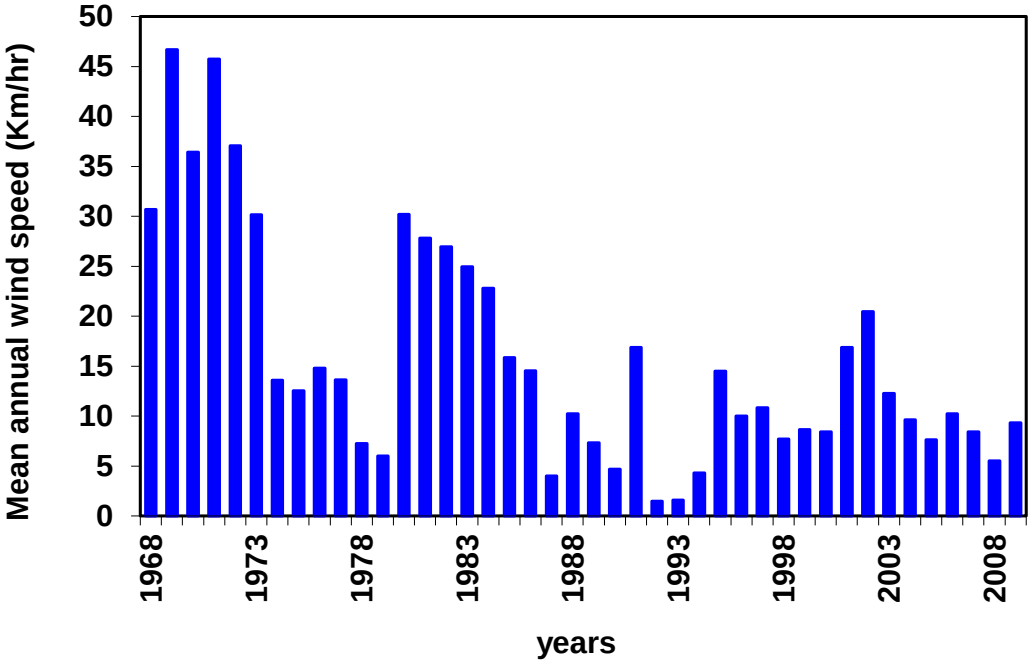

Figure 3.10: Mean annual wind speed at Domel

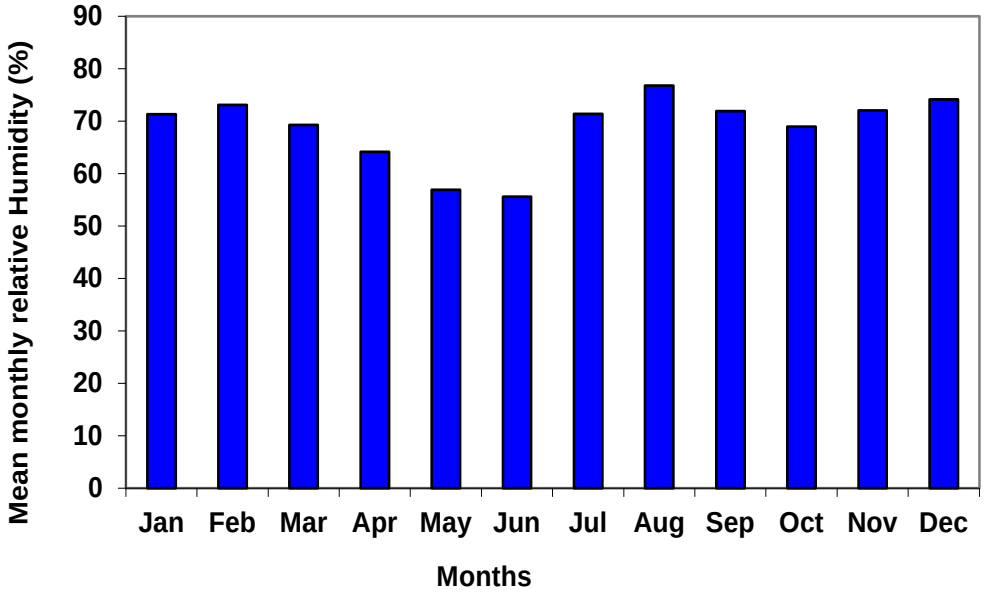

Figure 3.11: Average monthly relative humidity (%) at Domel

The annual average relative humidity values from 1968 to 2009 are presented in Figure 3.12, with the highest value for 1997 at 78%. The annual average relative humidity shows a slight rising trend over time.

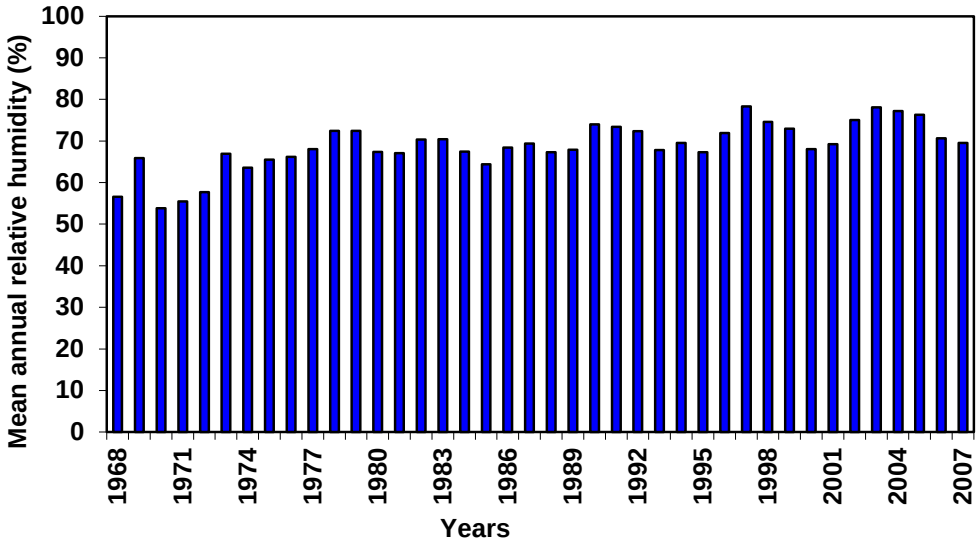

Figure 3.12: Mean annual relative humidity (%) for Domel

Seasons of the Mangla basin

Based on variation of climatic factors, including temperature, precipitation, humidity and evaporation, the following five climatic seasons can be recognized:

Pre-monsoon season (May –] June)

This is the hottest and driest season. Daytime temperature rises up to about 40°C.

Monsoon season (July – September)

Monsoon is the main rainy period. The cool monsoon winds followed by heavy rains lower the temperature to some extent. The groundwater levels start rising and reach a peak towards the end of season. The pre-monsoon and monsoon seasons are also called the summer season.

Post monsoon season (October – November)

The temperature generally decreases during this season. Ground water levels remain constant with the exception of a few places where withdrawal is exercised.

Winter season (December – February)

This season has low temperatures, strong northern cold winds, low rains and low evapotranspiration. Groundwater levels remain near to peak due to low evapotranspiration.

Spring season (March – April)

During this season temperatures remain pleasant due to light rain. The groundwater level starts declining as the evapotranspiration increases, coupled with excessive pumping.

3.3 Land-uses

The major part of the Mangla basin is grassland as it receives moderate rainfall in all months. The slope of the area ranges from 0 to 37% but is between 0 to 2.5 % for most areas (Figure 3.13). The basin is at a high altitude as shown by its contour map (Figure 3.14).

Irrigated agricultural land

Irrigated agricultural land is the major land cover in the Mangla basin. The irrigated land is mostly found on flat plains and gentle slopes, forming terraces and comprising post flooding or irrigated croplands, rainfed crop land and mosaic crop land. In total, the irrigated agricultural areas cover an area of approximately 55% of the total basin. Maize, wheat and rice are the main crops grown in the area. Fruits, including apples, apricots, peaches, walnuts, almonds, plums, pears, cherries, strawberries, citrus and guava are grown locally under irrigation. Sugarcane is a new introduction and is cultivated in limited areas. Vegetables are also grown locally, and kitchen gardens are gaining popularity in the area.

The small agro-based industries are not finding much favour compared to other parts of the country. This is mainly due to relatively low income generation from these enterprises compared to foreign remittances. The other reason for a lack of interest in agriculture is the dearth of cultivatable land in this area, the majority of the area being mountainous. The only sizeable cultivatable land is located in the south of Mirpur district, where the land holdings are still too small to be economic for a household.

On the other hand, poultry and dairy farming are developing rapidly in the area to meet the ever increasing need of meat and milk. Many locals have interests in the dairy business and are setting up dairy farms.

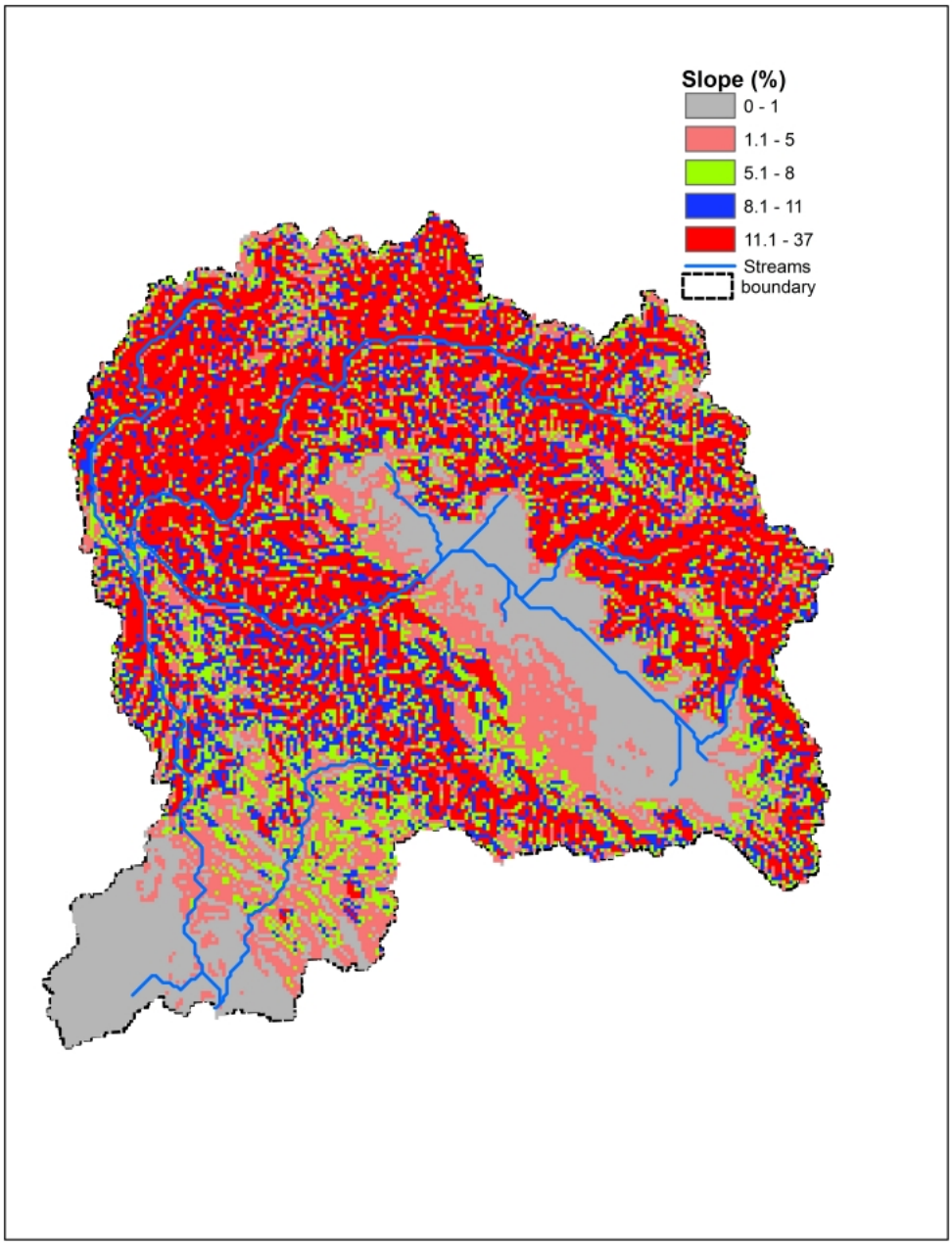

Figure 3.13: Slope map of the Mangla basin (%)

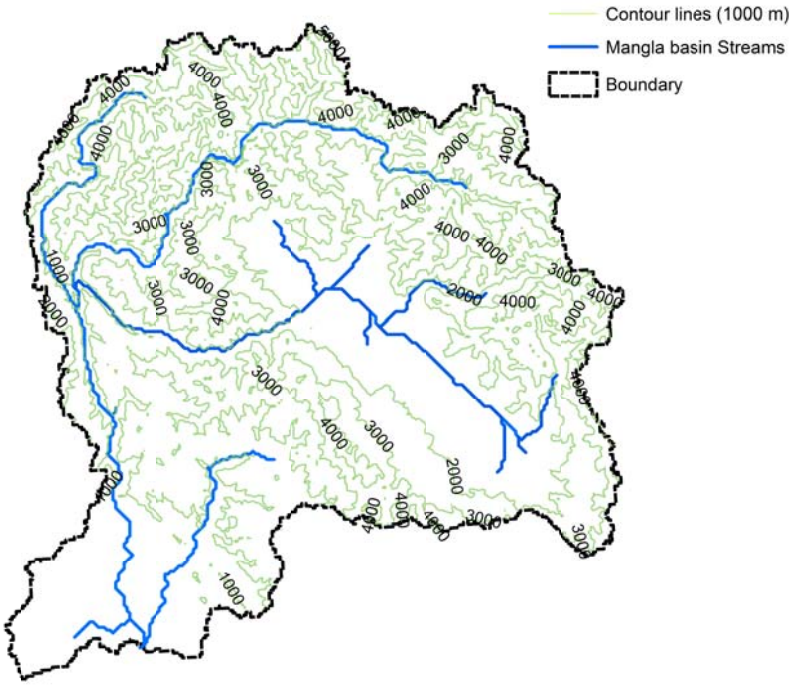

Figure 3.14: Contour map of the Mangla basin. Contour lines start from 1 000 up to 5 000 m with an interval of 1 000 m

Length of growing period

The length of the plant/crop growing period (days) is defined as days with mean monthly temperature greater than 7°C and a moisture supply from rainfall of half or more of the potential evaporation, which is recognised as necessary for plant/crop growth. Based on the climatic diagrams for Mangla, Kotli and Muzaffarabad meteorological stations, the length of the plant/crop growing periods (days) are:

Mangla	Summer (i.e. Kharif)	=	108 days
	Winter (i.e. Rabi)	=	112 days
Kotli	Summer (Kharif)	=	184 days
	Winter (Rabi)	=	136 days
Muzaffarabad	Summer (Kharif)	=	171 days
	Winter (Rabi)	=	137 days

From the above calculations, it is concluded that the southern low land area is the drier one and will need supplementary irrigation from surface or ground water for crop growth and maturation to attain high yields.

Forest

Forested areas are mainly located in the upland and central part of the basin. The forest cover can be further classified into: (i) broadleaved evergreen or semi deciduous forest, (ii) broadleaved deciduous forest, (iii) needle leaved evergreen forest, and (iv) mixed broadleaved forest. It covers an area of approximately 15% of the total basin.

In pre-historic times, all land facets from valley bottoms to upper mountain slopes in the Jhelum River basin were under different forest cover depending upon the altitudinal climate and soil conditions. Currently, the forest cover has been reduced significantly from most of the land facets that have been converted to grazing or agricultural land. Most current forest cover is confined to mountain slopes between 457m and 5000 m elevation. This includes: i) dry subtropical

broadleaved (*Olea-Acacia modesta*) chir pine forests, ii) moist chir pine forests, iii) moist temperate conifer and broadleaved forests, and iv) dry temperate forests.

Above these forests, subalpine forests with pastures occur between elevations of 3200m and 3810m, and alpine pastures at 4200 m elevation. These pastures are dominated by shrubs and short grasses used for sheep and goat grazing during the summer season. Snow fields occur above elevation 4200 m and are devoid of vegetation. They are, however, important from a basin standpoint.

Rangeland and wetland

Rangeland is usually found upland of the basin, comprising about 25% of the basin, and contains a generally natural landscape in the form of grassland, shrubs, woodland and wetland. Almost all of the rangelands in the Mangla basin are in degraded form from their original. These occur in wooded shrub land, shrub grassland or grassland, interspersed with forests, between 457 m and 4572 m elevation.

Overuse of these mountain rangelands through excessive grazing and trampling by a large number of transhumant and sedentary nomadic livestock have substantially degraded the rangeland. Consequently, their fertility has been lowered and so has their productivity. Currently they are producing much below their production potential. This has caused a serious imbalance, particularly in the subtropical zone, between the forage production and livestock forage requirement. The animals are underfed with low body weight, low milk and meat yield and low quality wool. They have low resistance against diseases and climatic harshness causing high mortality.

Due to degradation of these rangelands, their physical and hydrological cycles have been disturbed. The soils, subsequent to removal of their vegetation cover, are diminishing in depth over the hard rock, losing their organic matter and clay content. Due to the decrease in vegetative cover and surface sealing as a result of trampling, surface runoff has increased and infiltration has decreased and so has the soil moisture content, leading to soil erosion and sedimentation.

The alpine and subalpine pastures are predominantly used by transhumant livestock during the summer season. Owing to their gentler topography, better soil moisture regime and dense vegetative cover, they are relatively stable and pose little soil erosion problem.

Urban land

The urban area is defined as “Artificial surface areas and associated areas in the global land cover”. The urban area is less than 1% of the total basin.

Permanent snow and water

The Mangla basin is mainly a rain-fed area but there are some areas in the uplands that are covered by snow for most of the year. The Mangla Reservoir and Wular Lake are the two important water bodies in the basin. They cover around 4% of the total basin.

The land-use and land cover map is given in Figure 3.15 and the area is classified into main groups that have distinct hydrological characteristics. The distribution characteristics of each land-use are discussed in detail in Chapter 6.

Wildlife resources

The migratory birds of the Mangla Dam include 20 species of ducks belonging to four orders, two species of cranes, four species of cormorants, eight species of herons and egrets, three species of storks, one species of flamingos and two species of gallinules. Most of the species are rare and endangered. In addition, two species of global endangered migratory falcons also come and reside in the surroundings of the dam. The endangered and rare species include: bare headed goose, grey-leg goose, ruddy shelduck, gad wall, spot billed duck, white eyed pochard, red crested pochard, great crested grebe, black necked grebe, marbled teal, white headed duck, red shank, green shank, whiskered tern, grey heron, black stork, common crane and demoiselle crane. A list of wildlife sanctuary, game reserves, National Park and lakes with their extent is given in Table 3.2.

Table 3.2: Wildlife sanctuary and reserve of the Mangla basin (MJV, 2003)

Category	**Name**	**Area (km^2)**
Wildlife Sanctuary	Salkhala	8.1
Game Reserve	Ghamot	272.8
	Hilan	4.2
	Moji	38.6
	Mori Said Ali	2.4
	Phala/Kuthnar	3.2
	Qazi Nag	48.3
	Vatala	4.5
National Park	Machiara	135.4
Lakes	Mangla	100.0
	RatiGali	N.A
	Banjosa	N.A

3.4 Soil characteristics of the Mangla basin

The soil data and soil properties used for this study are derived from ISRIC-WISE (Batjes, 2006), a global soil data set with a resolution of 5×5 arc minutes as shown in Figure 3.16. The soil properties such as texture, soil bulk density,

soil available water capacity, soil electric conductivity and soil composition for sand, silt and clay are also available from the data set. There are some data available for soil composition at various gauging stations in the Pakistan part of the basin. There is only a slight difference in the composition compared to global data sets and therefore global data set values were used for this study.

The soil map of the Mangla basin can be classified further into eight groups that have similar soil properties. The properties of these eleven types are described in Table 3.2. As seen from Table 3.2 and Figure 3.16, sandy loam (48%), light clay (24%) and loam (22%) are the dominant soils in this region. The texture of the soil helps to define soil hydrologic groups (A, B, C, and D). In this sense, soils having similar runoff potentials under similar storm conditions are grouped in the same class. Further details for hydrological grouping of soils in SWAT can be found in Neitsch and Arnold (2005).

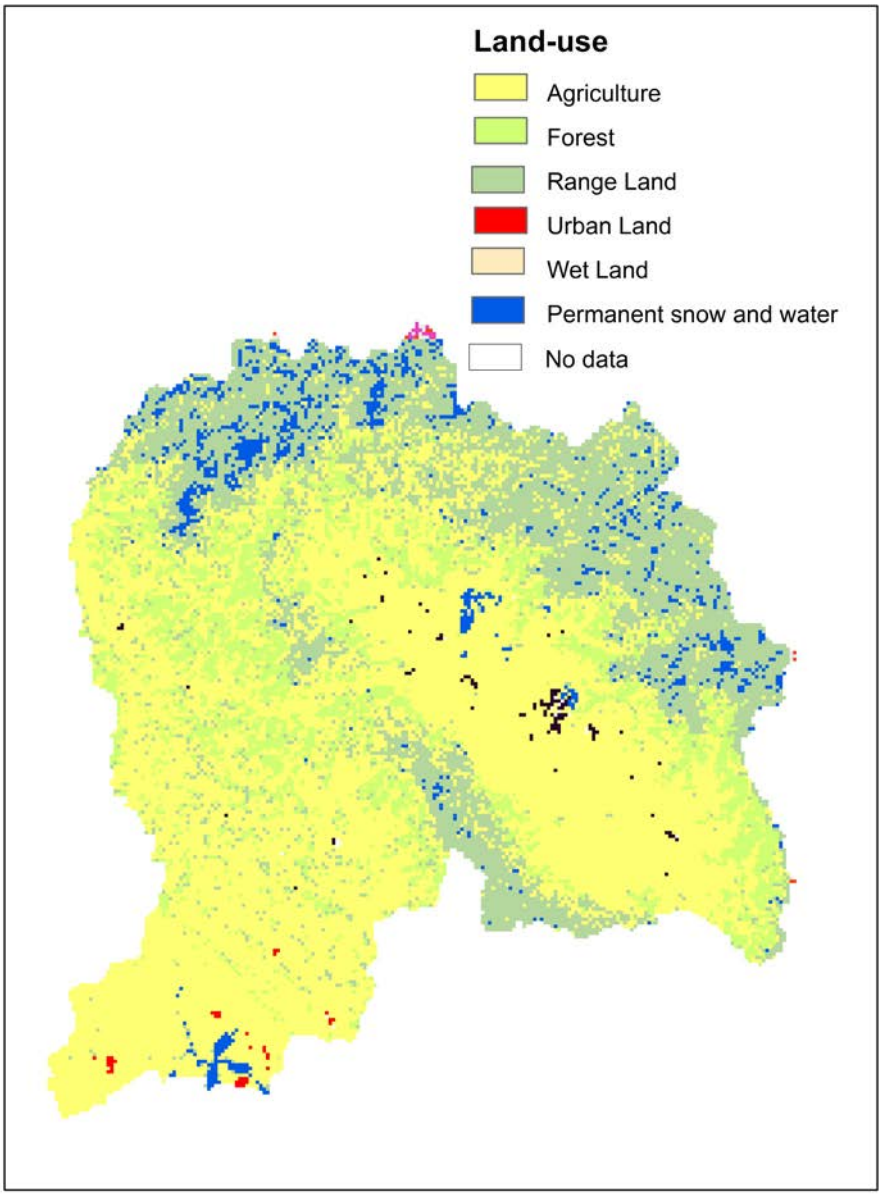

Figure 3.15: Land-use map of the Mangla basin

Table 3.3: Soil properties of the Mangla basin

Soil Type	Percentage of basin area (%)	Texture	Soil bulk density (g/cm^3)	Hydrologic Group	Soil available water capacity (mm/mm)	Hydraulic conductivity (mm/h)	Composition (%)			Soil electric conductivity (ds/m)
							Clay	Silt	Sand	
1	1	Loam	1.39	B	0.02	24	34	23	43	1.73
2	1	Light clay	1.41	B	0.02	29	22	36	42	0.10
3	24	Light clay	1.24	C	0.05	7.8	48	30	22	1.40
4	1	Clay loam	1.40	B	0.05	40	22	36	42	1.40
5	22	Loam	1.39	C	0.07	34	23	36	41	0.10
6	48	Sandy loam	1.40	C	0.15	40	22	36	42	0.41
7	2	Loam sandy	1.39	D	0.01	35	23	34	43	1.40
8	1	NA[1]	NA	NA	NA	NA	NA	NA	NA	NA

[1]No data available.

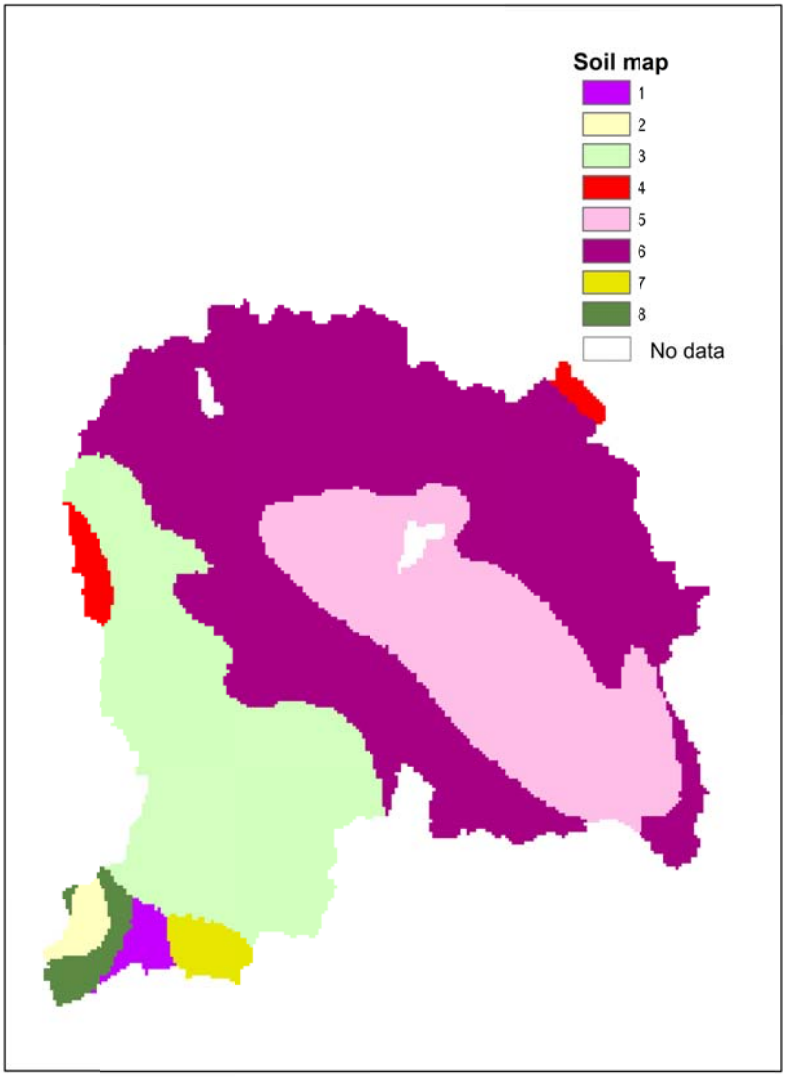

Figure 3.16: Soil type map of the Mangla basin (detail attributes of each soil types are listed in Table 3.2)

3.5 Water budget of the Mangla basin

There is great variation in runoff due to the difference in topographic conditions and rainfall pattern. The Jhelum River has an average annual discharge between 300 and 330 m^3/s at Chinari and Domel gauging stations above the Neelum confluence; 328 m^3/s at Muzzafarabad, and 828 m^3/s at Kohala, based on the record from 1990 to 2009 (Figure 3.17). The contribution of Poonch and Kanshi tributaries are negligible compared to Jhelum. The other two tributaries, Neelum

and Jhelum (upper and lower), produce a large portion of the runoff in spring to summer seasons (Figure 3.18).

The variation in discharge during spring in the basin is greater than in the monsoon season. This is due to the fact that Kunhar and Naran tributaries are fed by snow melt, whereas Jhelum River is mostly rainfed. The Kanshi and Poonch tributaries receive high flows from monsoon rainfall rather than snow melt. The seasonal variation of discharge of Jhelum River (Upper and lower), Neelum River, Kunhar River, Kanshi River and Poonch River is shown in Figure 3.19.

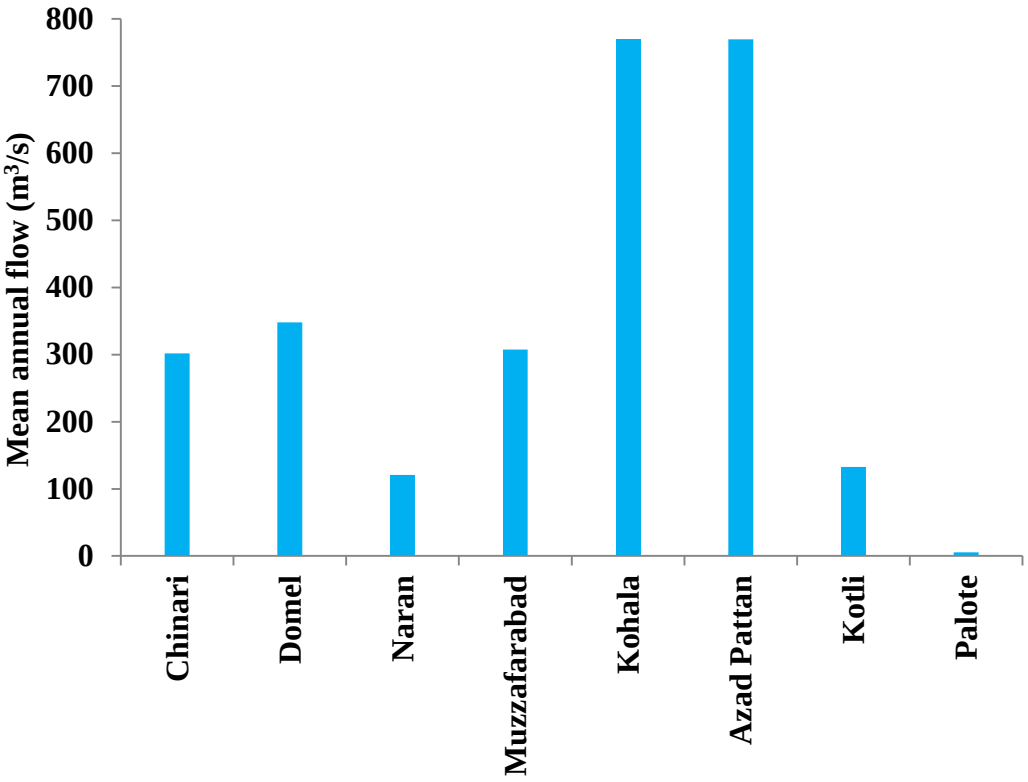

Figure 3.17: Mean annual flow at the Mangla basin flow gauging stations

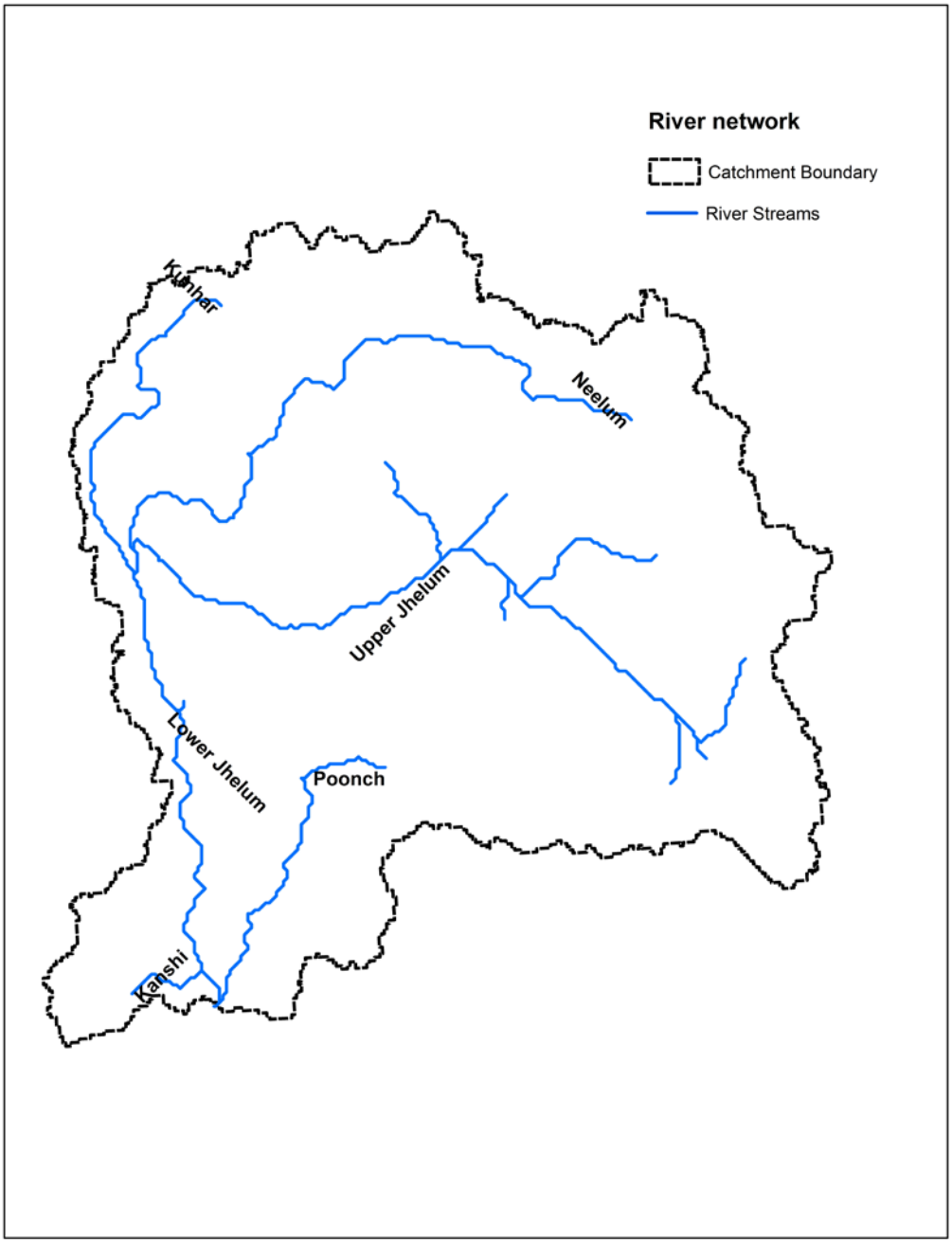

Figure 3.18: River network in the Mangla basin

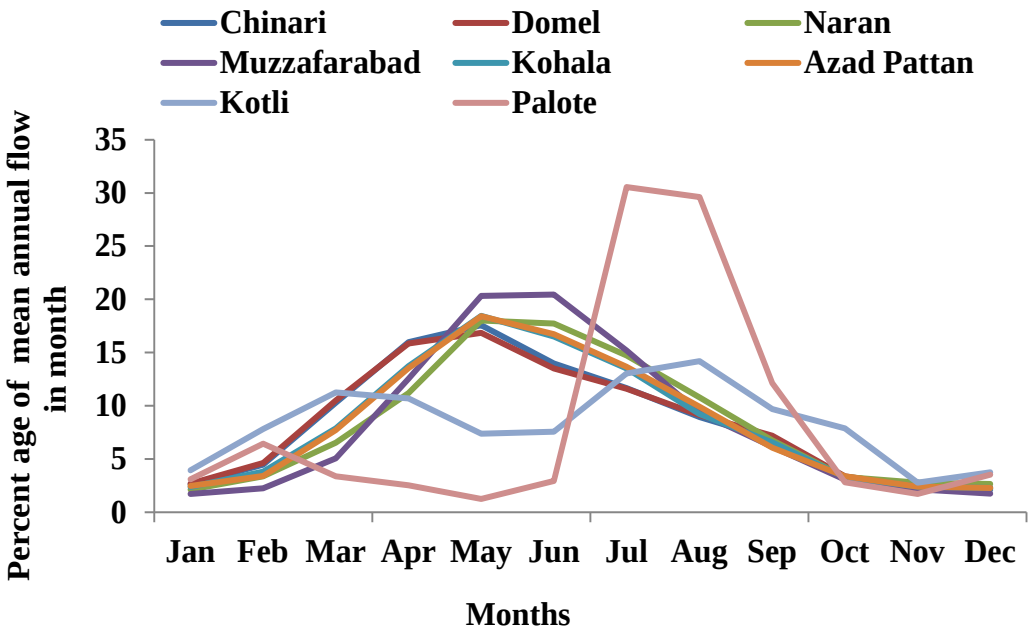

Figure 3.19: Mean monthly flows in percentage of annual flows at the flow gauging stations in the Mangla basin

3.6 Sediment characteristics

Most of the sediment load is produced from the geological erosion and seismic activity in the area. Landslides occur almost all the time along the Jhelum River. It is believed that the landslide activity in the region has enhanced after the 2005 earthquake (KHPP, 2008). The other sources of sediment are sheet erosion by rain and gully erosion. An important factor contributing to the soil erosion is land-use change such as deforestation, cattle grazing and road construction (KHPP, 2008). The sediment discharge data at Chinari, Hattian Bala, Domel, Chattar Kallas, Kohala, Naran and Azad Pattan stream gauging stations were collected from the SWHP, WAPDA. Table 3.4 lists the basin areas, available record of suspended sediment and average suspended sediment per year.

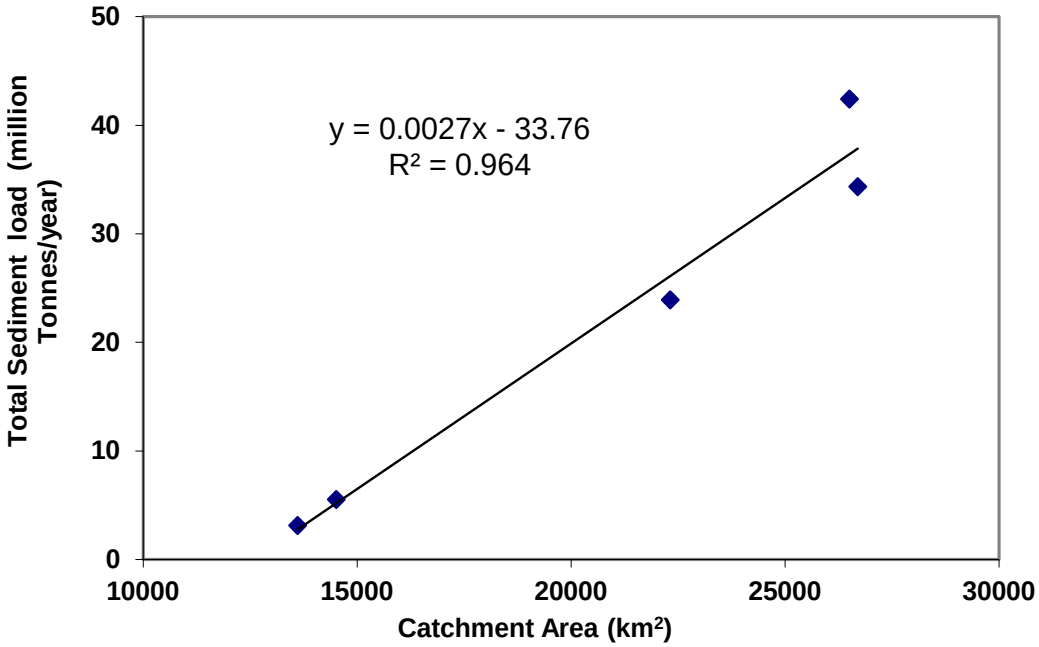

Figure 3.20: Total sediment load for the Jhelum River as a function of distance

Figure 3.20 depicts the suspended sediment load characteristics of the Jhelum River as a function of the basin area. The specific suspended sediment load increases linearly with the increase in basin area from Chinari to Karot.(SWHP,2005)

Specific suspended sediment yields of various gauging stations are shown in Figure 3.21 for Chinari, Domel, Kohala and Chattar Kallas, whereas the percentages of sand, silt and clay in suspension at the various stream gauging stations are shown in Figure 3.22.

No information is available on the specific suspended sediment yields in the Indian Kashmir, particularly upstream and downstream of the Wular Lake to estimate the sediment deposition rate in the lake. Wular Lake has reduced a lot of sediment loads to its downstream due to the sediment trapping ability of a large lake.

Table 3.4: Sediment gauging station characteristics of the Mangla basin

Sediment gauging station	**Sediment gauging Status**	**Basin area (km^2)**	**Data availability period**	**Mean annual suspended sediment (M tonnes)**
Chinari @ Jhelum	Closed	13,609	1970–1995	2.50
Hattian Bala @ Jhelum	Operating	13,792	1997–2005	1.95
Domel @ Jhelum	Operating	14,516	1980–2005	3.91
Chattar Klass @ Jhelum	Operating	24,790	1997–2005	12.54
Kohala @ Jhelum	Closed	24,890	1965–1995	19.32
Azad Pattan @ Jhelum	Operating	26,507	1979–2005	34.02
Karot @ Jhelum	Closed	26,699	1970–1979	–
Muzaffarabad @ Neelum	Operating	7,284	1963–2005	7.12
Garhi Habib Ullah @ Jhelum Kunhar	Operating	2,385	1960–2005	3.19

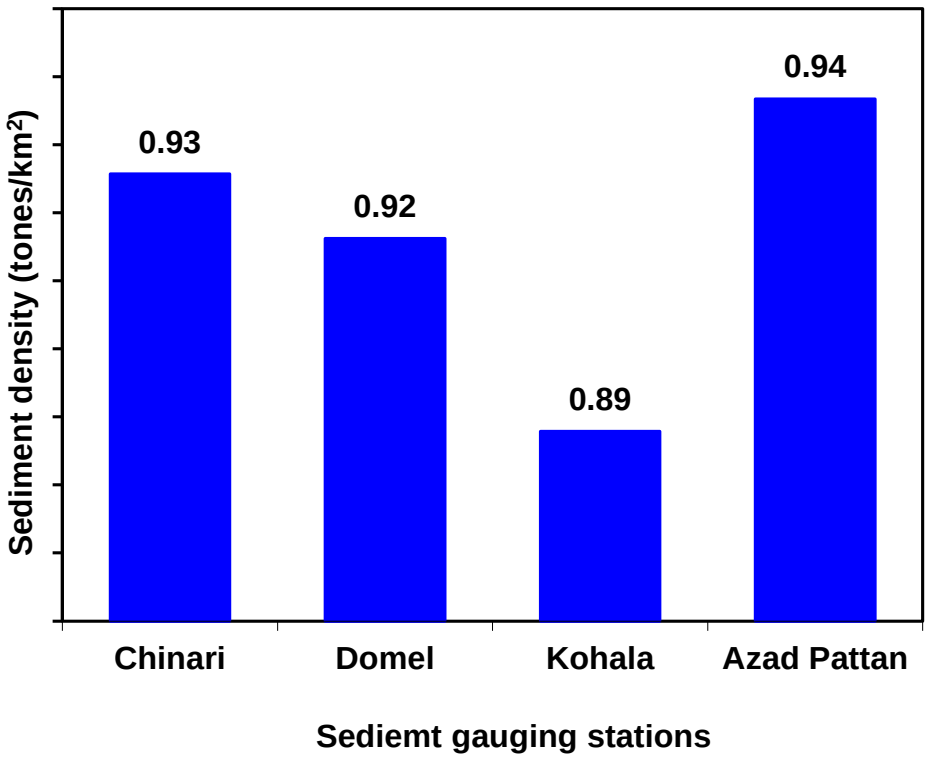

Figure 3.21 : Specific suspended sediment yields per annum at stream gauging stations

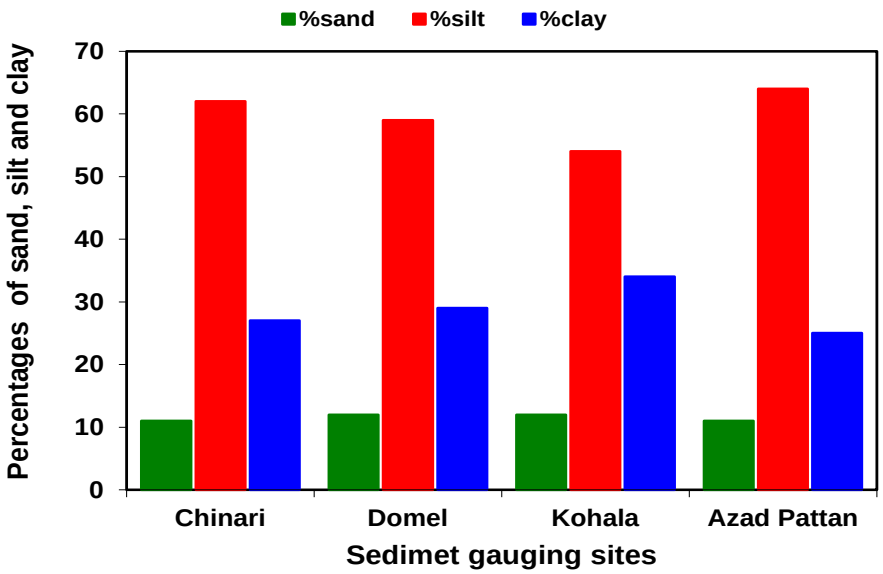

Figure 3.22: Percentages of sand, silt and clays per annum at various gauging stations

CHAPTER FOUR
HYDROLOGICAL AND SEDIMENT MODELLING IN THE STUDY AREA

This chapter describes the details of the Hydro/Sediment Routing-Climatic (HSRC) module of the integrated framework. Firstly, the input data is discussed, and then outputs (flow and sediment discharge) that are obtained from the model after calibration and validation. Finally, the impact of extreme rainfall events on sediment load is discussed.

4.1 Hydrological and sedimentation model

The SWAT (Soil and Water Assessment Tool) is a river basin model primarily developed to quantify the impact of land management practice in large, complex basins (Bosch et al., 2004). The model can be classified as semi-distributed as it divides the basin into sub-basins, which in turn are divided into Hydrologic Response Units (HRUs), while the distributed model can be described as a "physical based model for the simulation of the different process of the land phase in the hydrological cycle" (El−Nasr et al., 2005). It requires hydrological details at several spatial levels: basin, sub-basin, and the Hydrologic Response Unit (HRU). For example, climate data are defined at sub-basin level, with the same data applied for every HRU inside a sub-basin. Soil and management data are processed for each HRU, whereas snow melt temperature or the flow routing method is defined for the whole basin. The input data required for the development of the model includes topographic data, land-use types, soil and climate (rainfall, temperature, relative humidity, wind speed and solar radiation or sunshine hours). The main data sources for this study are from Pakistan Meteorological Department, Surface Water Hydrology Project (SWHP) of the

Water and Power Development Authority Pakistan, Soil Survey of Pakistan, and global data publically available.

4.1.1 Digital elevation model (DEM) of the study area

The topography is defined by the Digital Elevation Model (DEM) that describes the elevation of a given area at a specific spatial resolution. The DEM for the Mangla basin is derived from the USGS database (http://edcdaac.usgs.gov/gtopo30/hydro1k) with consistent coverage of 1 km resolution (Figure 4.1).

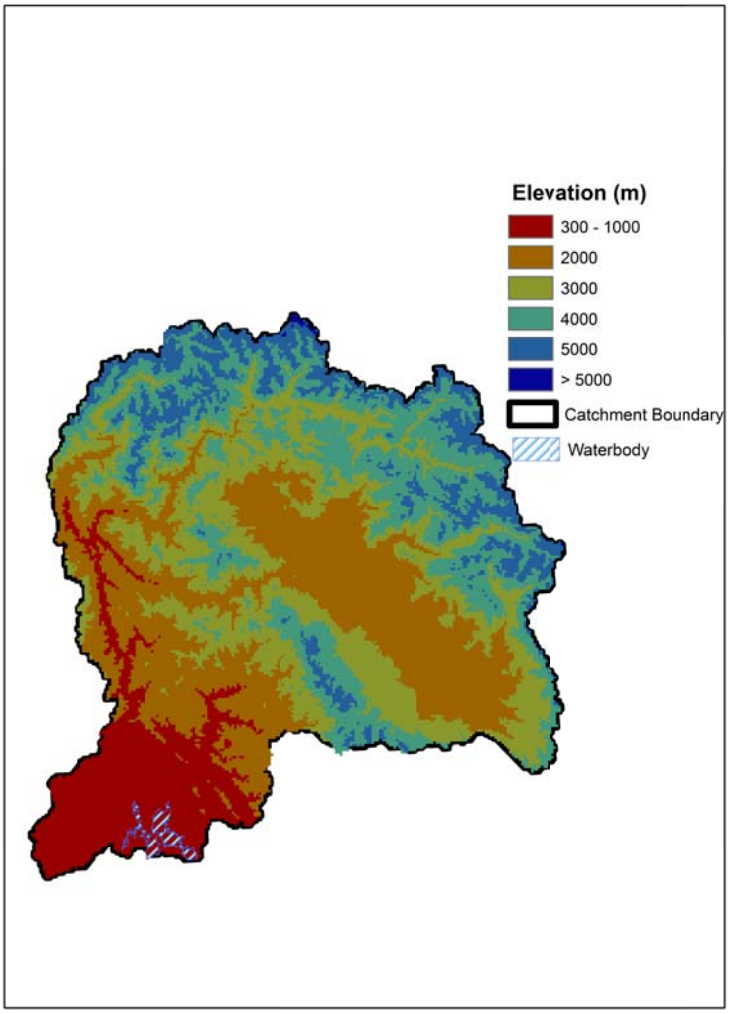

Figure 4.1: Digital Elevation Model (DEM) of the Mangla basin

4.1.2 Digital Stream Network

Stream network in the SWAT model is used to define location of the streams. The locations of the streams in the basin are defined by simply digitizing the digital elevation model (DEM).

4.1.3 Climate data

Climate data is needed by the SWAT model to simulate the hydrological process. The data required for this study was collected for seven stations within and around the study area: Astore, Domel, Naran, Palandari, Kotlti, Rehman Bridge and Mangla (Figure 3.2). The data consist of rainfall, maximum and minimum temperature, relative humidity, sunshine hours and wind speed. The data are in daily time series. A description of the data is shown in Table 4.1.

Table 4.1 Meteorological data collected for the study area

Station	**Lat (°)**	**Long (°)**	**Observation period**				
			Rainfall	**Tempera-ture**	**Relative Humidity**	**Evapora-tion**	**Wind Velocity**
Astore	35.2	74.54	1990–2009	1990–2009	No data	No data	No data
Domel	34.38	73.49	1990–2009	1990–2009	1970–2009	1970–2009	1970–2009
Naran	34.9	73.64	1990–2009	1990–2009	No data	No data	No data
Palandari	33.72	73.69	1990–2009	1990–2009	No data	No data	No data
Kotli	33.49	73.88	1990–2009	1990–2009	No data	No data	No data
Rehman Bridge	33.48	73.88	1990–2009	No data	No data	No data	No data
Mangla	33.12	73.63	1990–2009	1990–2009	No data	No data	No data

The rainfall and temperature (maximum and minimum) data are available for almost all gauging stations, but relative humidity, evaporation, wind speed, solar radiation and sunshine hour data are only available for Domel. The SWAT model has a built-in weather generator to generate climate data for the whole basin using time series data of a single gauging station, which was used by School and Abbaspour (2006) in an application of SWAT for West Africa. The 19 years of data from Domel station from 1990 to 2009 was used to parameterise the weather generator in SWAT to fill the missing data for other stations.

4.1.4 Soil and land-use maps

Land-use and soil data are used in SWAT to determine the topographic features and hydrological parameters for each land and soil category. The soil and land-use data can be either in grid or polygon (shape) format. In this study, the land-use map was generated from global land cover data (http://www.esa.int/due/ionia/globcover) at 300 m grid resolution.

4.1.5 Hydrological and sediment data

Hydrological data are required for performing sensitivity analyses, calibration and validation of the SWAT model. Flow and sediment data is maintained by and was collected from the Surface Water Hydrology Project (SWHP), Water & Power Development Authority Pakistan. The data included the discharge at Chinari, HattianBala, Domel and Kohala for Jhelum River; Naran for Kunhar River; Muzzafarabd for Neelum River; Palote for Kanshi River and near Kotli for Poonch River (Figure 3.2). The data are available on a daily scale from 1990 to 2009. The suspended sediment data are also processed by the same agency but recorded fortnightly. SWHP computes the annual total sediment based on the

rating curves from gauging stations. The sediment data (fortnight sediment discharge) and annual sediment deposited were also obtained from SWHP from 1990 to 2005. More detail of the data is shown in Table 4.2.

Table 4.2: Hydrological data collected for the study area

Gauging Station	Name of River	Latitude	longitude	Data collected (Years)
Chinari	Upper Jhelum	34.17	73.75	1970–1996
HattianBala	Upper Jhelum	34.16	73.74	1997–2009
Domel	Upper Jhelum	34.37	73.47	1976–2009
Muzaffarabad	Neelum	34.37	73.47	1990–2009
Naran	Kunhar	34.91	73.65	1990–2009
Kohala	Lower Jhelum	34.21	73.50	1990–2009
Palote	Lower Jhelum	33.22	73.43	1990–2009
Kotli	Punch	33.47	73.88	1990–2009

4.2 Data processing

The quality of the input data has a large impact on the performance of the model. Therefore it is essential to check the outliers and consistency in the input data. In this study, climate data (rainfall, temperature, wind speed and relative humidity) and flow data were checked for outliers and consistency or homogeneity based on Smirnov-Kolmogorov (S-K) Test (Ang, 1990) and double mass curve analysis (Adeloye and Montaseri, 2002). The S-K test was applied for sub-basin 1 (Chinari and Domel stations). The monthly data were divided into two parts, i.e., 1980 to 1989 and 1990 to 2005. The cumulative density function results show consistency between the two data series (Figure 4.2). Double mass curves were developed for Chinari, Domel, Naran, Muzzafarabad, Azad Pattan, Kotli and Palote on mean

monthly flows from 1990 to 2009 (Figure 4.3). The results indicate that all the series are consistent, since curves are sufficiently smooth in the presentation of the monthly accumulation of the flows for long-term observations. Furthermore, Chinari flow data are compared with the downstream gauging station of Domel. There is no break in the slope of the straight line indicating that flow measured at Domel is consistent with Chinari (Figure 4.4).

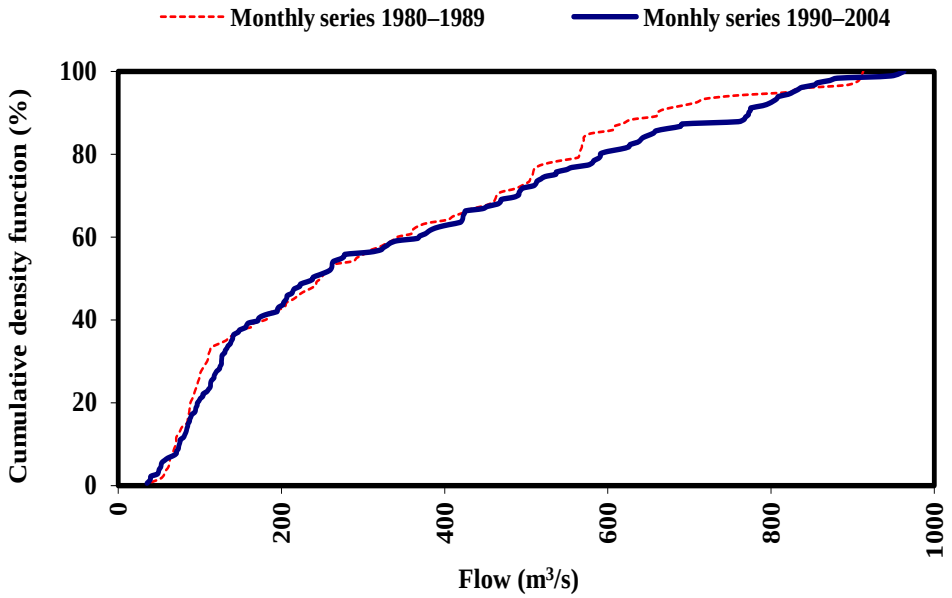

Figure 4.2: Cumulative density function of flow data of Domel gauging station for 1980–1989 and 1990–2005

4.3 SWAT model setup

The SWAT version 2009 was used in this study and ArcSWAT 2009 was used to build the model for the study area. ArcSWAT is the version of the SWAT model built in ArcGIS (Winchell et al., 2010). All the spatial analysis functions required by SWAT are carried out by ArcGIS such as delineation of basin and sub-basins and calculation of the Hydrological Response Units (HRU).

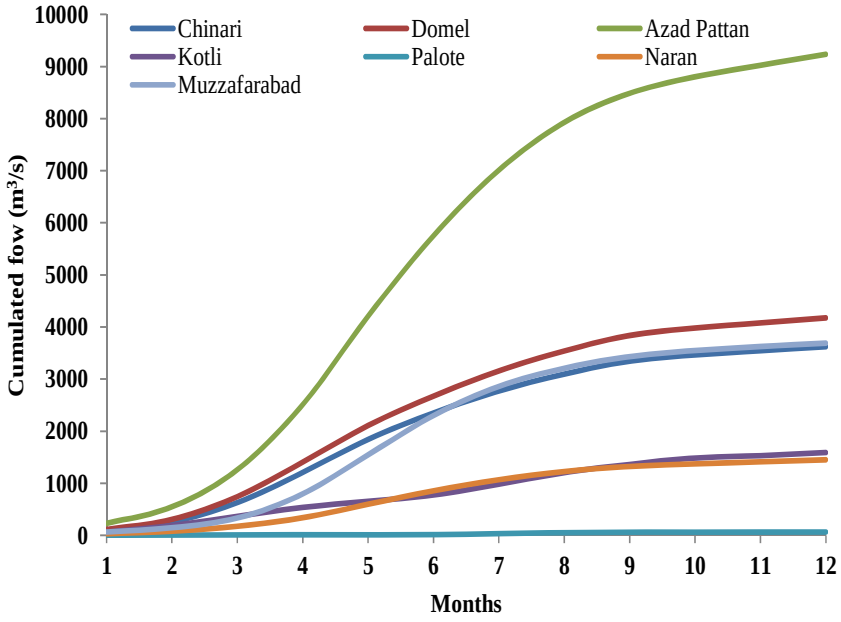

Figure 4.3: Accumulated flows for various flow gauging stations of the Mangla basin from 1990 –2009

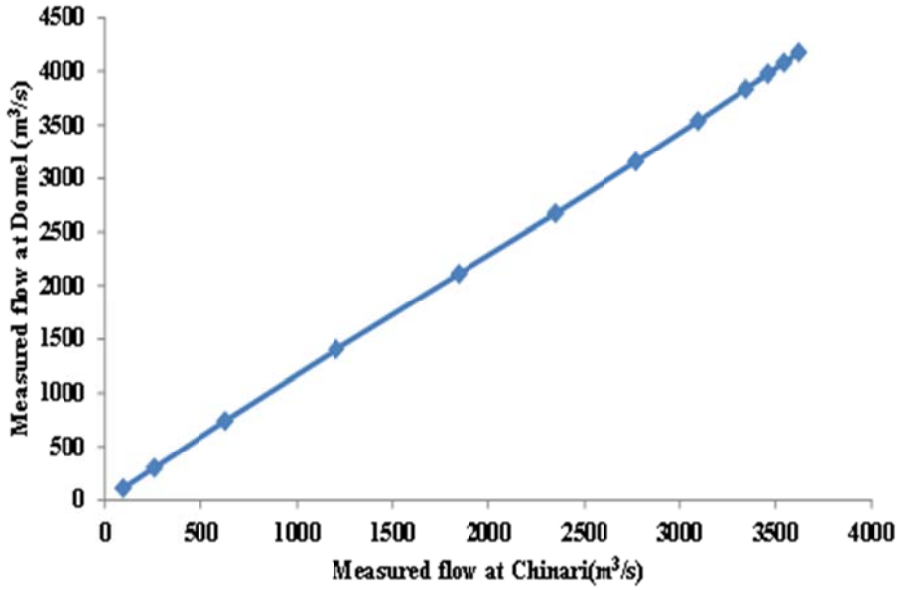

Figure 4.4: Double mass curve for Chinari (upstream) and Domel (downstream) flow gauging stations from 1990–2005

4.3.1 Basin delineation

ArcSWAT uses DEM data to delineate basin and sub-basins. This involves the analysis of the DEM to provide topographic information of a basin and create sub-basins on the basis of the flow directions and flow accumulations. In this study, this is done using manual delineation procedures within the model. Manual delineation provides the flexibility to edit sub-basin shapes and outlets.

4.3.2 DEM setup

The first step of the basin delineation is the DEM set up. Firstly DEM is required to be in proper projection. For this study, Lambert Conformal Conic projection was selected. A mask of the Mangla basin was created to set the boundaries of the basin. SWAT processes the mask section of the DEM to delineate the basin into sub-basins. Stream network of the Mangla basin is utilized in the delineation process as it improves sub-basin delineation and hydrological segmentation. Finally, false sinks are removed in the processed basin data as they may cause inaccurate flow direction rasters. Filling false sinks is very important for successful hydrological analysis and generating correct geographical and flow-related information.

4.3.3 Stream definition

For large hydrological basins like the Mangla basin, the stream definition is defined using available climate data, size of the basin and the objectives of the study. The Mangla basin is a trans-boundary basin, with more than half of its area lying in India. It is very difficult to obtain climate data from India as there is no treaty between Pakistan and India to share climatic and hydrological information.

Personal communications were used to obtain the climatic data for the Indian part. Unfortunately only data for Srinagr gauging station (Figure 3.2) was available. Considering the limitation of the climatic data and the objectives of the study, the whole basin was divided into six sub-basins, and the sediment load from each sub-basin computed to simulate the total sediment at the outlet of the basin (i.e., the Mangla Dam).

The purpose of the study was to assess climate change impact on the total sediment of the Mangla Dam. First, the information of sediment concentration from each sub-basin was required. The river discharge data was available for Jhelum River tributaries, i.e. Domel/Chinari for Upper Jhelum River, Muzaffarabad for NeelumRiver, Kotli and Palote for Poonch River, and thus it was more appropriate to delineate the basin on these points for the purpose of model calibration and validation. Therefore, the sub-basin delineation was done on the basis of the river tributary, i.e., Upper Jhelum basin, Neelum River basin, Kunhar River basin, Kanshi and Palote sub-basins (Figure 4.5).

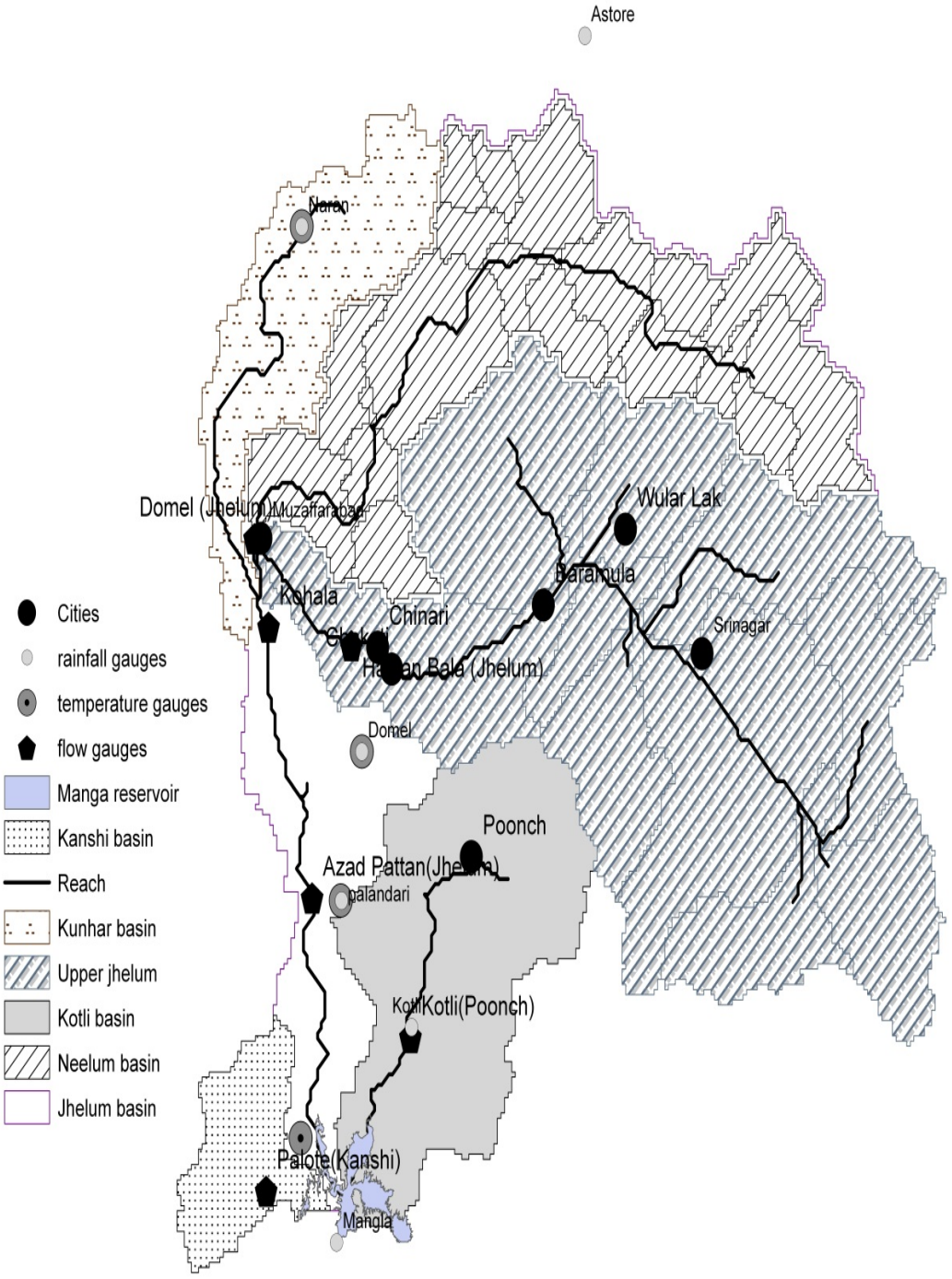

Figure 4.5: River basins of the Mangla basin

4.3.4 Outlet and inlet definition

The outlet definition in the basin determines the total number of sub-basins in the drainage network. For the present study six outlet points based on individual sub-basins (Upper Jhelum, Kunhar, Neelum, Poonch, Kanshi and Mangla sub-basins) were selected as shown in Figure 4.5. The catchment area of these sub-basins is 13885 km^2, 9245 km^2, 4454 km^2, 2039 km^2, 4192 km^2 and 4642 km^2, respectively.

4.3.5 Land-use and Soil data

Land-use and soil properties affect runoff, evapotranspiration and surface erosion. They are used by distributed hydrological models to determine the area and model parameters according to the land-use type and soil category for each sub-basin. For this study, land-use is reclassified based on the specific land cover types and the respective crop parameter according to SWAT database. A look up table for different categories of land cover/land-use is prepared to relate each grid value to SWAT land cover/land-use class. The different land-use types and their coverage are listed in Table 4.3.

The SWAT model requires soil textural and other soil physical/chemical properties such as available water content, hydraulic conductivity, bulk density and organic carbon content for different layers of soil. The study area was divided into nine soil groups. Physical soil properties, i.e., soil moisture content, bulk density and saturated hydraulic conductivity were calculated for the top two layers each 10 cm in depth. The properties of each soil are shown in Table 3.2, Chapter 3

Table 4.3: Description of land cover data

Land-use Type	Area (km^2)	Percentage of basin area (%)
Agricultural Land-Close-grown	7410	19.27
Agricultural Land-Row Crops	7414	19.28
Agricultural Land-Generic	6668	17.34
Forest-Evergreen	138	0.36
Forest-Deciduous	3896	10.13
Forest-Mixed	1527	3.97
Range-Grasses	7737	20.12
Wetland	4	0.01
Residential-Medium Density	23	0.06
Range-Brush	2134	5.55
Water	1507	3.92

4.3.6 Hydrologic Response Unit (HRU) analysis

SWAT further divides the sub-basin into Hydrologic Response Units (HRUs). Each HRU has the same land cover, soil group and slope. SWAT computes runoff and other hydrological outputs independently for each HRU and routes the runoff and sediment for the whole basin. The erosion and sediment for each HRU is estimated based on the Modified Universal Soil Loss Equation (MUSLE). It firstly computes the amount of runoff then uses the runoff to simulate erosion and sediment runoff for each HRU (SWAT, 2000), with runoff as the driving force in generating sediment. The splitting of sub-basins into smaller parts provides a better description of the water balance of the basin and enhances the model efficiency for flow and sediment calculation.

The HRU distribution is determined by the HRU definition. In the HRU definition, a threshold percentage to the sub-basin area was used to eliminate

HRU classification for small areas. Land-uses, soils or slope classes which have less than the threshold are ignored in the HRU classification. The threshold value defines the amount of detail required. For this study, the aim was to predict the impact of climate and land-use changes on the sediment generation, and therefore it was appropriate to obtain the maximum detail of land-use classes at a sub-basin level. Hence, no threshold values were assigned for the land-use, soil classes or slope in order to encompass maximum spatial details. The whole basin was divided into 174 HRUs based on land-use, soil and slope categories.

4.3.7 Importing climate data

SWAT calculates moisture and energy, which control the water balance. The climatic variables used for the calculation were rainfall, temperature, relative humidity, wind speed and solar radiation. Daily rainfall data from 1990–2009 for Astore, Naran, Domel, Palandari, Mangla and Kotli were incorporated in the SWAT model, while daily maximum and minimum temperature data from 1990–2009 for Naran, Domel, Palandari and Mangla were used. The weather generator in SWAT was used to fill data gaps, particularly solar radiation and wind, since the consistent daily record of sunshine hours and wind speed was not available. The parameterization of the weather generator was based on a 40 year (1970-2009) monthly record from Domel station.

4.4 Sensitivity analysis

Sensitivity analysis was carried out for sub-basins 1, 5 and 6. The total number of 25 SWAT parameters, which are important for hydrological and sediment modelling, was selected to analyse their relative sensitivity to the model result. Table 4.4 lists the 19 parameters that were the most sensible for the model result.

Table 4.4: Sensitivity rank of the SWAT parameters for sub-basins

Rank	Parameter	Symbol
1	Soil moisture curve number	CN2
2	Threshold water level in shallow aquifer for base flow	GWQMN
3	Base flow recession flow	ALPHA_BF
4	Soil evaporation compensation factor	ESCO
5	Surface runoff lag coefficient	SURLAG
6	Deep aquifer percolation fraction	RCHRG_DP
7	Channel curve number	CH_N2
8	Slope of the channel	SLOPE
9	Maximum canopy storage	CANMX
10	Moist soil albedo	SOL ALB
11	Snow fall temperature	SMTMP
12	Snow pack temperature for lag factor	TIMP
13	Snow melt base temperature	SMTMP
14	Soil erodibility factor	USLE_K
15	Soil available water capacity	SOL_AWC
16	Support practice factor	USLE_P
17	Manning "n" for overland flow	OV_N
18	Maximum rooting depth of soil profile	SOL Z
19	Saturated hydraulic conductivity	SOL_K

The surface flow parameter, CN2, was the most sensitive parameter for all sub-basins, since the SWAT uses the US Soil Conservation services approach (SCS curve number) methodologoy for flow calculations. For sub-basin 1, base flow parameters such as GWQMN and ALPHA_BF also showed high sensitivity similar to CN2. Also, the parameter SOL_AWC was sensitive for sub-basin 1. The high sensitivity of GWQMN and ALPHA_BF and SOL_AWC demonstrates that groundwater plays an important role in contributing flow for sub-basin 1. The slope parameter (SLOPE) shows high sensitivity for sub-basin 6, indicating that the sub-basin is characterized by variations in the topographic conditions. The range of final optimum parameters is shown in Table 4.5.

Table 4.5 Final parameter values of the sensitivity results

Parameter	Description and unit	Initial Range	Final parameter value for outlet location		
			Sub-basin 1	Sub-basin 5	Sub-basin 6
CN2	SCS curve number for moisture condition II	35-98	44-90	36-83	45-84
GWQMN	Depth of water in shallow aquifer for base flow (mm)	0-5000	11-475	0	33-450
ALPHA_BF	Base flow alpha factor (days)	0-1	0.02-1	0.1-0.80	0.43-1
ESCO	Soil evaporation compensation factor	0-1	0-0.90	0-0.80	0.4-0.9
RCHRG_DP	Deep aquifer percolation fraction	0-1	15-25	0.05	0.15
SOL_Z	Depth from soil surface to bottom layer (mm)	0-3000	1200	1260-1625	1300
SOL_AWC	Available water capacity of the soil layer	0-1	0.04-0.95	0.1-0.3	0.1-0.3
GW_REVAP	Groundwater revap coefficient	0.02-0.2	0.04-0.19	0.02	0.18
CH_N2	Channel Manning's coefficient	0.01-0.3	0.024	0.024	0.016
CH_K2	Effective hydraulic conductivity of the channel alluvium	0-150	9	15	6.26

4.5 Calibration and validation of the model for flows

After the sensitivity analysis of the parameters, an initial model run was performed. The observed and simulated flows were compared for sub-basins 1, 5, and 6. Model calibration was done manually because it was easier than the auto-calibration method to check the physical meaning of the parameter based on expert judgment before accepting the results. CN2 was 79 for sub-basin 5 and 92 for sub-basin 6. The smallest value of CN2 78 was for sub-basin 1, which can be associated with soil properties such as high permeability or high percentage of sand in the soil. The high value of CN2 in sub-basin 6 may be due to intensive

agriculture in that sub-basin and may also be associated with more clay in the soil with low infiltration rate. This could reduce the amount of infiltration and thus more surface runoff. The soil attributes of bulk density, soil available water capacity, hydraulic conductivity, texture (content of clay, silt, sand) and soil electric conductivity were extracted from global data sets and adjusted according to the local conditions without calibration. For example, Sol_AWC, the hydraulic conductivity was set to 0.09 for sub-basin 1 because of the high amount of fine grained (clay-loam) soils in this sub-basin, while for sub-basins 5 and 6 they were set to 0.015 and 0.05, respectively.

The soil evaporation compensation factor, ESCO, controls the depth distribution of the soil water to meet the soil evaporation requirement. The evaporative demand not met by the soil layer will result in a reduction in actual evapotranspiration for the HRU (Neitsch and Arnold, 2005). At basin level, it was reduced from the SWAT default value of 0.95 to 0.75 to increase the amount of evapotranspiration that was very likely for semi-humid regions such as the Mangla basin.

ALPHA_BF defines the groundwater contribution to the surface flow. A high value was obtained for sub-basin 1, showing that there is high groundwater contribution in this sub-basin. The Mangla basin is mostly a rainfed basin, however, there is significant contribution of snow melt for sub-basin 1. ALPHA_BF also reflects groundwater flow response to changes in recharge. It is directly related to the groundwater recession constant (days). Similarly GWQMN is related to base flow generation for the shallow aquifer.

The performance of the model was evaluated for upstream and downstream of the Mangla basin according to a statistical evaluation of the simulated results, graphical representation of hydrographs at different outlets of the basin, water balance of the whole basin and finally representation of sediment at different outlets and the main Mangla basin outlet.

Firstly, the water balance of the whole basin was calculated from 1993–2002. The results show that the model simulated the annual water balance well with the observations, with an annual mean difference of only 17.76 mm, less than 1.5% (Table 4.6). The slight difference in the water balance may be due to model error, but may be also associated with soil water. The evapotranspiration calculated by the model was about 51% of the annual rainfall.

Table 4.6 Annual water balance of the basin from 1993- 2002

Water component	Amount (mm)	
	Observed	Computed
Precipitation	1356	
Evapotranspiration		693
Surface runoff		475
Lateral flow		7
Ground water recharge		164
Total	1356	1338

In addition to the water balance, the model performance was evaluated with other statistical indices of coefficients of determination (R^2) and the Nash Sutcliffe efficiency (E_{NS}) as a measure of fitness of model prediction. The coefficient of determination (R^2) is the square of the Pearson's product-moment correlation coefficient. It means that there is a linear relationship between observed and predicted values, its value ranges from 0 to 1 describing the agreement of the observed and predicted values (Equation 4.1), while the Nash Sutcliffe efficiency

(E_{NS}) defines the coefficient of efficiency which ranges from minus infinity to 1 with higher values indicating better agreement. Physically, E_{NS} is the ratio of the mean square error to the variance in the observed data subtracted from the variance as shown in Equation 4.2 (Legates and McCabe Jr, 1999). This indicates how well the plot of observed versus the simulated value fits the 1:1 line. If the measured value is the same as all predictions, E_{NS} is 1. If the E_{NS} is between 0 and 1, it indicates deviations between measured and predicted values. If E_{NS} is negative, predictions are poor, and the average value of output is a better estimate than the model prediction (Nash and Sutcliffe, 1970). The coefficient of determination (R^2) evaluates the linear relationship between the variables so it is insensitive to additive and proportional differences between the model simulation and observed values, while the Nash Sutcliffe efficiency (E_{NS}) is also sensitive to differences in the observed and simulated means and variables. These indicators have been widely used to evaluate the performance of the hydrological and climate change assessment studies (Pandey et al., 2008; Steenhuis et al., 2009).

$$R^2 = \frac{\left(\sum_i^n (O_i - O_{av})(P_i - P_{av})\right)^2}{\sum_i^n (O_i - O_{av})^2 (P_i - P_{av})^2} \quad 4.1$$

$$E_{NS} = \frac{\sum_i^n (O_i - O_{av})^2 - \sum_i^n (P_i - O_{av})^2}{\sum_i^n (O_i - O_{av})^2} \quad 4.2$$

where R^2 is Coefficient of determination, n is the total number of observations in the data set, O_i is the observed value at each point and P_i is the predicted value at each point.

The model is validated for sub-basins 1, 5 and 6. Sub-basin 1 is the largest one, which covers about 53% of the basin. The calibration and validation of the model

was done by accumulating the daily modelled result to monthly values and comparing the accumulated monthly result to observed monthly data. The year 1996 was selected for sub-basin 1 as the calibration period.

The performance of the calibration is shown in Figure 4.6. The model simulates the flows very well. The Coefficient of determination (R^2) for the simulated flows was 0.90 and the Nash Sutcliffe Coefficient (E_{NS}) was 0.75.

The model was validated by accumulating the daily simulated result to monthly values and compared with observed monthly flow of 1990–2009 for sub-basin 1 (Figure 4.7). Validation was only performed on a monthly basis because the primary purpose of the model was to compute the sediment budget of the whole basin and the monthly time-step was already sufficient. The validation reveals that the model efficiently simulated the monthly flows for sub-basin 1 (upper Jhelum), although the early spring flows were not modelled as efficiently as the monsoon months, which may be due to the complexity of snow melt effect and the limited number of precipitation gauge stations at higher altitudes for model variables (Figure 4.8). For sub-basins 5 and 6, the results show that SWAT simulated flows very well, especially for monsoon months. The results are presented in Figure 4.9 to Figure 4.12 and statistical indices are shown in Table 4.7.

Table 4.7: Statistics analysis for the validation period

Sub-basins	Coefficient of determination ($R^{2)}$	Nash Sutcliffe coefficient (E_{NS})	Error in mean monthly flow (m^3/s)
Sub-basin 1	0.81	0.78	0.1
Sub-basin 5	0.84	0.81	0.24
Sub-basin 6	0.62	0.60	0.35

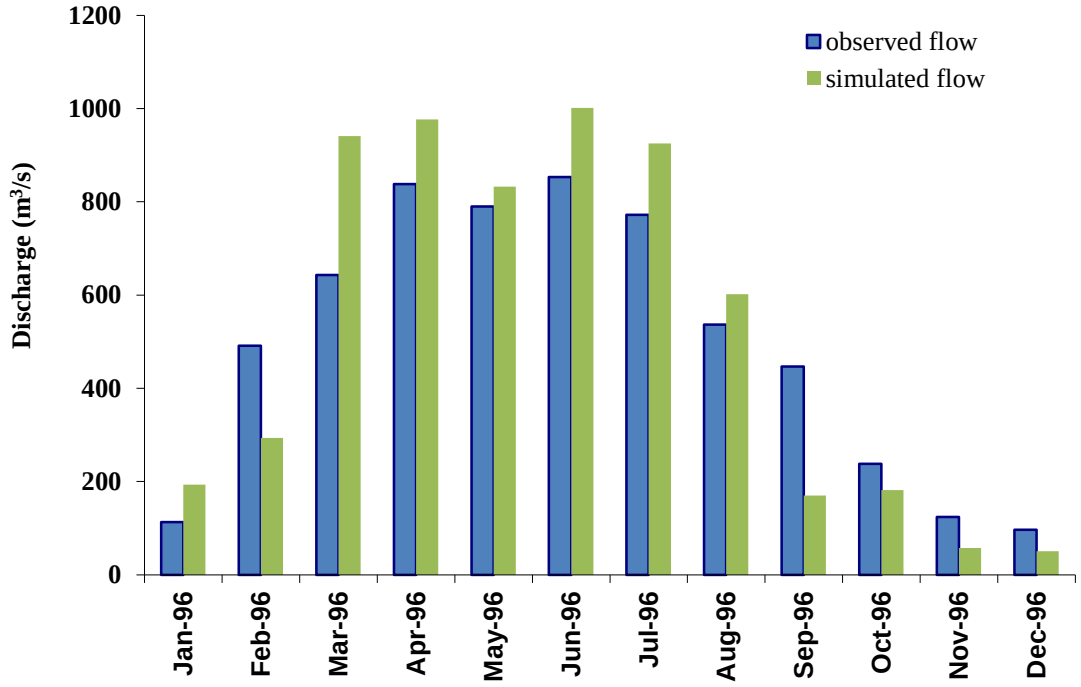

Figure 4.6: Observed and calibrated discharge for sub-basin 1 for 1996 at accumulated monthly basis

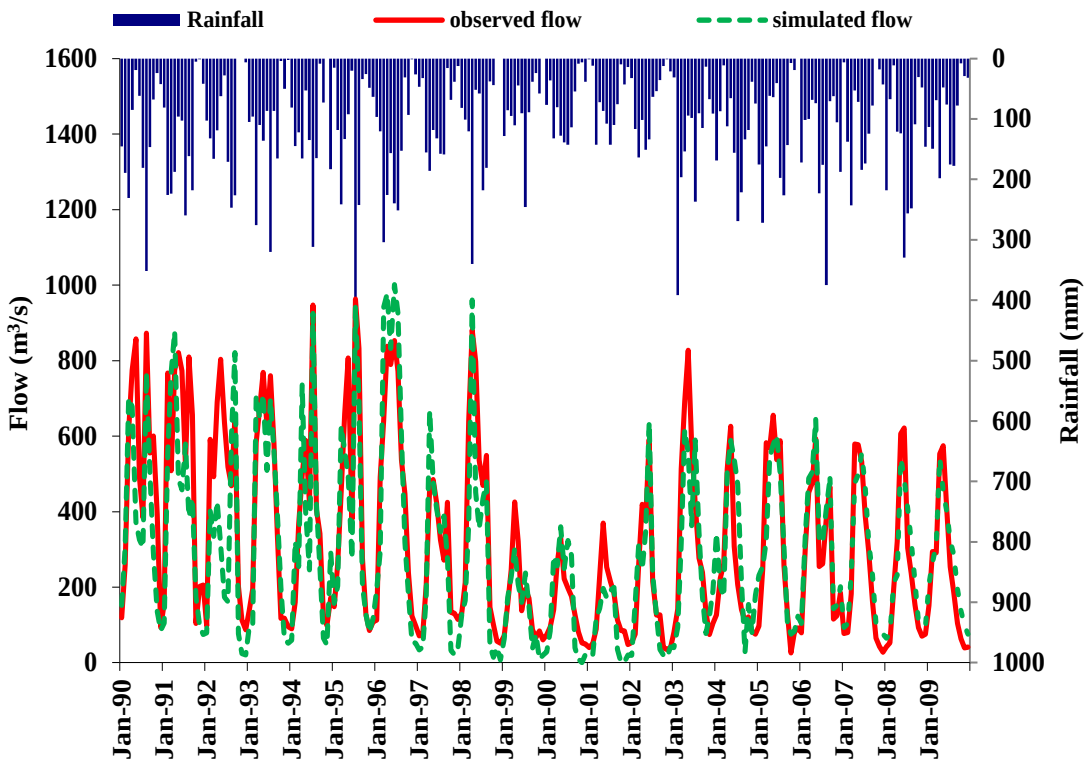

Figure 4.7: Comparison between observed and simulated flow at sub-basin 1 from from January 1990 to December 2009 on an accumulated monthly basis

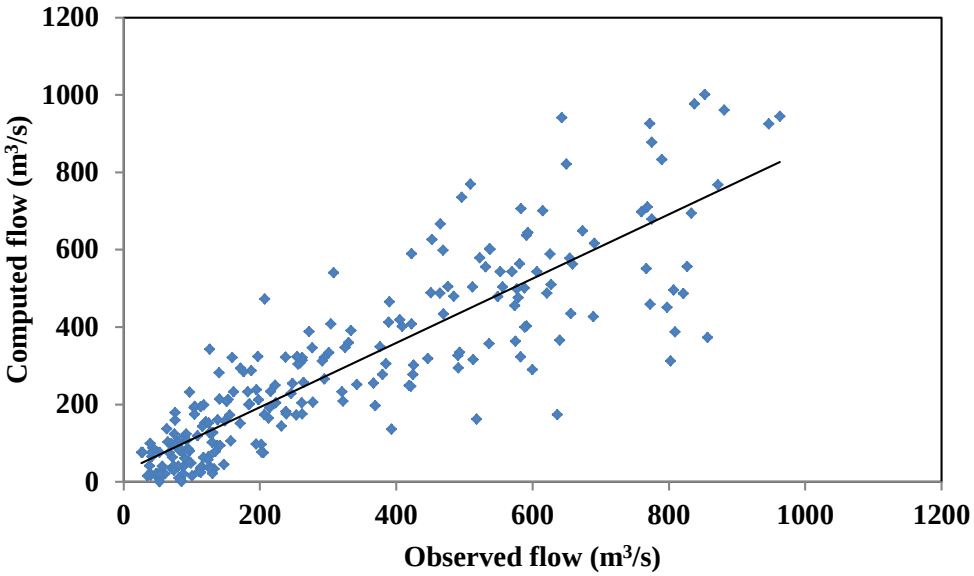

Figure 4.8: Rating Curve between observed and simulated monthly flow for sub-basin 1 from January 1990 to December 2009

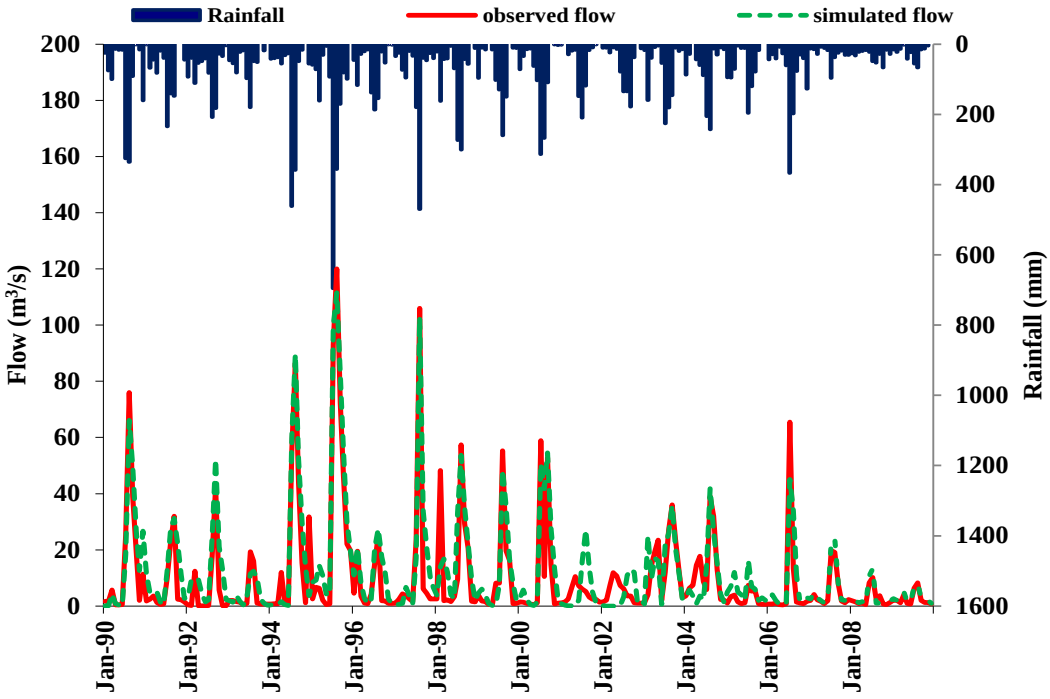

Figure 4.9: Comparison between observed and computed flows on an accumulated monthly basis for sub-basin 5 from January 1990–December 2009

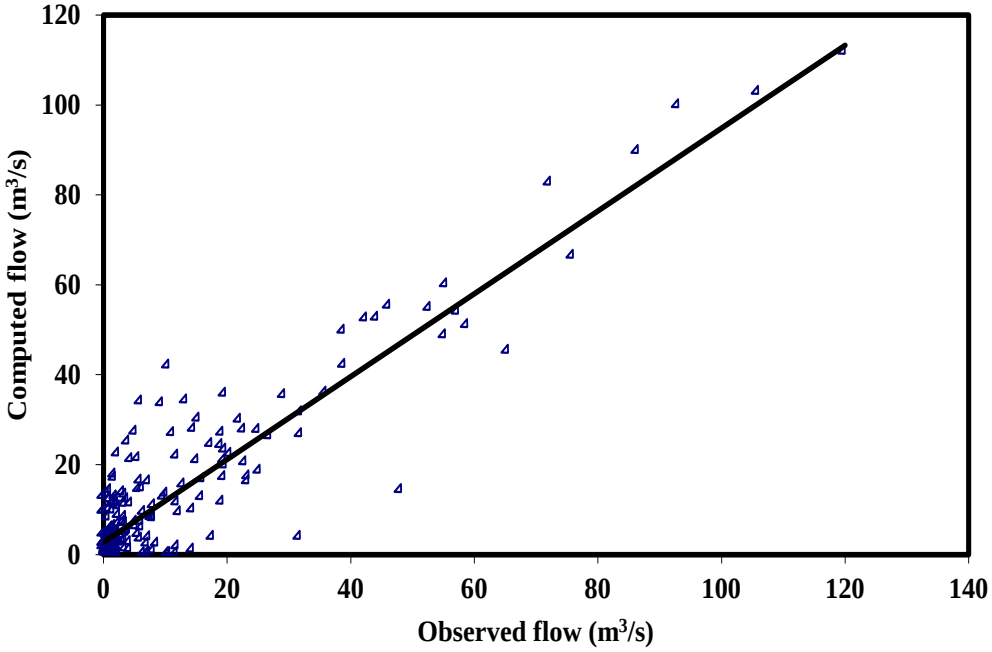

Figure 4.10: Scatter plot between observed and simulated monthly flow for sub-basin 5 from January 1990–December 2009

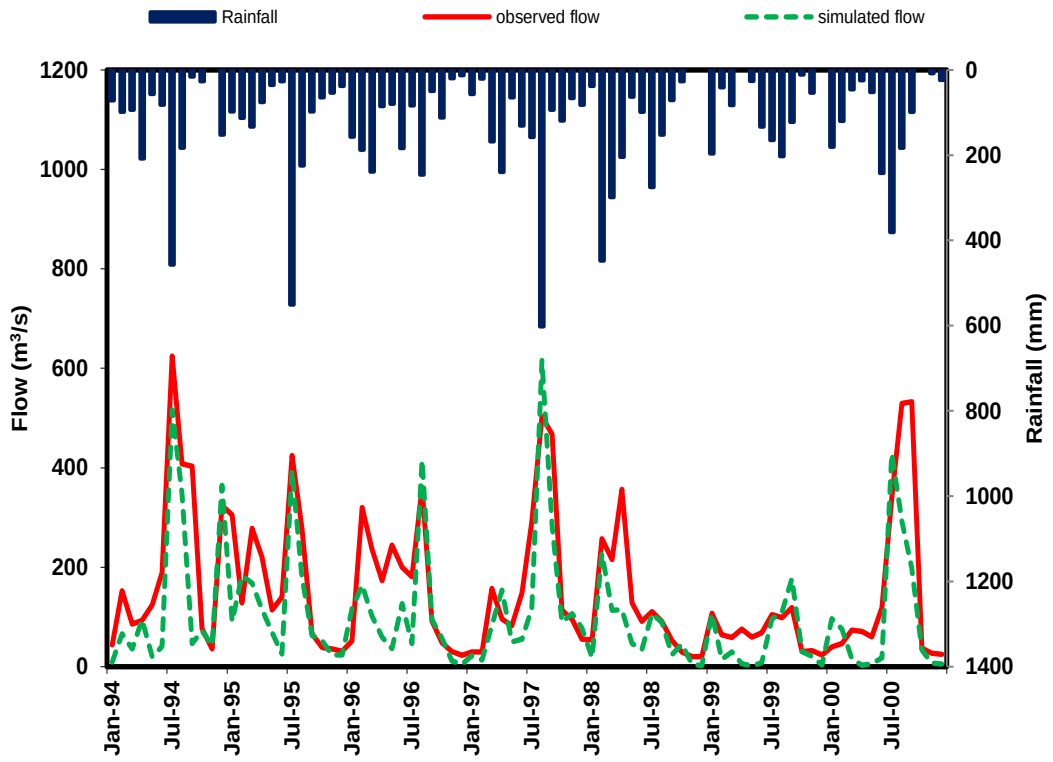

Figure 4.11: Observed and computed flows for sub-basin 6 with accumulated monthly rainfall from 1993–2004

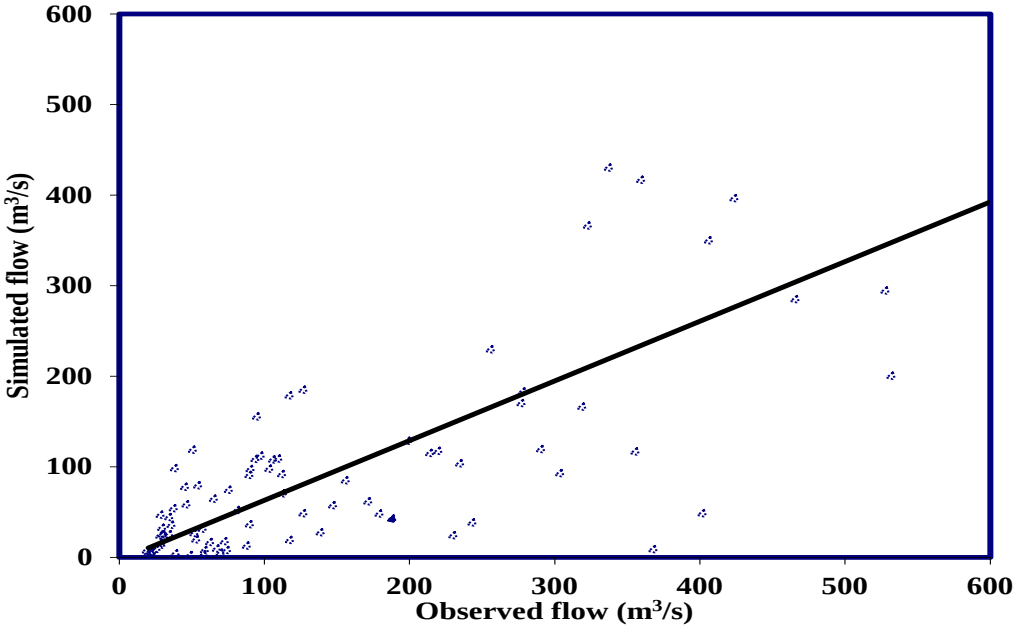

Figure 4.12: Scatter plot between observed and simulated monthly flow for sub-basin 6 from January 93–December 2002

4.6 Validation of the model for sediment

There was no sediment discharge record available on either a daily or monthly basis. The only available record was on a yearly basis, although there were some fortnightly observations of the sediment along with the instantaneous flow data. In order to obtain monthly data for validation purposes, rating curves were developed from the instantaneous flows and instantaneous sediment for sub-basins 1, 5 and 6. The results show that instantaneous flow was correlated well with suspended sediment for all sub-basins as shown in Figures 4.13, 4.14 and 4.15. A time series data of sediment was derived from daily flow data using these rating curves from 1990–2005. The sediment obtained from mean daily flows were verified by accumulating it on a yearly basis and comparing it with observed sediment data on a yearly basis published by the Surface Water Hydrology Project WAPDA Pakistan. The daily data were accumulated on a monthly basis for the validation of the SWAT model results.

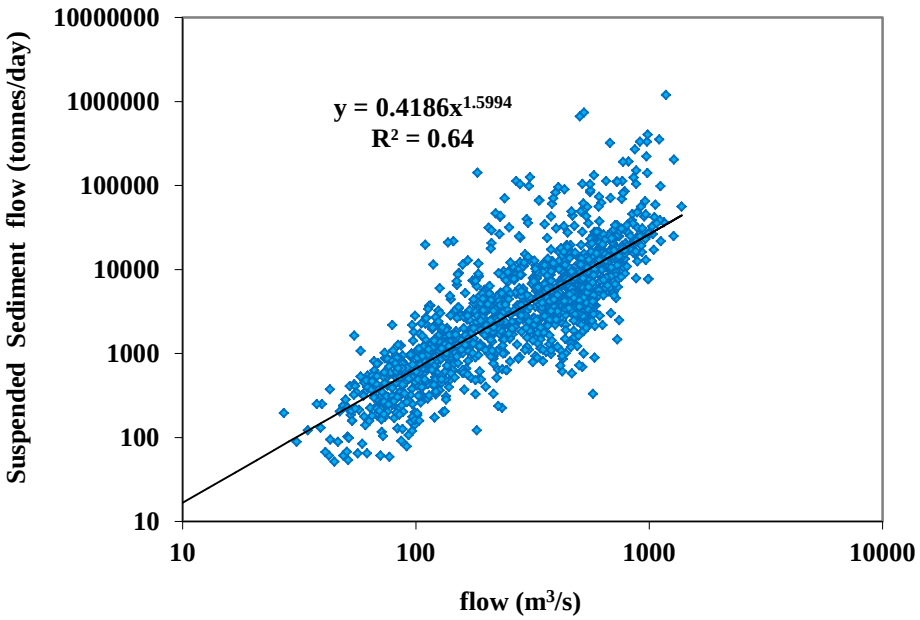

Figure 4.13: Correlation between observed river discharge and calculated suspended sediment discharge for sub-basin 1

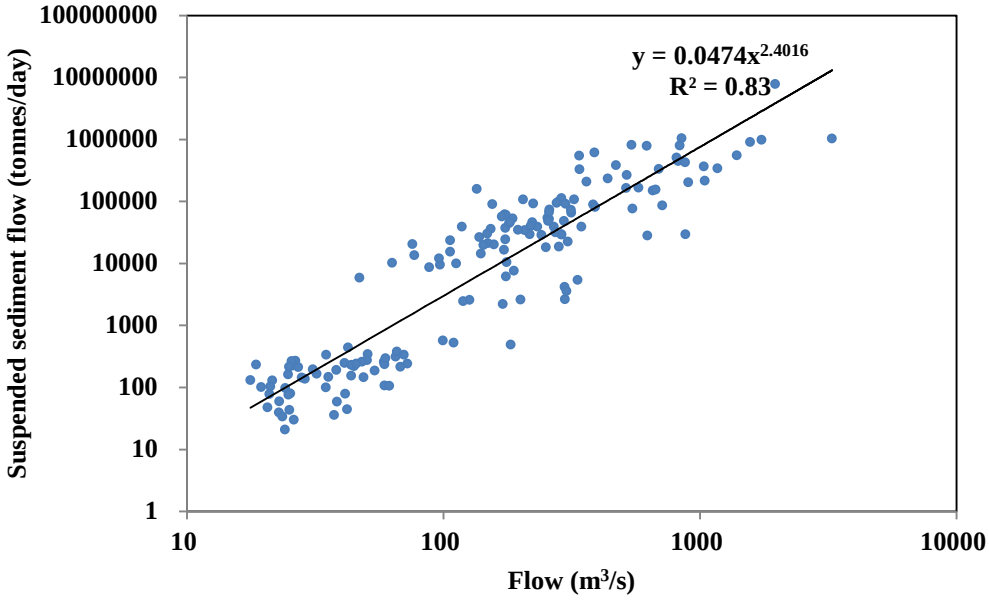

Figure 4.14: Correlation between observed river discharge and calculated suspended sediment discharge for sub-basin 5

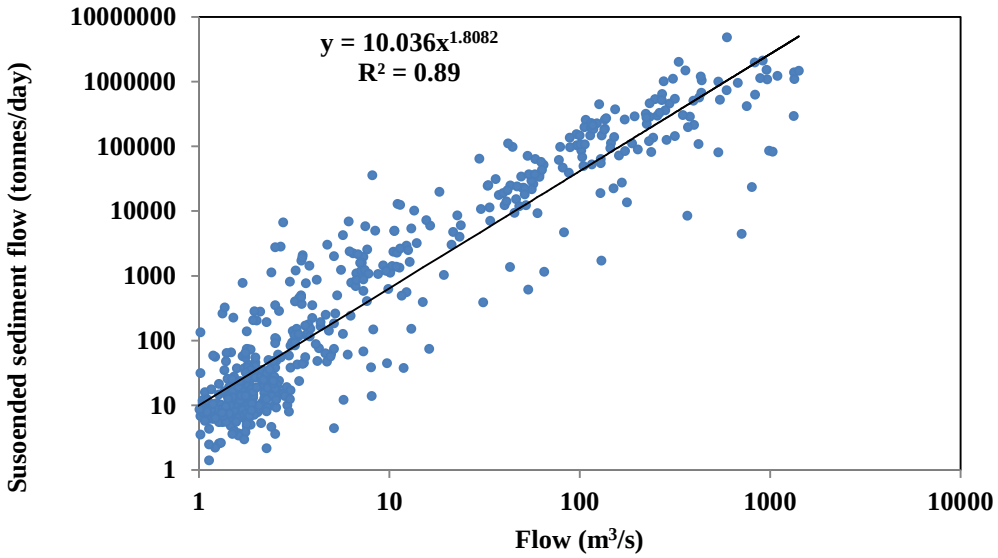

Figure 4.15: Correlation between observed river discharge and calculated suspended sediment discharge for sub-basin 6

The sediment discharge simulated by the SWAT model was validated for sub-basins 1, 5 and 6 with generated sediment load for these sub-basins with satisfactory results. The Model simulates the sediment very well for sub-basins 1 and 5, but less so for sub-basin 6 (Figure 4.16 and Figure 4.17). The statistical performance of the model for sediment simulation was also evaluated.

The results revealed that the model simulated sediment well for sub-basins 1 with an R^2 value of 0.825 and E_{NS} of 0.70. The R^2 and E_{NS} for sub-basins 5 are 0.64 and 0.44, respectively, whereas for sub-basin 6 they are relatively low at 0.52 and 0.39.

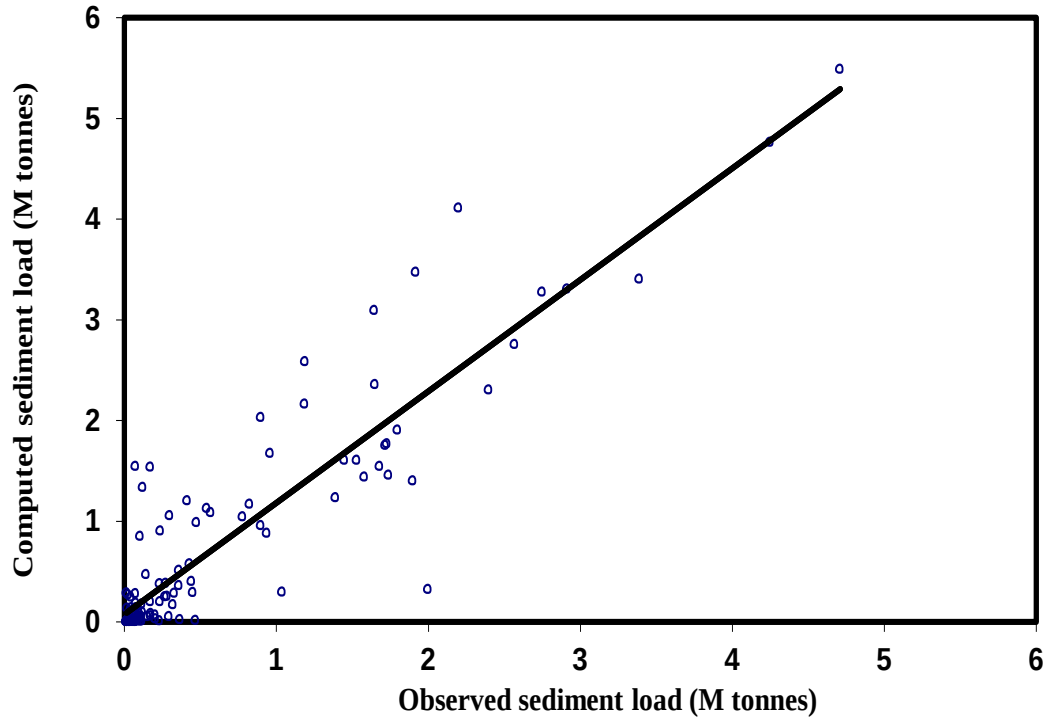

Figure 4.16: Scatter plot between observation derived monthly sediment and modelled monthly sediment for sub-basin 1

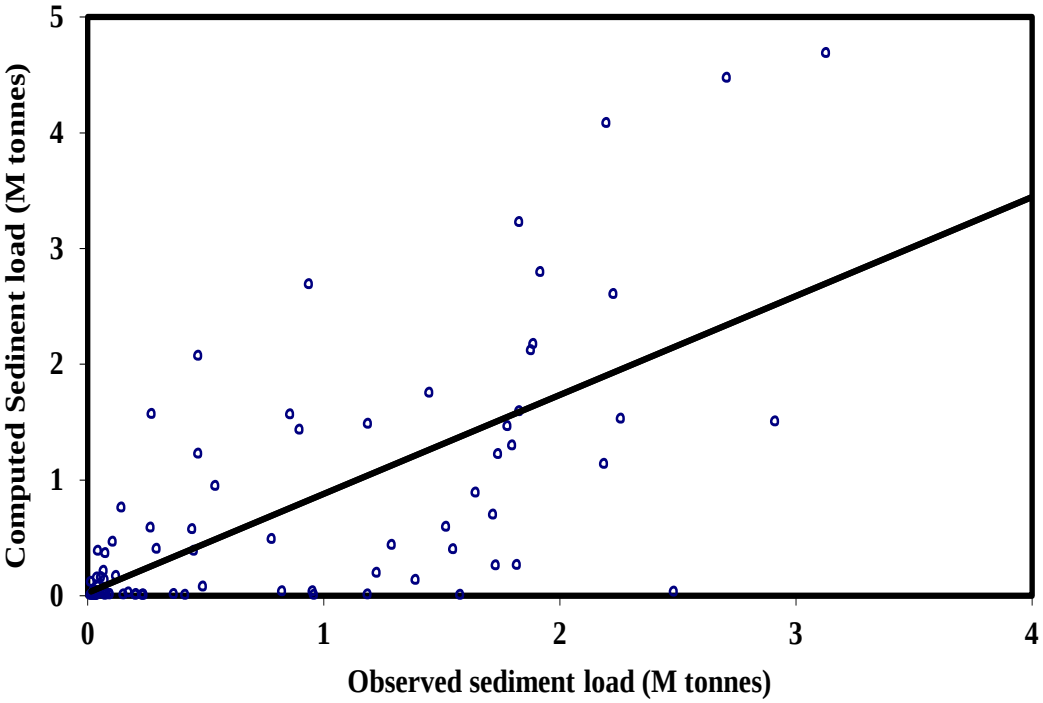

Figure 4.17: Scatter plot between observation derived sediment and modelled monthly sediment for sub-basin 6

4.7 Reservoir life

The Mangla basin of the Mangla Dam has an area of 38,434 km^2, out of which Jhelum River is the main tributary, whereas the Neelum, Kunhar, Poonch and Kanshi Rivers are other tributaries that contribute flow and sediment to the Jhelum River (Figure 4.18). The sediment load is computed for the whole basin, i.e., sediment contribution from sub-basins 1, 2, 3, 4, 5 and 6. To validate the sediment load computed by the model for the whole basin, it is necessary to determine the suspended sediment and bed load from the sediment measurement record or hydrological survey. The Water and Power Development Authority Pakistan (WAPDA) maintains the record of suspended sediment at Palote and Kotli. The record of sediment discharge was obtained from WAPDA from 1990 to 2005.

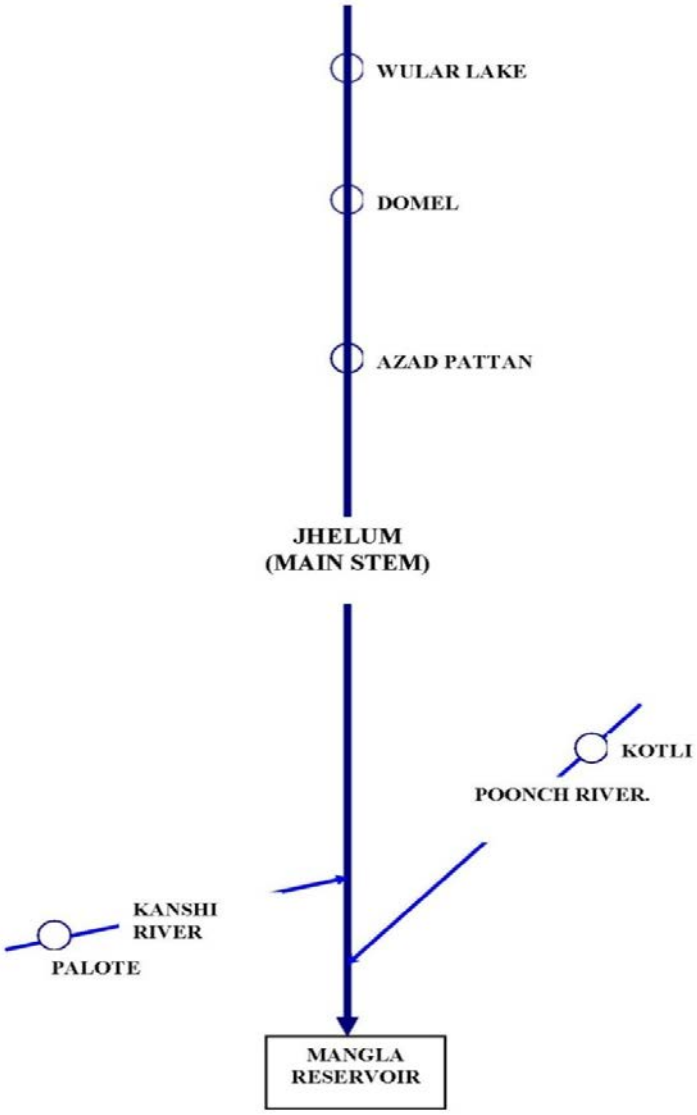

Figure 4.18: Layout of the Mangla basin

To determine the total suspended sediment load at the outlet at the Mangla Dam, a linear relationship between sediment and area was used to estimate the sediment of the un-gauged area as shown in Equation 4.3. The linear relationship between sediment load and area can easily be used because the un-gauged area was very small as compared to total area.

$$Sedimnet_{Mangla} = Sed_{A.Pattan} + Sed_{km} \times Ungauged\ area + Sed_{Palote} + Sed_{km} \times Ungauged\ area + Sed_{Kotli} + Sed_{km} \times Ungaugedarea \quad 4.3$$

where

$Sediment_{Mangla,}$ total sediment transported at the outlet of Manga from the whole basin (million tonnes);

$Sed_{A.\ Pattan,}$ sediment of the upper Jhelum basin up to Azad Pattan (million tonnes);

Sed_{Palote}, sediment of the Palote basin up to Palote gauging station (million tonnes);

$Sed_{Kotli,}$sediment of the Kotli basin up to Kotli gauging station (million tonnes);

Sed_{Km}, sediment of the basin per km^2

Un-gauged area is the basin area not covered by the gauged record (km^2).

The sediment load can be categorized as suspended sediment and bed load. Suspended sediment can be defined as sediment that moves with the flow in the river, whereas bed load is the rate of movement of sediment particles along the stream bed in the process of rolling, sliding and/or hopping (saltation). Generally the amount of bed load transport by a large deep river is about 5 to 25% of the suspended sediment (Simons and Şentürk, 1992). For the current study, 10% bed load of suspended sediment was assumed considering previous studies in the basin. The total sediment calculated from WAPDA record (1990 to 2005) is shown in Table 4.8.

Using the SWAT model the sediment load was computed for the whole basin and showed very good resemblance compared to sediment from the WAPDA record based on Equation 4.3. This indicates that runoff is the driving force for

sub-basins, the model in general predicts the sediment well. However, the model was unable to simulate the sediment for years that had high flooding, such as 1992 as shown in Figure 4.19. Therefore a separate analysis (impact of extreme event for sediment load) was carried out to compare the load of a high flood event and is explained in Table 4.9 below.

Table 4.9: Total sediment yield at the Mangla Dam outlet

Year	Total sediment yield (million tonnes)	Year	Total sediment yield (million tonnes)
1990	135	1998	107
1991	171	1999	34
1992	288	2000	21
1993	166	2001	8
1994	163	2002	29
1995	198	2003	26
1996	183	2004	24
1997	66	2005	35

The monthly distribution of sediment was estimated using SWAT from 1990 to 2000. The average seasonal magnitude varied from approximately 80% from March to September and 20% from October to February (Figure 4.20). The sediment deposition starts in late March and peaks in September. The minimum sediment was observed in November or December. The large drop in sediment in the winter season was attributed to low flow in the rivers. Jhelum River is the rainfed river, contributing sediment mainly in the monsoon months. Neelum and Kunhar tributaries, on the other hand, are influenced by snow melt that also produces maximum flows in the early spring and consequently most of the sediment is produced starting from early spring. The year 1992 shows the maximum amount of sediment simulated and the year 1999 had the minimum

sediment simulated. Figure 4.21 presents the long-term monthly mean distribution of the sediment in the Mangla Reservoir.

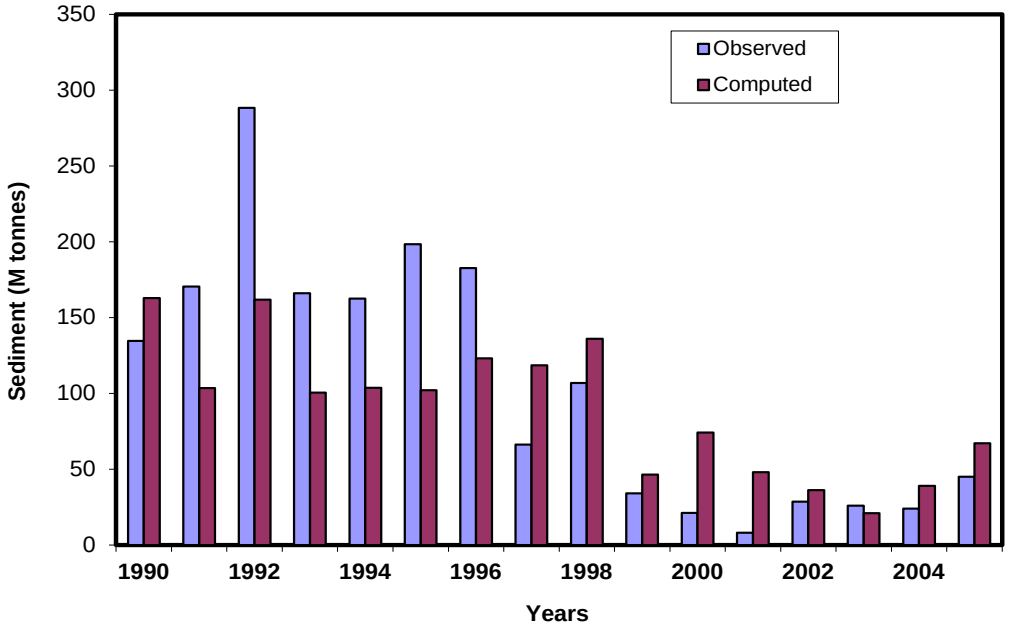

Figure4.19: Observed and computed annual sediment load for the Mangla Reservoir

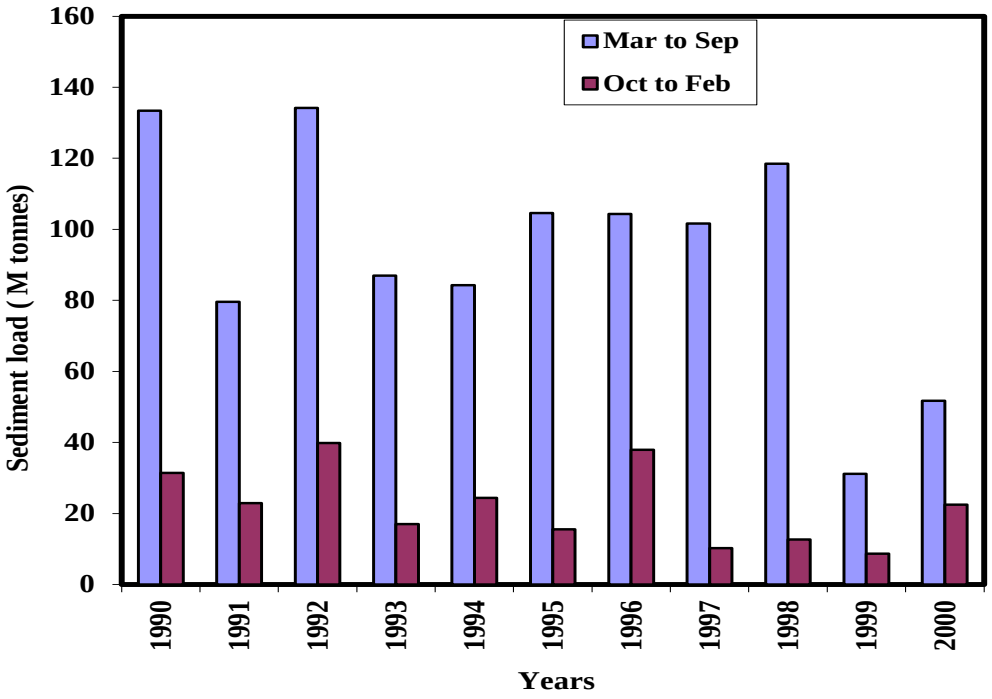

Figure 4.20: Sediment load deposition in the Mangla Reservoir for two seasons

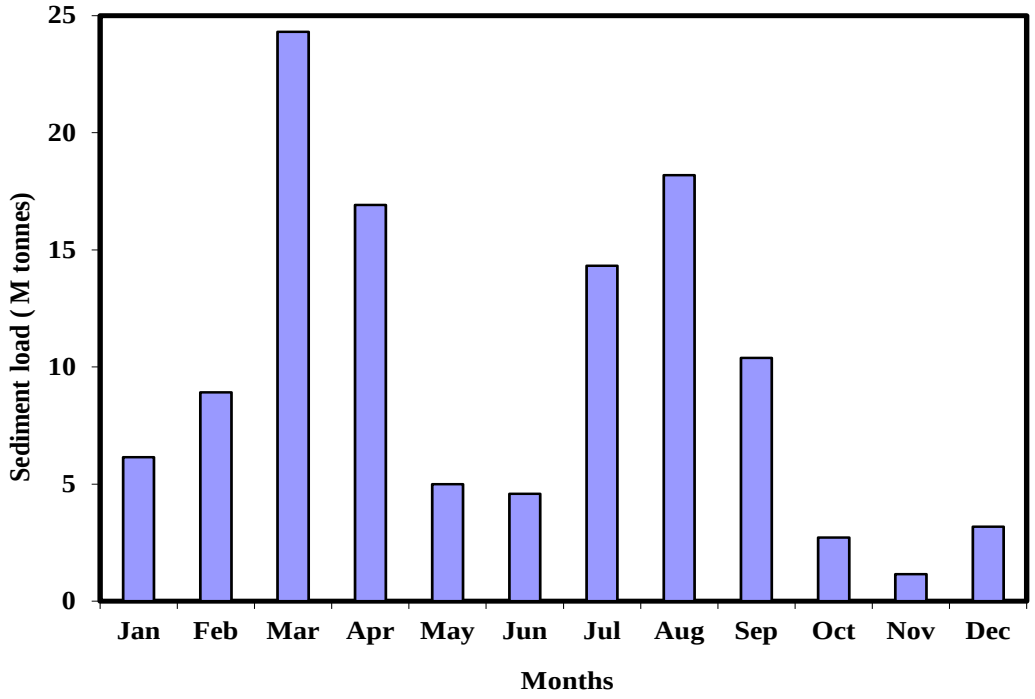

Figure 4.21: Mean monthly sediment load deposition for the Mangla Reservoir

4.8 Correlation between sediment and extreme events

Pakistan experienced an extremely high rainfall in July 2010, resulting in one of the most devastating flooding which affected one third of the country's surface area (Figure 4.22) The flood caused devastation in terms of lives lost as well as infrastructure damage and more than 2.5 million people were affected directly or indirectly (BBC, 2010). July and August of 2010 were the hottest months on record for Pakistan (NOAA, 2010), causing high runoff from the snow and glacier melt, whereas above average monsoon rainfall aggravated the flooding as the rivers already filled to their full capacity.

The Mangla basin is located in arid to semi-arid zones characterized by monsoon rainfall with two discrete rainfall patterns (details in Chapter 3). The intensity of monsoon rainfall evenst is sometimes very high and most of the sediment is

produced by these events. Extreme rainfall events play an important role in sediment deposition, and can produce debris flows, mass movement and sometimes slope failure (Cheng et al., 2005; Crosta and Frattini, 2008), hence generating much higher sediment than normal rainfall events. Therefore it is essential to analyse the impact of extreme events on sediments and to include it as a component of the integrated model. Due to the limitation of the data availability, the impact of extreme rainfall on sediments was analysed in two steps. Firstly, the annual rainfall of the six gauging stations and total sediment at the Mangla Dam outlet was analysed from 1990 to 2005, and secondly, the relationship between extreme event and sediment generation was analysed through a single extreme event.

The annual rainfall data (1990 to 2004) of Domel, Bagh, Naran, Palandari, Kotli and Mangla, and their average rainfall is shown in Figure 4.23. The annual rainfall and annual sediment of the 15 years are divided into groups of three years (Figure 4.24). As shown in Figure 4.24, the combined rainfall of the Mangla basin and sediment amount relates very well, with a linear coefficient of 0.86. Butt et al. (2011) found a correlation coefficient (R^2) of 0.94 for combined rainfall and sediment deposited at the Mangla Dam outlet. In their study, the annual rainfall data used was from Chillas, Garidupata, Jhelum, Kakul, Kotli, Murree, Muzzafarabad and Skardu for 1967 to 2005. Most of these gauging stations lie outside of the Mangla basin, except Garidupata, Kotli and Muzzafarabad. It is apparent that the Mangla basin sediment is strongly linked with total rainfall of the basin e.g., maximum sediment (441 million tonnes) was deposited from 1990 to 1992 when rainfall was at its maximum (25,623 mm).

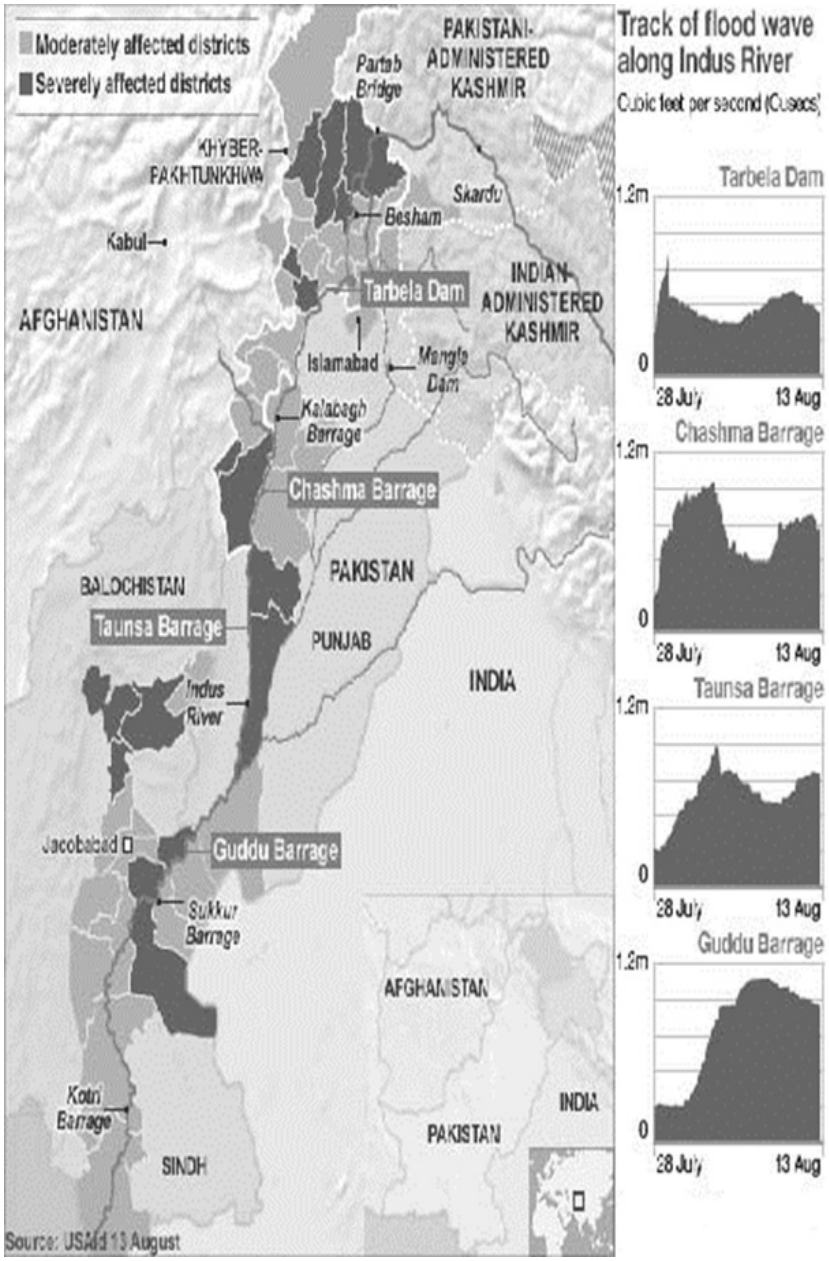

Figure 4.22: Flood affected area map of Pakistan in 2010 and the track of flood wave along the Indus river (Sources: USAID & Pakistan Meteorological Department)

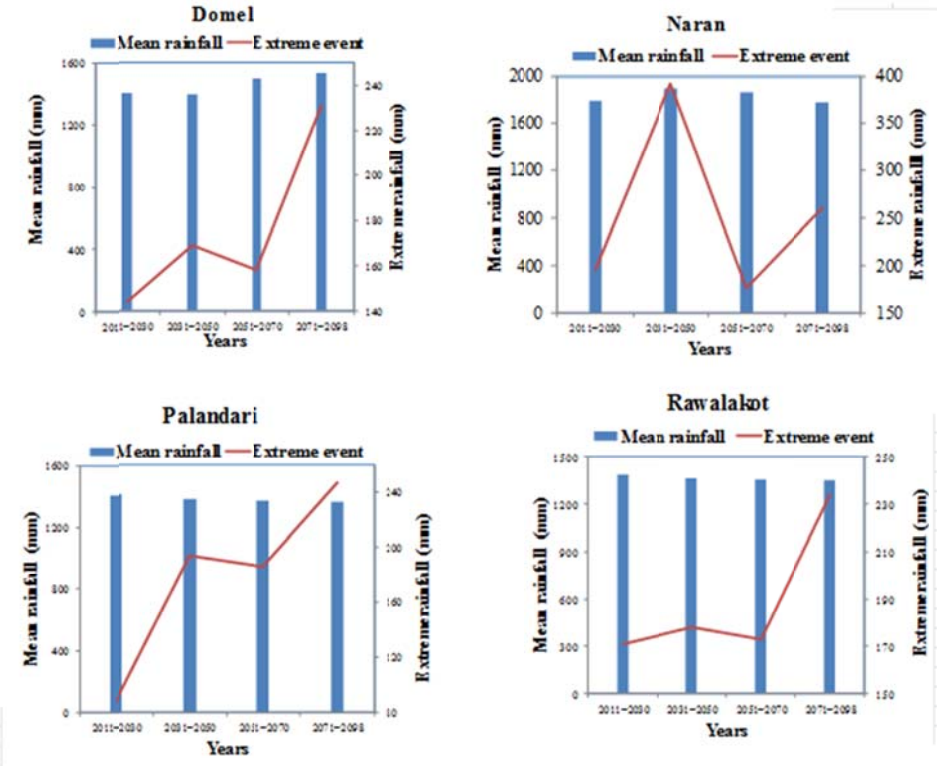

Figure 4.23: Annual total rainfall for gauging stations for Magla basin (blue line) with average annual rainfall (red line)

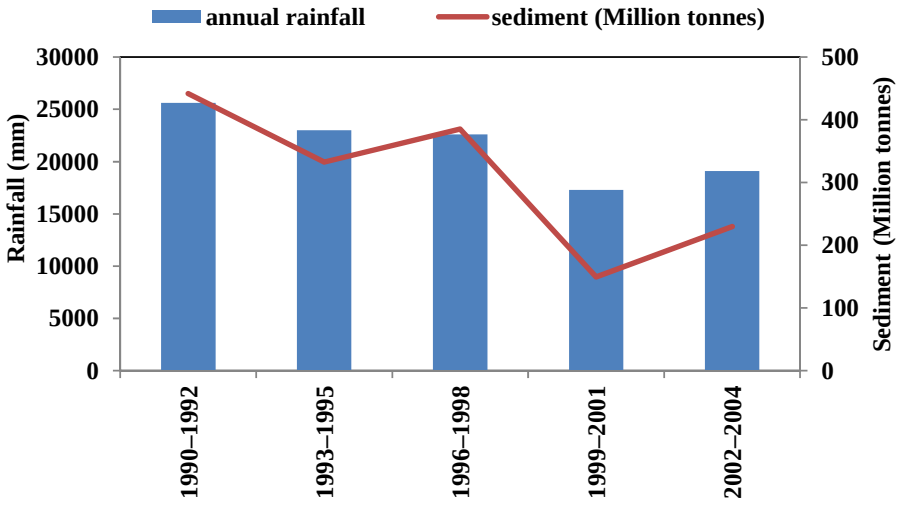

Figure 4.24: Pattern of events based on three year mean annual rainfall and sediment with a fifteen year mean rainfall in the Mangla Reservoir

Due to the limitation of the data availability, the extreme event analysis was done based on a single heaviest rainfall event in the Jhelum River basin to assess its impact on sediment deposition using the Domel gauging station data. Domel is the confluence of Jhelum River and Neelum River. The flow was recorded for Jhelum at this junction, facilitating analysis of the Jhelum River itself. For the period of 1980 to 2005, the maximum 24 hour rainfall of 294 mm was recorded on September 9, 1992 at Domel (Figure 4.25). The maximum daily flow was 1,936 m^3/s on the same day.

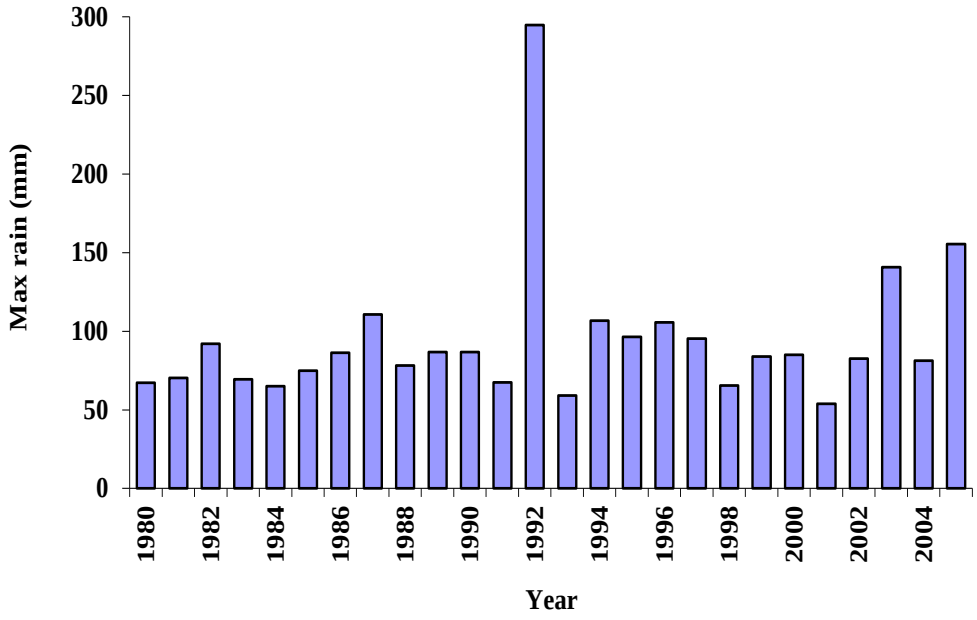

Figure 4.25: Annual maximum 24 hour rainfall at Domel

Extreme event analysis was carried out by applying the General Extreme Value (GEV) distribution for annual maximum daily rainfall data from 1980 to 2005. It focused on a block maximum value over an entire year. This frequency distribution is very flexible for specifying the centre of the distribution, size of the deviation, and shape parameter of the distribution governing how rapidly the upper tail decays (Katz, 2010). The results show that extreme high rainfall is about 317 mm for a 100 year return period (Figure 4.26).

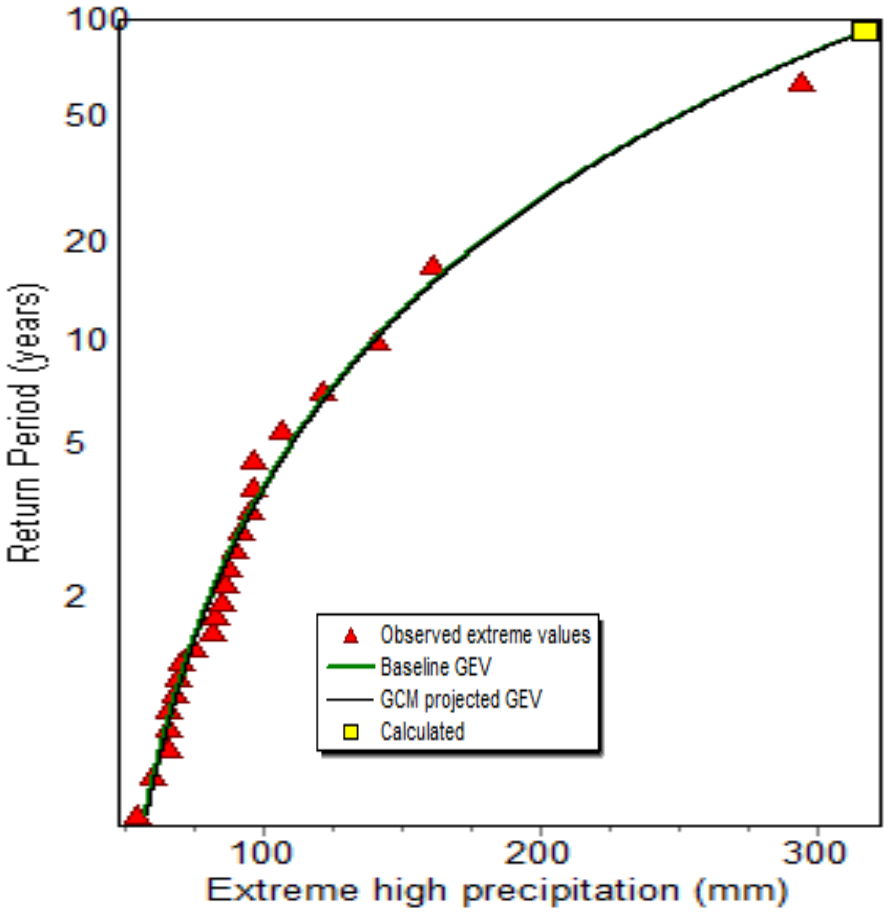

Figure 4.26: Plot of GEV distribution for Domel annual maximum daily rainfall from 1980–2005

The daily time series of rainfall and flow data at Domel gauging station for the year 1992 is shown in Figure 4.27. The rainstorm of September, 1992 resulted in the most severe flood in the Jhelum River. The mass curve for the rainstorm is presented in Figure 4.28 which clearly shows that the duration of the extreme rainstorm remained for more than 24 hours.

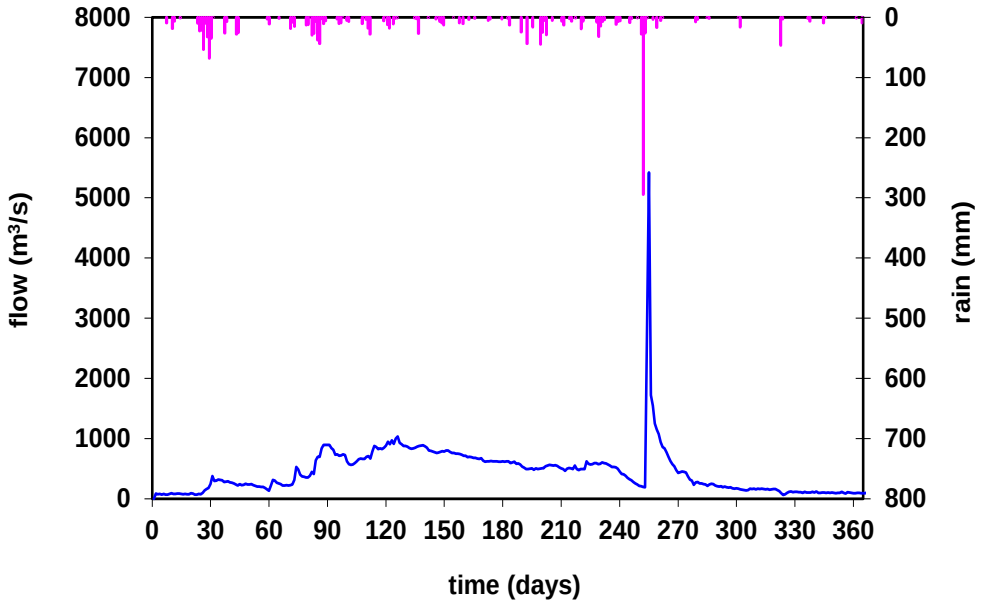

Figure 4.27: Observed daily flow and daily rainfall at Domel gauging station for the year 1992

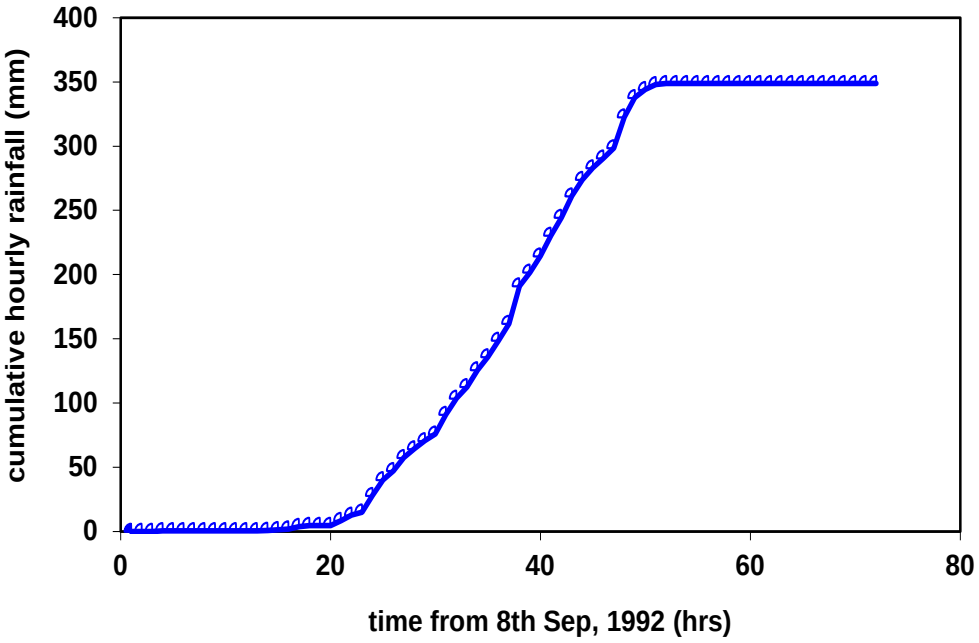

Figure 4.28: Mass curve of the rainfall for the extreme rainstorm of 1992

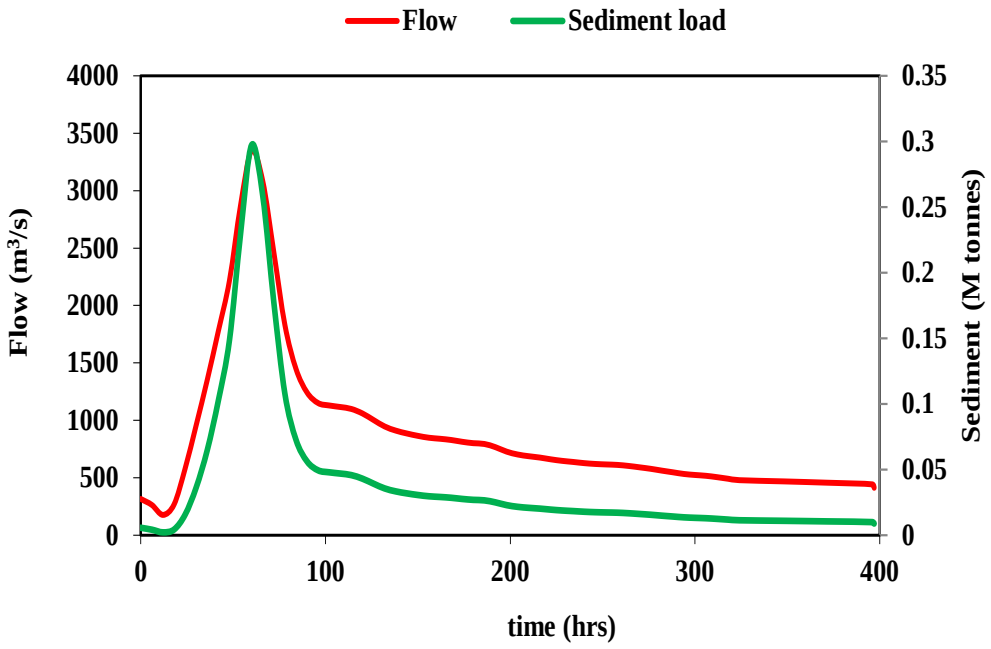

Figure 4.29: Comparison of flow and sediment for the extreme event

The model-computed sediment consists of five sets of 6 hours with respect to rainfall and flow. The amount of sediment load shows similar trends to the flow. The computed sediment load using the long-term sediment and flow rating curve is 0.005 million tonnes at the start of the event, increasing with flow and peaking at 0.63 million tonnes to gradually decline to 0.04 million tonnes at the end of the event (Figure 4.29). This indicates that an extreme event can increase sediment load 0.63 million tonnes in less than 48 hours and the influence of the extreme event remains for almost 100 hours.

4.9 Conclusion

In this chapter, the hydrological model SWAT was applied to the study area. The computation was done on an HRU basis for the whole basin, although results are shown for individual sub-basins.

The runoff of the whole basin was calculated to verify the water balance of the study area. Flow and sedimentation load was computed from various sub-basins on a monthly basis as shown in section 4.5 and 4.6. For the monthly river flow, model validation gave an R^2value of 0.85, 0.88 and 0.60 for sub-basins 1, 5 and 6, respectively. For the sediment load, R^2values for the validation period were 0.82, 0.64 and 0.52 for sub-basins 1, 5 and 6, respectively. Sediment load for the Mangla Dam outlet was calculated using a flow rating curve for the gauging stations representing the Mangla basin on an annual basis. Sediment load was also calculated to verify sediment computed by the SWAT model.

The impact of an extreme event on sediment load was analysed using a statistical approach. A unit hydrograph was constructed for the extreme rainfall event of 1992 and its impact on the sediment load generation was analysed based on computed sediment load. The general extreme value (GEV) distribution was adopted to simulate the annual maximum daily rainfall. The results reveal that there is strong correlation between extreme rainfall events and sediment load for the Mangla basin. The next two chapters (Chapters 5 and 6) will discuss how the climate change component and land-use component were developed.

CHAPTER FIVE
CLIMATE CHANGE SCENARIO DEVELOPMENT

The reservoir sedimentation is a dynamic process that is influenced by continuous climate and land-use conditions. Human-induced climate change is also a dynamic process that is controlled by the socio-economic development of human society. To study climate change impacts on sedimentation requires transient climate data that can represent the dynamics of future climate change. This chapter focuses on a method of statistical bias correction (BC) that applies an equal distance-based quantile-to-quantile mapping method to correct the GCM daily precipitation and temperature data based on observed daily precipitation and temperature data in order to generate transient climate change scenarios for the study area.

The three GCMs used in this study were obtained from the new IPCC AR5 CMIP5 database (Table 5.1). Only the GCM experiments driven by IPCC A2 emission scenario for the 21st century were available when this part of the research was carried out. The IPCC A2 scenario is based on a heterogeneous world with continuously increasing population and a technologically fragmented economic development, which represents one of the highest emission scenarios (but not the highest). A GCM under IPCC A2 scenario normally generates a larger than average future climate change condition.

5.1 Statistical bias correction methods

The reservoir sedimentation is a dynamic process that is influenced by continuous climate and land-use conditions. Human-induced climate change is also a

dynamic process that is controlled by the socio-economic development of human society. To study climate change impacts on sedimentation requires transient climate data that can represent the dynamics of future climate change. This chapter focuses on a method of statistical bias correction (BC) that applies an equal distance-based quantile-to-quantile mapping method to correct the GCM daily precipitation and temperature data based on observed daily precipitation and temperature data in order to generate transient climate change scenarios for the study area.

Table 5.1: The three GCMs from the CMIP5 database

Model	**Model Name**	**Institute**	**Country**	**Resolution (Lat×Long)**
CSM	NCAR CSM	National Centre for Atmospheric Research	USA	$2.82^{o} \times 2.82^{o}$
CanESM2	Canadian Earth System Model	Canadian Centre for Climate Modelling and Analysis	Canada	$2.82^{o} \times 2.82^{o}$
NorESM	Norwegian Earth System Model	Bjerknes Centre for Climate Research	Norway	$2^{o} \times 2^{o}$

The three GCMs used in this study were obtained from the new IPCC AR5 CMIP5 database (Table 5.1). Only the GCM experiments driven by IPCC A2 emission scenario for the 21st century were available when this part of the research was carried out. The IPCC A2 scenario is based on a heterogeneous world with continuously increasing population and a technologically fragmented economic development, which represents one of the highest emission scenarios

(but not the highest). A GCM under IPCC A2 scenario normally generates a larger than average future climate change condition.

5.2 Statistical bias correction methods

The basic procedure of bias correction is to develop a statistical relationship or transfer function between the GCM outputs and historical observed values and then apply the transfer function to GCM future projections in order to eliminate the possible systematic errors in GCM outputs (Ines and Hansen, 2006; Piani et al., 2010). It has been widely applied in downscaled GCM outputs. Currently, almost all BC methods are applicable to only a single downscaled time series versus a single observed time series. One of the simple bias correction methods is pattern scaling (Santer et al., 1990). Various pattern scaling techniques have been used in climate change scenario constructions (Hanssen-Bauer et al., 2003; Diaz-Nieto and Wilby, 2005; Widmann et al., 2010). For the simplest pattern scaling method, a rescaling (multiplicative) factor during the baseline period was calculated to correct the bias of the mean monthly GCM rainfall. This was done as follows:

$$x_i' = x_i \frac{\overline{X}_{OBS}}{\overline{X}_{sim}} \qquad 5.1$$

Where x_i and x_i' refer to the GCM and corrected rainfall on day *i*, and $\overline{X}_{sim}$ and $\overline{X}_{OBS}$ is the long-term monthly mean rainfall from the GCM and observations for a given month. It is clear that the sole objective of the scaling procedure is to adjust rainfall amount in order to reproduce the long-term mean observed rainfall

for a specific month, without any operation to correct the systematic error in frequency or intensity distribution (Ines and Hansen, 2006).

Another bias corrected method is called rescaling or quantile-based mapping cumulative distribution function (CDF matching) (Panofsky and Brier, 1968; Law and Kelton, 1982). The typical procedure is to map the distribution of GCM daily data, i.e., the CDF of daily rainfall or temperature in a specific month onto that of observed data. The corrected GCM data x' on day *i* during the baseline period can be derived as

$$x_i' = F_{obs}^{-1}(F_{sim\_B}(x_i)) \quad 5.2$$

where F(•) and F^{-1}(•) denote the CDF of either the observations (*obs*) or GCM results (*sim*) and its inverse during the baseline period. To bias-correct GCM values for a future period, the method needs firstly to find the corresponding percentile values for these future values on the CDF of the GCM values during the baseline period and then search for the observed values on the CDF of the observations at the same percentile locations. Thus, the original GCM results are replaced by those values found on the CDF of the observations.

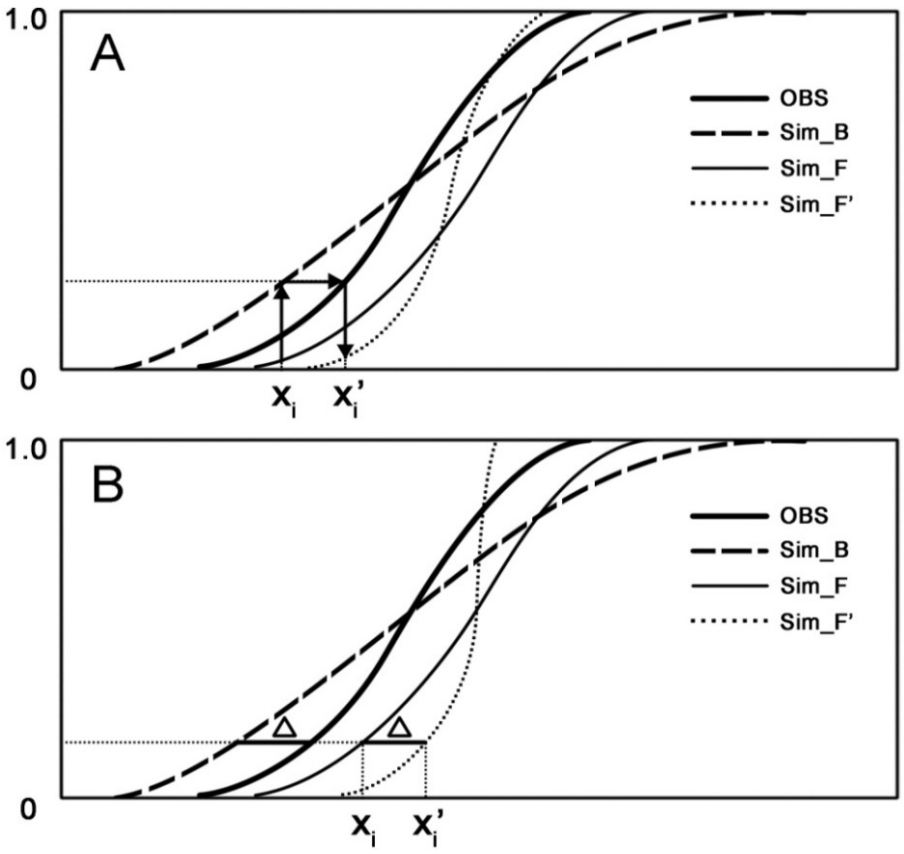

Figure 5.1: Scheme of bias correction methods of (A) CDFP and (B) EDCDF (modified after Li et al., 2011)

Because this BC procedure is based on CDF and replacement, it is hereafter termed CDFP. Figure 5.1 (A) illustrates how this worked.

The above BC method has been successfully used in hydrologic and crop simulations as well as many other climate impact studies (Ines and Hansen, 2006; Cayan et al., 2008; Piani et al., 2010). The significant characteristics of the method is that it adjusts all moments (i.e., the entire distribution matches that of the observations for the baseline period), while maintaining the rank correlation between the GCM results and observations. However, the method was based on an important assumption; namely, the precipitation and temperature distributions do not change over time. In other words, the future climate will still follow the same statistical characteristics of the observed (e.g., the variance and skew) during

the baseline period and only the mean will change. However, some studies have shown that, at least for precipitation, climate characteristics would change over time (Meehl et al., 2007; Benestad et al., 2008; Milly et al., 2008).

In view of these facts, an equal distance-based CDF mapping method (EDCDF) was proposed to correct the GCM daily precipitation and temperature. This method was different from the above traditional method in that the information from the CDF of the GCM was also incorporated into the BC procedure. For a given percentile, it was assumed that the difference between the GCM and observed value during the baseline period also applies to the future period. Thus, the corrected GCM data x' on day *i* for the future period can be calculated as

$$x_i' = x_i + F_{obs}^{-1}(F_{sim\_F}(x_i)) - F_{sim\_B}^{-1}(F_{sim\_F}(x_i)) \quad 5.3$$

where F(•) and F^{-1}(•) denote the CDF of either the observations (*obs*) or GCM results (*sim*) and its inverse during the baseline period (*_B*) and future period (*_F*). Figure 5.1(B) illustrates how this BC procedure performed. As can be seen from the figure, the difference between the GCM and observed values during the baseline period at each percentile was considered as the systematic error to be superimposed upon the CDF of the GCM values at the corresponding percentile during the future period. This was the reason why the method was termed the equidistant CDF matching method. Compared with CDFP, the difference between the CDFs for the future and baseline periods was also taken into account in EDCDF. However, the two methods will generate an identical BC result if the distribution for the future climate is the same as that for the baseline period. Moreover, if the changes in variability are small, results from both methods will be close to each other.

The above two BC methods are all based on CDF and rely on the statistical relationships between the two CDFs (observed, GCM baseline period) to correct the third one (GCM result for the future period). Indeed, the differences between the GCM results of the future and baseline period could also be superimposed onto the observed CDF to construct new projections. The above two methods involved the operation of taking the inverse of the CDFs. In practice, the CDFs can be either empirical (i.e., sorted arrays of observations) or fitted to some theoretical distribution such as the gamma distribution (Ines and Hansen, 2006; Piani et al., 2010), Log-Logistic (e.g, Shoukri et al., 1988) or exponential distribution (Madi and Raqab, 2007). However, a single theoretical distribution does not always work well for regions with very complicated climate types and orographic features such as the case study area (Vlcek and Huth, 2009). Moreover, fitting a distribution often needs long-term observed precipitation data. For simplicity, only the empirical distribution was considered in order to represent observed and GCM precipitation intensities. The EDCDF method was used in generating the climate scenarios for this study.

5.3 Bias correction of precipitation

Unlike temperature, the daily precipitation event is intermittent in nature, especially for arid and semi-arid regions. Hence, to separate daily precipitation into frequency (fraction of precipitation days, or wet days) and intensity (rainfall per wet day) in modelling allows for a more accurate precipitation simulation. Correcting the bias of the two rainfall components will also correct the monthly total rainfall itself. A two-step BC procedure is therefore proposed to simultaneously adjust the two components of GCM rainfall to make it

approximate the long-term observed distribution for each gauge station in the study area as shown in Figure 5.2.

To perform a bias corrected operation, the observed precipitation was firstly truncated using a threshold value of 0.1mm ($\bar{x} = 0.1$) to obtain an ideal frequency distribution. Then the GCM daily precipitation during the baseline period was fitted into an empirical frequency distribution. By finding a threshold $\bar{x}_{sim}$, this distribution was truncated so as to ensure that its frequency above the threshold would approximate the observed precipitation frequency (Ines and Hansen, 2006). The threshold $\bar{x}_{sim}$ was calculated from the empirical observed and GCM cumulative precipitation distribution as,

$$\bar{x}_{sim} = F^{-1}_{sim_B}\left(F_{obs}\left(\tilde{x}\right)\right) \qquad 5.4$$

where F(•) and F^{-1}(•) denote a cumulative distribution function (CDF) and its inverse, $\tilde{x}$ represents the truncated observed time series at a threshold $\bar{x} = 0.1$, and the subscripts of *sim* and *obs* indicate GCM or observed daily precipitation, while the *_B* indicates the baseline period. Moreover, this threshold $\bar{x}_{sim}$ was also used to truncate the GCM precipitation during the future period.

The above correction procedure was only applicable when the precipitation frequency was overestimated, which is common for the GCM-based precipitation (Dai, 2006; Ines and Hansen, 2006). If frequency was underestimated, the frequency was not corrected or was offset by adding some artificial precipitation events. Ines & Hansen (2006) suggested that only drizzles (0.1 mm rainfall) should be used, but they pointed out that such a procedure might distort the corrected frequency distribution. Therefore, in this study, precipitation events

were randomly selected from the historical data and to offset the frequency deficit. Moreover, the corrected percentage of the frequency deficit between GCM data during the baseline period and observed data was used to correct the GCM precipitation frequency for the future period.

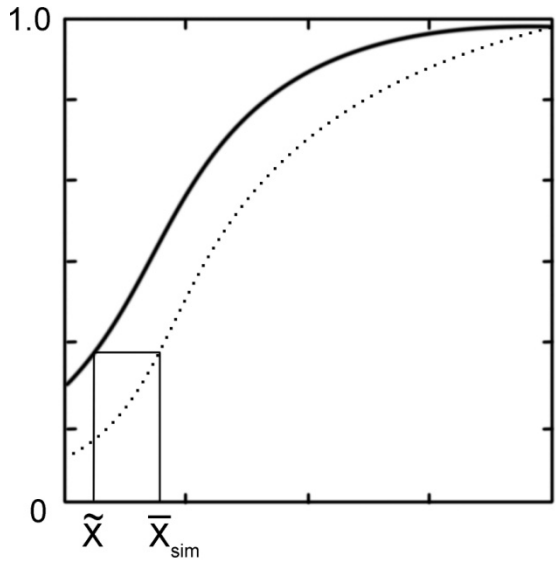

Figure 5.2: Threshold to truncate the CDF of the original GCM daily precipitation (dashed line). The $\bar{x}_{sim}$ for the GCM data, having the same CDF value as the truncated observed data at x=0.1(thick line)

After correcting precipitation frequency, the intensity distribution of the truncated GCM daily precipitation could be further adjusted by the equal distance-based CDF mapping method (EDCDF). An adjustment of Equation 5.5 was used and given in the following equation.

$$x_i' = \begin{cases} x_i + F_{obs}^{-1}(F_{sim\_F}(x_i)) - F_{sim\_B}^{-1}(F_{sim\_F}(x_i)), & x_i > \bar{x}_{sim} \\ 0, & x_i < \bar{x}_{sim} \end{cases} \quad 5.5$$

In practice, an iteration process is necessary for the BC process. Generally, five iteration steps were sufficient.

5.4 Data and result

To match the GCM simulations for present-day climate, only the period from 1980–2004 for rainfall and 1990–2004 for temperature were used, which are termed the baseline period. The precipitation time series were from three GCMs i.e. CSM, CNRM, CanESM2 and NorESM. Future projections of rainfall and temperature (maximum and minimum) were calculated to the year 2098 under the SRES A2 Scenario.

The bias correction (BC) procedure was performed on a daily basis, and all evaluations were carried out on a daily basis. Based on the observed probability distribution functions (PDFs), the performance of the BC method was evaluated for the first two moments of the PDFs: the mean (SDII) and the standard deviation (ppSD). The corrected SDII for daily rainfall and maximum and minimum temperature were very accurate. In terms of rainfall intensity, Figure 5.3 shows the observed and bias corrected mean rainfall for wet days (1980-2004). The bias corrected results of all GCM's showed very similar patterns for mean rainfall. The total number of wet days of GCMs after the bias corrected procedure fits very well with observation as shown in Figure 5.4. The bias corrected procedure must have had an impact on the second moment of the PDF daily rainfall- ppSD. These effects on a daily basis are shown in Figure 5.5. All the bias corrected ppSDs approximated the observed ppSD no matter where they were in the distribution. Each point in the figure corresponds to a single gauging station for a specific GCM, with the X-axis representing the observed value and the Y-axis, the bias correct one. All three GCMs showed similar results with NorESM slightly better than the other two. As shown in these figures, errors are almost negligible and

there was no bias toward either high or low values, including at the tails of the distribution (large or small observed values).

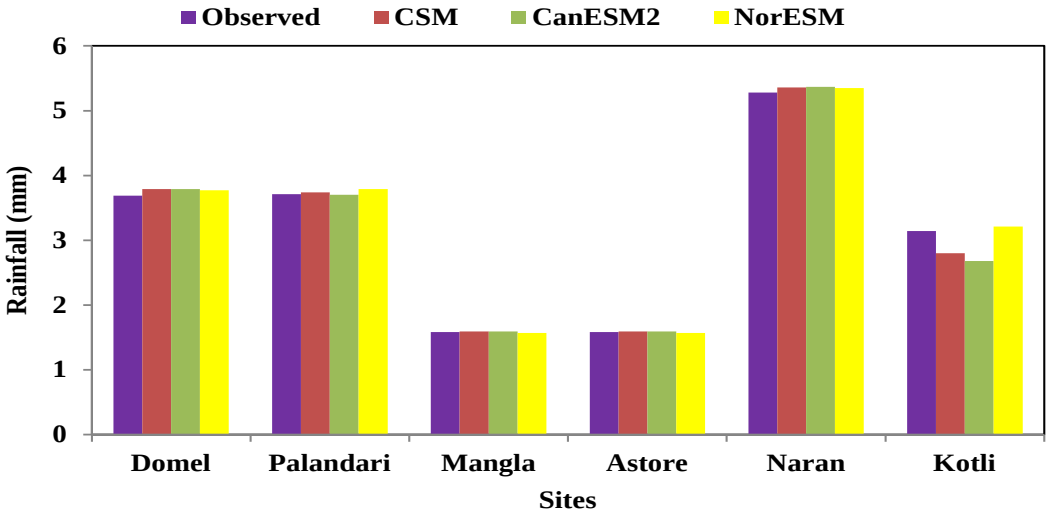

Figure:5.3 Mean daily rainfall of wet days for observed BC data of various GCMs from 1980–2004

The daily temperature (maximum and minimum) for five gauging stations Bagh, Kotli, Naran, Palandari and Mangla are also bias corrected for GCM's. The results of the temperature data reveal that the BC procedure corrected the GCM's data very well. The results are evaluated on the first two moments of the PDF: the mean (SDII) and standard deviation (ppSD). Figure 5.6 and 5.7 presents the mean maximum and mean minimum temperature on a daily basis from 1990–2004 and Figure 5.8 and 5.9 shows the scatter plots of standard deviation (ppSD) for observed and bias corrected maximum and minimum temperatures, respectively. Good results were found for minimum and maximum temperature data, although NorESM bias corrected data for minimum temperature showed little variation in standard deviation values.

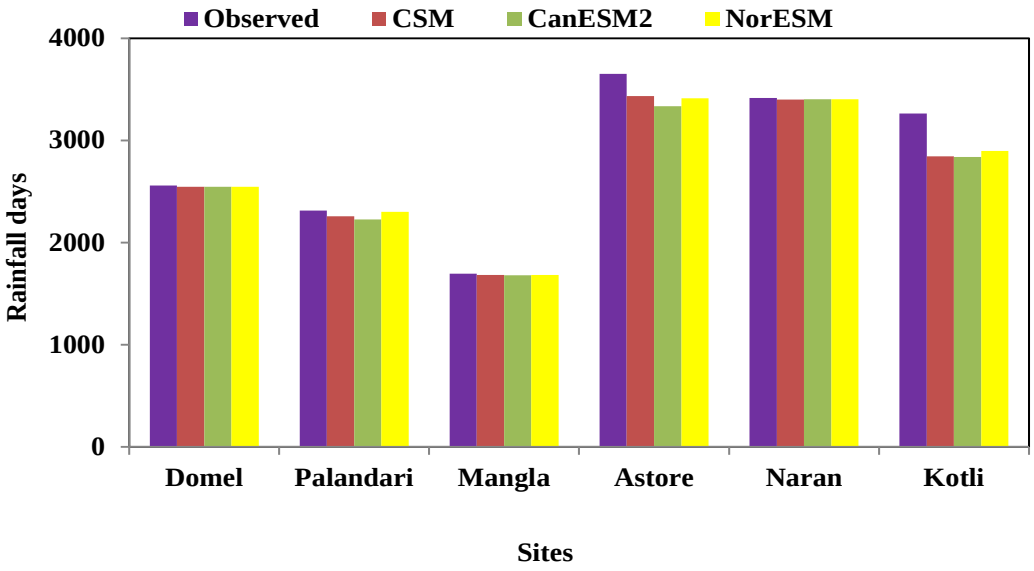

Figure 5.4: Total wet days from 1980–2004 for observed and BC data of various GCMs

.

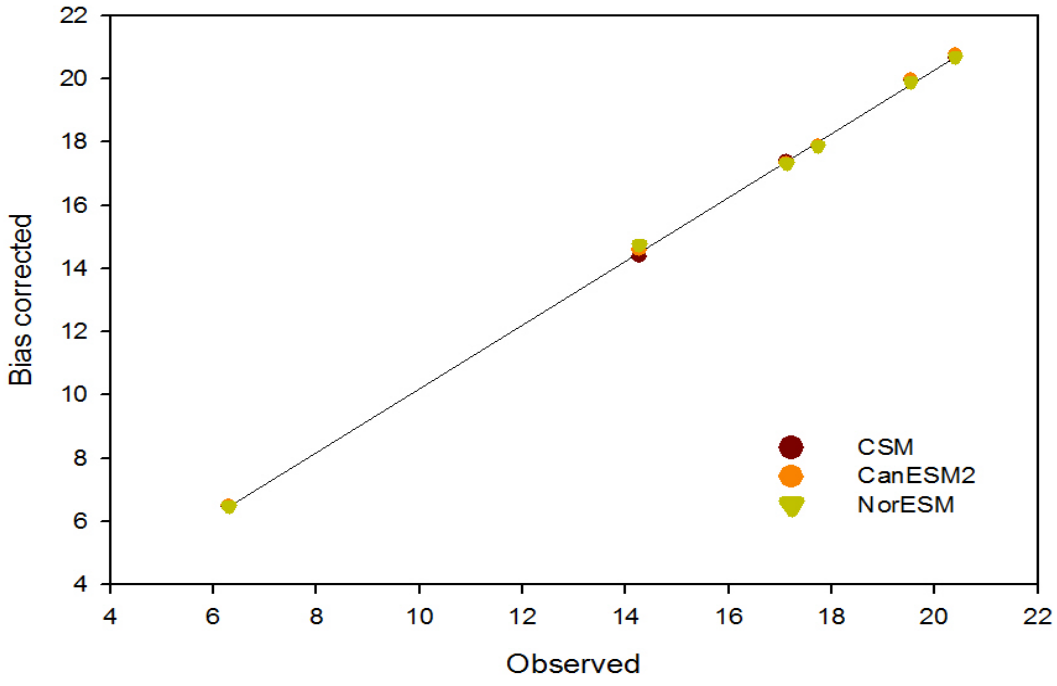

Figure 5.5: Scatter plot of observed versus Bias Corrected standard deviations (ppSD) from 1980–2004

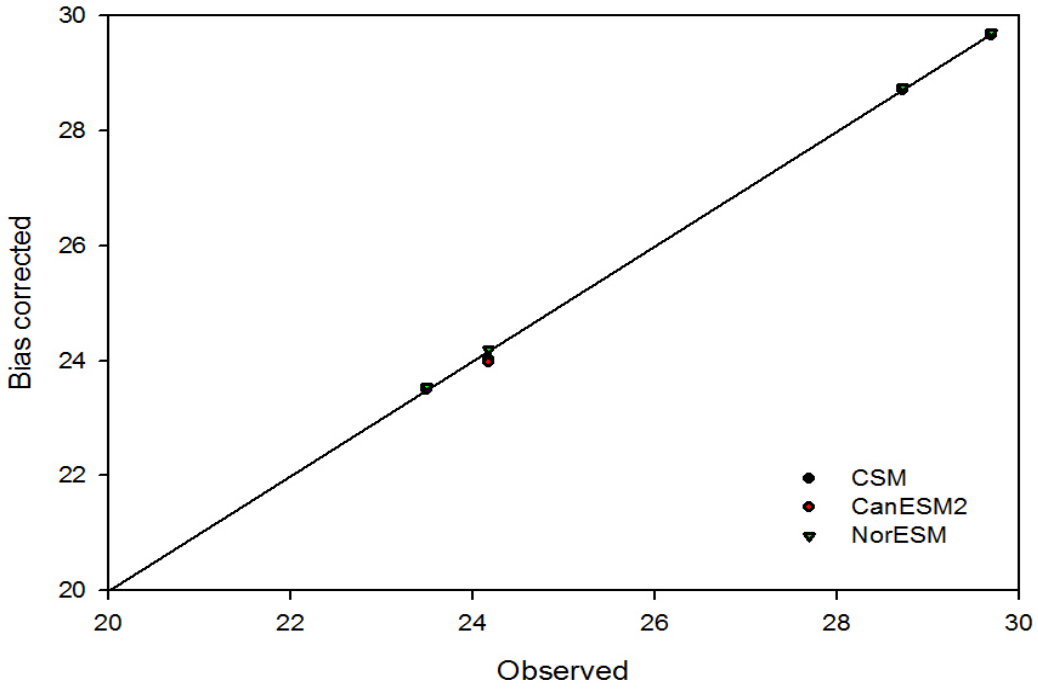

Figure 5.6: Scatter plot of observed versus Bias corrected mean daily maximum temperature (^{o}C) for various GCMs from 1990–2004

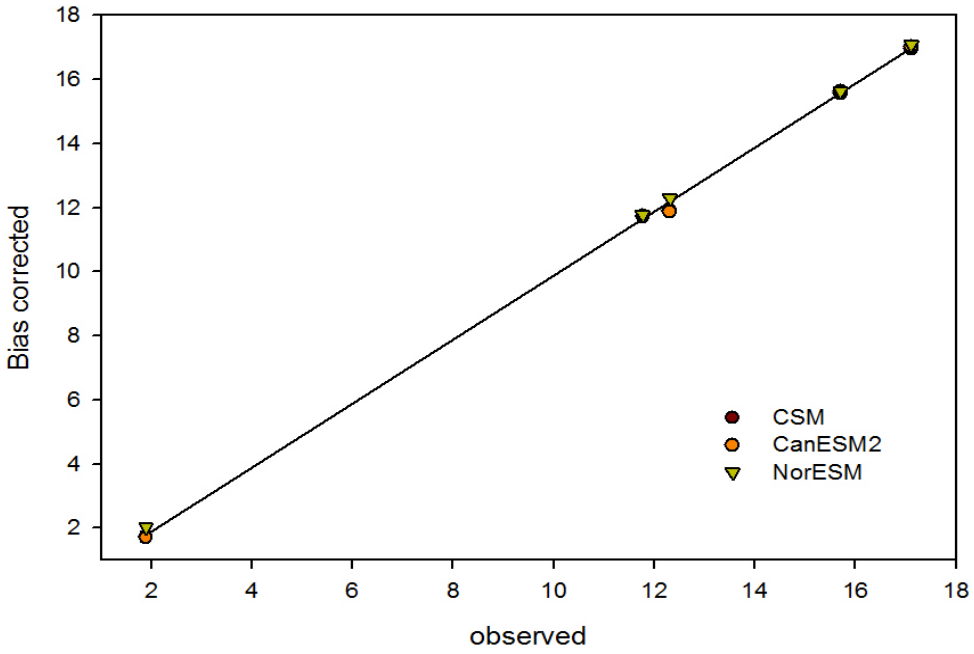

Figure 5.7: Scatter plot of observed versus Bias corrected mean daily minimum temperature (^{o}C) for various GCMs from 1990–2004

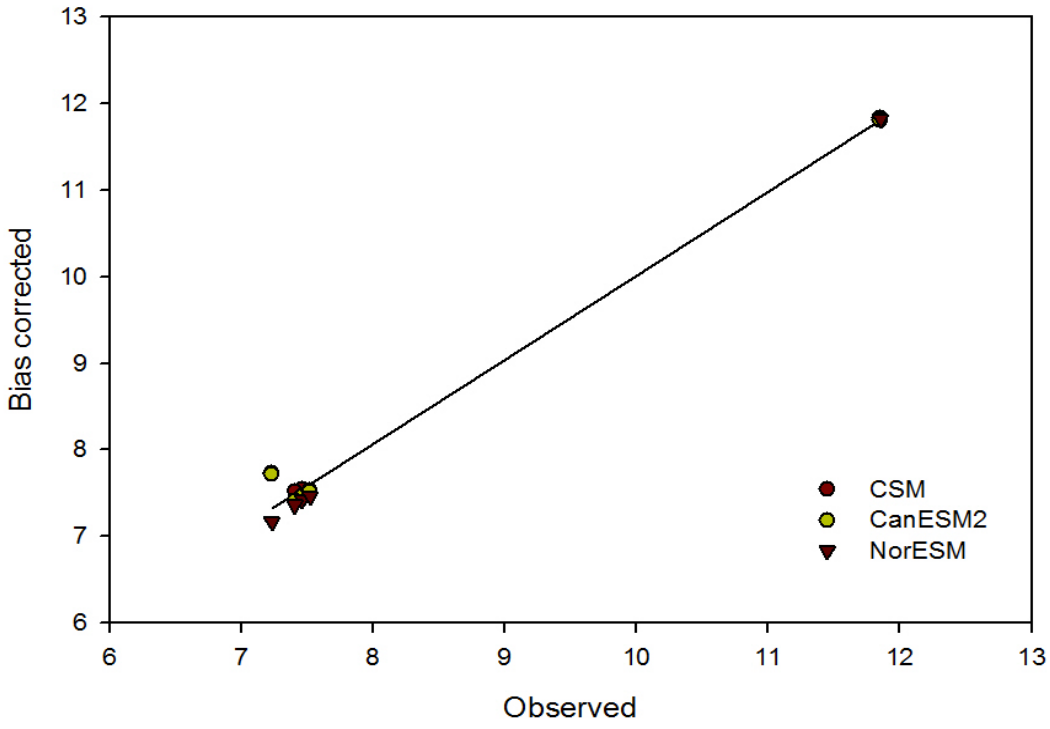

Figure 5.8: Scatter plot of observed versus Bias Corrected standard deviations (ppSD) of maximum daily temperature from 1990 –2004

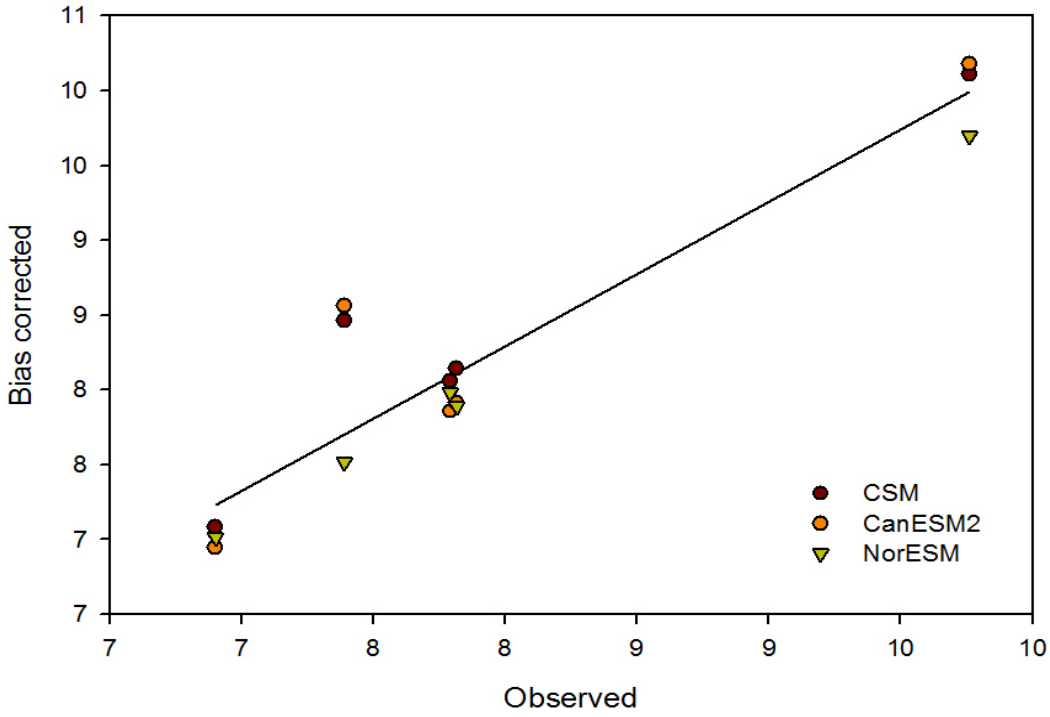

Figure 5.9: Scatter plot of observed versus Bias Corrected standard deviations (ppSD) of minimum daily temperature from 1990–2004

In addition to statistical indices, the performance of the bias corrected rainfall data was evaluated by hydrograph analysis. The SWAT model was run using these original rainfall data, bias corrected rain and GCM rainfall and keeping all the other parameters the same for baseline analysis. The results reveal that bias corrected rainfall predicted the flows very well, whereas the GCM rainfall was not able to simulate observed flow. The bias corrected rainfall picked all the high and low flows throughout the baseline period and the shape of the hydrograph was very similar compared to observed flows, whereas the GCM data under-predicted the flow for all seasons. The statistical indices for bias corrected rainfall and GCM rainfall for NorESM climate scenario is shown in Table 5.2.

Table 5.2: Statistical indices for flow using observed, bias corrected and GCM rainfall data from 1990–2004

Simulated flow	Rainfall type used to simulate flow		
	Observed	Bias Correction	Global Circulation Model
Mean flow (m^3/s)	307	281	36
Maximum flow (m^3/s)	963	996	355
Minimum flow (m^3/s)	35	10	7
Standard deviation	258	249	50

5.5 Conclusions

The climate change scenarios have been constructed as a part of the development of an integrated model. Three sets of GCM simulations driven by a high emission scenario (SRES A2) were selected for the current study: NorESM, CSM and

CanESM2. The transient time series data of rainfall and temperature (max, min) was generated from 2011–2098 for various gauging stations in the Mangla basin. The GCM's data for rainfall and temperature was corrected using bias corrected procedure. The output results were evaluated using the first two moments of the PDF: the mean (SDII) and standard deviation (ppSD) both for rainfall and temperature. The results indicate that BC rainfall and temperature data show very good agreement with observed data. In addition to these statistical tests, bias corrected rainfall and GCM rainfall data were also evaluated on a hydrological basis. The comparison of a hydrograph was made using these rainfall data (observed, BC and GCM) in the Mangla basin. The results show that BC rainfall data present almost the same shape of hydrograph compared to observed rainfall, whereas the GCM was unable to predict low or high flows.

CHAPTER SIX
LAND-USE SCENARIO BUILDING

6.1 Land-use component

For over a decade, understanding what causes changes in land-use and how to model these changes has become a very important scientific topic (Irwin and Geoghegan, 2001). It is believed that human-induced land-use changes can significantly influence regional and local climate (Pielke Sr et al., 2002). At a basin scale the changes can alter hydrological systems that may threaten water resources or cause more frequent floods.

There are many causes of changes in land-use or land cover. They may be classified as the i) proximate causes and ii) underlying causes (Geist and Lambin, 2001). The proximate causes are those directly affecting land cover. For example, shifting cultivation that leads to deforestation. In terms of scale, the proximate causes work locally. The underlying causes are the fundamental forces that drive the proximate causes from a higher hierarchy and are normally associated with socio economic factors such as population, household income, government policies, etc. (Turner II and Ross, 1993; Wood and Porro, 2002). The underlying causes can work at all scales from local, regional to national. Hence, the land-use changes are scale-dependent. Land-use change derived from biophysical factors such as environmental changes and climate change plays an important role in shaping landscape at a large regional scale, while slope, elevation, soil fertility, etc. are more important factors for land-use change on a more local scale (Jha et al., 2011).

There are many methods for modelling land-use, which have been developed based on various approaches such as remote sensing for monitoring as well as inventories (Kaufmann and Seto, 2001; Gross et al., 2006), probability models (Geoghegan et al., 1997), multiple regression models (Lin et al., 2011), and economic approach models (Anselin and Bera, 1998; Pinkse and Slade, 2010; Brady and Irwin, 2011). An early review was done by Lambin (1997) and the methods were classified based on the methodologies of how land-use changes may occur in the future, and what factors influence these changes. Irwin et al. (2001) also provided a review on land-use models, particularly spatially explicit models.

6.2 Selecting and adapting the appropriate method/model

Ideally, a land-use model for an integrated assessment should generate spatial land-use change scenarios at any time in the future, i.e. can answer questions of when and where the land-use change is likely to happen in the future. In addition, the model needs to be able to accommodate various policy interferences so that the impacts of such policy interference can be directly reflected in the land-use pattern. Therefore, policy-relevant driving factors or the underlying causes of the changes can be assessed. Based on these requirements, the dynamic spatial simulation model would be the ideal candidate for this study. The spatial system model employs general systems theory (Von Bertalanffy, 1968) and system modelling techniques (Odum, 1983) to identify the major components (stocks) and their relations (flows) for a land-use change system (Huang et al., 2007). It has been used in a variety of land-use applications with different scales, foci and locations (Santoso, 2003; Lonergan, 2005). This method is spatially explicit and can be

implemented through GIS software that includes neighbourhood connectivity functions or user-defined filters for convolution operation. During the modelling process, the neighbourhood cells are given certain values according to the degree of their influence on the cell in the centre when this central cell is transforming from one state to another. The assigned values are dependent on their states and distances from the centre. The resulting value from the neighbourhood cells will determine the new state of the nearby cell. However, the dynamic spatial simulation model requires a large amount of data and is highly computational demanding, making it inappropriate for this study. The Mangla basin is located in a trans-boundary region between Pakistan and India. It is a conflict area with loose boundary demarcation, hence is very difficult to collect the required spatial data. Data collected by authorities are normally confidential by nature and not available for public use. However, some spatial data were obtained from the Planning and Development Department, Muzzafarabad, for the Pakistan region. Considering the data availability, spatial information of the area and the purpose of the study, a land-use model was built using map algebra techniques.

What the proposed integrated model requires from the land-use components are scenarios that can be linked easily to the hydrological components. The model using map algebra has an advantage of directly processing the generated land-use patterns and displaying the output in the form of spatial distributions as required by the hydrological component, based on given underlying causes and proximate causes for land-use changes.

In this study, the underlying causes and the proximate causes are pre-selected to run the model. They are chosen with the aim of conducting sensitivity analysis

of the impacts of land-use changes on stream flows and reservoir sedimentation. This work does not intend to produce accurate or even practical future land-use scenarios but rather to analyse the changes of land-use under various driving causes or human interventions and the impact on sediment load generation.

6.3 How the scenarios are generated

The map algebra method has been successfully used for modelling land-use changes by many researchers (e.g., Youssef et al., 2010; Shirabe, 2012). The map algebra technique was firstly used by Tomlin & Berry (1979). It has the ability to develop a spatial system model and analyse complex land-use change systems. Huang et al. (2007) used this technique to analyse land-use changes for the Taipei metropolitan region in Taiwan.

Map algebra organizes and processes spatial data from different layers and produces an output layer based on specific criteria. It is widely used for analysing and synthesizing digital cartographic data. Map algebra decomposes the layers into fundamental components so that recombination of these components generates a wide range of flexibility. It defines the input layers by numeric values so that unequivocal mathematical operations can be created. The map algebra mathematical operations can be categorized into three classes: i) local, ii) focal and iii) zonal. In the local function, a new value is attributed to each location specified in the layer, whereas focal function assigns a new value as a function of all locations in the neighbourhood, and zonal assigns new values within a zone specified in the layer (Tomlin, 1994).

In this study, a simple spatial model was built on map algebra rules for the transition being defined with simple spatial analysis. Before constructing the

transition rules, there was a need to analyze the behaviour of land-use change, its distribution, and the possible driving factors of the change.

6.4 Behaviours of land-use change in the study area

Information about the characteristics and behavior of land-use changes is necessary for defining transition rules. It is also useful for assigning values to cells that may be influenced by changes in nearby cells.

A general hierarchical transition of land-uses in Himalaya has been reviewed by (Schickhoff, 1995). According to his finding, the forest cover of the Kaghan valley (lies in the Mangla basin) has decreased markedly (45%) since the 19th century. He argued that socio-economic conditions played the most important role in the dynamics of the land-use transformation.

A general transition hierarchy of land-use in Pakistan shows a pattern of land-use transition from rural to urban conditions. The urban area is at the top of the hierarchy. Inside the urban area, the open space can change to settlement, constructions and industries; in the area surrounding the urban area, agriculture can change to settlements; and in rural areas forest or rangeland can change to agriculture. In the next section, the pattern of future land-use transition for the Mangla basin is analysed on the basis of socio-economic conditions with available data from the Mangla basin lying inside Pakistan.

6.5 Socio-economic analysis

The main sources of income of the people are services, small businesses, rental income from properties in Mirpur and Islamabad and remittances from the UK

and other countries. People prefer government jobs, currently Kashmiri muhajir families mainly from Bagh and Bhimber districts, belong to the service group.

People who have settled abroad have the maximum proportion of their income from rental of their properties located in Mirpur, Jhelum, Islamabad, Rawalpindi and Dina. There is not much interest in investment in industry or other commercial development projects. Nevertheless, small-scale investments in Mirpur city have been being made in small businesses. The spatial distribution of human population in the Mangla basin was analysed using global population data (Gridded population of the World, version 2, (CIESIN) as shown in Figure 6.1. Mostof the area of the basin has less than 5000 people per km^2. There are only a few dense points of population in the basin: Srinagr, Muzzafarabad, Kotli and Mirpur, where average population is about 15000 people per km^2.

From 1981 to 1997 population growth rate was 2.4%, whereas the growth for the year 2007 is about 2.41% with a total population of 2972500 for Pakistan Kashmir. The most populated areas are Muzzafarabad (21.5%) and Kotli (19.5%).

The number of households in the same period (1981-1997) increased with an average annual growth rate of 7.69% for the Kashmir valley, whereas 48% of the people migrated from rural to semi-urban or urban areas from 1981 to 1997 (AJK, 1998). In comparison to the population growth, the number of households and urbanization grew very rapidly.

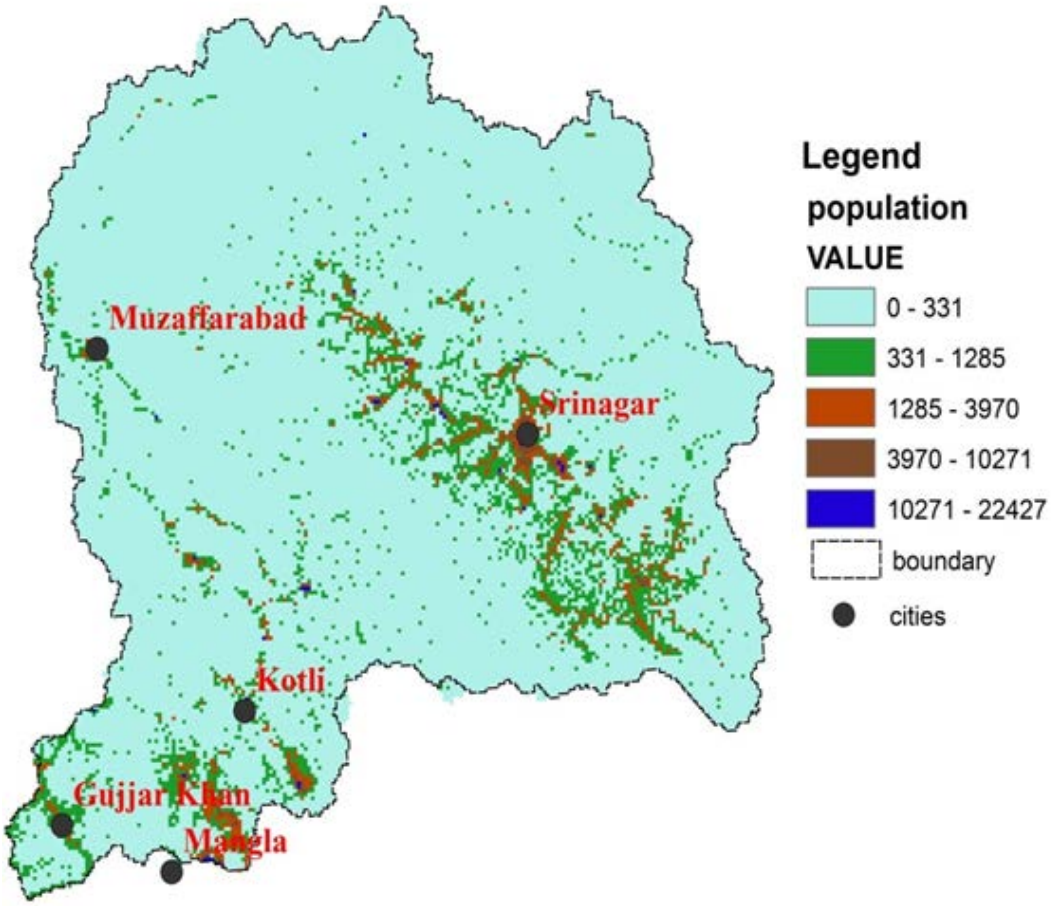

Figure 6.1: Spatial population distribution in the Mangla basin (people/km^2)

The increase in industrialization is one important underlying cause for the rapid expansion of urbanization. The total number of industry units in 1998 was 867 in Kashmir with poultry and woodwork being the two major industries with 552 and 255 units, respectively (AJK, 1998), increasing to 1,465 industry units in 2007 (AJK, 2007). The increase in population is also significantly related to the increase of conversion of forest to agricultural land. The growth in agricultural crop area has been about 0.59% annually from 1990 to 1998 (AJK, 1998) and accelerated to 1.34% for 1998 to 2007 (AJK, 2007). Khan (2009) assessed the linkages between poverty and deforestation in the Swat valley which

is situated in the Northwest of Pakistan. According to his finding, forest cover has shrunk since 1969 along with an increase of 27% in agriculture land.

From this statistical information of the study area, the literature review regarding land-use change in Pakistan, and expert knowledge based upon field observations in October 2009 and March 2011, the information of the likely transition from one land-use type to another type is summarized as follow:

- The forest area shrinkage is due to an increase in agriculture area
- The increase in agriculture area is due to an increase in population size
- The increase in urban area is affected by the number of industries and schools.

It should be noted that there are no consistent criteria about land-use conversion hierarchy. It is also likely that agricultural area can be converted into settlement/industrial areas, or forest into settlement/industrial areas (Santoso, 2003).

6.6 Rules of transitional hierarchy in the study area

A schematic hierarchy of land-use transition in the study area can be drawn from the above discussion and Figure 6.2. The purpose of this figure is to illustrate a simple transition rule for main land-use types. In reality, land-use transition from one type to another is much more complicated, and involves detailed transition rules between land-use types or even for one land-use type itself, such as evergreen forest, mixed forest to close row grown crops or generic agriculture, and transition from one agriculture type to another agriculture type. Land-use

conversion may not have a sequential order, but for the study area it has to follow the transition rule from a low state in the hierarchy to a higher state due to the socio-economic development needs.

For the present study, forest was regarded as the lowest state in the land-use change hierarchy and settlement, the highest. It is very likely that forest can change to rangeland, agriculture and settlement, whereas the probability of settlement to forest or agriculture is very low unless it is forced by outside human interventions such as legislations or regulation by government.

6.7 Influence of physical factors on land-use distribution

Land-use is influenced by the land characteristics such as slope, elevation, and distance from the main road. In general the urban areas are located mostly on flat land. The slope for the urban area is between 0.1 to 1%. The average slopes for three agricultural classes AGRC, AGRR and AGRL is 3.14%, 9.80% and 7.75%, respectively. Most of the agriculture in the basin is located on flat lands with 46% of the agriculture land having a slope between 0 to 5%. However, there is about 2% agricultural land that has a slope of 20% or above. The average slopes of the forest land and rangeland is 11% and 12%, respectively (Figure 6.3).

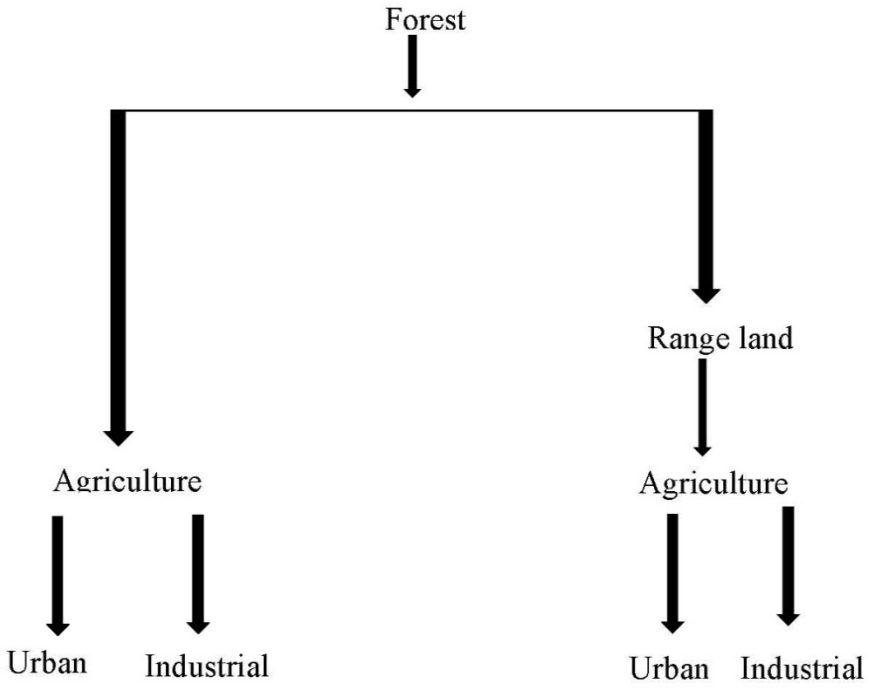

Figure 6.2: Land-use transition in the Mangla basin

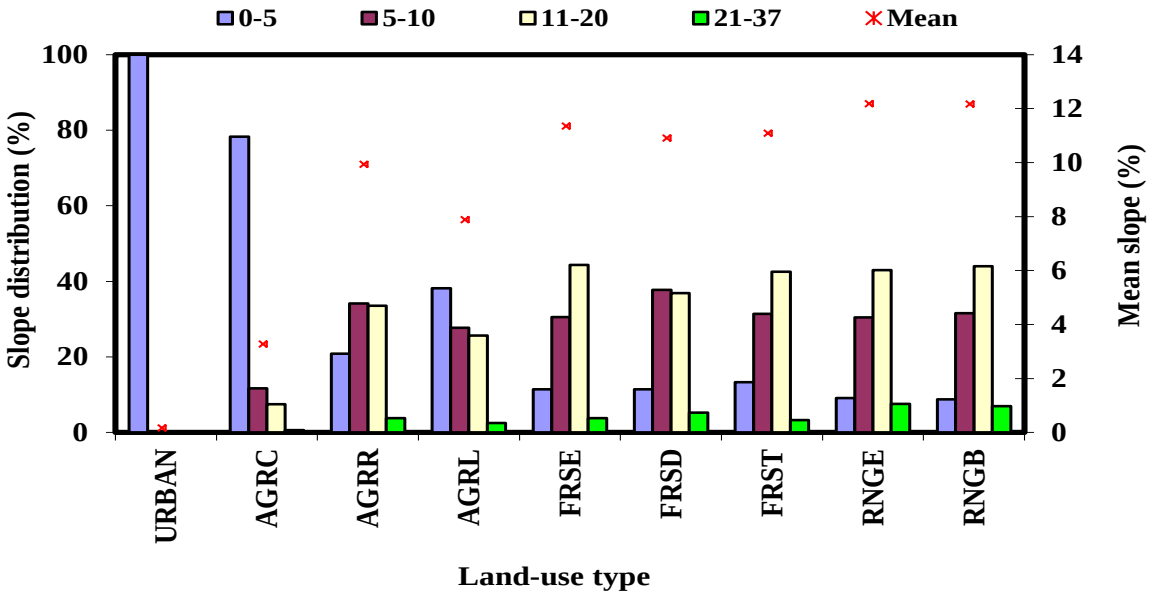

Figure 6.3: Distribution of land-use types with respect to slope where URBAN, AGRC, AGRR, AGRL, FRSD, FRST, RNGE and RNGB are SWAT model land-use types and represent urban land, Agricultural Land-Close-grown, Agricultural Land-Row Crops, Agricultural Land-Generic, Forest-Evergreen, Forest-Deciduous, Forest-Mixed, Range-Grasses and Range-Brush

The urban area is distributed on relatively low elevations from 340 m to about 460 m with a mean elevation of 400 m. Agriculture and rangeland are distributed over

a wide range of elevations from 340 m to about 4000 m. The mean elevation of the various agricultural classes in the basin is about 1800 m, while mean elevation of the forest and rangeland is about 2250 m and 3500 m. Usually rangeland is located at high altitudes. The mean elevation of each land-use class and distribution of elevation between 0–1,000 m and more than 3,500 m is shown in Figure 6.4.

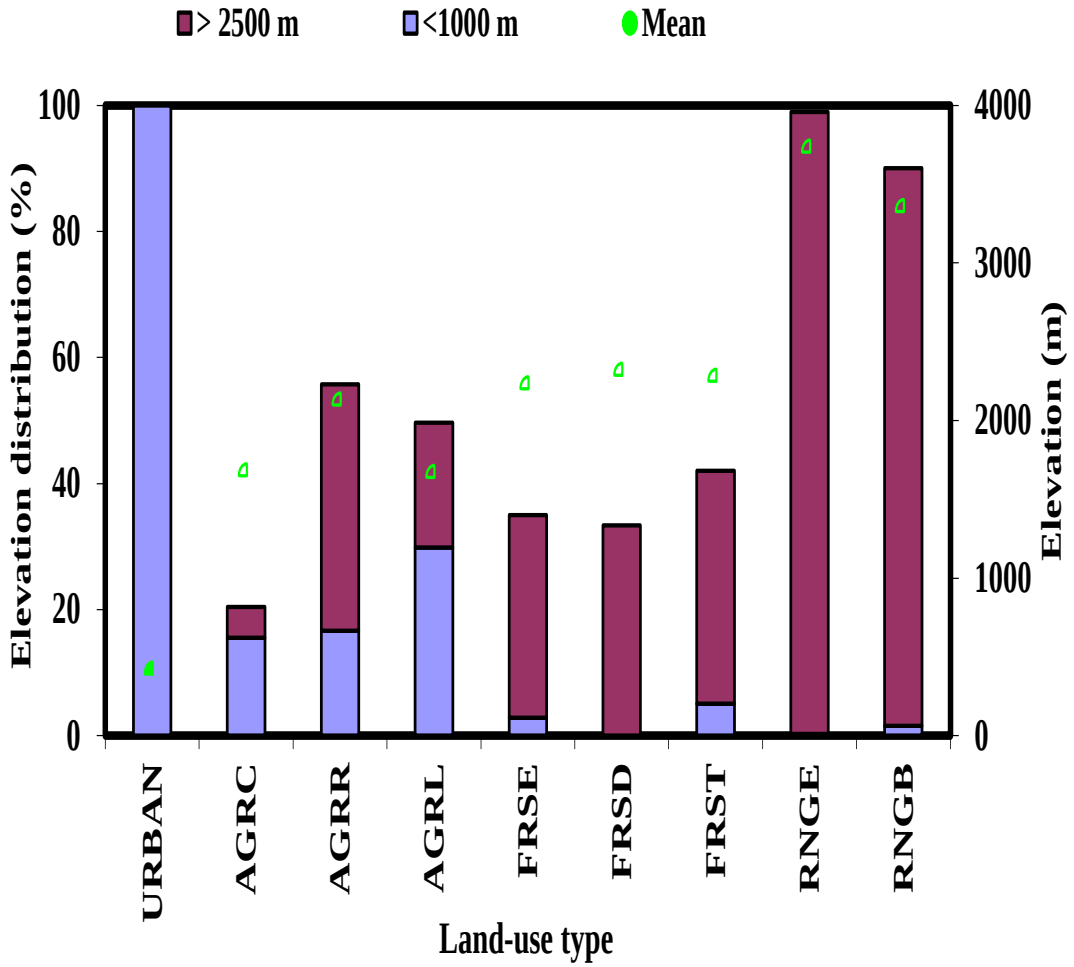

Figure 6.4: Distribution of land-use types with respect to elevation where URBAN, AGRC, AGRR, AGRL, FRSD, FRST, RNGE and RNGB are SWAT model land-use types and represent urban land, Agricultural Land-Close-grown, Agricultural Land-Row Crops, Agricultural Land-Generic, Forest-Evergreen, Forest-Deciduous, Forest-Mixed, Range-Grasses and Range-Brush.

Road network plays a vital role in shaping the land-use. When constructing the scenarios of land-use patterns, the road network information is required in order to develop realistic scenarios of land-use change patterns. In particular, urban areas prefer to be located adjacent to the main road. It is also preferable for some agricultural land to be located near roads for easy access to market. The main road is considered to have no influence in land-use distribution beyond a certain distance. Santoso (2003) found that beyond 3500 m, the main roads had no influence on the distribution of the land-use for his study area in Indonesia.

Figure 6.5 shows the distribution of urban areas with respect to the distance from the main road. It shows that the majority of urban areas are located mostly very close to the main road (0–1000 m) with mean distance of 438 m, whereas agricultural land is distributed between 0 to 11000 m with the average distance of 1458 m. More than 54% of agricultural land is located from 0 to 1000 m and only 5.4% agricultural land lies above 4500 m away from main roads. Forests and rangeland locate far away from main roads with a mean distance of 2000 m and 2347 m, respectively. Clearly, there is a preference for urban areas to be located in places that are easily accessible, indicating that increases in urbanization in the future are likely to take place near the main road provided that sufficient space is available.

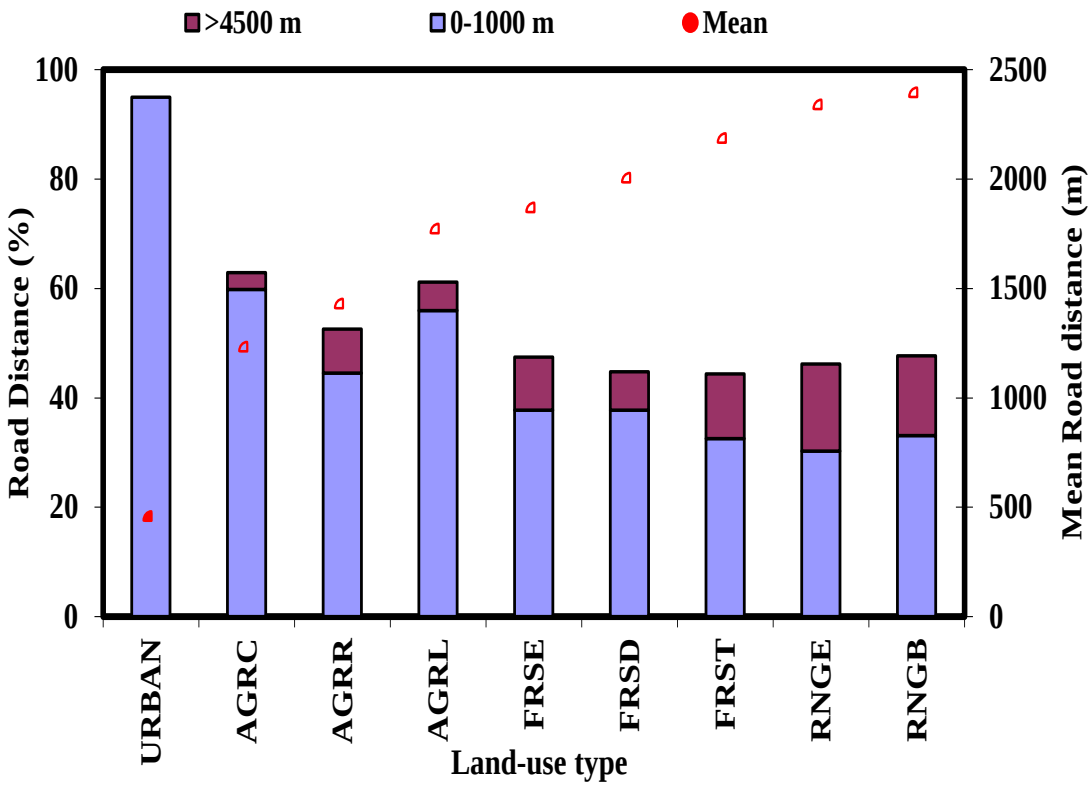

Figure 6.5: Distribution of land-use types with respect to road distance where URBAN, AGRC, AGRR, AGRL, FRSD, FRST, RNGE and RNGB are SWAT model land-use types and represent urban land, Agricultural Land-Close-grown, Agricultural Land-Row Crops, Agricultural Land-Generic, Forest-Evergreen, Forest-Deciduous, Forest-Mixed, Range-Grasses and Range-Brush.

6.8 Using GIS for generating land-use scenarios

A GIS spatial model was used to construct the scenarios based on map algebra techniques. Firstly maps for land-use, slope, road and population density, and a digital elevation model were prepared for the study area. The population data were extracted from the global data set. The land-use and slope maps have already been discussed in section 3.3 Chapter 3, the digital elevation model of the study area is discussed in section 4.1.1 Chapter 4, and the population density map is discussed in section 6.5, Chapter 6. The road map of the study area was prepared using

topographical sheets of the region at 0.25 m from the Survey of Pakistan (http://www.surveyofpakistan.gov.pk/).

Map algebra techniques were used to construct new scenarios. The input layers of population, slopes, elevations and road distance were used to generate the new land-use type layer; the attribute value assigned to each raster in the output layer is the function of the independent value associated with location of input layers.

Three possible scenarios for the future have been selected with possible land-use patterns. Each scenario comprises some defined conditions based on socio-economic analysis and physical factors that will determine the future patterns of the land-use. The scenarios are: business-as-usual, pro-industrialization, and pro-agriculture. These are given below.

- **Business-as-usual**

The business-as-usual scenario was based on conditions that land-use change is kept constant and there is no large change in agriculture or forest. It can be termed as a reference scenario. In this scenario population growth has increased but there is no increase in urban area or agriculture.

- **Pro-industrialization**

The pro-industrialization scenario is based on the conditions that some agricultural land is expected to become part of urbanization and settlements. Industrialization usually provides more job opportunities in various sectors such as transportation, services, etc. in the cities so that more people relocate to the urban area, which in turn causes an increase in urbanization and demand for settlements (Santoso, 2003). For the current study, considering the population

density and other socio-economic indicators of the area, it was assumed that agricultural land with a population of more than 15000 and relatively low slope (2 to 4%) and closer to roads will convert into urban area.

- **Pro-agriculture**

In this scenario, the agricultural sector is encouraged. It is assumed that most of the land that is suitable for agriculture and currently not used will be transitioned to agricultural practices. For example, the forest or rangeland close to the roads and suitable for agriculture in terms of slope and elevation that has more than 5,000 people per km^2, is expected to change into agriculture land. The rates of change for the land-use must be known for generating a time series of change in land-use pattern, at least the rate of change of the land-use at the highest state in the hierarchy, which is the urban area. By knowing the rate of change of the urban area, the growth of the urban area for a specific year can be calculated. Subsequently, a time-series for change in land-use can be produced.

However, the rate of urbanization in the study area has not been well studied or documented. The rate of urbanization in Pakistan is about 3% per annum (Wareing and Shei, 2010). There has been a significant increase in agricultural area in the selected study area during the last decade or so, with the cropped land increasing by 13% from 1997 to 2007 in the Kashmir (AJK, 2007).

For this study, the rate of land-use change relies only on the growth rate of the socio-economic parameters (population growth rate) and physical parameters such as slope, elevation and road distances. Population growth was considered the main driver for land-use change because it controls directly the demand from

society. The characteristics used for the generation of the scenarios are given in Table 6.1 as shown below.

The map algebra process was employed for the transition of land-use type fulfilling all four conditions, i.e., agricultural land will be converted to urban land if population in that specific cell is more than 20,000, elevation is more than 750 m, slope is more than 4% and distance from the main road is 1,500 m.

Table 6.1: Summary of factors influencing land-use transition for the 2030 scenario

	Influencing factors	**Change of land-use type**		
		Agriculture to urban	**Forest to agriculture**	**Rangeland to agriculture**
Business-as- usual	Population (people/km^2)	> 20,000	> 10,000	> 10,000
	Elevation (m)	< 750	< 1,800	< 1,800
	slope (%)	< 4	< 7	< 7
	distance from main road (m)	<1,500	< 3,500	< 3,500
Pro-industrialization	Population (people/km^2)	> 15,000	> 12,000	> 12,000
	Elevation (m)	< 800	< 1,800	< 1,800
	slope (%)	< 5	< 7	< 7
	distance from main road (m)	<1,500	< 3,500	< 3,500
Pro-agriculture	Population (people/km^2)	> 15,000	> 5,000	> 5,000
	Elevation (m)	< 750	< 2,000	< 2,000
	slope (%)	< 4.5	< 10	< 10
	distance from main road (m)	<1,500	< 4,000	< 4,000

6.9 Conclusions

The land-use change scenarios have been constructed as part of the development of an integrated model. Three sets of policy-relevant scenarios have been developed: business-as-usual, pro-industrialization, and pro-agriculture. Each scenario generates a time-series of land-use change patterns for the year 2030.

These land-use change patterns have been created, based on the principle of map algebra technique. The socio-economic and physical factors have been considered for the generation of scenarios. The land-use change patterns can also be transformed into a time series by knowing the rate of change of the most important land-use types that drive the whole change in pattern. The land-use future scenarios for year 2030 are shown in Figures 6.6 to 6.9. The results show that there is a 38% increase in the urban area in the pro-agriculture scenario and an almost 200% increase in urban area for the pro-industrial scenario with respect to the business-as-usual scenario. Similarly, agricultural area is increased by 1.50% for the pro-agriculture scenario. The increase in agricultural area is also justified from the historical statistics of the study area.

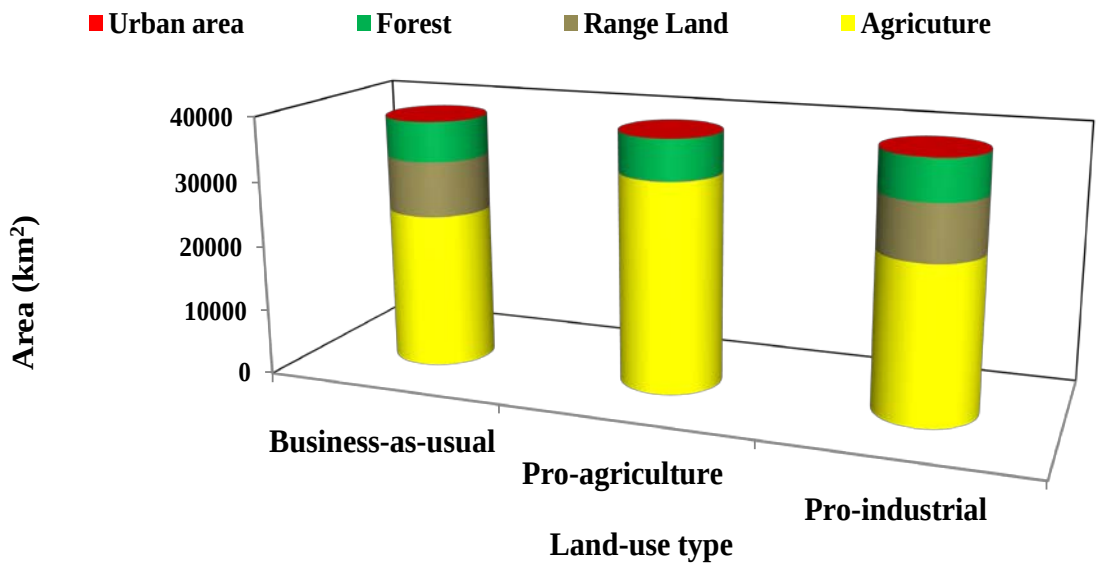

Figure 6.6 Summary of factors influencing land-use transition for the 2030

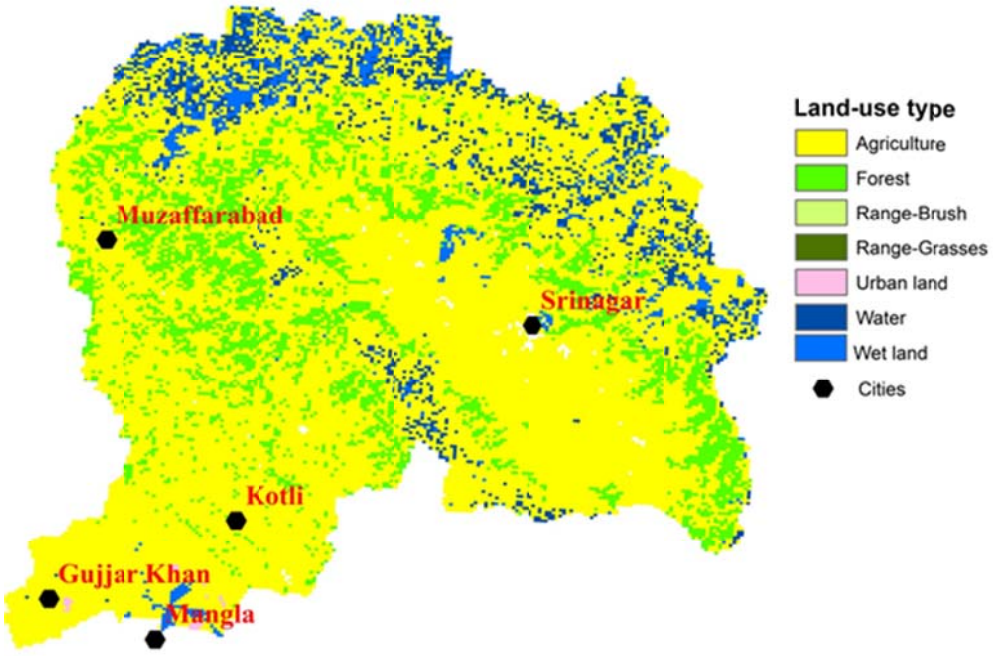

Figure 6.7: Land-use scenario business-as-usual for 2030

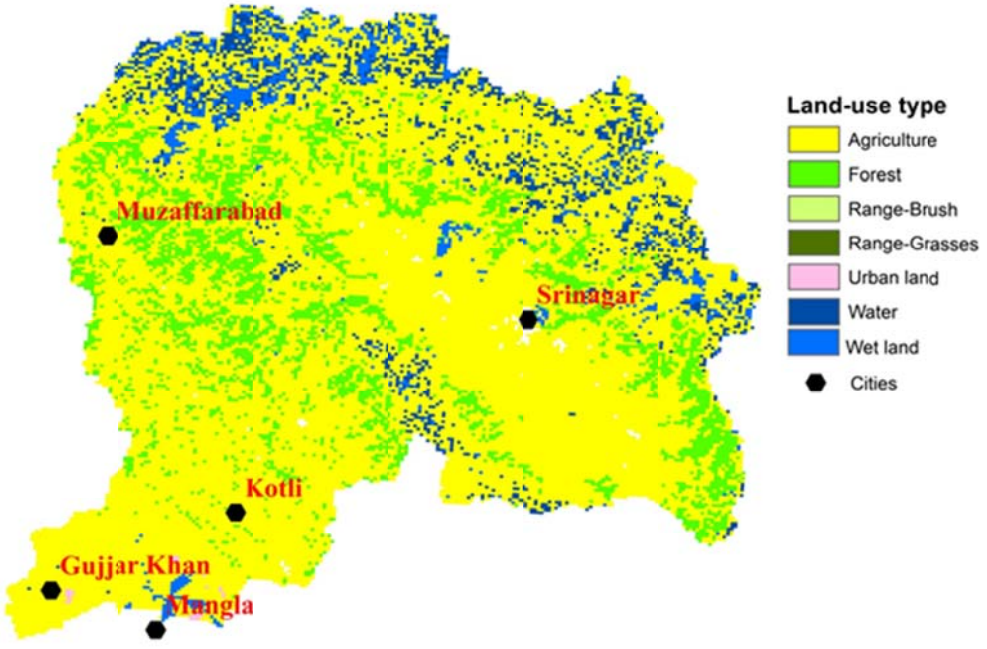

Figure 6.8: Land-use scenario pro-agriculture for 2030

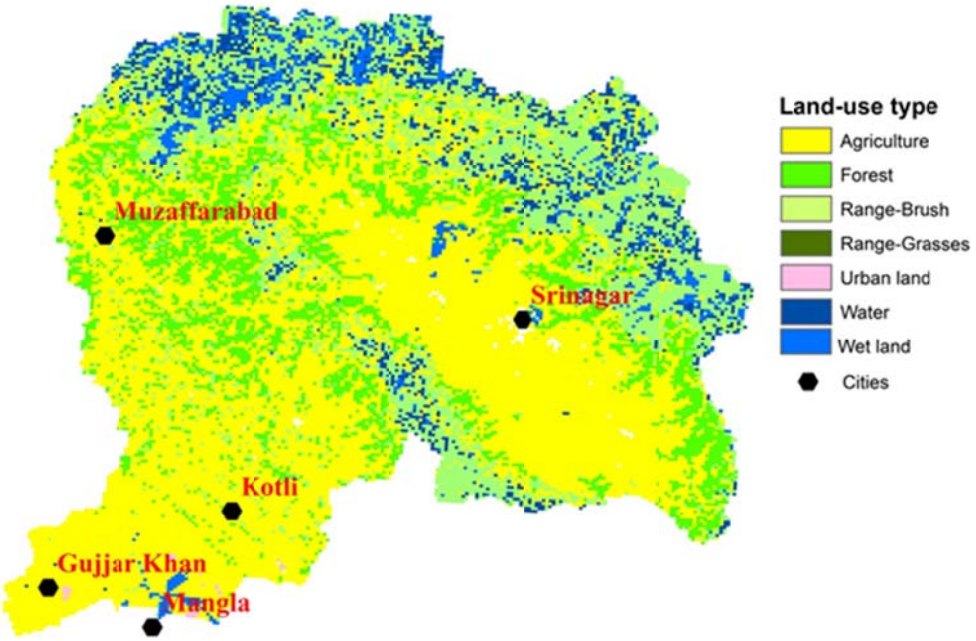

Figure 6.9: Land-use scenario pro-industralization for 2030

CHAPTER SEVEN
RESULTS OF THE INTEGRATED MODELING SYSTEM

The previous chapters discussed the development of a reservoir life assessment model by integrating the land-use, climate and sediment components in one framework. The model has the specific purpose of conducting sensitivity analysis on reservoir sedimentation with respect to changes in land-use and climate, and combinations thereof. The model has been applied to the Mangla Reservoir basin and this chapter discusses the application results with detailed assessment of the effects of land-use and climate changes on the reservoir sedimentation and reservoir life. The assessment is conducted for various land-use change and climate change scenarios, as well as for their various combinations. Land-use management as an adaptation option is assessed based on its effects on reservoir life. Finally, this chapter makes an evaluation of the integrated model based on the assessment results.

7.1 Controlling parameters and simulation conditions

The model simulation was carried out under the following conditions:

a) All the parameters/assumptions used on hydrological/sedimentation characteristics of the basin were obtained or calibrated based on historical data and remained the same for future climate change scenarios.

b) Sediment load simulated by the model for the period of 1990 to 2005 is used as the baseline condition.

c) Economic analysis was based on the data of the statistical year book of Azad Jammu and Kashmir (2007), and farm inputs were derived from the Mangla Dam Raising Project, Project Planning Report (2003).

The integrated model allows simulation experiments of climate change under various conditions. Ideally, impact results from multi GCMs on the basin sedimentation and reservoir life are needed in order to reveal not only the potential changes but also the range of changes resulting from climate change. For the present study three GCMs (i.e., CSM, CanESM2 and NorESM) were used for daily outputs from 1990 to 2098 driven by the IPCC SRES A2 emission scenario. A bias correction technique was applied to the GCM outputs to produce the localized daily rainfall and daily temperature data from 2011 to 2098. The data was then used to drive the hydrological model and simulate reservoir sedimentation and reservoir life for future climate change impact assessment.

7.2 Climate change impact on sedimentation and reservoir life

There are only three transient climate scenario data from GCM results. Although very limited, the combination of these data may still provide an opportunity to determine the range of uncertainty of the climate change projections. The climate change impact on the annual sedimentation was assessed for 2030, 2050, 2070 and 2098 relative to the baseline conditions (1990–2004) (Figure 7.1). The annual average sediment between 2010–2030 for NorESM and CanESM2 increased by 13 and 14%, respectively, from the baseline, whereas it remained unchanged for the CSM scenario. All the scenarios showed an annual sediment load increase for periods after 2030 from the baseline, with a maximum increase of 22% for CanESM2 for the period 2071–2098. The mean annual sediment increase for the whole period of 2012 to 2098 for NorESM, CanESM2 and CSM are 15, 8 and 14%, respectively, from the baseline. For the same period, the variation in the sediment amount for different GCMs is quite large. As the rainfall amount and

rainfall frequency are the driving forces in generating sediment, the large variation between GCMs might be due to the natural rainfall variability in the GCM simulation, but most likely it implies high uncertainties represented by the differences of GCM used.

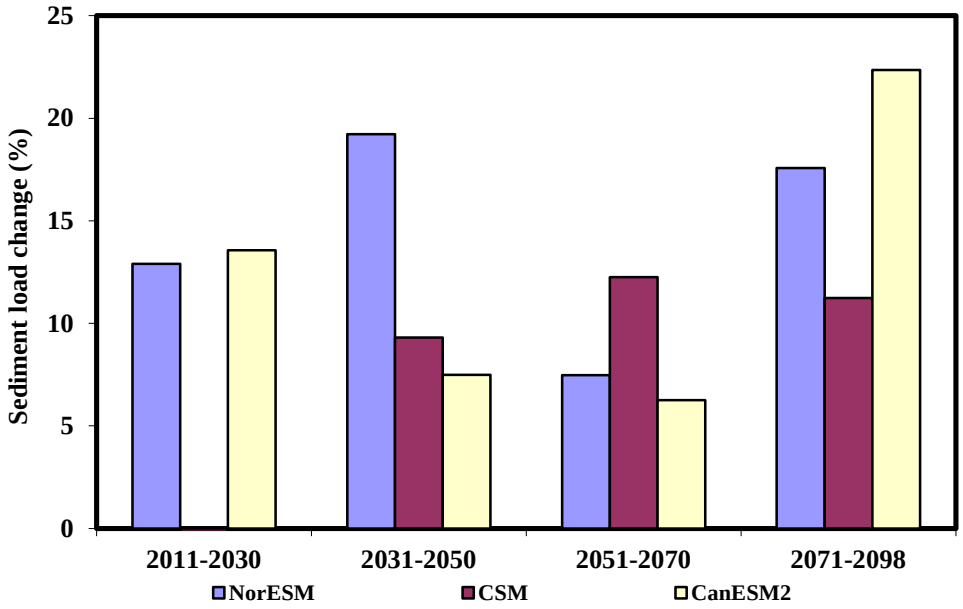

Figure 7.1: Sediment discharge changes to the baseline period (1990–2004) at basin outlet for the three GCM scenarios

For the same GCM, the variation in sediment for different time spans (Figure 7.1) can be explained by variations in extreme rainfall events in the future. There is large variation in rainfall magnitude for extreme events in GCM data for various gauging stations. The magnitudes of rainfall for a 20 year return period (NorESM scenario) with mean annual rainfall for various time spans is shown in Figure 7.2. The results indicate that the magnitude of rainfall for extreme events is very different for all the gauging stations in the future and may produce a large variation in sediment load. There is a large variation in extreme rainfall in Domel, Naran and Palandari gauging stations, whereas change in mean annual rainfall is not markedly high. As discussed in Chapter 4, extreme rainfall events can produce

a large amount of sediment load that may cause strong variability in sediment load in each time span.

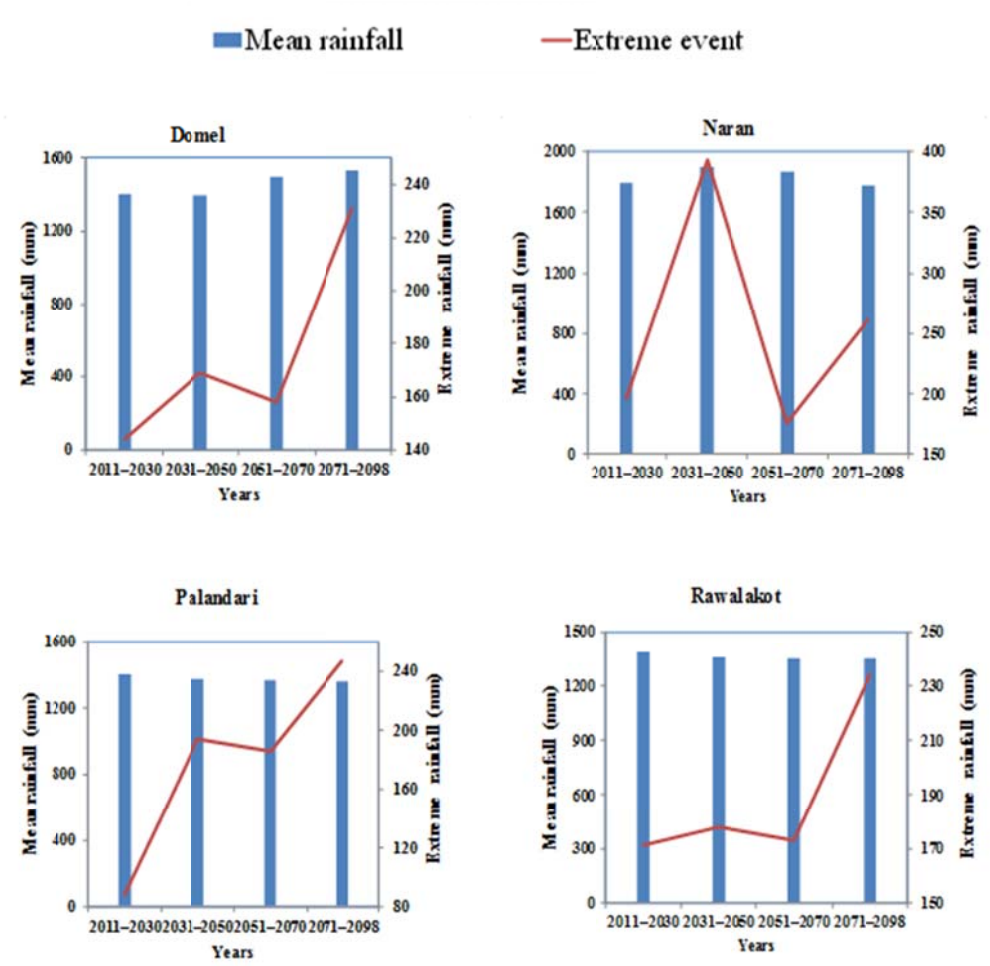

Figure 7.2: NorESM mean annual rainfall and extreme rainfall events for twenty years return period for various gauging stations in the Mangla basin

To support the simulated sediment calculations, the model has been further evaluated with the rainfall pattern. Figure 7.3 shows the annual mean rainfall pattern for the periods 2012–2030, 2031–2050, 2051–2070 and 2071–2098 of NorESM. The results indicate that rainfall is generally higher for the 2031–2050 scenario compared to 2012–2030 with a varied change pattern. The seasonal and inter-annual variability of rainfall have caused the variation in the sediment

transported in the river reaches. The spatial sediment variation driven by the NorESM scenario for the whole basin is shown in Figure 7.4. The spatial variation in the sediment shows that most of the sediment amount is generated in sub-basin 4. This is due to a prominent increase in the flow of the river Jhelum after the Domel gauging station.

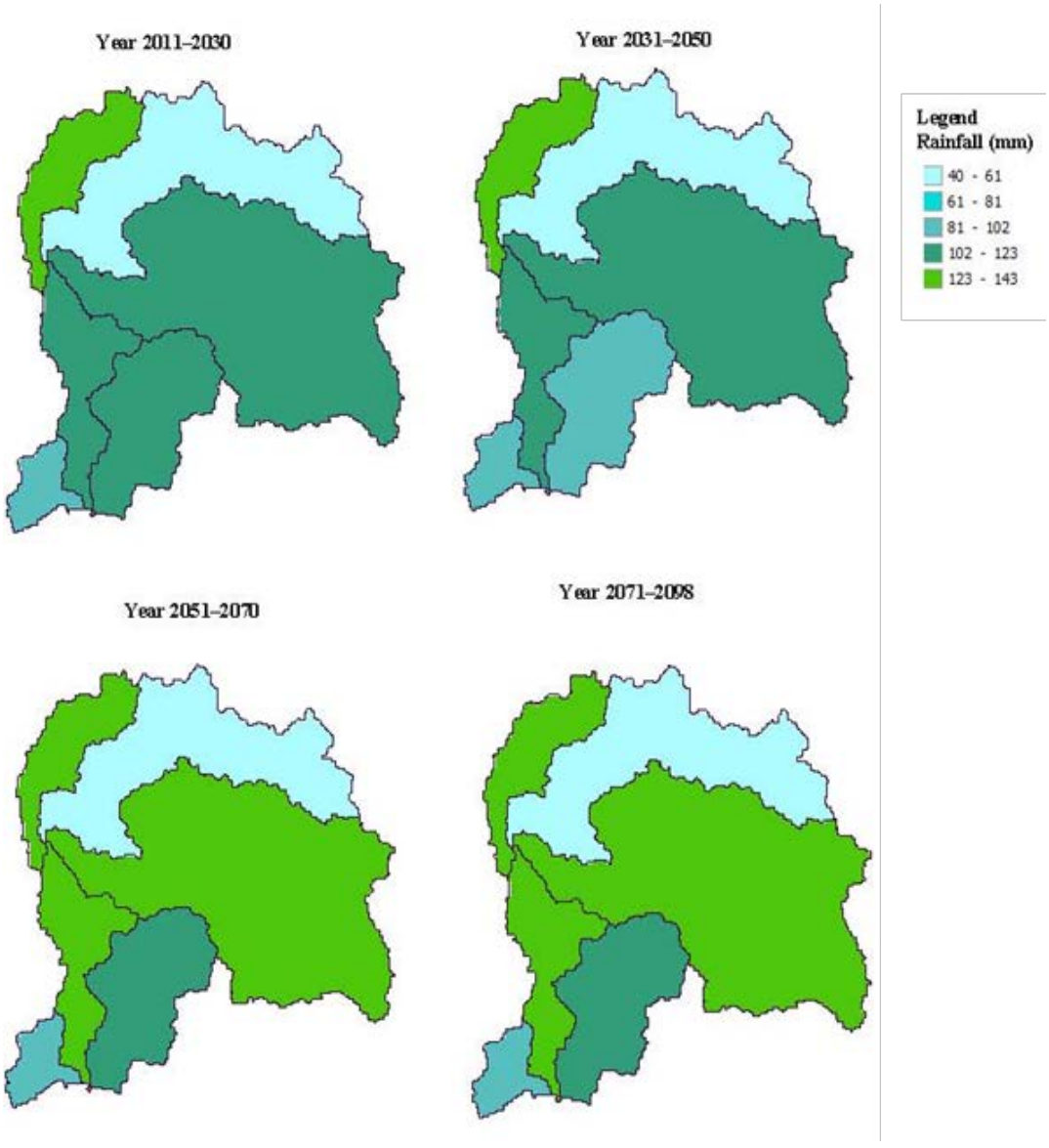

Figure 7.3 NorESM mean annual rainfall projection for each sub-basin (mm)

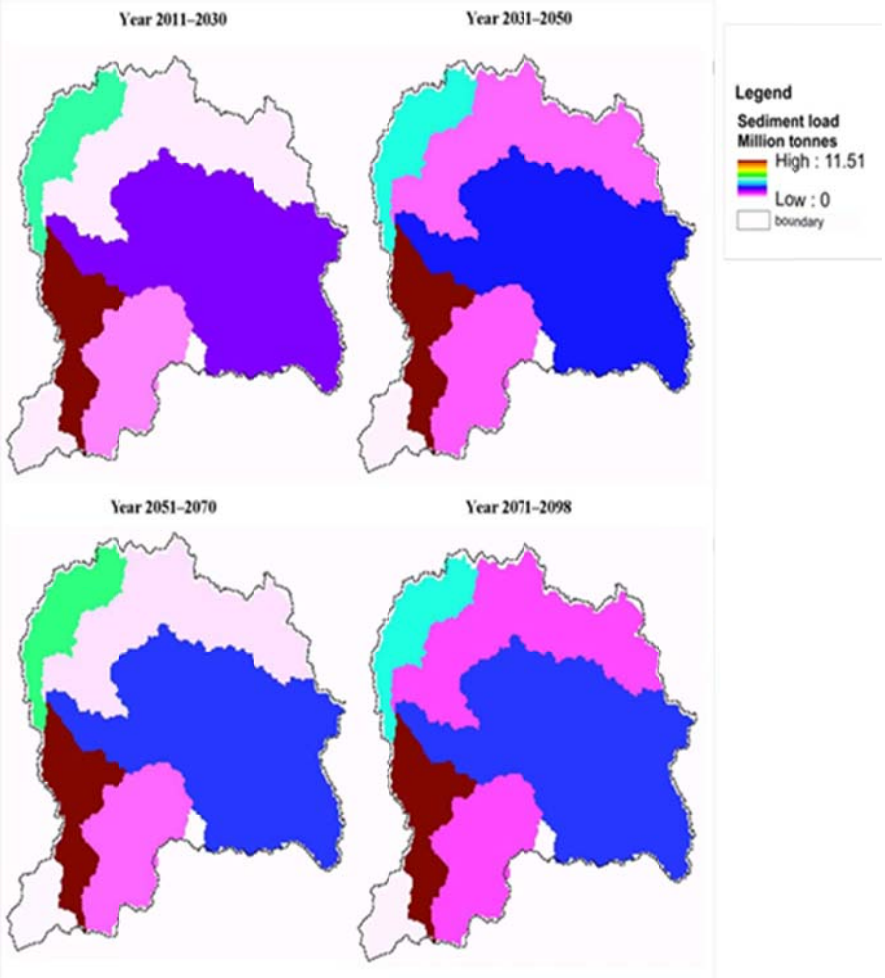

Figure 7.4: NorESM projected mean annual sediment load (Million Tonnes) from each sub-basin

Figure 7.5 demonstrates the seasonal variation of the sediment discharge. There is an increase in sediment deposition at the Mangla outlet for the monsoon season (July to September) for all the scenarios. CanESM2 also simulates higher sediment for the spring season compared to baseline. The variation in sediment in the spring can be linked with early snow melt in the basin due to high temperatures in the spring, whereas during the monsoon there is a probability of more frequent and intense rainfall. The sediment depositions for NorESM,

CanESM2 and CSM are about 27%, 45% and 26%, respectively. Clearly, the monthly results suggest that the increase in sediment mostly occurs in the monsoon season.

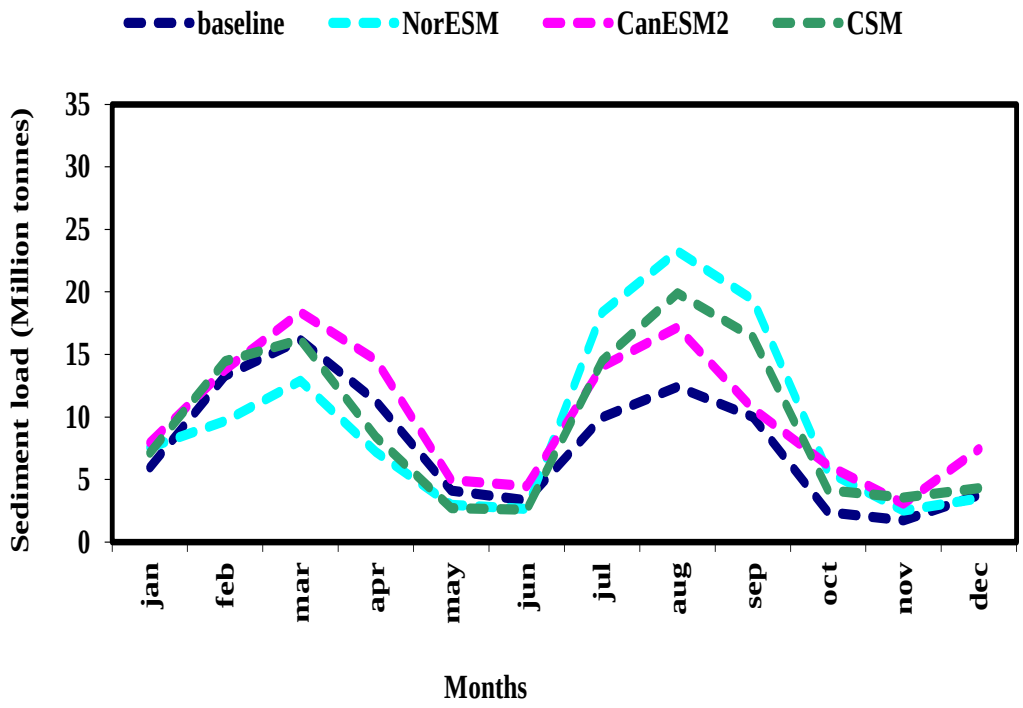

Figure 7.5: Long term monthly sediment load at Mangla Dam outlet for various climate change scenarios

7.2.1 Seasonal variation in the sediment

The seasonal sediment load variability can be derived from the sediment load in different seasons. The maximum sediment in the Mangla Reservoir sediment occurs in the spring and Monsoon seasons from March to September. The total sediment load in these months is about 71% for the baseline period (1990–2005). The future projection shows variability in the sediment load in the seasons. The NorESM scenario produces about 74% sediment load of the mean annual sediment load from spring to the Monsoon season between (2011–2098), whereas the CanESM2 scenario projects less sediment load from March to September

(68%) and the CSM scenario virtually shows no change in seasonal sediment load variability for the period (2011–2098) compared to baseline (Figure 7.6). In many cases, the changes in seasonal variability may also be followed by a change in the overall annual sediment load that may obscure the changes in variability. The seasonal variation in the sediment load reflects the variation of rainfall pattern and frequency in this region.

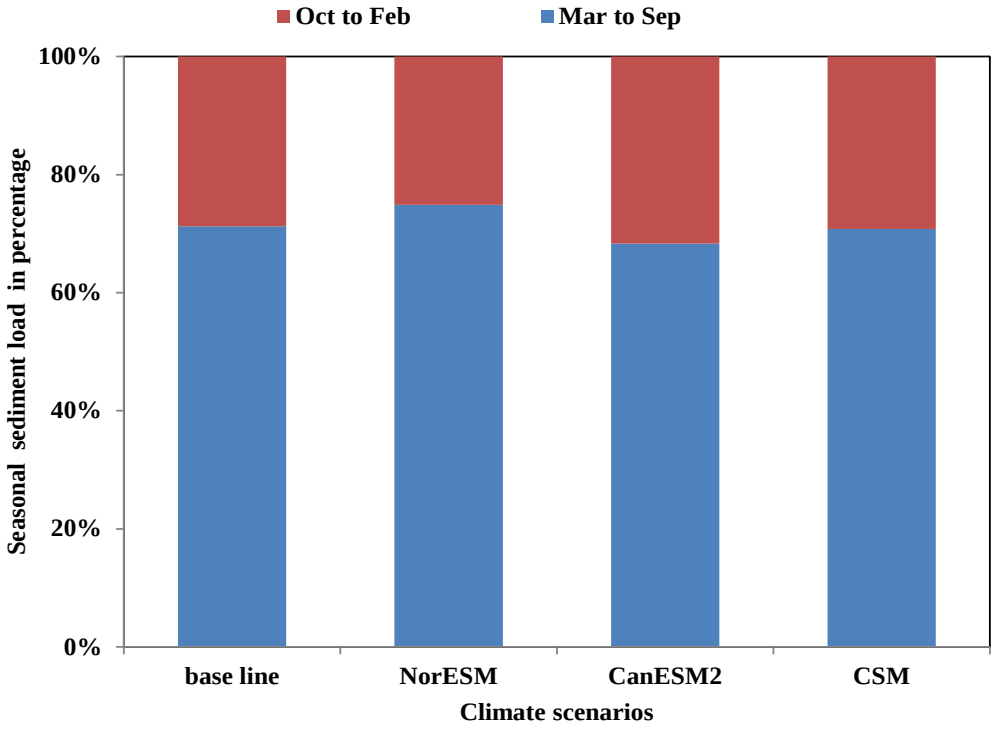

Figure 7.6: Seasonal sediment load pattern for various climate scenarios relative to the total sediment load.

7.2.2 Climate change impact on reservoir life

The loss of storage capacity has always been recognized as an issue which affects both the long-term operation of the Mangla Reservoir and future storage developments on the Jhelum River and its tributaries. The reservoir life is computed in time-series with respect to the selected policy scenarios. The climate data from three GCM runs (i.e., CSM, CanESM2 and NorESM) under the SRES

A2 scenario were used. A transient simulation was carried out starting from 2011 to 2098 using the Brune curve (1953). This curve relates the inflowing sediment load proportion retained in the reservoir to the volume of the reservoir. The Mangla Dam is planned to be raised by 9.14 m with a 0.60 m high wave protection wall on the crest. This would raise the maximum reservoir conservation level by 12.19 m. The proposed capacity of the dam after the raising project will be 6461 Mm^3 (MJV, 2003). Currently the project is in construction phase. Sediment density is calculated for the reservoir using standard unit weight and the USBR equation. Trap efficiency of the reservoir is considered to be 90%.

The results show that reservoir life is depleted very rapidly with the NorESM and CanESM2 climate scenarios and relatively slow depletion for CSM. The remaining capacity of the reservoir for the year 2098 is projected as 2080 Mm^3, 2114 Mm^3 and 2553 Mm^3 for NorESM, CanESM2 and CSM scenarios, respectively (Figure 7.7). The reservoir life capacity will be about 2897 Mm^3 in the year 2098 by considering the baseline sediment load deposition in the Mangla Dam outlet from 2011–2098.

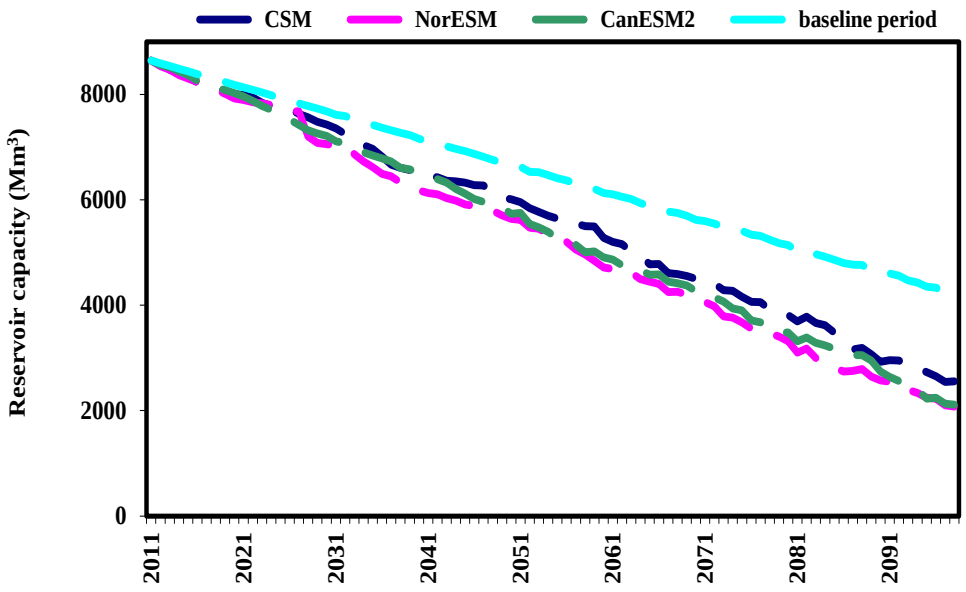

Figure 7.7: Reservoir capacity change from baseline and various GCM climate scenarios

7.3 Combined climate and land use change impact on reservoir

The previous sections discussed the influence of climate change on river sedimentation and reservoir life for the Mangla basin. Reservoir sedimentation and reservoir life was further analysed for the combined influence of climate and land-use changes, using the three policy-related land-use change scenarios discussed in chapter 6. There are a number of combinations of the land-use and climate change scenarios and this section only focuses on selected combinations of land-use and climate change scenarios. In general, the pro-agriculture scenario produces the highest annual sediment load among all change scenarios. The effect of this scenario is greater with time, when more land is shifted towards agriculture. The pro-industrialization scenario shows an increase in the annual sediment load, whereas the business-as-usual shows almost no change in the annual sediment load. The mean annual increase in sediment load for 2031-2098 is about 43% from

baseline with the pro-agriculture land-use scenario under NorESM, but increases 15% if there is no land-use change for the same period. The pro-industrialization land-use change produces similar results for the same GCM, with the annual increase in sediment being about 39% from baseline with land-use change from 2031-2098. It is clear that land-use change will have a marked impact on the sedimentation of the study area later in the century, as sediment load is reduces from 2051-2070 from the baseline without climate change, while it will continue to increase under the pro-agriculture and pro-industrialization scenarios as shown in Figure 7.8. This might be due to intensification of cultivation area in pro-agriculture and pro-industrialization land-use scenarios.

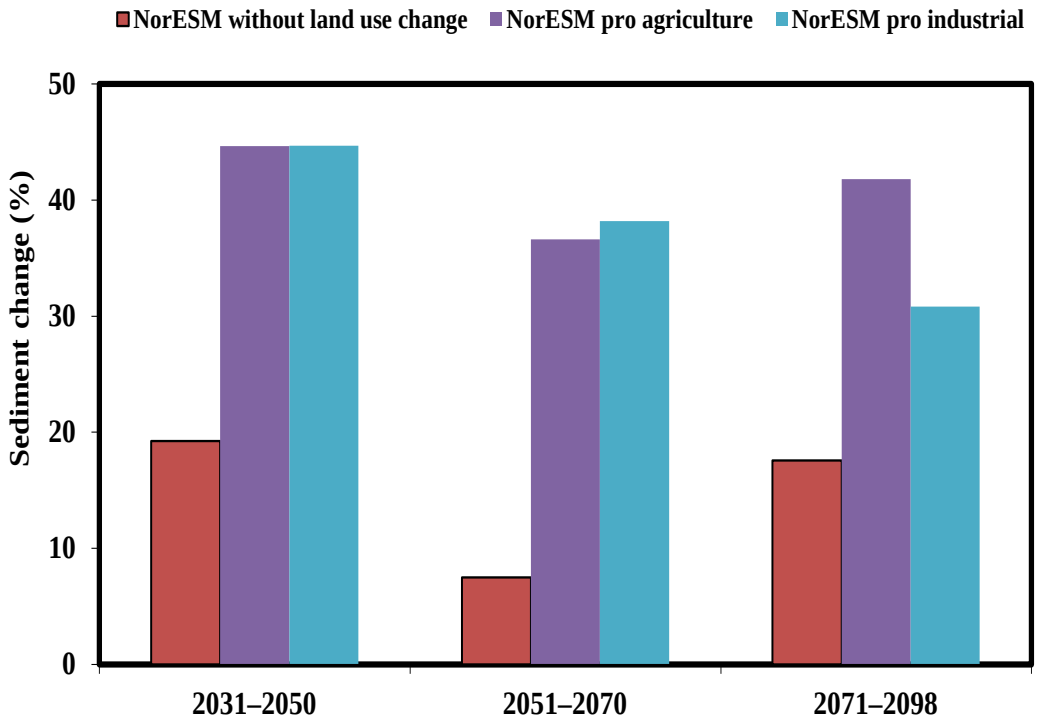

Figure 7.8: Change in annual sediment discharge at the Mangla Dam outlet from baseline for various climate and land-use scenarios

The land-use change can exacerbate the climate change impact as shown in Figure 7.8. The pro-agriculture scenario produces much higher sediment load annually

but the variation in the two seasons (March to September and October to February.) is not significant. This shows that sediment load discharge is primarily driven by rainfall, although the land-use can aggravate the sediment load in the basin and in the river reaches with the pattern in sediment discharge remaining almost same (Figure 7.9). The amount of sediment produced is much higher in the early spring (March and April) and monsoon seasons (July to September) compared to the NorESM scenario without land-use changes. The monthly variation in the sediment is shown in Figure 7.10.

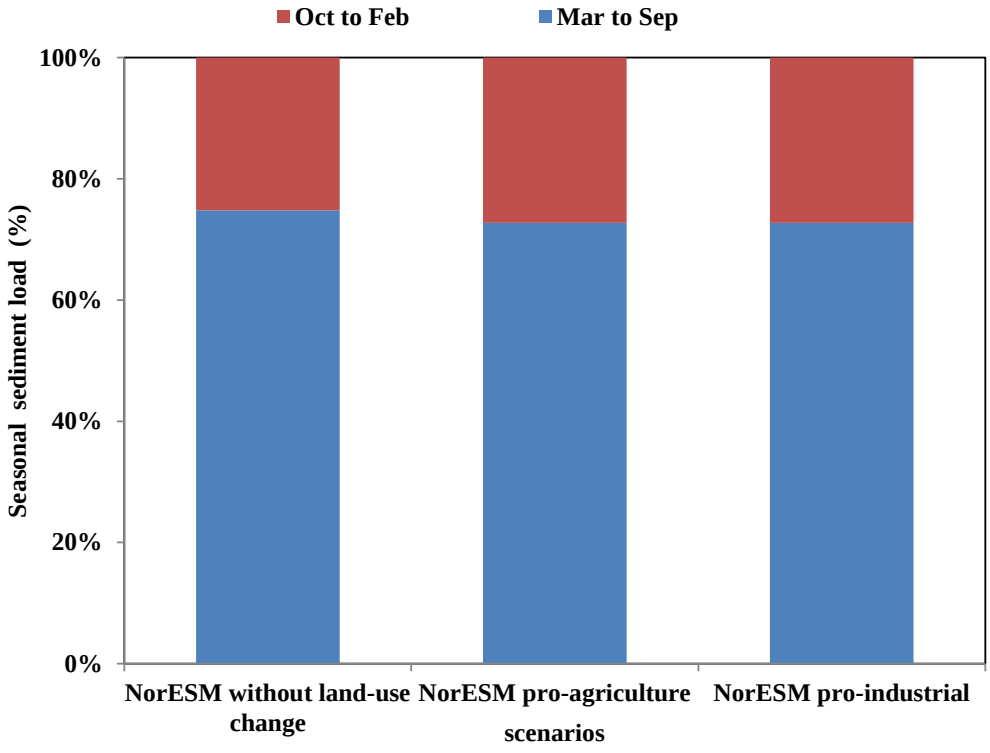

Figure 7.9: Projected seasonal sediment discharge ratio change at the Mangla Dam outlet for climate scenario for 2031-2098 and two land-use scenarios

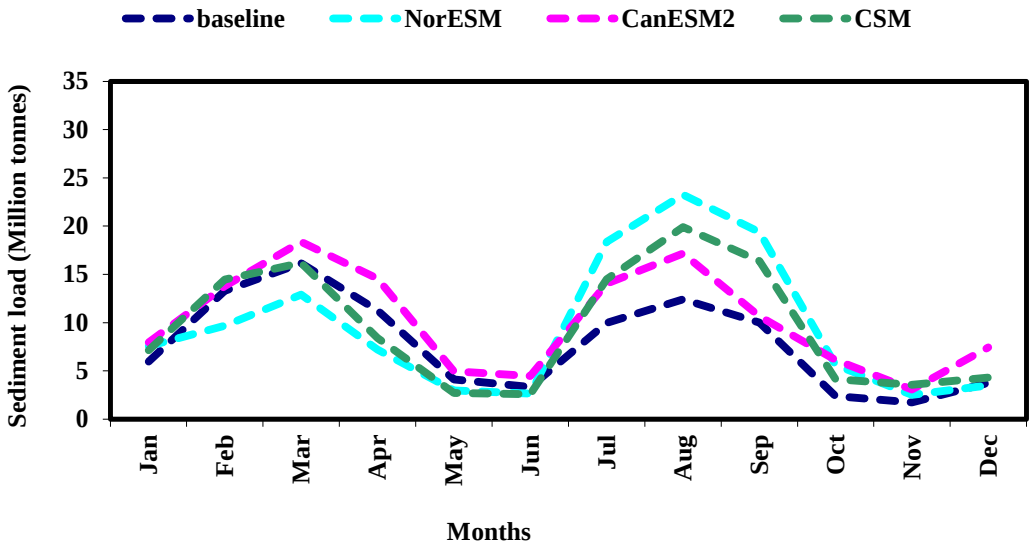

Figure 7.10: Projected long term mean monthly discharge for the period 2031-2098 under NorESM with pro-agriculture and pro-industrialization

7.3.1 Reservoir life under combined effect of climate and land-use changes

The reservoir life can also be computed by the integrated model for various combinations of climate and land-use change. For the current study, reservoir life was computed with three possible scenarios using the NorESM scenario with business-as-usual, the NorESM scenario with the pro-agriculture scenario and NorESM with the pro-industrialization scenario (the details of these scenarios can be found in Chapter 6). For all these scenarios, land cover was kept the same as the baseline period up to 2030. New projected land-use covers were used in the model from 2031–2098. ra (Figure 7.11).

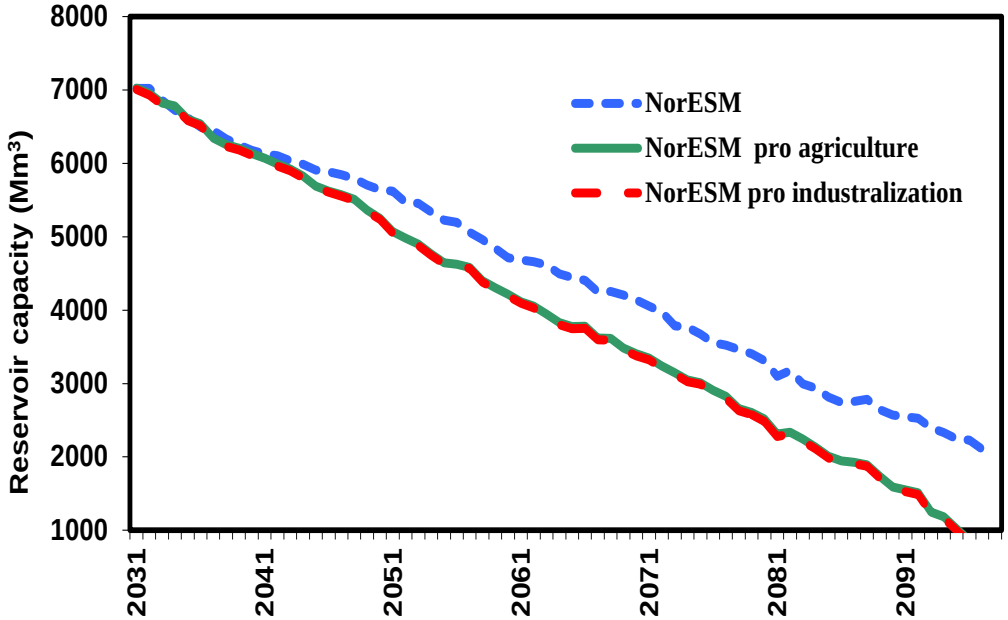

Figure 7.11: Reservoir capacity change for various climate and land-use scenarios

7.3.2 Spatial variation of the sediment

The integrated framework allows a spatial analysis for examining the variation due to climate or land-use change. This spatial analysis can be performed on sub-basin or hydrological response units (HRU's). The area of Mangla catchment is very large so analysis for the current study was carried out on HRU basis. Figure 7.12 shows changes in average annual sediment load for base line period while Figure 7.13 shows mean annual sediment load from 2083–2098 for pro-agriculture with the NorESM scenario. The results show that there is large variation in sediment load at HRU scale. The sediment load varies from 1 to 542 tonnes in the Mangla basin although mean sediment load is 52 tonnes per hectare for base line period while mean annual sediment load for future scenario is about 77 tonnes per hectare. The prominent increase of sediment load in the HRU's

existing sub-basin 4 is obvious for base line and future scenario as sediment is primarily driven by flow and all the river streams are combined in this sub-basin.

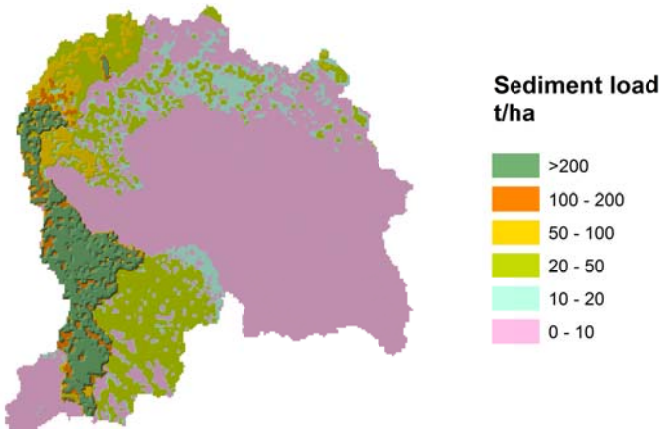

Figure7.12: HRU mean annual sediment load for base line period (tonnes per hectare)

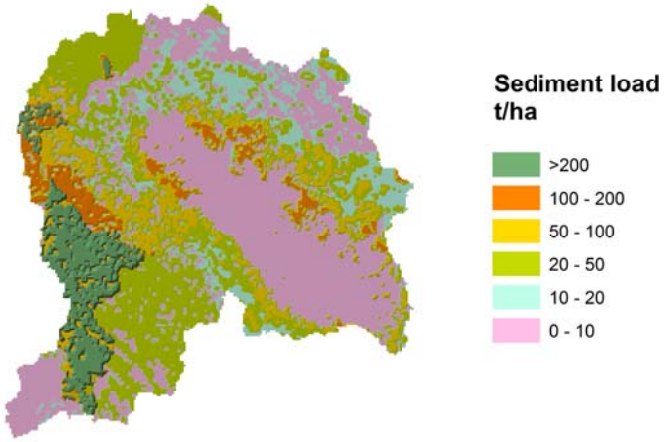

Figure7.13: HRU mean annual sediment load for 2083-2098 under NorESM climate and pro-agriculture scenario (tonnes per hectare)

7.4 Trends of extreme rainfall events in the Mangla basin

Climate extremes are multifaceted meteorological phenomena that can be characterized in terms of intensity, duration or frequency. The frequency analysis based on return period is very common and is an effective index to represent possible extreme value changes in the future (Kharin et al., 2010). In this study, the return period is quantiles of distribution of annual extremes and was estimated from a generalized extreme value (GEV) distribution. The GEV analysis was carried out using the SimCLIM software (Warrick, 2009).

The intensity and frequency of extreme rainfall events are projected to increase in the future with global warming, even for regions with projected decrease in annual mean rainfall (Kharin and Zwiers, 2000; Kaufmann and Seto, 2001; Wehner, 2004; Kharin and Zwiers, 2005). Pakistan received unusually high monsoon rainfalls in 2010 in most parts of the country that was changed into one of the most devastating floods in history. The monsoon rainfall was again more than the 2011 average. The variations in the monsoon rainfall in this region represent one of the largest variations of the global climate system (Turner and Slingo, 2009). Given that sediment load can just be generated by large floods caused by extreme rainfall events, it is essential for climate change impacts on sediment studies to include projections of extreme event changes under climate change impacts studies.

For the present study, the annual extreme daily rainfall data for two gauging stations, Domel and Garhi Duppata, were analysed. Both stations are situated in the Upper Jhelum part of the basin (sub-basin 1). The daily time series rainfall data of three GCM's: NorESM, CanESM2 and CSM from 1980 to 2098 were

used. The impact on extreme rainfall was analyzed for the three GCMs for the baseline period (1980-2004) and the two future periods (2011–2050 and 2051–2098) is shown in Figures 7.14 and 7.15. The results demonstrate that little extreme rainfall change is projected for the near future (2011–2050) for both stations, particularly for relatively short return period events (less than 20 years). Long return period events (larger than 20 years) are projected by the three GCMs to become less intensified for Domel and one GCM (CanESM2) for Garhi Duppata. However, the other two GCMs (NorESM and CSM) project stronger than baseline extreme rainfall event intensities for Garhi Duppata. The variations of the extreme event change projection for the near term reflect the uncertainties between GCMs on the one hand, while on the other hand, the climate change signal may be still too weak to be identified in the near term and the analysed result may be influenced by the natural climate variability included in the GCM simulated data.

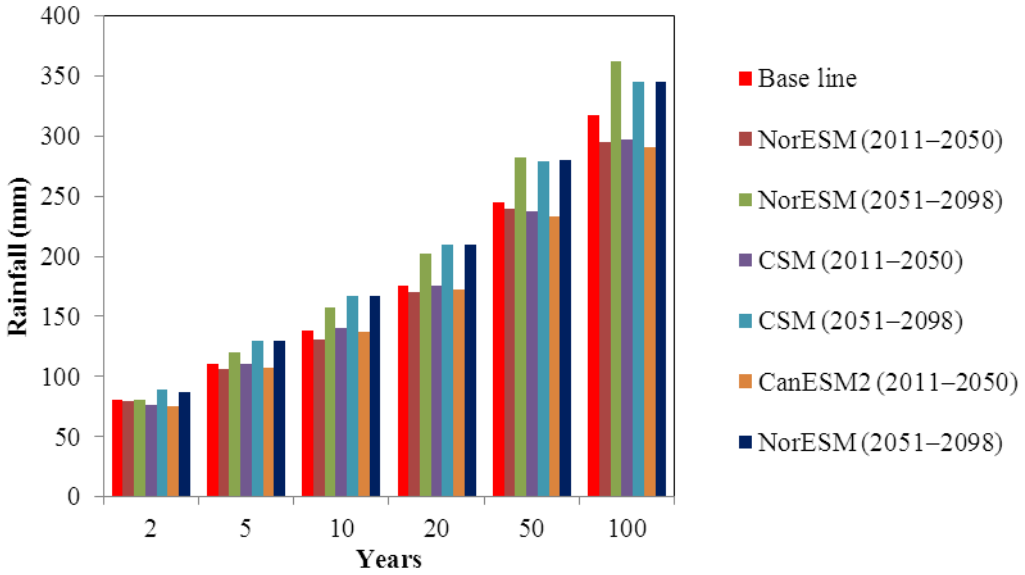

Figure 7.14: Extreme rainfall (mm) for Domel for baseline and NorESM scenarios

In contrast, towards the end of this century (2051–2098), the results indicate increase of intensity for all extreme events for both stations with the only exception of CSM's 100 year return event for Garhi Duppata. Although the projection of extreme rainfall intensity changes for the near future is still uncertain, the NorESM scenario projected 10% to 14% intensity increases for extreme rainfall events of 2 to 100 year return for Domel. The results of NorESM for Garhi Duppata also indicate increases in rainfall intensity for all return periods with a maximum 27% intensity increase for the 100 year return rainfall. Similar results can also be found from those of CanESM2 and CSM scenarios for the two stations, except for a slight intensity decrease projected by CSM for Garhi Duppata. The consistency of GCM projections for both stations for 2051–2098 indicates a strong likelihood that the extreme event intensity will increase along with global warming trends.

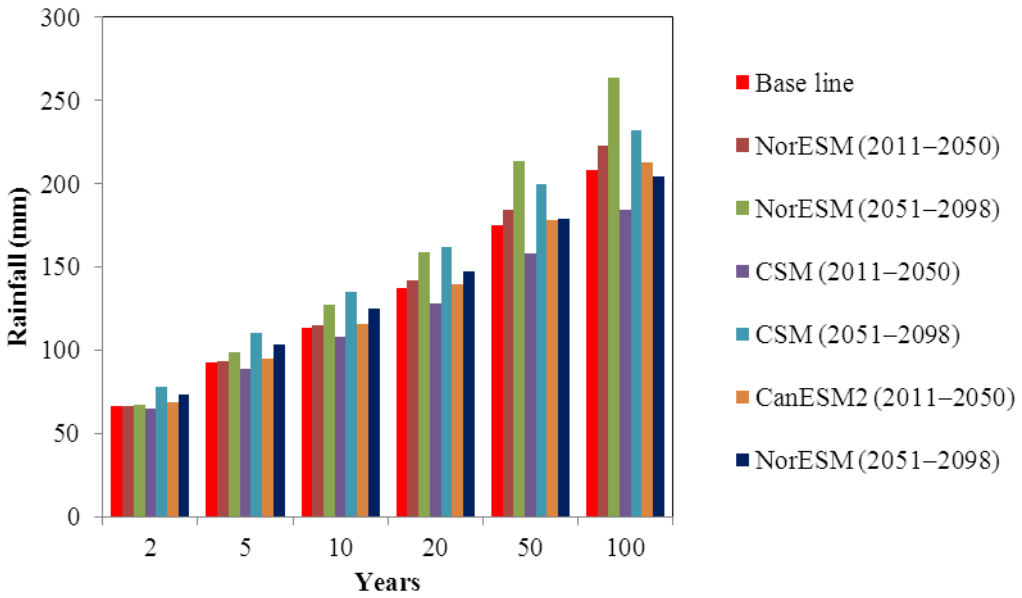

Figure 7.15: Extreme rainfall (mm) of Garhi Duppata for baseline and NorESM scenarios

The results also justify the SWAT model results for various GCM's (discussed earlier in sections 7.3 and 7.4) as there is a prominent increase in sediment from 2070 onwards for all the scenarios. This might be due to more frequent extreme events projected late in the century by various GCM's. As discussed in Chapter 4, an individual extreme event can cause as much as 20% of whole year sediment in less than a week. More frequent extreme events in the future will produce more sediment even though the mean annual rainfall may be projected to decrease.

7.5 Adaptation scenario

The flux of sediment transported by the water in the Mangla Reservoir has increased in magnitude since its operation started. It became evident from this study that the rate of sediment deposition will continue to increase in the future due to climate and land-use changes. Therefore it is imperative to take adaptation measures into account to reduce the vulnerability of sedimentation in order to maintain the designed reservoir's life span.

Several adaptation options can reduce the vulnerability of the sedimentation and enhance the reservoir life such as raising dam height, dredging, flushing and basin land-use management. A project for raising dam height has already been in construction phase to increase the reservoir conservation level by another 12.12 m. The reservoir's storage capacity with the additional dam height is projected to be depleted in 80 to 90 years (WAPDA, 2007). World-wide experience of sediment flushing and dredging from reservoirs is very limited, particularly for large reservoirs. Therefore for the present study, land-use management was considered as the only adaptation measure to abate the impact of climate. Various

land-use scenarios were generated for the Mangla basin as management adaptation options.

7.5.1 Adaptations scenario 1

Scenario 1 considered the business-as-usual scenario for the next 20 years (2011–2030). After that Government will need to implement basin management practices to reduce reservoir vulnerability. In this adaptation option, all the agricultural land that is situated above 2000 m and rangeland above 3000 m would be converted to forest (Figure 7.16). The model results reveal that annual sediment accumulation is about 7.37% and 4.48% less than the pro-agriculture and pro-industrial scenarios, respectively, after 2030.

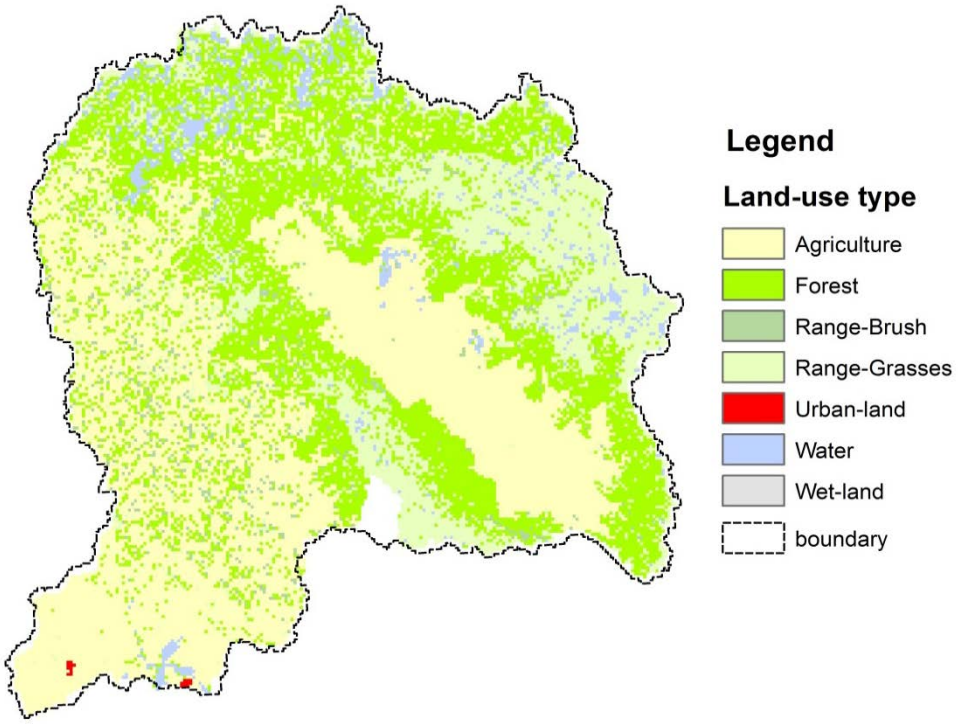

Figure 7.16: Land cover change for scenario 1

7.5.2 Adaptation scenario 2

Under scenario 2, land-use practices are again kept as business-as-usual up to 2030. Thereafter, Agricultural Land-Generic crops[1] (AGRL) land-use type, which is 17% of the basin, will be converted to mixed forest land class (Figure 7.17). This scenario shows a prominent decrease in the sediment discharge and sediment deposition at the Mangla Dam outlet. The mean annual sediment discharge entering into Mangla Dam is about 43.57% and 41.82% less compared to pro-agriculture and pro-industrial scenarios, respectively.

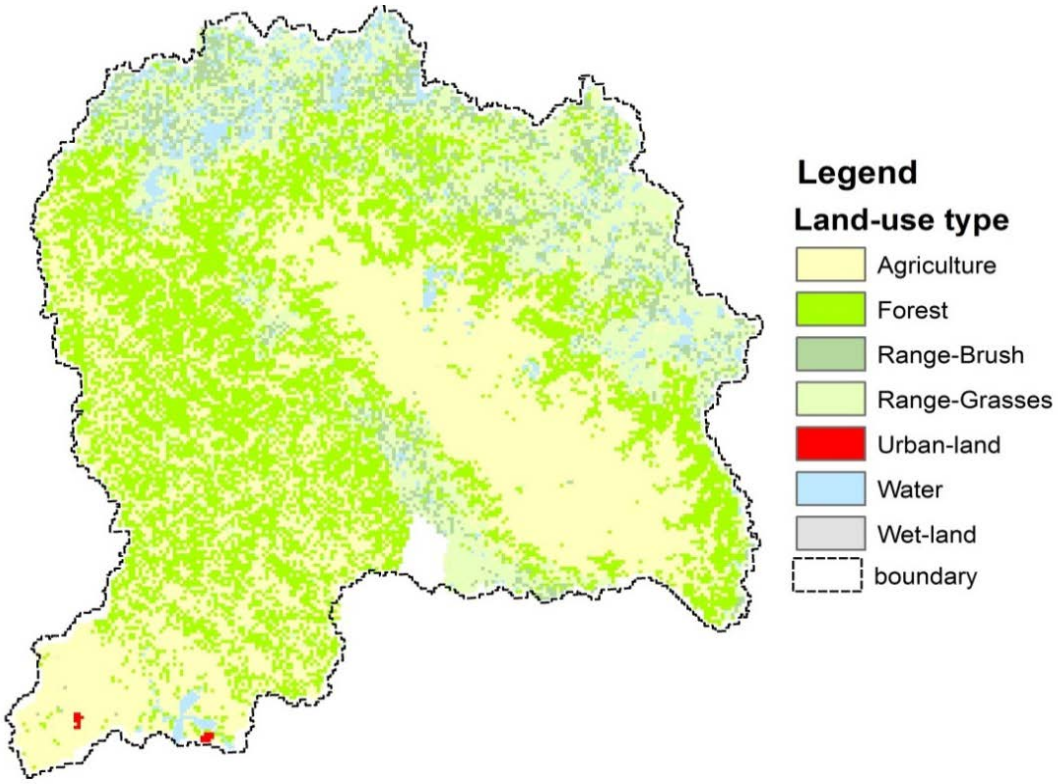

Figure 7.17: Land cover change for scenario 2

[1]The Mangla basin consists of three types of agricultural land: Agricultural Land-Close-grown (AGRC), Agricultural Land-Row Crops (AGRR), Agricultural Land-Generic (AGRL) and forest with a mixture of Forest-Evergreen (FRSE), Forest-Deciduous (FRSD) and Forest-Mixed (FRST). For the adaptation simulations, both the agricultural land types and forest land types are combined.

7.5.3 Adaptation scenario 3

Dairy farming may be a good adaptation option to replace agriculture. This option was assessed by converting AGRL land-use type to pasture land (PAST) from 2031 onward, as shown in Figure 7.18. Pasture land produces less sediment compared to agriculture or industrial areas. The mean annual sediment discharge under this adaptation is about 121 million tonnes from year 2031–2098, which is about 16.45% and 13.85% less than pro-agriculture and pro-industrialization scenarios, respectively. The reservoir life for these various adaptation options is shown in Figure 7.19.

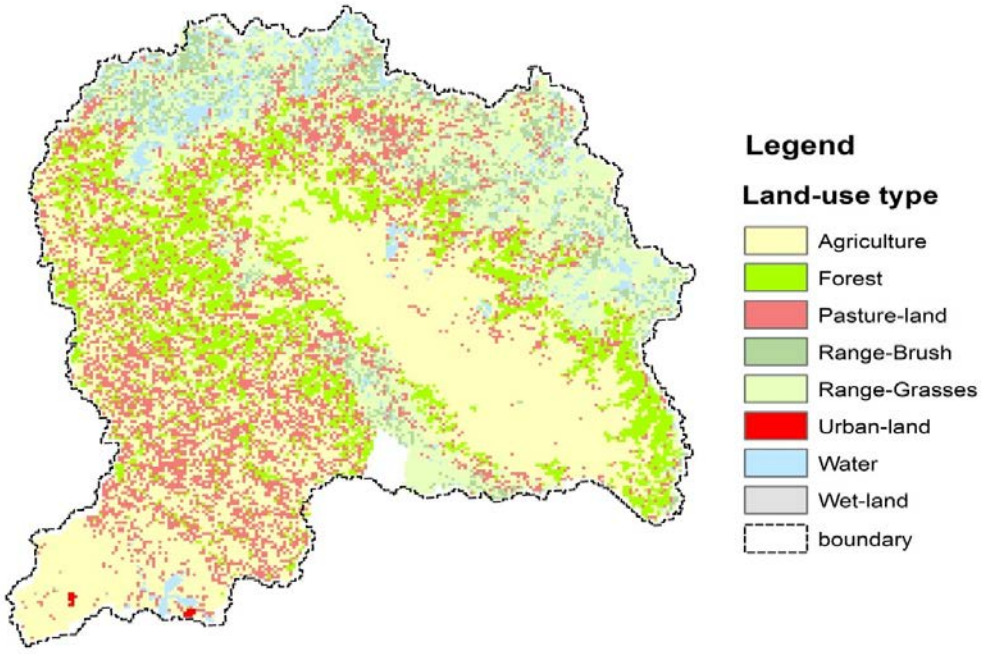

Figure 7.18: Land-use change for scenario 3

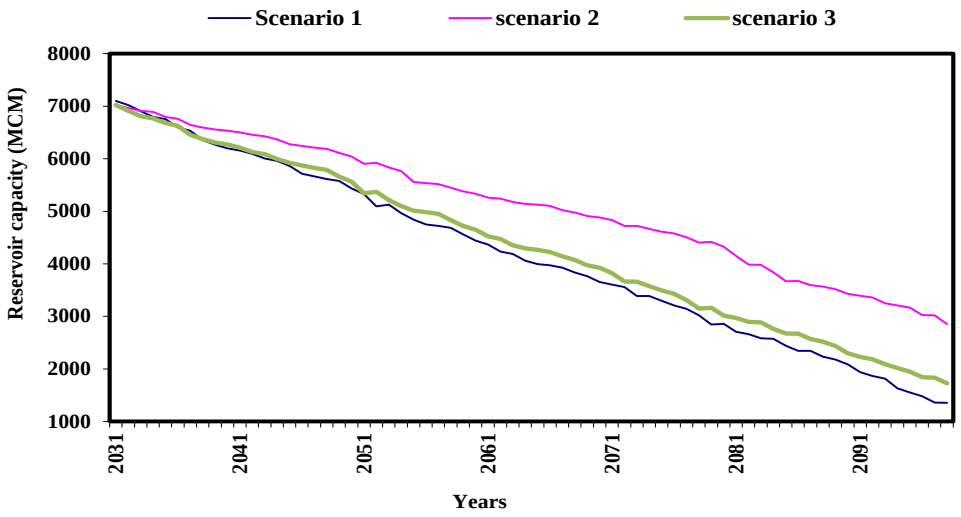

Figure 7.19: Reservoir capacity change for various adaptation scenarios

7.6 Economic analysis

Economic analyses are important in climate change impact assessments. They provide critical information for stakeholders to take the impact of climate change and land-use change into their decision making process. As discussed in Chapter 1, the primary purpose of the Mangla Dam is to store water for irrigation and power generation. Thus, the economic analysis was carried out by translating irrigation and power benefits from the dam into monetary terms (Pakistan Rupee or PKR) to support a simple cost-benefit analysis.

7.6.1 Valuation of the irrigation water

To estimate the benefits attributed to water supply, the value of irrigation releases has been estimated on the basis of provincial data for irrigated area and irrigation water use. MJV(2003) calculated the value of water for Kharif (summer) and Rabi (winter) seasons for the Indus basin in 2002. To estimate the benefits attributed to increases in irrigation water supply, the value of irrigation releases has been estimated on the basis of Provincial data for irrigated acreage and irrigation water use. Agronomic data estimated at the provincial level and comprising cropping

pattern, intensities, crop yields, farm inputs and cultural practices for canal-irrigated areas have been collected and analysed for recent years.

Based on the agronomic data, crop budgets for each province have been developed (MJV, 2003). Net crop income from the crop budgets has been combined with the reported irrigated area in each province to provide a measure of income at economic prices from irrigated lands. The net income values divided by the reported quantities of irrigation water, both surface water and groundwater, give the estimated value of water. The value of water was revised and taken as PKR1.07/m^2 and PKR0.48/m^2 at root zone[1] and source[2] respectively, for the current study. The results are shown in Table 7.1

Table 7.1: Value of water for the Indus basin (MJV 2003)

Description	Years	Kharif	Rabi	Annual
Canal withdrawals ($\times 10^6$ m^3)	1996–1997	87232	45947	133179
	1997–1998	80966	42617	123583
	1998–1999	87392	45330	132723
	1999–2000	89255	37757	127012
	2000–2001	74983	27272	102256
	2001–2002	69161	25188	94349
Average during 1996–97 to 2001–02		81499	37352	118850
Average availability of water assuming average efficiency ($\times 10^6$ m^3)		36348	16659	53003
Pumpage ($\times 10^6$ m^3)				
(i)Kharif Rabi distribution		1	0	1
(ii)Pumpage at farm gate[3]		33501	28543	62044
(iii)Field application efficiency @ 80%		26804	22832	49635
Total water availability ($\times 10^6$ m^3)				
(i)At root zone		63152	39491	102638
(ii)At source		141595	88546	230476
Total net present value (Million PKR)		4.07	14.12	27.48
Value of water (PKR/m^2)				
(i)At root zone		0.07	0.13	0.33
(ii)At source		0.11	0.19	0.14

[1]The price of irrigation water at farmer's field
[2]The price of irrigation water at Mangla Reservoir

[3] The farm gate pumpage is the net pumpage required for crops at the agriculture farm

7.6.2 Irrigation benefits

Water from the Mangla Reservoir is mainly released for the Rabi (summer) season crops but also sometimes in late or early Kharif (winter) in years when water shortages are acute. It is expected that this pattern of release will continue with the raised dam height in the future. Thus, irrigation benefits will accrue mostly from Rabi crops but the risk of water shortage in Kharif is also reduced. A high certainty that water will be available in Kharif as well as Rabi encourages farmers to expand their cultivated area and avoid applying more expensive water inputs from other sources thereby resulting in high yields. Therefore, the major reason for raising the Mangla Dam is to improve the certainty of irrigation supply with restored storage in the Indus system.

However, improvement of the certainty in water supply can also be achieved from adaptation options. The accumulated irrigation benefit from reducing the sedimentation in the reservoir is PKR31,252 million, PKR137,562 million and PKR61,686 million, respectively, for the three adaptation scenarios by the end of this century (in today's value as shown in Figure 7.20), although the conversion of agricultural land to forest will have an impact on the economy of the country.

The loss of net crop income due to adaptation options was estimated and compared with the net profit in terms of irrigation water saving. The total cropped area of Kashmir is about 2476.23 million m^2. Maize, rice, wheat, vegetables and fruit are the major crops of the area. The cropping yield was estimated using data from the Department of Agriculture and Livestock Muzzafarabad. The yield of the important crops for 2007-2008 is shown in Table 7.2 (AJK, 2007).

Table 7.2: Agriculture yield for the Kashmir valley for major crops (kg/hectare)

Crops	Maize	Rice	Wheat	Potato	Gram pulses	Oil seed	Vegetables	Fruits
Yield	1239	2556	1063	8117	988	865	4765	6041

Farm inputs (seed, fertilizer, pesticides, use of bullock, electricity and labour) data was used for Khyber Pakhtoonkhawa province for 2003–2004 that has very similar topographic conditions. The net value of production was calculated by subtracting the expenses from crop incomes for the Kashmir valley. The details are shown in Table 7.3. The net value of crop production per hectare (10,000 m^2) is PKR 0.52 million. For the adaptation options 1 and 3, about 4,500 and 6,010 km^2 is proposed to convert from agriculture to forest. Considering the same crop value for the whole basin, the net loss from agriculture will be about PKR 23.4 million and PKR 31.25 million per year for the 2 options, respectively. The results of the economic analysis shows that adaptation option 2 is more appropriate compared to adaptation option 1 as crop value lost due to option 2 is much less compared to benefits achieved from irrigation water and power generation, while adaptation option 3 could be a good option but more investigation and analysis is required to further explore the impact of pasture farming in the basin.

Table 7.3: Net value of production for major crops in Azad Jamu and Kashmir, Pakistan

Crops	**Maize**	**Rice**	**Wheat**	**Potato**	**Gram pulses**	**Oil seed**	**Vegetables**	**Fruits**
GROSS VALUE OF PRODUCTION (PKR)								
Gross Revenues	22298	29434	25253	119768	29986	25950	90526	302038
CROP PRODUCTION EXPENSES (PKR)								
Ploughings	2178	1103	933	1103	679	679	1103	
Seed	679	404	1321	28951	508	205	26000	
Fertilizer N	1386	1277	1459	1240	474	1277	1240	
Fertilizer P	588	706	784	745	275	941	745	
Fertilizer K	0	0	0	231	0	0	231	
Sprays	293	195	117	195	0	0	195	
Hired Labour	638	1425	788	1920	270	780	1920	
Family Labour	3113	4275	1463	2880	1080	2220	2880	
Total cost	8874	9385	6865	37266	3286	6102	34315	
Value of sticks	1804	627	650	0	0	0	0	
NET VALUE OF PRODUCTION (PKR)								
	15228	20676	19038	82502	26700	19848	56211	277038

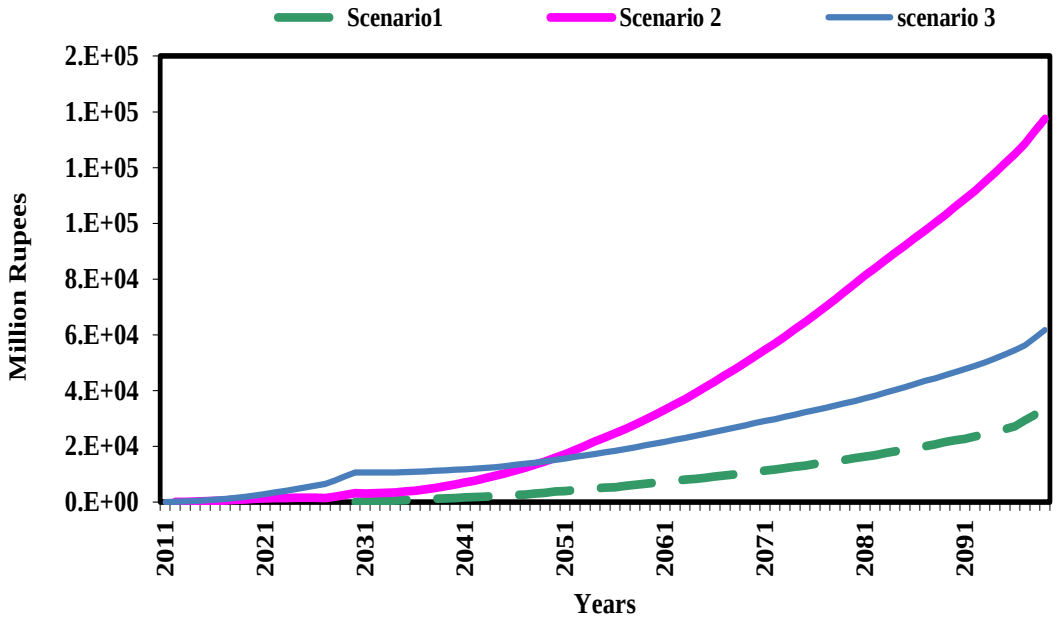

Figure 7.20: Net value of production for major crops in Azad Jamu and Kashmir, Pakistan

7.6.3 Power and energy benefits

Historically the Mangla Reservoir has been operated with priority for irrigation and the generation of electricity has been incidental. It is operated on 10-day indents along with irrigation water releases, and does not provide firm capacity but incremental energy. The additional energy provides a cost-saving by substituting energy that otherwise would be generated by fossil fuel plants. The Mangla power station has been operating as peaking plant for most of the time and as base load plant (minimum amount of power that must be available) only during flood seasons and periods of high irrigation demand. During peaking operation, water from the Mangla Reservoir is in excess of demand and is stored in the Rasul Barrage from where it is re-regulated to suit the requirements of downstream irrigation networks. For the current study, the monetary value of

power and energy benefit was not calculated because input data, such as reservoir level and 10 daily discharges, are not available.

7.6.4 Flood alleviation

The Mangla Dam already provides flood alleviation benefits to the downstream area. A major part of the small to medium floods is absorbed and peaks of large floods are also significantly reduced by the reservoir. This minimizes loss of human and animal lives from flooding downstream. In addition, damage to crops and infrastructure is also reduced

7.7 Implication of results for the study area

The results from the model indicate that the projected sediment may increase or decrease depending on the selected land-use and climate change scenarios. These findings have significant implications for the study area. These may help policymakers and land-use planners to anticipate and take proactive action on the impact of future climate change conditions.

The three policy-related land-use change scenarios resulted in various effects on reservoir life. In general, the pro-agriculture scenario produces higher annual sediment than the other land-use scenarios. The effect of this scenario is greater with time, i.e., when more land is converted. Pro-industrialization scenarios show little less sediment than pro agriculture scenarios, whereas sediment deposition for the business-as-usual is very small. These may also help policymakers and land-use planners to anticipate the impacts of future climate conditions. It should be noted, however, that these are scenarios and not future predictions. Some implications from the results are discussed below.

7.7.1 An increase in annual sediment load

A possible increase in monthly sediment has been noted in particular under a combination of the CSM climate change pattern and the pro-agriculture land-use scenario. The high sediment may increase the risk of reservoir life. Minimizing the risk may require, for example, development of basin management techniques. The risk of floods may also be minimized by implementing a specific land-use policy, such as reforestation, in order to reduce sedimentation.

7.7.2 Spatial variation in annual sediment load

Spatial changes in sediment are influenced by both the climate and land-use. In general, climate change causes a gradual change in local variation, whereas the land-use change causes a more distinct change. This suggests that there are opportunities for controlling the sediment load locally in order to manage the entire river sediment, as part of an integrated basin management.

7.7.3 Evaluation of the integrated model for preliminary assessment

The integrated frame is useful for conducting impact assessments by comparing impacts with and without change of conditions (Major and Frederick, 1997). The purpose of the integrated model is to bring together the complex relationship between land-use, climate and hydrological components into one system for comparing the impact (i.e. sensitivity analysis) under various conditions (i.e. 'what if' questions). The integrated model is, therefore, evaluated based on the ease of conducting this kind of sensitivity analysis and whether it helps the policymakers and planners in examining the impacts under various pre-determined scenarios of

land-use changes and climate changes. In addition, this evaluation serves as a base for future improvement or development of this model.

7.8 Conclusions

This chapter demonstrates the application of the integrated model for conducting sensitivity analysis of the effects of land-use and climate change on the river sedimentation and reservoir life. The model is suitable as a decision support tool for examining the possible changes in land-use patterns and how these changes could affect the river flows.

This integrated model results from a range of land-use change scenarios and climate change scenarios, allowing a comprehensive analysis for exploring “what if” questions. Compared to the baseline period (1990–2005), the model can identify scenarios that may produce significant changes in the river sedimentation and thus will have significant impacts on the study area. The results will be useful for policymakers and other stakeholders to make scientifically informative decisions and take pro-active actions.

It was found from the model results that changes in seasonal river sedimentation can result from land-use or climate change or both. Climate change has large impacts on the sediment pattern at a regional scale, while the land-use change has a distinct influence at a local scale. This opens up opportunities to manage the variation in the river sediment as an adaptation option to mitigate the climate change impact. Finally, an economic analysis was carried out to assess the financial benefits that can be achieved through basin management.

CHAPTER EIGHT
SUMMARY AND CONCLUSIONS

8.1 Overview of the key issues

During the 20th century the increase in freshwater use by humans outstripped the global population growth. As per future projections, the global population will increase by another 40 to 50% within the next fifty years (www.worldwatercouncil.org). The escalating population growth coupled with industrialization, urbanization, climate change and associated enhanced climate variability will not only result in global water scarcity but also have serious consequences on the environment. Pakistan – a country of over 170 million people, has also been experiencing high water stress due to increasing population and urbanization. Historically, dams and reservoirs have been used to provide freshwater storage for human use. In Pakistan, the current capacity of dams and reservoirs are not sufficient to preserve the surface water produced by glacier melt and rainfall. Furthermore, the capacity of the existing dams is decreasing at an alarming rate due to sedimentation. An example of such a reservoir is the Mangla Dam, the second largest dam in the country. Due to sedimentation it has lost almost 20% of its water storage capacity since its impoundment in 1967.

8.2 Summary of the research objectives and methodologies

The aim of this dissertation was to study the changes in climate and land-use on reservoir sedimentation and identify adaptation options to increase the resilience of the reservoir life based on an integrated water resources management model.

In order to understand the water budget and sediment produced and its transportation to the outlet, the basin area was studied from a broad perspective and as part of the river basins contributing to the Mangla Dam.

This study developed an integrated model system incorporating a distributed hydrological model based on SWAT and a climate change impact assessment model for understanding the hydro-sediment dynamics under different climate and land-use scenarios. The hydrologic model was calibrated and validated for flow and sediment for the study area. There was a close agreement between the observed and model simulated flows and sediment for both sub-basins and the overall trend of the flow and sediment transported at the outlet of the basin. A rating curve was developed for all the gauging stations between flow and sediment in order to compute the monthly sediment outputs. Since there was no sediment observation at the outlet of the basin, sediment contribution from all the sub-basins was computed at this junction using the relationship between sediment and un-gauged area.

Reservoir sedimentation is a dynamic process that is influenced by continues climate and land-use changes. The impact study, therefore, required transient climate and land-use change scenarios. The following future scenarios were produced to simulate the response of the reservoir sedimentation and reservoir life under the impact of climate and land-use changes up to the end of the 21st century.

- A transient daily time series of climate scenario was created through bias correction of three IPCC AR5 GCM daily outputs. The GCM runs are driven by the IPCC SRES A2 emission scenario, which projects one of the fast climate changes in the future;

- The land-use change scenarios were built using a map algebra method. Three scenarios were constructed based on socio-economic and physical conditions of the study area: i) pro-agriculture scenario; ii) pro-industrialization scenario, and iii) business-as-usual scenario. Land-use change scenarios were also analysed as adaptation options to reduce the sediment based on various land management practices.

8.3 Summary of the results

The results of this study reveal that river flow and sediment pattern varied greatly in the study area. Statistical indicators such as scatter plots and the Nash Sutcliffe Efficiency coefficient (N_{SE}) and the comparison of hydrographs indicated that the model generally simulates flow and sediment very well for the monsoon season, and is satisfactory for low flow season (December to February). There was good agreement in the annual water balance and the N_{SE} values were greater than 0.5 for flow validation at all outlets. The $\underline{N_{SE}}$ values were relatively low for sediment simulation. The lower value of N_{SE} for sediment might be due to insufficient sediment data in constructing the flow-sediment rating curve. Extreme event analysis for the single heaviest rainfall showed that a single extreme rainfall event can produce a significant amount of sediment that is about 20% of the yearly total.

Climate change will impact on the Mangla Reservoir's life span but with a considerable range of uncertainties between different GCMs. However, all GCM projections show a prominent increase in sediment load for 2011–2098. The difference in projected temporal rainfall change pattern also gave rise to variations in the simulated sediment. However, in general, there will be more sediment transported in the monsoon season and less sediment in the dry conditions

(winter). Spatial distribution of all the scenarios showed that most of the sediment is transported by the Jhelum River after the confluence of Kunhar and Neelum tributaries.

A superimposed effect of land-use change in addition to climate change can have an exacerbating impact on sediment. The sediment transported under the pro-agriculture scenario compared to baseline was shown to be the highest.

It is clear that Reservoir life of the Mangla basin is highly vulnerable due to climate and land-use changes. The reservoir life is reduced by 28, 27 and 12% under the NorESM, CanESM2 and CSM scenarios, respectively, even without considering land-use change. With additional land-use changes, the reservoir life will be depleted even more quickly. Adaptation options can, however, reduce the vulnerability of reservoir life to projected climate and land-use changes. Several adaptation options with regard to basin management have been explored in this study.

- Conversion of the agricultural land to forest that is situated above 2,000 m and rangeland above 3,000 m could reduce annual accumulation of sediment
- Conversion of 34% of the agricultural area (AGRL class) to mixed forest after 2030 was projected to markedly decrease sediment discharge and deposition at the Mangla Dam outlet Pasture farming was considered as another adaptation option. Like option 2, conversion of 34% of the agricultural land to pasture after 2030 may reduce sediment accumulation

It was evident from the adaptation scenarios that among all land-use types, agricultural land was the greatest contributor to erosion and sediment in the

Mangla basin since loose soil is eroded in ploughing and harvesting time. Basin management is perhaps the best adaptation option for controlling this sediment. Since extreme events can produce a disproportionate amount of sediment, special adaptation options may be needed to counteract their impact, such as diverting runoff from agricultural land to the empty dug wells or ponds in the monsoon season before runoff becomes part of the rivers. The dug wells could be designed in areas with intense agriculture to serve as sand and sediment deposits.

Economic analyses carried out on the value of water for irrigation indicated that reservoir capacity increased with adaptation options for saving water for irrigation downstream of the basin. The results showed that there were irrigation benefits from adaptation options 1, 2 and 3 until 2098 but that economic loss from adaptation options could be expected due to the reduction of agricultural area inside the basin. At the same time, additional benefits will be gained from power generation and flood alleviation.

The findings suggest that climate change has a great influence on the variability of sediment load in the basin but that the pronounced change in sediment is more likely caused by land-use change. Therefore, the issue of land-use management as part of the integrated management program in order to achieve sustainable development is very relevant.

8.4 Broader implication and contribution to knowledge

The thesis has implications for increasing awareness of the importance of an integrated framework that can be applied to examine possible changes in sediment behaviour of the basin and consequently the sedimentation due to its transportation into the reservoir. The results of change were calculated for both

climate and land-use change patterns. In particular, they showed the importance of climate and land-use components in assessing the possible future sediment variability of the basin.

Specifically, the thesis contributes to knowledge in several ways:

Firstly, it contributes to the integrated work that links the climate component and land-use into a hydrological and economic analysis for assessing the impacts in the basin. Secondly, the thesis has proposed policy-related land-use management options for the study area based on the socio-economic analysis. Thirdly, this kind of integrated work linking climate change, land-use, hydrology and economics is unique for the Mangla basin. So far, there have been no such integrated studies in Pakistan.

8.4.1 Limitations of the model and suggested future work

Despite certain limitations with respect to data availability and data quality, this thesis was able to show the importance of developing an integrated system for a more realistic perspective of the factors influencing reservoir life expectancy. Nevertheless, the limitations should not be ignored, and these are described on a component basis as follows:

8.4.1.1 Hydrological component

The data for the upstream catchment (Indian part) was not available for the study although time series flow data of almost two decades of the downstream catchment were available for calibration and validation of the model. The biggest constraint was sediment data that was not available on daily or monthly basis so rating curves were developed to obtain sediment loads at various stations in the Mangla catchment. The land-use and soil attributes used for the model were from

globally based data. Consequently, some assumptions had to be made for calculating soil parameters of the basin. Extreme event analysis was done using paucity of data for the extreme event analysis also made it difficult to carry out detailed studies of the impact of extreme events in the basin.

In summary, there were some constraints for achieving a comprehensive investigation of the contribution of the hydrological component because of the lack of long-term data.

8.4.1.2 Land-use component

The land-use scenarios were created using a static model technique of “map algebra”. A different approach for generating land-use change scenarios would require replacing the static model with a dynamic model for better land-use change allocation procedures. Due to the lack of socio-economic data for the Mangla basin, land-use scenarios were generated using socio-economic data from the Pakistan part. The available data were point data, i.e., socio economic information was available on a regional basis, making it difficult to examine the socio-economic conditions of the basin spatially. Due to unavailable dynamic land cover change data, the land-use component was not able to be validated.

The land-use model uses a limited number of physical factors, which include slope, elevation and distance to the main road. However, soil fertility and groundwater conditions may also have contributed locally to the land-use distribution patterns, but these data were not available. For socio-economic analysis only population growth was considered as the major driving factor for land-use changes. Detailed analysis is required to determine other relevant factors

for the land-use change, such as economic parameters and industrial growth in the study area.

8.4.1.2 Climate Component

Transient daily rainfall and temperature data for climate change scenarios were developed for the study area using GCM results. Because data were not available from a broader range of GCMs, only three GCM results driven by a high emission scenario were used. The resolution of the GCMs is rather coarse (about 2 arc latitude-longitude degrees) making it difficult to incorporate topographic features of the area.

8.5 A possible way forward

As mentioned in the previous section (8.5), data availability was the main limitation in the integrated work for examining current and future climate, and land-use. In particular, it prevented extensive and detailed calibration and validation of the model. Good long-term data and data on well-distributed climate, flow, sediment and land-use upstream of the Jhelum basin would be required for analysing and validating the results of the upper part of the basin. It remains a challenging study topic for further research.

A wider range of climate scenarios would be useful for sensitivity and uncertainty analyses. More importantly, downscaled GCM output is more suitable than GCM output itself as was done for this research. Downscaled GCM outputs incorporate environmental factors that influence the local climate condition, such as topography, and such factors are possibly ignored by GCM due to its coarse resolution. Hence the use of downscaled GCM data instead of GCM will

potentially increase the accuracy of results. However, dynamic downscaled data (RCM) are not available for the study area, and carrying out statistical downscaling of GCM outputs requires good quality, long-term observed data which is also not available. Currently the dynamic downscaling work is underway to produce an improved generation of regional climate change projections for the AR5 series (Giorgi et al., 2009). There is no doubt that further research will improve the findings of this study when these data become available.

An in-depth research of extreme events and their relationship with sediment generation also requires high quality daily (or sub-daily) rainfall data, as well as corresponding sediment observations, neither of which are so far available. Given the importance of the impacts of the extreme rainfall events on sediment generation, further research is required and the first step to support such research would be setting up of daily sediment observations for the key tributaries in the study area so that future sediment patterns due to extreme events can be analysed.

REFERENCES

Adams, S., R. Titus, K. Pietersen (2001). Hydrochemical characteristics of aquifers near sutherland in the Western Karoo, South Africa Journal of Hydrology, 241(1-2): 91-103.

Adeloye, A., M. Montaseri (2002). Preliminary streamflow data analyses prior to water resources planning study/analyses préliminaires des données de débit en vue d'une étude de planification des ressources en eau. Hydrological Sciences Journal 47(5): 679-692.

AJK (1998). Azad Kashmir statistical year book (1998). Ministry of Economic Affairs and Statistics, Azad Jamu and Kashmir, Pakistan.

AJK (2007). Azad Kashmir at a glance. Government of Azad Jamu and Kashmir, Pakistan.

Al Ali, Y., J. Touma, P. Zante (2008). Water and sediment balances of a contour bench terracing system in a semi-arid cultivated zone (El Gouazine, central Tunisia). Hydrological Sciences Journal 53(4): 883-892.

Alcamo, J., P. Döll, T. Henrichs (2003). Global estimates of water withdrawals and availability under current and future business-as-usual" conditions." Hydrological Sciences Journal 48(3): 339-348.

Altaf-ur-Rehman (2004). Sediment management for reservoirs. 69th annual session proceedings Pakistan Engineering Congress, Lahore Pakistan, A-One Publishers.

Ang, A. (1990)..Probability concepts in engineering planning and design, Vol. II Decision, risk, and reliability, John Wiley & Sons, NY.

Anselin, L. and A. K. Bera (1998). Spatial dependence in linear regression models with an introduction to spatial econometrics. Statistics Textbooks and Monographs 155: 237-290.

Archer, D. and H. Fowler (2008). Using meteorological data to forecast seasonal runoff on the river jhelum, pakistan. Journal of Hydrology 361(1-2): 10-23.

Archer, D., N. Forsythe, H. Fowler (2010). Sustainability of water resources management in the indus basin under changing climatic and socio economic conditions. Hydrology and Earth System Sciences 14(8): 1669-1680.

Arnell, N. W. (1999). Climate change and global water resources .Global Environmental Change 9: S31-S49.

Arnold, J. G. and P. M. Allen (1999). Automated methods for estmating baseflow and ground water recharge from stream flow records. JAWRA Journal of the American Water Resources Association 35(2): 411-424.

Arnold, J. G., P. M. Allen and D. S. Morgan (2001). Hydrologic model for design and constructed wetlands. Wetlands 21(2): 167-178.

Arnold, J. G., R. Srinivasan, R. S. Muttiah (1998). Large area hydrological modeling and asseement part 1: Model development. JAWRA Journal of the American Water Resources Association 34(1): 73-89.

Arnold, J., J. Williams, R. Srinivasan (1996). SWAT manual, USDA. Agricultural Research Service and Blackland Research Center, Texas.

Ashmore, P., M. Church (2001). The impact of climate change on rivers and river processes in Canada. Bulletin 555, Geological Survey of Canada, Ottawa.

Batjes, N. H. (2006). Isric-wise derived soil properties on a 5 by 5 arc-minutes global grid (version 1.0). Wageningen: ISRIC—World Soil Information.

BBC (2010). (british broadcasting corporation),' 2.5m people affected' by pakistan floods. Http:// www.BBC.Co.Uk/news/world-south-asia-10834414, BBC (accessed 12 October 2010).

Beasley, D., L. Huggins and E. Monke (1980). Answers: A model for watershed planning. Transactions of the ASAE 23(4).

Benestad, R. E., I. Hanssen-Bauer and D. Chen (2008). Empirical-statistical downscaling, World Scientific Pub Co Inc., Singapore

Berga, L. (2008). Berga, l. 2008. Dams for sustainable development. Paper presented at high-level international forum on water resources and hydropower, Beijing, 17-18 October 2008.

Bicknell, B. R., J. C. Imhoff, J. L. Kittle Jr (1996). Hydrological simulation program–Fortran, user's manual for release 11. US EPA.

Bingner, R. and F. Theurer (2001). AnnAGNPS technical processes: Estimating sediment yield by particle size for sheet and rill erosion. In Proc.7th Federal Interagency Sedimentation Conference: Sedimentation Monitoring, Modeling, and Managing, vol. 1: I1,I- 7. Washington, D.C.: Interagency Advisory Committee on Water Data, Subcommittee on Sedimentation.

Boardman, J., and D.T. Favis-Mortlock. (1993). Simple methods of characterising erosive rainfall with reference to the South Downs, southern England. In: S. Wicherek (ed), Farm Land Erosion in Temperate Plains Environment and Hills. Elsevier, Amsterdam, 17-29.

Borah and M. Bera (2004). Watershed-scale hydrologic and nonpoint-source pollution models: Review of applications. Transactions of the ASAE 47(3): 789-803.

Borah, D., R. Xia, M. Bera (2002). Dwsm-a dynamic watershed simulation model. Mathematical models of small watershed hydrology and applications: 113-166.

Bosch, D., J. Sheridan, H. Batten (2004). Evaluation of the SWAT model on a coastal plain agricultural watershed,. Transactions of the American Society of Agricultural Engineers 47 (5): 1493-1506.

Bosch, D., J. Sheridan, H. Batten (2004). Evaluation of the SWAT model on a coastal plain agricultural watershed, Transactions of the American Society of Agricultural Engineers 47(5): 1493-1506.

Brady, M. and E. Irwin (2011). Accounting for spatial effects in economic models of land use: Recent developments and challenges ahead. Environmental and Resource Economics 1-23.

Bruijnzeel, L. (2004). Hydrological functions of tropical forests: Not seeing the soil for the trees. Agriculture, Ecosystems & Environment 104(1): 185-228.

Butt, M. J., A. Waqas and R. Mahmood (2010). The combined effect of vegetation and soil erosion in the water resource management. Water resources management 24(13): 3701-3714.

Butt, M. J., R. Mahmood and A. Waqas (2011). Sediments deposition due to soil erosion in the watershed region of Mangla dam. Environmental monitoring and assessment: 1-11.

Caston, C. B., W. H. Nowlin, A. Gaulke (2009). The relative importance of heterotrophic bacteria to pelagic ecosystem dynamics varies with reservoir trophic state. Limnology and Oceanography 54(6): 2143-2156.

Cayan, D. R., E. P. Maurer, M. D. Dettinger (2008). Climate change scenarios for the California region. Climatic Change 87: 21-42.

Chaudhry, M. and N. Akhtar (2009). Assessment of sediment flushing efficiency of reservoirs. Pakistan Journal of Science 61(3): 181-187.

Cheng, J., Y. Huang, H. Wu (2005). Hydrometeorological and landuse attributes of debris flows and debris floods during typhoon toraji, july 29-30, 2001 in central Taiwan. Journal of Hydrology 306(1-4): 161-173.

Chow, V., D. Maidment and L. Mays (1988). Applied hydrology, 572 pp. Editions McGraw-Hill, New York.

Christensen, J. H., T. R. Carter, M. Rummukainen (2007). Evaluating the performance and utility of regional climate models: The prudence project. Climatic Change 81: 1-6.

Christensen, N. S., A. W. Wood, N. Voisin (2004). The effects of climate change on the hydrology and water resources of the colorado river basin. Climatic change 62(1): 337-363.

Chu, T. and A. Shirmohammadi (2004). Evaluation of the swat model's hydrology component in the piedmont physiographic region of maryland. Transactions of the ASAE 47(4): 1057-1073.

Ciesin, I. (2000). Gridded population of the world (GPW), version 2Center for International Earth Science Information Network (CIESIN) Columbia University, International Food Policy Research Institute (IFPRI) and World Resources Institute (WRI), Palisades, NY.

Coulthard, T. J. and M. G. Macklin (2001). How sensitive are river systems to climate and land-use changes? A model-based evaluation. Journal of Quaternary Science 16(4): 347-351.

Crosta, G. B. and P. Frattini (2008). Rainfall-induced landslides and debris flows. Hydrological Processes 22(4): 473-477.

Dai, A. (2006). Precipitation characteristics in eighteen coupled climate models. Journal of Climate 19(18): 4605-4630.

De Araújo, J. C., A. Güntner and A. Bronstert (2006). Loss of reservoir volume by sediment deposition and its impact on water availability in semiarid brazil. Hydrological Sciences Journal 51(1): 157-170.

Diaz-Nieto, J. and R. L. Wilby (2005). A comparison of statistical downscaling and climate change factor methods: Impacts on low flows in the river thames, united kingdom. Climatic Change 69(2): 245-268.

Downer, C. W., F. L. Ogden, W. D. Martin (2002). Theory, development, and applicability of the surface water hydrologic model casc2d. Hydrological processes 16(2): 255-275.

Eckhardt, K. and J. Arnold (2001). Automatic calibration of a distributed catchment model. Journal of Hydrology 251(1-2): 103-109.

El-Nasr, A. A., J. G. Arnold, J. Feyen (2005). Modelling the hydrology of a catchment using a distributed and a semi-distributed model. Hydrological processes 19(3): 573-587.

Etienne, L., F. Anctil, A.N.N.V.A.N. Griensven (2008). Evaluation of streamflow simulation by swat model for two small watersheds under snowmelt and rainfall Hydrological Sciences–Journal–des Sciences Hydrologiques 37-41.

Falkenmark, M., J. Lundqvist and C. Widstrand (1989). Macro-scale water scarcity requires micro-scale approaches, Wiley Online Library.

FAO. (2000). New dimension in water security. Water, society and ecosystem services in the 21st century. Food and agriculture organization of the unitied nations, land and water development division. Rome.

Favis-Mortlock, D. and J. Boardman (1995). Nonlinear responses of soil erosion to climate change: A modelling study on the UK South downs. Catena 25(1-4): 365-387.

Fonseca, R., F. Barriga and W. Fyfe (1998). Reversing desertification by using dam reservoir sediments as agriculture soils. Episodes 21: 218-224.

Frederick, K. D. and D. C. Major (1997). Climate change and water resources. Climatic Change 37(1): 7-23.

Gadgil, A. (1998). Drinking water in developing countries. Annual review of energy and the environment 23(1): 253-286.

Gardner, R. and A. Gerrard (2003). Runoff and soil erosion on cultivated rainfed terraces in the middle hills of nepal. Applied Geography 23(1): 23-45.

Gasith, A. and V. H. Resh (1999). Streams in mediterranean climate regions: Abiotic influences and biotic responses to predictable seasonal events. Annual Review of Ecology and Systematics 51-81.

GCISC (2005). Water resources of Pakistan by Dr Imtiaz Ahmad. South Asia Regional Training work shop on watershed modelling, Global Change Impact Studies Centre (GCISC), Islamabad, Pakistan.

Geist, H. J. and E. F. Lambin (2002). Proximate causes and underlying driving forces of tropical deforestation. BioScience 52 (2): 143-150.

Geoghegan, J., L. A. Wainger and N. E. Bockstael (1997). Spatial landscape indices in a hedonic framework: An ecological economics analysis using GIS. Ecological Economics 23(3): 251-264.

Giorgi, F., C. Jones and G. Asrar (2009). Addressing climate information needs at the regional level: The Cordex framework. WMO Bulletin 58(3): 175.

Gomez, B., L. Carter and N. A. Trustrum (2007). A 2400 yr record of natural events and anthropogenic impacts in intercorrelated terrestrial and marine sediment cores: Waipaoa sedimentary system, New Zealand. Bulletin of the Geological Society of America 119(11-12): 1415.

Gomez, B., Y. Cui, A. Kettner (2009). Simulating changes to the sediment transport regime of the waipaoa river, New Zealand, driven by climate change in the twenty-first century. Global and Planetary Change 67(3-4): 153-166.

Goudie, A. (2006). The human impact on the natural environment: Past, present, and future, Wiley-Blackwell.

Green, C. and A. Van Griensven (2008). Autocalibration in hydrologic modeling: Using swat2005 in small-scale watersheds. Environmental Modelling & Software 23(4): 422-434.

Gross, J. E., R. R. Nemani, W. Turner (2006). Remote sensing for the national parks. Park Science 24(1): 30-36.

Hamdy, A., R. Ragab and E. Scarascia-Mugnozza (2003). Coping with water scarcity: Water saving and increasing water productivity. Irrigation and drainage 52(1): 3-20.

Hanssen-Bauer, I., E. Forland, J. Haugen (2003). Temperature and precipitation scenarios for norway: Comparison of results from dynamical and empirical down-scaling. Climate Research 25(1): 15-27.

Haq I and S. T. Abbas (2006). Sedimentation of tarbela and Mangla reservoirs. 70th Annual Session Proceedings, Pakistan Engineering Congress, pp. 23-46, A- One Publishers Lahore Pakistan.

Haregeweyn, N., J. Poesen, J. Deckers (2008). Sediment-bound nutrient export from micro-dam catchments in northern ethiopia. Land Degradation & Development 19(2): 136-152.

Himesh, S., C. Rao and A. Mahajan (2000). Calibration and validation of water quality model. CSIR Centre for Mathematical Modelling and Computer Simulation.

Horak, J. and Owsinski, J.W. (2004) TRANSCAT project and prototype of DSS.Proceedings of 10th EC-GIS workshop. http://wwwlmu.jrc.it/ Workshops/10ec-gis/papers/25june_horak.pdf. Warszawa, Poland, 23-25.06.2004

Huang, B., W. Sun, Y. Zhao (2007). Temporal and spatial variability of soil organic matter and total nitrogen in an agricultural ecosystem as affected by farming practices. Geoderma 139 (3-4): 336-345.

Huang, S. L., W. C. Kao and C. L. Lee (2007). Energetic mechanisms and development of an urban landscape system. Ecological modelling 201(3-4): 495-506.

Hudson, P. and R. Kesel (2006). Spatial and temporal adjustment of the lower mississippi river to major human impacts. Zeitschrift für Geomorphologie, Supplementband 143: 17-33.

Huntington, T. G. (2006). Evidence for intensification of the global water cycle: Review and synthesis. Journal of Hydrology 319 (1-4): 83-95.

ICWE. (1992). The Dublin Statement and Report of the Conference. International Conference on Water and the Environment: Development Issues for the 21st century. 26–31 January. Dublin.

Ines, A. V. M. and J. W. Hansen (2006). Bias correction of daily gcm rainfall for crop simulation studies. Agricultural and Forest Meteorology 138(1-4): 44-53.

IPCC (2007a). Climate change 2007: Impacts, adaptation and vulnerability. Contribution of working group ii to the fourth assessment report of the intergovernmental panel on climate change, cambridge, Cambridge University Press, UK.

IPCC (2007 b). Climate change 2007: The physical science basis. Contribution of working group i to the fourth assessment report of the intergovernmental panel on climate change Cambridge, United Kingdom and New York, USA. Cambridge University Press.

Irwin, E. G. and J. Geoghegan (2001). Theory, data, methods: Developing spatially explicit economic models of land use change. Agriculture, Ecosystems & Environment 85 (1-3): 7-24.

Ito, A. (2007). Simulated impacts of climate and land-cover change on soil erosion and implication for the carbon cycle, 1901 to 2100. Geophysical research letters 34(9): L09403.

Jayakrishnan, R., R. Srinivasan, C. Santhi (2005). Advances in the application of the swat model for water resources management. Hydrological Processes 19(3): 749-762.

Jha, M., P. W. Gassman, S. Secchi (2004). Effect of watershed subdivision on swat flow, sediment, and nutrient predictions1. JAWRA Journal of the American Water Resources Association 40(3): 811-825.

Jha, S., C. M. Bacon, S. M. Philpott (2011). A review of ecosystem services, farmer livelihoods, and value chains in shade coffee agroecosystems. Integrating Agriculture, Conservation and Ecotourism: Examples from the Field: 141-208.

Jønch-Clausen, T. (2004). Integrated Water Resources Management (IWRM) and water efficiency plans by 2005: Why, what and how. TEC Background Papers No. 10, Global Water Partnership Technical Committee (TEC), Stockholm, Sweden. Available at:http://www.gwpforum.org/gwp/library/TEC10.pdf

Katz, R. W. (2010). Statistics of extremes in climate change. Climatic Change 100 (1): 71-76.

Kaufmann, R. K. and K. C. Seto (2001). Change detection, accuracy, and bias in a sequential analysis of landsat imagery in the pearl river delta, china: Econometric techniques. Agriculture, Ecosystems & Environment 85(1-3): 95-105.

Khan, S. R. (2009). Assessing poverty–deforestation links: Evidence from SWAT, Pakistan. Ecological Economics 68(10): 2607-2618.

Kharin, V. V. and F. W. Zwiers (2000). Changes in the extremes in an ensemble of transient climate simulations with a coupled atmosphere-ocean GCM. Journal of Climate 13(21): 3760-3788.

Kharin, V. V. and F. W. Zwiers (2005). Estimating extremes in transient climate change simulations. Journal of Climate 18(8): 1156-1173.

KHPP (2008) Feasibility and Detailed Design Report of Kohala Hydropower Project, Water and Power Development Authority, Pakistan

Kiersch, B. and S. Tognetti (2002).Land-water linkages in rural watersheds: Results from the fao electronic workshop. Land Use Water Resour. Res 2 1.1-1.6.

Klein, R. J. T., S. E. H. Eriksen, L. O. Næss (2007). Portfolio screening to support the mainstreaming of adaptation to climate change into development assistance. Climatic Change 84(1): 23-44.

Konikow, L. F. and J. D. Bredehoeft (1992). Ground-water models cannot be validated. Advances in Water Resources 15(1): 75-83.

Kumar, C. P. (2000). Ground water flow models. Technical notes: Http://www.Angelfire.Com/nh/cpkumar/publication/.

Kuylenstierna, J., P. Najlis and G. Björklund (1998). The comprehensive assessment of the freshwater resources of the world-policy options for an integrated sustainable water future. Water International 23(1): 17-20.

Lahlou, A. (1996). Environmental and socio-economic impacts of erosion and sedimentation in north africa. IAHS Publications-Series of Proceedings and Reports-Intern Assoc Hydrological Sciences 236: 491-500.

Lambin, E. F. (1997). Modelling and monitoring land-cover change processes in tropical regions. Progress in Physical Geography 21(3): 375-393.

Law, A. M. and W. D. Kelton (1982). Simulation modeling and analysis, McGraw-Hill Book Co, USA.

Leavesley, G. H. and G. Survey (1983). Precipitation-runoff modeling system: User's manual, US Geological Survey.

Legates, D. R. and G. J. McCabe Jr (1999). Evaluating the use of goodness-of-fit measures in hydrologic and hydroclimatic model validation. Water Resources Research 35(1): 233-241.

Lin, Y. P., H. J. Chu, C. F. Wu (2011). Predictive ability of logistic regression, auto-logistic regression and neural network models in empirical land-use change modeling–a case study. International Journal of Geographical Information Science 25(1): 65-87.

Liu, J., B. Liu and K. Ashida (2001). Reservoir sedimentation management in Asia. World 1: 11.18.

Lonergan, C. (2005). Modelling land use changes in Navua, Fiji: Improvement to vulnerability and adaptation assessment of climate change impacts in the pacific. Intenational Global change Institue (IGCI). University of Waikato, University of Waikato. Master of Philosophy.

Macklin, M. G. and J. Lewin (2003). River sediments, great floods and centennial-scale holocene climate change. Journal of Quaternary Science 18(2): 101-105.

Madi, M. T. and M. Z. Raqab (2007). Bayesian prediction of rainfall records using the generalized exponential distribution. Environmetrics 18(5): 541-549.

Mahmood, K. (1987). Reservoir sedimentation: Impact, extent, and mitigation. Technical paper, International Bank for Reconstruction and Development, Washington, DC (USA).

Malone, E. and E. Rovere (2004). Assessing current and changing socio-economic conditions, chapter 6. Adaptation Policy Framework for Climate Change: Developing Strategies, Policies and Measures, UNDP.

Mamede, G. L., J. C. De Araujo and A. Bronstert (2007). Global change scenarios in the prediction of reservoir sedimentation and water availability. IAHS-AISH publication: 137-141.

Martin, J. M. and M. Meybeck (1979). Elemental mass-balance of material carried by major world rivers. Marine chemistry 7 (3): 173-206.

McKinney, M. L. and J. L. Lockwood (1999). Biotic homogenization: A few winners replacing many losers in the next mass extinction. Trends in Ecology & Evolution 14 (11): 450-453.

Meehl, G. A., C. Covey, T. Delworth (2007). The wcrp cmip3 multimodel dataset. Bull. Am. Meteorol. Soc 88: 1383-1394.

Meybeck, M. and C. Vorosmarty (2005). Fluvial filtering of land-to-ocean fluxes: From natural holocene variations to anthropocene. Comptes Rendus Geosciences 337(1-2): 107-123.

Milly, P., J. Betancourt, M. Falkenmark (2008). Stationarity is dead: Whither water management? Earth 4: 20.

MJV (2003). Mangla Dam Raising Project, Project Planning Report, Water & Power Development Authoriy, Pakistan.

Morris, G. L. and J. Fan (1998). Reservoir sedimentation handbook: Design and management of dams, reservoirs, and watersheds for sustainable use, McGraw-Hill Professional.

Nash, J. E. and J. Sutcliffe (1970). River flow forecasting through conceptual models part i—a discussion of principles. Journal of Hydrology 10 (3): 282-290.

Neitsch, S. and J. Arnold (2005). Soil and water assessment tool theoretical documentation. Version 2005. Temple, Texas, USA, grassland. Soil and Water Research Laboratory, Agricultrual Research Service and Blackland Research Center, Texas Agricultural Experiment Station.

NOAA (2010). State of the climate, global analysis, july 2010, national climate data center. Http:/www.Ncdc.Noaa.Gov/sotc/global/2010/8 (accessed 29 December 2011).

Odum, H. T. (1983). Systems ecology; an introduction: An introduction. Wiley, New York, 644 pp.

O'Reilly, C. and R. Silberblatt (2009). Reservoir management in mediterranean climates through the european water framework directive. Hydrology, water resources collections and archives, university of california water resources center, uc berkeley. University of California, Berkeley.

Owens, P., R. Batalla, A. Collins (2005). Fine-grained sediment in river systems: Environmental significance and management issues. River research and applications 21 (7): 693-717.

Palmieri AF, Shah F, Annandale G, Dinar A. 2003.Reservoir Conservation Volume I: The RESCON Approach. World Bank: Washington, DC; 101.

Pandey, A., V. Chowdary, B. Mal (2008). Runoff and sediment yield modeling from a small agricultural watershed in india using the wepp model. Journal of Hydrology 348(3-4): 305-319.

Panofsky and Brier, 1968 H.A. Panofsky, G.W. Brier Some Applications of Statistics to Meteorology. The Pennsylvania State University (1968)

PEPA (2005). State of environmental report 2005 (draft) Pakistan Environmental Protection Agency (PEPA), Ministry of Environment, Government of Pakistan.

Piani, C., J. Haerter and E. Coppola (2010). Statistical bias correction for daily precipitation in regional climate models over europe. Theoretical and Applied Climatology 99(1): 187-192.

Piegay, H., D. E. Walling, N. Landon (2004). Contemporary changes in sediment yield in an alpine mountain basin due to afforestation (the upper drôme in france). Catena 55(2): 183-212.

Pielke Sr, R. A., G. Marland, R. A. Betts (2002). The influence of land-use change and landscape dynamics on the climate system: Relevance to climate-change policy beyond the radiative effect of greenhouse gases.P hilosophical Transactions of the Royal Society of London. Series A: Mathematical, Physical and Engineering Sciences 360(1797): 1705-1719.

Pimentel, D., C. Harvey, P. Resosudarmo (1995). Environmental and economic costs of soil erosion and conservation benefits. Science 267(5201): 1117.

Pinkse, J. and M. E. Slade (2010). The future of spatial econometrics. Journal of Regional Science 50(1): 103-117.

Planning Commision of Pakistan (2005). The medium term development framework 2005-2010.

Postel, S. L., G. C. Daily and P. R. Ehrlich (1996). Human appropriation of renewable fresh water. Science 271(5250): 785.

Pruski, F. and M. Nearing (2002). Climate-induced changes in erosion during the 21st century for eight us locations. Water Resources Research 38(12): 1298.

Raclot, D. and J. Albergel (2006). Runoff and water erosion modelling using wepp on a mediterranean cultivated catchment. Physics and Chemistry of the Earth, Parts A/B/C 31(17): 1038-1047.

Refsgaard, J. and B. Storm (1995). Mike she. Chapter 23 in computer models of watershed hydrology, 809-846. VP Singh ed. Water Resources Pub., Highlands Ranch, CO.

Rode, M., B. Klauer, P. Krause (2002). Integrated river basin management: A new ecologically-based modelling approach. Ecohydrology & Hydrobiology 2(1-4): 177-185.

Rosen, C. (2000). World resources 2000-2001: People and ecosystems; the fraying web of life, Elsevier Science.

Santer, B. D., T. M. L. Wigley, M. E. Schlesinger (1990). Developing climate scenarios from equilibrium gcm results. Report no. 47, Max-Planck-Institut-für-Meteorologie, Hamburg, 29 pp.

Santoso, H. (2003). Towards an integrated model for assessing the effects of changes in climate and land use patterns on the quantity and variability of river flows in indonesia. International Global Change Institue (IGCI). University of Waikato, University of Waikato.

Savenije, H. and P. Van der Zaag (2008). Integrated water resources management: Concepts and issues. Physics and Chemistry of the Earth, Parts A/B/C 33(5): 290-297.

Schickhoff, U. (1995). Himalayan forest-cover changes in historical perspective: A case study in the kaghan valley, northern pakistan. Mountain Research and Development: 3-18.

Schuol, J. and K. Abbaspour (2006). Calibration and uncertainty issues of a hydrological model (swat) applied to west africa. Advances in Geosciences 9: 137-143.

Shiklomanov, I. A. and J. C. Rodda (2003). World water resources at the beginning of the twenty-first century, Cambridge University Press Cambridge, UK.

Shirabe, T. (2012). Prescriptive modeling with map algebra for multi-zone allocation with size constraints. Computers, Environment and Urban Systems.

Shoukri, M., I. Mian and D. Tracy (1988). Sampling properties of estimators of the log-logistic distribution with application to canadian precipitation data. Canadian Journal of Statistics 16(3): 223-236.

Sidle, R. C., A. D. Ziegler, J. N. Negishi (2006). Erosion processes in steep terrain--truths, myths, and uncertainties related to forest management in southeast Asia. Forest Ecology and Management 224(1-2): 199-225.

Simons, D. B. and F. Şentürk (1992). Sediment transport technology: Water and sediment dynamics, Water Resources Pubns.

Singh, V. P. and D. K. Frevert (2002). Mathematical models of largewatershed hydrology. Highlands Ranch, Colorado, Water Resources Publications.

Small, I., J. Rowan and R. Duck (2003). Long-term sediment yield in crombie reservoir catchment, angus; and its regional significance within the midland valley of scotland. Hydrological sciences Journal 48(4): 619-635.

Solomon, S., D. Qin, M. Manning (2007). The physical science basis. Contribution of working group I to the fourth assessment report of the Intergovernmental Panel on Climate Change: 235-337.

Srinivasan, R. and J. G. Arnold (1994). Integration of a basin scale water quality model with GIS1. JAWRA Journal of the American Water Resources Association 30(3): 453-462.

Steenhuis, T. S., A. S. Collick, Z. M. Easton (2009). Predicting discharge and sediment for the abay (blue nile) with a simple model. Hydrological processes 23(26): 3728-3737.

SWAT (2009). Soil & water assessment tool. Theoretical documentation version 2009. Texas WaterResources Institute Technical Report No. 406

Syvitski, C. J. Vörösmarty, A. J. Kettner (2005). Impact of humans on the flux of terrestrial sediment to the global coastal ocean. Science 308(5720): 376.

Syvitski, M. D. Morehead and M. Nicholson (1998). Hydrotrend: A climate-driven hydrologic-transport model for predicting discharge and sediment load to lakes or oceans. Computers & Geosciences 24(1): 51-68.

TAMS Consultants Inc., H. W. L. I. o. H. (1997). Tarbela dam sediment management study – inception report, commissioned by Pakistans Water and Power Development Authority (WAPDA).

Tate, E. L. and F. A. K. Farquharson (2000). Simulating reservoir management under the threat of sedimentation: The case of tarbela dam on the river indus. Water Resources Management 14(3): 191-208.

Taylor, C. M., E. F. Lambin, N. Stephenne (2009). The influence of land use change on climate in the Sahel.

Tomlin, C. D. (1994). Map algebra: One perspective. Landscape and Urban Planning 30(1): 3-12.

Tomlin, C.D., and J.K. Berry. (1979). A mathematical structure for cartographic modeling in environmental analysis. In: Proceedings of the American Congress on Surveying and Mapping, pp. 269-83.

Tong, S. T. Y. and W. Chen (2002). Modeling the relationship between land use and surface water quality. Journal of Environmental Management 66(4): 377-393.

Turner II, B. and R. Ross (1993). Relating land use and global land cover change. Global Change The IGBP Series.

Turner, A. G. and J. M. Slingo (2009). Uncertainties in future projections of extreme precipitation in the indian monsoon region. Atmospheric Science Letters 10(3): 152-158.

United Nations (2006). World water development report 2 : Water, a shared responsibility. UNESCO. Paris: 601.

Verstraeten, G. and J. Poesen (1999). The nature of small-scale flooding, muddy floods and retention pond sedimentation in central belgium. Geomorphology 29(3-4): 275-292.

Vlcek, O. and R. Huth (2009). Is daily precipitation gamma-distributed?:: Adverse effects of an incorrect use of the Kolmogorov-Smirnov test. Atmospheric Research 93(4): 759-766.

Von Bertalanffy, L. (1968). General system theory-foundations and developments. New York: George Braziller, Inc: l0.

Vörösmarty, C., B. Fekete, M. Meybeck (2000). A simulated topological network representing the global system of rivers at 30-minute spatial resolution (stn-30). Global Biogeochemical Cycles 14: 599-621.

Walling, D. (2006). Human impact on land-ocean sediment transfer by the world's rivers. Geomorphology 79(3-4): 192-216.

Walling, D. and D. Fang (2003). Recent trends in the suspended sediment loads of the world's rivers. Global and Planetary Change 39(1-2): 111-126.

Wareing, M. and K. Shei (2010) Pakistan: Urbanization, sustainability, & poverty, http://pages.Uoregon.Edu/aweiss/intl442_542/pakistan%20report%202.Pdf. (accessed 12 May 2011).

Warrick, R., (2009). Using SimCLIM for modelling the impacts of climate extremes in a changing climate: a preliminary case study of household water harvesting in Southeast Queensland. Paper presented at 18thWorld IMACS/MODSIM Congress, Cairns, Australia,13_17 July 2009. Available from http://mssanz.org.au/modsim09.

WCD. (2000). Dams and development: A new framework for decision-making: The report of the world commission on dams. London, Earhscan

Wehner, M. F. (2004). Predicted twenty-first-century changes in seasonal extreme precipitation events in the parallel climate model. Journal of Climate 17(21): 4281-4290.

White, WR. (2005). World Water: Resources, Usage, and the role of man-made reservoirs. Foundation for Water Resources. Allen House, The Listons, Liston Road, Marlow, Bucks SL7 IFD, U.K.

Widmann, M., Bretherton, C.S., Salathé E.P., (2003).Statistical precipitation downscaling over the Northwestern United States using numerically simulated precipitation as a predictor. J. Clim. 16, 799–816.

Williams, J. R. and H. D. Berndt (1972). Sediment yield computed with universal equation. Journal of the Hydraulics Division 98(12): 2087-2098.

Williams, J., M. Nearing, A. Nicks (1996). Using soil erosion models for global change studies. Journal of Soil and Water Conservation 51(5): 381-385.

Winchell, M., R. Srinivasan, M. di Luzio (2010). Arc SWAT interface for SWAT 2009. Available from http:// swat.tamu.edu/software/arcswat/-United States

Winchell.M.,Srinivasan,R., Di Luzio,M., and Arnold. J. (2010). Arc SWAT interface for SWAT 2009. Users'guide. Grassland, Soil and Water Research Laboratory, Agricultural Research Service and Blackland Research Center, Texas Agricultural Experiment Station: Temple, Texas 76502, USA, 495.

Wischmeier, W.H., Smith, D.D., (1978). Predicting Rainfall Erosion Losses A Guide to Conservation,Agricultural Handbook 537. Planning, Science and Education Administration. US Department of Agriculture, Washington, DC, 58 pp.

Wood, A. W., D. P. Lettenmaier and R. N. Palmer (1997). Assessing climate change implications for water resources planning. Climatic Change 37(1): 203-228.

Wood, A. W., L. R. Leung, V. Sridhar (2004). Hydrologic implications of dynamical and statistical approaches to downscaling climate model outputs. Climatic Change 62(1): 189-216.

Wood, C. H. and R. Porro (2002). Land use and deforestation in the amazon. Deforestation and land use in the Amazon. Gainesville: University Press of Florida: 1-38.

World Bank, (2005). Pakistan Country Water Resources Assistance Strategy: Water Economy: Running Dry World Bank South Asia Region, Agriculture and Rural Development Unit

World Water Council (2006). Final report of the 4thworldwater forum. Mexico city, National Water Commission of Mexico: 262.

Yang (2006). Erosion and sedimentation manual, United States. Bureau of Reclamation. Denver office. Technical service center, Government Printing Office.

Yang, D., S. Kanae, T. Oki (2003). Global potential soil erosion with reference to land use and climate changes. Hydrological Processes 17(14): 2913-2928.

Young, R., C. Onstad, D. Bosch (1987). Agricultural non-point source pollution model (agnps). A Watershed Analysis Tool. USDA Conservation Research Report 35.

Youssef, A. M., B. Pradhan and E. Tarabees (2010). Integrated evaluation of urban development suitability based on remote sensing and gis techniques: Contribution from the analytic hierarchy process. Arabian Journal of Geosciences 4(3-4): 463-473.